

Doctoral Dissertation

**Monotonic and Dynamic Strength Characteristics of
Discontinuous Plane in Ring Shearing**

(リングせん断における不連続面の単調および動的強度特性)

by

Nguyen Van Hai

**Division of System Design and Engineering
Graduate School of Science and Engineering
Yamaguchi University, Japan**



March, 2017

ABSTRACT

This thesis represents a laboratory-based experimental study into the monotonic and dynamic strength characteristics of discontinuous plane in ring shearing. It is well-known that the residual shear strength is an essential property in evaluating long-term stability of reactivated landslides in geotechnical engineering. According to previous studies, earthquake-induced landslides may occur on discontinuous planes, such as bedding planes between weathered and unweathered mudstones having different cementation properties resulting from diagenesis. However, the monotonic and dynamic shear behavior at contact surfaces between cemented and non-cemented soil layers has not yet been sufficiently investigated. The objective of this study is to elucidate the ring-shear characteristics of artificial bedding planes that model actual behaviors of slip surfaces occurring between two layers having different degrees of cementation. Additionally, in order to simulate realistic mechanical behavior of naturally cemented clay, artificial cementation bonds were created by adding a cementing agent at different ratios to clay slurry. A series of monotonic and dynamic ring-shear tests was performed under various conditions on non-cemented and cemented kaolin, as well as two-layered specimen combined by attaching cemented kaolin to non-cemented kaolin.

(1) *Monotonic ring-shear tests*: A series of ring-shear tests was performed on reconstituted and cemented one-layer clay specimens, and on two-layered specimens made from clay layers having varied levels of cementation to artificially reproduce a bedding plane. Total nine types of sample were performed. The shear displacement rate, the normal stress, and the curing time were varied in order to better elucidate the influence of these factors on the residual strength characteristics of the discontinuous plane. The test results showed that the residual friction angle of two-part combinations of non-cemented and cemented kaolin was approximately 33.6% lower than that of pure kaolin. In contrast, the residual friction angle of cemented kaolin may be as much as 6.2° greater than non-cemented kaolin. The stress ratio of 2% cemented kaolin increased as the shear

displacement rate increased. The degree of increase was not significant as the cement content increased beyond 2%.

Furthermore, additional multistage ring-shear tests under different normal stresses and shear speeds performed on four sample types showed that the residual friction angle was significantly different corresponding to types of sample, with a range of 0.5 to 6.2°. Additionally, the effect of cementation on the residual cohesion intercept was identified according to the testing methodology. The stress ratio of combined samples in single-stage and multistage ring-shear tests increased with a similar tendency as the shear displacement rate increased. This increase is different for 0% and 4% cemented kaolin, which indicates that the multistage technique may give erroneous results for these clayey soils.

(2) *Dynamic ring-shear tests*: Experimental tests were carried out by using a consolidation-constant volume cyclic loading ring-shear apparatus. Three levels of vertical consolidation stress, σ_N , (98 kPa, 196 kPa, and 294 kPa); four over-consolidation ratios (OCR) (1, 2, 3, and 4); and three shear-torque amplitudes (30 kPa, 60 kPa, and 90 kPa), were applied. The response of four types of samples of cemented and non-cemented kaolin under above mentioned various conditions were carried out to investigate the effects of these factors on the cyclic degradation. The cyclic degradation parameter, t , which evaluate the rate of cyclic degradation with the number of cycles, was mainly used to analyze test results. The experimental results revealed that t decreases with increasing σ_N , shear-torque amplitude, and OCR. For 2%+0% combined-cement specimen, the effect of σ_N on the cyclic degradation was not significant. As OCR increased from 1 to 4, the value of t reduced approximately 25.7% and 58.6% for 0% and 2% normal cemented kaolin samples, respectively. On the other hand, positive and negative cyclic pore water pressure may be generated inside the 2% cemented specimen. This trend also suggests that the cyclic pore water pressure build-up may not be a dominant factor contributing to the cyclic degradation of cemented clay. For combined specimens with a bedding plane, the stress paths barely reached their residual strength line. The cyclic shear resistance of discontinuous plane materials decreased significantly as compared with static residual strength.

CONTENTS

ABSTRACT	i
CONTENTS	iii
LIST OF FIGURES	vi
LIST OF TABLES	xiii
LIST OF SYMBOLS AND ABBREVIATIONS	xiv
Chapter 1 INTRODUCTION	1
1.1 General background	1
1.2 Objectives and Scopes.....	6
1.3 Organization of thesis	7
Chapter 2 LITERATURE REVIEW	10
2.1 Residual strength behavior of clays	10
2.1.1 Introduction.....	10
2.1.2 Relationship between residual strength with soil index properties	12
2.1.3 Nonlinearity of residual failure envelope.....	19
2.1.4 Residual shearing mechanism	21
2.1.5 Effect of shear displacement rate on residual strength.....	23
2.1.6 Residual shear strengths of clays and its application to the evaluation of landslides stability.....	26
2.2 Characteristics of naturally cemented clay.....	30
2.3 Residual strength characteristics of cemented clay soils.....	33
2.4 Multistage ring-shear test technique	35
2.5 Cyclic degradation in clay in dynamic ring-shear test device.....	36
2.6 Review of typical earthquake-induced landslides occurring along the bedding plane in Japan	38
Chapter 3 EXPERIMENTAL TESTING PROGRAMME	43
3.1 Introduction.....	43
3.2 Monotonic ring-shear apparatus.....	44
3.3 Dynamic ring shear apparatus.....	48
3.4 Material and Specimen.....	52
3.5 Preparation of normal and combined specimens.....	53

3.6	Preparation of over-consolidation samples	58
3.7	Test procedure for monotonic ring shear test.....	58
3.8	Test procedure for dynamic ring-shear test.....	59
3.9	Determination of residual strength.....	60

Chapter 4 SHEAR BEHAVIOR OF DISCONTINUOUS PLANE MATERIALS IN MONOTONIC RING-SHEAR TEST 62

4.1	Shear behaviour and strength properties of normal and combined specimens	62
4.2	Effects of combination conditions on shear behaviour for combined specimens	77
4.3	Stress ratio versus normal stress	79
4.4	Effects of cement content in normal and combined specimens	81
4.5	Effects of curing time on the residual strength of normal specimens	84
4.6	Residual state characteristics of multistage ring-shear tests	87
4.7	Observation the slickensides after test	95
4.8	Summary	96

Chapter 5 RATE EFFECT ON RESIDUAL STRENGTH OF DISCONTINUOUS PLANE MATERIALS 98

5.1	Rate effects on residual strength at the contact surface between non-cemented and cemented clays	98
5.2	Effect of increasing shear-rate multistage ring-shear test on the residual strength of cemented and non-cemented kaolin samples	105
5.3	Summary	107

Chapter 6 CYCLIC DEGRADATION OF DISCONTINUOUS PLANE MATERIALS IN DYNAMIC RING-SHEAR TEST 109

6.1	Introduction of cyclic degradation	109
6.2	Effect of confining pressure on cyclic degradation of discontinuous plane materials	111
6.2.1	Evaluation of the change of in the degradation parameter t under different confining pressure	111
6.2.2	Evaluation of the normalized cyclic stress ratio under different confining stress levels	121
6.3	Effects of the shear-torque amplitude on cyclic degradation of discontinuous plane materials.....	122
6.4	Effect of the over-consolidation ratio on the cyclic degradation of discontinuous plane materials.....	126
6.4.1	Change in the degradation parameter t under different over-consolidation ratios	127
6.4.2	Partial evaluation of pore water pressure based on normal stress change during cyclic loading for over-consolidated cemented and non-cemented specimens	131

6.4.3 Mobilized cyclic stress ratio versus the number of cycles under different over-consolidation ratios	132
6.5 The stress paths based on a comparison between the shear strength of dynamic and monotonic ring-shear test.....	133
6.6 Summary	136
Chapter 7 CONCLUSIONS AND RECOMMENDATIONS FOR FUTURE RESEARCH	138
7.1 Conclusions.....	138
7.2 Recommendations for future research.....	144
REFERENCES	146
ACKNOWLEDGMENTS	157

LIST OF FIGURES

Figure 1.1 Typical case of earthquake-induced landslide in the 2004 Mid Niigata Prefecture Earthquake (PWRI, 2006).	4
Figure 1. 2 Flowchart of the research	9
Figure 2.1 Diagrammatic stress-displacement curves at constant normal stress (Skempton, 1985).....	11
Figure 2.2 Relationship between the residual friction angle and the clay fraction (Lupini et al., 1981).	13
Figure 2.3 Relationship between the residual friction angle and plasticity index (Seycek, 1978).	13
Figure 2. 4 The variation of residual shear strength angle with liquid limit (Hatipoglu et al., 2013).	14
Figure 2. 5 Relationship between the secant residual friction angle and liquid limit, clay fraction, and the effective normal stress (Stark and Eid, 1994).....	15
Figure 2. 6 Relationship between the secant residual friction angle and liquid limit, clay fraction, and the effective normal stress (Stark et al., 2005).	15
Figure 2. 7 Variation in ϕ_r with clay fraction and liquid limit (Tiwari and Marui, 2005).	17
Figure 2. 8 Variation in ϕ_r with plasticity index and proportion of smectite (Tiwari and Marui, 2005).	18
Figure 2. 9 Field residual strength for London clay (Skempton, 1985).....	19
Figure 2. 10 Effect of clay mineralogy on drained residual failure envelopes (Stark and Eid, 1994).....	20
Figure 2. 11 Ring shear tests on sand-bentonite mixtures (after Lupini, Skinner and Vaughan, 1981).....	22

Figure 2. 12 Summary of the observed rate-dependent phenomena for residual strength (Tika et al., 1996).....	24
Figure 2. 13 Rate effect of residual strength observed in various soils (after Nakamura and Shimizu, 1978; Scheffler and Ullrich, 1981; Lemos et al., 1985; Okada and So, 1988; Yatabe et al. 1991; Suzuki et al., 2000).....	26
Figure 2. 14 Reactivated shear strength versus displacement for different times of aging: (a) Duck Creek shale; (b) Otay bentonitic shale (Stark et al., 2005).....	28
Figure 2. 15 Summary of published strength recovery test results for effective normal stress of 100 kPa or less (Stark, 2010).....	30
Figure 2. 16 Schematic diagram showing one-dimensionally consolidation and drained shear behaviors in (a) void ratio and effective normal stress relation and (b) shear stress and shear strain relation for cemented and non-cemented soils, respectively (Suzuki et al, 2007)	32
Figure 2. 17 (a) Microfabric of uncemented clay and (b) Structure of the induced cemented clay (Horpibulsuk et al., 2003)	33
Figure 2. 18 Relationship between friction angle and cohesion intercept versus cement content of induced cemented Bangkok and Ariake clays (Horpibulsuk et al., 2005)...	34
Figure 2. 19 The effect of vertical consolidation on cyclic degradation for two samples of kaolin (Mortezaie et al 2013)	37
Figure 2. 20 Landslide dam in the 2004 Niigata Prefecture Chuetsu Earthquake (taken by Prof. Suzuki)	38
Figure 2. 21 Bedrock Sliding Tufaceous sandstone on slip surface at Yokowatashi in Nagaoka city (taken by Prof. Suzuki).....	39
Figure 2. 22 Large-scale landslide in the 2004 Niigata Prefecture Chuetsu Earthquake (taken by Prof. Suzuki)	39
Figure 2. 23 A cross section of “Kuchi-Otani” landslide (Grachev et al. (2005).....	41
Figure 2. 24 Geographic location and cross section of Iwagami landslide (Tiwari et al., 2005).....	42

Figure 3.1 Essential features of ring-shear test apparatus.	45
Figure 3.2 Front view of ring shear-test apparatus	46
Figure 3. 3 Shear box containing test sample	46
Figure 3. 4 A typical testing specimen for monotonic ring-shear test.....	47
Figure 3. 5 Essential features of consolidation-constant volume cyclic loading ring-shear apparatus.	49
Figure 3. 6 Front view of consolidation-constant volume cyclic loading ring-shear apparatus.	50
Figure 3. 7 Shear box containing test sample	50
Figure 3. 8 A typical testing specimen for dynamic ring-shear test	51
Figure 3. 9 Basic features of normal and combined specimens.....	53
Figure 3. 10 Flow chart shows test procedure	54
Figure 3. 11 Soil specimen in process of pre-consolidation.....	55
Figure 3. 12 A soil specimen in process of trimming.....	56
Figure 3. 13 Removing the inside soil core to make an annual specimen.....	56
Figure 3. 14 Completing specimen before transferring to the shear box.....	56
Figure 3. 15 Transferring a soil specimen to the shear box	57
Figure 3. 16 Final setting before ring shear test	57
Figure 3. 17 Schematic diagram for determining the residual strength by a hyperbolic curve approximation.	61
Figure 4. 1 Shear stress and shear displacement curves for (a)-(c) normal and (d)-(f) combined specimens.	67
Figure 4. 2 Peak and residual drained failure envelopes for (a)-(c) normal and (d)-(f) combined specimens.	68

Figure 4. 3 Comparison of (a) peak and (b) residual drained failure envelopes for normal specimen with different cement contents.....	69
Figure 4. 4 Comparison of (a) peak and (b) residual drained failure envelopes for combined specimens with different cement contents.	70
Figure 4. 5 Internal friction angle versus cement content for normal specimen.....	71
Figure 4. 6 Friction angle versus cement content for normal and combined specimens.	71
Figure 4. 7 Sketch pictures exhibit the theories using to explain the significantly increasing residual friction angle: (a) a cemented clay specimen before shearing, (b) development of slip surface based on previous researches, and (c) slip surface was undulated and wavy observing in this study.....	72
Figure 4. 8 Cohesion versus cement content for normal specimen.	75
Figure 4. 9 Cohesion versus cement content for normal and combined specimens.	75
Figure 4. 10 Stress paths of normal specimen with different cement contents.	76
Figure 4. 11 Stress paths of combined specimen with different cement contents.	77
Figure 4. 12 Influence of combined time on shear behavior for normal specimens with different cement content.	78
Figure 4. 13 Relationship between mobilized stress ratio (τ/σ_N) at peak and residual states and normal stress for normal specimens with different cement contents.	80
Figure 4. 14 Relationship between mobilized stress ratio (τ/σ_N) at peak and residual states and normal stress for combined specimens with different cement contents.....	81
Figure 4. 15 Shear stress and shear displacement curves for cemented kaolin clay with various cement contents.....	82
Figure 4. 16 Relationship between (a) peak and (b) residual drained shear strength and cement content for normal specimen.	83
Figure 4. 17 Relationship between (a) peak and (b) residual drained shear strength and cement content for combined specimen.....	84

Figure 4. 18 Shear stress and shear displacement curves under different curing time for cemented kaolin specimen.	86
Figure 4. 19 Relationship between peak and residual strength, and curing time for 2% and 4% cement kaolin specimens.	86
Figure 4. 20 Shear stress-displacement curves for four kinds of specimens by increasing (a) and reducing (b) load MRST.	88
Figure 4. 21 Normal stress-settlement relationship for all specimens conducted by (a) method 2 and (b) method 3.	89
Figure 4. 22 Residual shear strength envelopes of all samples obtained by various testing methods.	91
Figure 4. 23 Residual friction angle obtained by all methods.	92
Figure 4. 24 Residual cohesion intercept obtained by all methods.	93
Figure 4. 25 Variation in residual strength for four kinds of specimen by all methods.	94
Figure 4. 26 Slickensides observed after ring-shear tests for (a) 0% cement, (b) 4%+0%, (c) 2%, and (d) 4% cemented kaolin specimens.	95
Figure 5. 1 Shear behaviors of normal and combined specimens tested under various shear displacement rate.	101
Figure 5. 2 Variation of stress ratio at (a) peak and (b) residual states with shear displacement rate for normal specimen with various cement contents.	103
Figure 5. 3 Variation of stress ratio at (a) peak and (b) residual states with shear displacement rate for normal and combined specimens.	104
Figure 5. 4 Shear displacement rate versus stress ratio for all specimens by increasing shear-rate in single- and multi-stage tests.	107
Figure 6. 1 Schematic illustrating the phenomenon of cyclic degradation and the definition of parameters.	110

Figure 6. 2 Typical time series data for CRSTs on 0%, 2%, 0%+2%, and 2%+2% cemented kaolin specimens: $f= 0.5$ Hz; shear-torque = 60 kPa; normal stress = 196 kPa.	114
Figure 6. 3 Relationship between the cyclic degradation index, δ^* , and the number of cycles, N , for all types of specimen under different normal stresses.....	117
Figure 6. 4 Comparison of the degradation index with the number of cycles, N , for all types of specimens under constant normal stress, $\sigma_N = 98$ kPa.....	117
Figure 6. 5 Comparison of the degradation index with the number of cycles, N , for all types of specimens under constant normal stress, $\sigma_N = 196$ kPa.....	118
Figure 6. 6 Effect of normal stress, σ_N , on the degradation parameter, t , for all types of specimens.....	119
Figure 6. 7 Comparison of the effect of σ_N on the degradation parameter, t_{20} , for all types of specimen.....	120
Figure 6. 8 Normalized cyclic stress ratio versus the number of cycles under the different normal stress at shear displacement, $\delta = 2$ mm.	122
Figure 6. 9 Relationship between the cyclic degradation index, δ^* , and the number of cycles, N , for all types of specimen under different cyclic stress ratios.	124
Figure 6. 10 The effect of the cyclic stress ratio, CSR, on degradation parameter, t , for all types of specimen.....	126
Figure 6. 11 Comparison of the effect of the cyclic stress ratio, CSR, on the degradation parameter, t_{20} , for all types of specimens.....	126
Figure 6. 12 Relationship between the cyclic degradation index, δ^* , the and number of cycles, N , for the 0% and 2% cemented kaolin specimens.....	128
Figure 6. 13 Effect of OCR on the degradation parameter, t , for the 0% and 2% cemented kaolin specimens.....	129
Figure 6. 14 Comparison of the effect of OCR on the degradation parameter, t_{20} , for the 0% and 2% cemented kaolin specimens.....	130

Figure 6. 15 Comparison of the vertical normal stress change during cyclic loading for the (a) 0% and (b) 2% cemented kaolin specimen with the different OCRs	131
Figure 6. 16 Mobilized cyclic stress ratio versus the number of cycles under the different over-consolidation ratio for the 0% and 2% cemented kaolin specimens.	132
Figure 6. 17 Stress paths and peak and residual strength line of the (a) 0% cement, (b) 2% cement, (c) 0%+2% cement and (d) 2%+2% cement specimen during cyclic shearing, respectively; $f = 0.5$ Hz, shear torque = 60 kPa.	136

LIST OF TABLES

Table 3. 1 Features of ring-shear apparatus from Universities and Institutes, compared with the device used in this study	47
Table 3. 2 Features of previous dynamic ring-shear apparatus, compared with the device used in this study.....	51
Table 3. 3 Physical properties of kaolin and cemented kaolin clay.....	52
Table 3. 4 Types of combination for combined-cement kaolin samples.....	53
Table 4. 1 Test cases and test results of cemented and non-cemented kaolin samples	64
Table 4. 2 Summary of shear strength parameters of cemented and non-cemented kaolin specimens under a normal stress of 196 kPa	68
Table 4. 3 Summary of stress ratio at residual state under various combined time and type of specimen for cemented and non-cemented kaolin specimens.....	79
Table 5. 1 Test cases and test results of cemented and non-cemented kaolin samples under different shear rates.....	99
Table 6. 1 Test cases and test results of cemented and non-cemented kaolin samples in dynamic ring-shear test.....	112

LIST OF SYMBOLS AND ABBREVIATIONS

Symbols

a	hyperbolic approximation parameter
b	hyperbolic approximation parameter
C	cement content
c_r	residual cohesion intercept
c_p	peak cohesion intercept
c'	effective cohesion intercept
e	void ratio
e_o	initial void ratio
f	cyclic frequency
G_{sN}	secant shear modulus in dynamic shearing test for the N th cycle
G_{s1}	secant shear modulus for cycles 1
h	annulus thickness of ring-shear test sample
I_p	plasticity index
N_f	number of cycles at pre-defined failure state
N th	number of N cycles in dynamic ring-shear test
p	vertical pressure in compression test
r	coefficient of correlation in determining the residual shear strength
r_o	outer diameter of ring-shear apparatus
r_i	inner diameter of ring-shear apparatus
R	coefficient of correlation
S_{ro}	initial saturation
t	cyclic degradation parameter
t_{20}	cyclic degradation parameter at the 20th cycle
u	pore water pressure
w_o	initial water content
w_L	liquid limit
w_P	plastic limit
ϕ'	internal friction angle
ϕ_r	residual friction angle
δ_{c1}	ring shear displacement for cycles 1

δ_{cN}	ring shear displacement for the N th cycle
δ	horizontally shear displacement in monotonic ring-shear test
ζ	cyclic degradation index in cyclic strain-controlled mode
ζ^*	cyclic degradation index in cyclic stress-controlled mode
γ_c	cyclic shear strain amplitude
ρ_{to}	initial wet density
τ	shear stress
τ_c	cyclic shear stress (shear-torque amplitude)
τ_f	cyclic shear resistance at presumed failure state in dynamic ring shear test
τ_r	drained residual shear stress
τ_{rec}	recovered shear strength
τ_{cN}	cyclic shear resistance in the N th cycle
v	vertical displacement
σ_c	vertical consolidation pressure
σ_{N0}	initial normal stress
σ_N	normal stress or vertical consolidation stress
σ	total normal stress on the shear plane
σ'	effective normal stress
θ	shear rotation angle in radian

Abbreviations

AI	activity index (plasticity index/clay fraction)
CF	clay fraction
CSR	cyclic stress ratio
CRST	cyclic ring shear test
LL	liquid limit
MRST	multistage ring shear test
NC	normal consolidation
OC	over consolidation

OCR	over-consolidation ratio
OPC	ordinary Portland cement
PI	plasticity index
RST	ring shear test
SDC	shear-displacement-controlled cyclic loading ring-shear test
SEM	scanning electron microscope
ST	shear torque
STC	shear-torque-controlled cyclic loading ring-shear test

Chapter 1 INTRODUCTION

1.1 General background

Landslides in soils such as shales, sandstone, and mudstone occur frequently in many parts of the world. The occurrence of earthquake-induced landslides in Japan has increased since the Mid Niigata Prefecture Earthquake of 2004. The scale and movement of earthquake-induced landslides, the constituent materials, and the locations of slip surface are quite different from those of rainfall-induced landslide. During an earthquake, for existing landslides that contain slickensided rupture, shear displacement will commonly occur along the existing slip surfaces because they are weaker than the surrounding soils. [Fig. 1.1](#) shows a typical case of an earthquake-induced landslide that occurred in the Mid Niigata Prefecture Earthquake. The landslide occurred on the boundary between weathered mudstone and un-weathered mudstone ([PWRI, 2006](#)). It should be noted that the majority of the landslides occurred along discontinuous surfaces, such as bedding planes, where the strength of the upper layer differs from that of the lower layers. However, the strength and deformation properties of the contact surface between different soil layers during static and dynamic loading remain to be clarified ([Sassa et al., 1995](#); [Onoue et al., 2006](#); [Wakai et al., 2010](#); [Kinoshita et al., 2013](#)).

An important feature of all naturally cemented clays is the bonding that takes place between particles as a result of diagenesis. This occurs because of carbonate precipitation and the growth of carbonate crystals on the soil grains. Natural cementation increases the resistance of soil to deformation. Therefore, when the cementation is broken, failure will occur, accompanied by a significant magnitude and rate of subsequent deformation. Landslide soils possess the mechanical properties of cemented soil owing to diagenetic bonding over an extended period ([Suzuki et al., 2007](#)). This results from the precipitation of cementing agents in marine and arid environments, weathering, or long-term crystal growth between grains ([Sangrey, 1972](#)). The unique behaviour of these soils has been attributed to bonding, or natural cementation between particles that developed in situ soon after deposition. The existence of cementing binder can cause chemical binding that results in over-consolidation. This leads to behaviour

similar to that of over-consolidated clays, such as strain softening and higher initial stiffness.

Many researchers have studied the behaviour of artificially cemented soils in order to model naturally cemented soils. To simulate the behaviour of natural clay cemented over many years, artificially cemented clay can be created by mixing clay with a small amount of Portland cement or similar agents. Using this method, laboratory cementation bonding occurs at a much faster rate than that of natural clays cemented via diagenetic processes. In recent decades, a number of investigations have been conducted on the stress-strain relationship and strength properties of cemented soils, which using triaxial, direct shear, unconfined compression, and ring-shear tests. Testing materials were usually artificially cemented samples. There are many common mechanical characteristics amongst different types of cemented soils, such as yield stress, initial stiffness, peak strength, residual strength, and dilatancy.

According to the literature, the concept of aging often refers to the cementation of clays forming over many years. The mechanical behaviour of aged clay is characterized by three main factors: delayed compression and cementation over a long period of geological time, a consolidation yield stress higher than the effective overburden pressure, and “stress overshooting” in an e -log p relation (Bjerrum, 1967). Leroueil and Vaughan (1990) revealed that the mechanical behaviours of naturally cemented soils such as claystone, sandstone, and weak rocks are similar, even when the cementation results from different causes. Consequently, the artificially cemented clay samples are expected to simulate many of the characteristics of naturally cemented clays. The effects of bonding in artificial clays are only significant for stresses below an apparent pre-consolidation stress value. They are considered to be sensitive to stress changes and the duration of loading during testing. It has been shown that artificially and naturally bonded soils were comparable with respect to yield compression stress and strain-softening behaviours (Cuccovillo and Coop, 1999). From these experimental studies, the behaviour of artificially cemented kaolin was found to be qualitatively similar to the behaviour of sensitive natural clays (Sangrey, 1972; Burland, 1990). Fischer et al. (1978) stated that cemented Drammen clay behaves as a non-cemented clay with the over-consolidation ratio of about 1.7. Kasama et al. (2000) indicated that the failure envelope of cemented clay is parallel to that of non-cemented clay based on the results of a series

of consolidated undrained triaxial compression tests conducted on cemented clay. Recent results by [Horpibulsuk et al. \(2004, 2005\)](#) revealed that the behaviour of cemented clays is very different from that of over-consolidated soil.

On the other hand, residual strength of these soils is one of the most important characteristics in evaluating the stability of reactivated landslides ([Skempton, 1964; 1985](#)). After Skempton's pioneering work, ring shear tests and reversal direct box shear tests were carried out to measure the residual strength of soil because of their advantages compared with the reversal direct box shear test and triaxial test on a pre-cut specimen ([Bishop et al., 1971; La Gatta, 1970; Yatabe et al., 1996; Toyota et al., 2009](#)). For various kinds of soils, physical and chemical properties, mineralogy composition, effective normal stresses, re-consolidation, over-consolidation ratio (OCR), and shear displacement rate were recognized as factors affecting the residual strength ([Lupini et al., 1981; Skempton, 1985; Lemos et al., 1985; Gibo et al., 1987, 2002; Moore, 1991; Yatabe, 1991; Stark and Eid, 1994; Tika et al., 1996; Suzuki et al., 2000, 2001; Vithana et al., 2012; Kimura et al., 2013](#)). The influence of cementation on the residual strength of landslide materials is especially important at bedding planes with low confining pressures, where effective cohesion plays an important role in the stability of landslide slope ([Mesri and Abdel-Ghaffar, 1993](#)). [Wissa et al. \(1965\)](#) reported that the residual strength is not affected by cementation and can be described by a single strength envelope that is independent of the amount of cementation. [Sasanian and Newson \(2014\)](#) pointed out that the residual strength of the cemented soil increases with increasing curing time or cement content and that the residual strength increases at a slower rate than the peak strength. Among these researches, relatively little literature has been published on the residual strength of materials composed of different cemented soil layers measured with a ring-shear test apparatus ([Suzuki et al., 2007](#)).

Therefore, there is a requirement for investigating the interface of artificially cemented clays that model the actual behaviour of slip surfaces between two soil layers subject to earthquake-induced rapid loading. The purpose of this study is to elucidate the residual strength characteristics of discontinuous planes that model the behaviour of realistic slip surfaces existing between two layers of different degrees of cementation. This is achieved using a ring-shear test apparatus, and is used to better assess the risk of earthquake-induced landslide. According to [Suzuki et al. \(2007\)](#), the concept of residual

strength for a cemented clay can be extended in terms of the disappearance of cementation, in addition to the reorientation of platy clay particles parallel to the direction of shearing. It should be noted that landslides involving such cemented clays occur frequently in many parts of the world. Thus, when considering the stability of a landslide slope consisting of naturally cemented clay such as mudstone, it is important to understand the residual strength characteristics of soil samples having natural cementation.

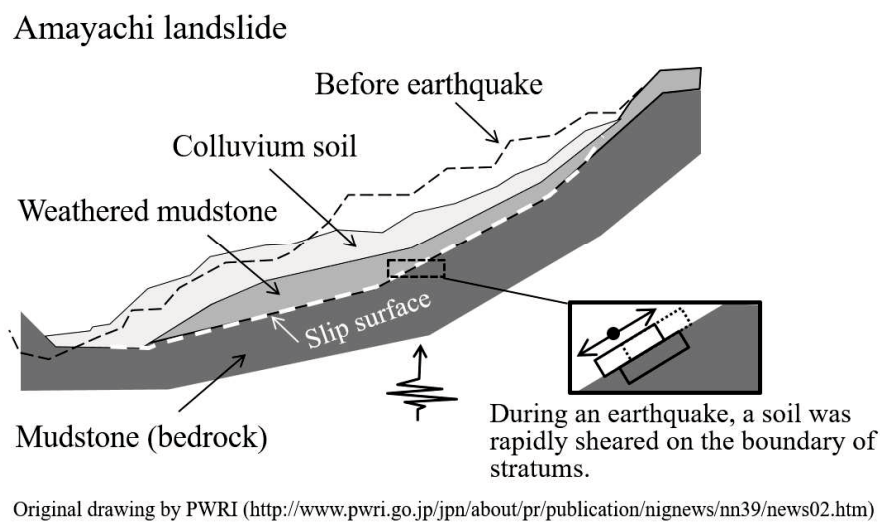


Figure 1.1 Typical case of earthquake-induced landslide in the 2004 Mid Niigata Prefecture Earthquake (PWRI, 2006).

Earthquake-induced slope failures and landslides in naturally cemented clays may result in tremendous hazards. Such soil layers generally subject cyclic shear stresses with different amplitudes and frequencies which can lead to reduce their stiffness and strength. Such a cyclic degradation may cause the deformations and the instability of natural slope. While the dynamic behavior of sandy soil have widely been conducted by many researchers up to the present, only a few studies have been carried out on clayey soils, especially naturally cemented clay soils. This lead to the requirement of further researches to determine the amount and degree of these soil deformation which occur under different kinds of monotonic and cyclic loads. Soil elements, in which initial static shear stresses act on the potential sliding surface, are subjected to additional cyclic shear stress during earthquakes (Jurko et al., 2008). Many factors affect the dynamic properties

of various kinds of soil, such as clay content, clay mineralogy, void ratio, effective confining pressure, shear strain amplitude, and number of cycles (Ansal and Erken, 1989; Grachev et al, 2006). Up to date, effect of dynamic loading on pre-existing shear surface of soil, especially cemented clayey soil, has not yet been sufficiently investigated. Additionally, the cyclic degradation of cemented clayey soil carried out by a dynamic ring-shear test has scarcely been published. Consequently, the change degree of the cyclic degradation of lightly cemented kaolin clay that model actual behaviors of new or pre-existing slip surfaces of soil require to be evaluated, as well as contribute the more deeply understanding to a largely unexplored area.

The residual strength is measured in laboratory by means of many kinds of testing devices. Conventional ring shear apparatus, basing on the Imperial College type ring shear apparatus developed by Bishop et al. (1971), has been commonly used to determine the residual strength because of its many advantages compared to other testing apparatus. The simplicity, convenience, less cost, and requirement of less sample volume are the main characteristics of the Bromhead ring shear apparatus, developed by Bromhead (1979), which has brought about it being popularly used for commercial testing. Based on previous researches, approximately comparable values of residual strength were found using various types of laboratory shear device and testing procedure (La Gatta, 1970; Bishop et al., 1971; Townsend and Gilbert, 1973; 1976). According to traditional single-stage ring-shear test method, each specimen is consolidated and then sheared for only a process without further followed any stages. Thus only a relationship between stress and displacement is described and obviously peak strength and residual strength are determined at failure state. This leads to the requirement a series of three or four specimens, which conducted at different normal stress levels, to supply sufficiently a set of data allowing to predict the exact shape of the failure envelope.

In contrast, a multistage test technique is defined in terms of a single specimen subjecting a number of increase or decrease in normal stress and then shearing to residual conditions, in order to define the full residual strength envelope. This method also may be applied to an individual specimen being sheared by gradually increasing shear rate, which is often used in evaluation of the effect of shear speed on the residual strength. Multistage ring-shear test has many considerable advantages as compared to single-stage ring-shear test. First, the failure envelope is plotted correctly because of a more

number of tested normal stresses. Second, the sample volume required for the test is less than that for individual sample testing. Third, test duration is significantly reduced. Fourth, it is possible to obtain a large quantity of strength parameters from each single specimen. On the other hand, the limitation in measuring the peak shear strength seem to be the main problem of this method.

Though one of the main reasons for the acceptability of the multistage technique is the independence of residual strength on stress history, which have been referred in the literature. Nevertheless, it can be stated that the application of multistage testing technique in ring-shear apparatus, which results in many residual stress state for each specimen, should be improved in further researches. Upon to date, relatively little literature has been published on the residual strength of cemented soil layers measured by multistage ring-shear test, in which the normal stress and shear rate level are being increased or decreased in each stage.

In summary, this thesis represents a laboratory-based experimental study into the monotonic and dynamic shear strength characteristics of discontinuous plane in ring shearing. Both monotonic and dynamic ring-shear apparatuses were used to investigate strength parameters of non-cemented and cemented kaolin clay. A series of monotonic and dynamic ring-shear tests was performed on reconstituted and cemented clay specimens, in addition to two-layered specimens made from clays having varied cementation to artificially reproduce bedding plane. In addition, laboratory-simulated cementation was achieved by adding various amounts of a cementing agent to kaolin clay. The experimental results were compared with literature data to analyse the effects of parameters on the strength properties of contact surface between cemented and non-cemented kaolin.

1.2 Objectives and Scopes

The overall objective of this research is to study the monotonic and dynamic ring shear strength characteristics of discontinuous plane materials.

The key objectives and scope of the research work were formulated as follows:

- Investigate the effect of parameters such as shear displacement rate, confining stress, and curing time on the strength properties of contact surface between cemented and non-cemented kaolin that model the behaviour of actual slip surface existing between two layers of different degrees of cementation. When the strength property of soil having a discontinuity such as bedding plane, the influence of discontinuity on stability of landslide slope can be assessed quantitatively.
- An additional study also was carried out for a comparable work base on the results obtained from single-stage and multistage ring-shear tests, in which conducted by increasing and reducing normal stress, as well as shear rate. Additionally, also to investigate whether the effect of cementation on the multistage technique for cemented clayey soils through some main parameters, such as residual friction angle, residual cohesion intercept, and shear rate.
- Evaluate the influence of parameters such as shear-torque amplitude, over-consolidation ratio, and vertical consolidation stress on the cyclic degradation and cyclic shear resistance of artificial discontinuous plane material. The cyclic degradation parameter, t , which evaluate the rate of cyclic degradation with the number of cycles, was mainly used to analyze test results.

1.3 Organization of thesis

This thesis consists of seven chapters in total. Flowchart of the research is shown in [Fig. 1.2](#). The introduction is given in this chapter 1, while the remainder of the thesis is structured as follows:

Chapter 2 presents the literature review with regard to the previous studies about residual strength behavior of clay soils, characteristics of naturally cemented clay soils. Some of works relating to multistage ring shear test are also briefly reported. In addition, the review of cyclic degradation of clays soils in dynamic shear is also included in this chapter. One additional presentation of history cases in relation to earthquake-induced landslides occurring at bedding plane in Japan is described because this is especially essential for the primary purpose of this research.

Chapter 3 describes the experimental testing program adopted in this study, including a description of testing materials, testing devices, general testing procedures, and analysis method of testing results. The selection and features of sample type are also explained in this chapter.

Chapter 4 is the first of three chapters on the experimental work. It presents the results of monotonic ring-shear tests on cemented and non-cemented kaolin samples to investigate the strength characteristics of discontinuous plane. The presented results are discussed and compared to available data from the literature. This chapter also presents an experimental investigation into the multistage ring-shear test for a comparable analysis.

Chapter 5 represents continuously the experimental results conducted using monotonic ring-shear apparatus, mainly concentrates on the mechanism of rate effect. The effect of shear rate on the residual strength of different types of samples was evaluated. On the other hand, a series of multistage ring-shear tests was carried out with varying shear displacement rates across multiple specimens in order to evaluate the residual strength characteristics of cemented and non-cemented clays subjected from slow to fast shearing.

Chapter 6 presents the experimental results and discussion from all dynamic ring-shear tests performed on cemented and non-cemented kaolin samples, as well as combined samples. This work was mainly analyzed on the basis of cyclic degradation parameter.

Finally, Chapter 7 summarizes the main conclusions derived from this study. A summary of the findings and conclusions from the conducted research work is presented and a number of recommendations for future work also given at the end.

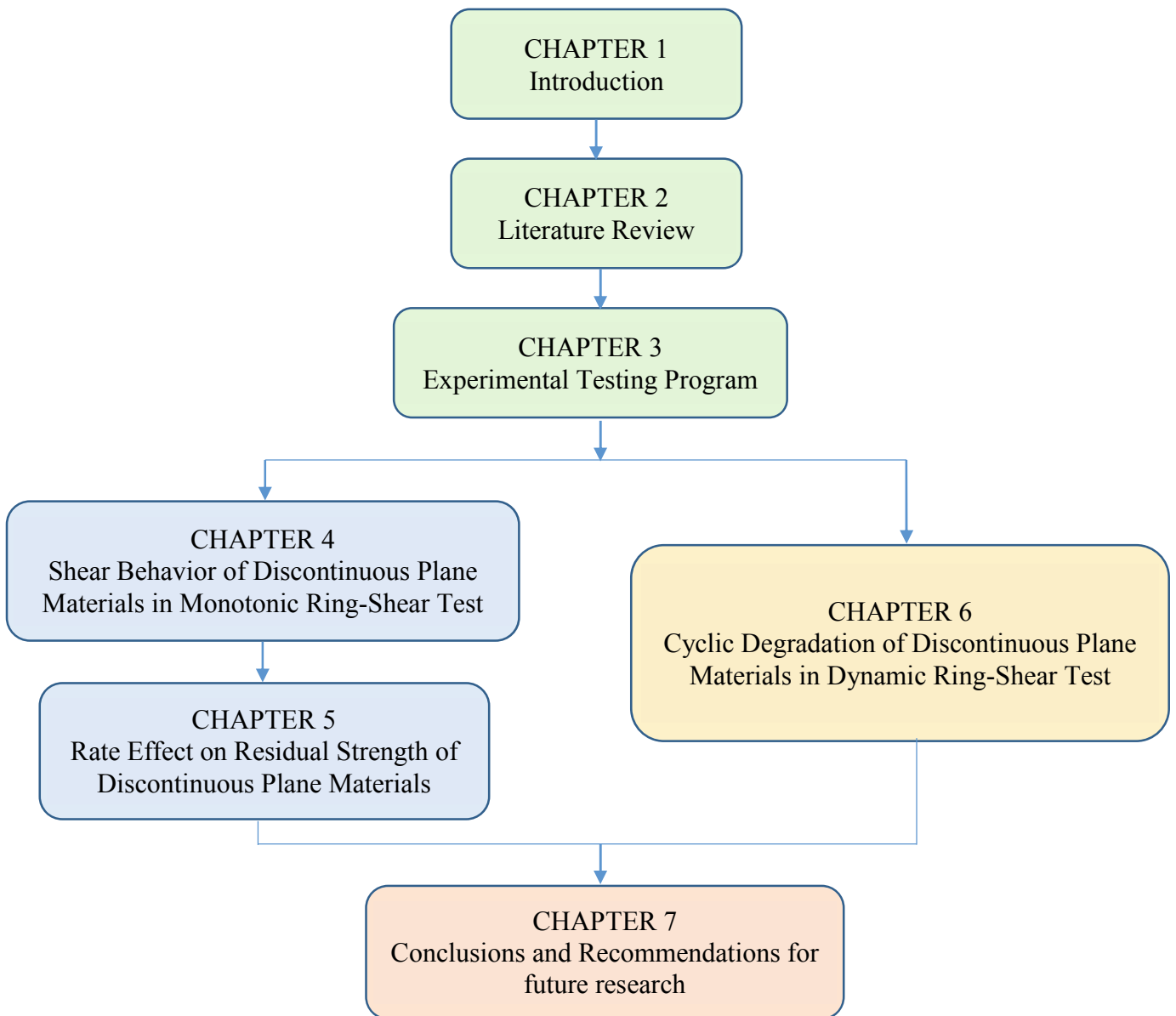


Figure 1. 2 Flowchart of the research

Chapter 2 LITERATURE REVIEW

2.1 Residual strength behavior of clays

2.1.1 Introduction

The residual shear strength is the minimum constant shear resistance attained in a soil at large displacement. It may be considered a fundamental soil property, substantially independent of stress history, original structure, initial moisture content and others factors. Furthermore, residual strength is frequently related to long-term stability problem and areas with landslide history, bedding planes or folded strata (Skempton 1985). Factors affecting the residual shear strength of clays include the type of clay mineral, the index properties of the soil, pore water chemistry, shear displacement rate, and other factors (Lupini et al., 1981; Mesri and Cepeda-Diaz, 1986; Stark and Eid, 1994, Tiwari and Marui, 2003, Ramiah et al., 1970, Suzuki et al., 2001),

Over the last few decades, a significant amount of research has been conducted to achieve better understanding the behavior of residual strength of clay soils (Skempton, 1985; Lupini et al., 1981; Stark and Eid, 1994, 1997) as well as improving the devices and testing techniques for more accurately measuring the residual strength (Stark and Eid, 1993; Garga and Infante, 2002; Meehan et al., 2006, 2007; Sassa et al., 2005). However, relatively little literature has been published on the residual strength of materials composed of different cemented soil layers measured with a ring-shear test apparatus (Suzuki et al., 2007).

Heavily over-consolidated clays have high peak strengths and generally exhibit a large decrease from peak to residual strength. The reduction in strength is accompanied by an increase in void ratio and water content. On the other hand, normally consolidated clays have lower peak strengths and exhibit a smaller decrease from peak to residual strength than over-consolidated clays. This decrease in strength is accompanied by a reduction in void ratio and is due entirely to the orientation of particles parallel to the direction of shearing. This typical soil behavior is illustrated in Fig. 2.1.

The residual strength of a clay is described in terms of residual friction angle, ϕ_r , and a residual strength cohesion intercept, c_r , as follows:

$$\tau_r = c_r + \sigma' \tan \phi_r = c_r + (\sigma - u) \tan \phi_r \quad (2.1)$$

Where: τ_r = residual shear stress

σ = total normal stress on the shear plane

u = pore water pressure

σ' = effective normal stress

For most natural soils, the residual strength cohesion intercept is close or equal to zero, and the residual friction angle is less than the peak friction angle. The residual strength behavior is commonly described by the shearing resistance ratio, $\tau_r / \sigma' = \tan \phi_r$ (for $c_r = 0$). Although the assumption of zero cohesion at residual states has been widely applied for designing purposes, [Tiwari et al. \(2005\)](#) reported residual cohesion values as large as 9.2 kPa obtained from the best fit residual strength envelope for some soils.

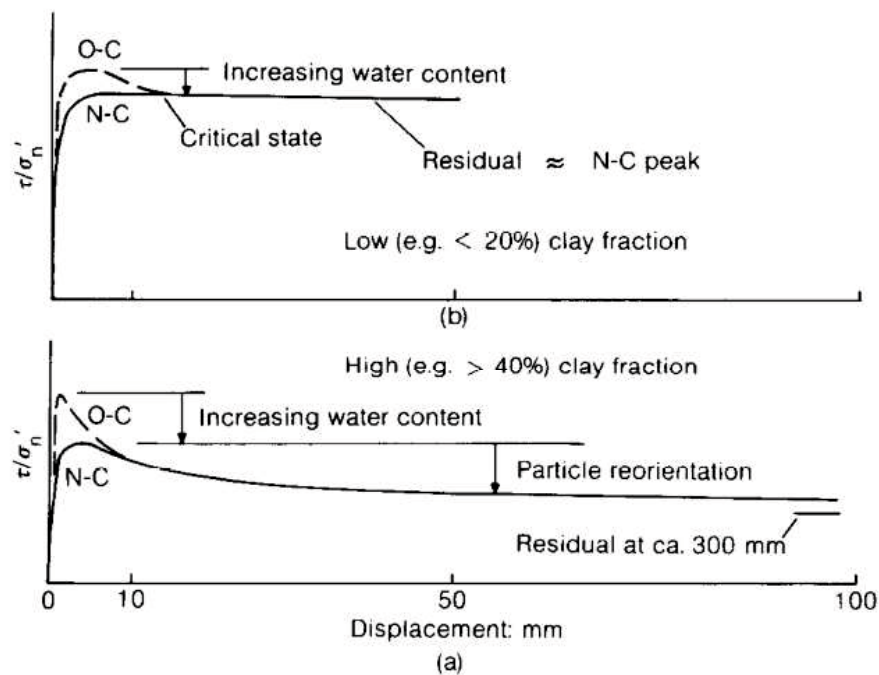


Figure 2.1 Diagrammatic stress-displacement curves at constant normal stress
([Skempton, 1985](#))

Early studies into the residual strength behavior of soils were carried out in the 1930's. The application of residual strength to the stability of slope led to the new

research into the changes that occur in soil during the transition from peak to residual strength, and required the development of new testing devices for determining the residual strength of soils. In the Fourth Rankin lecture, Skempton (1964) presented evidence to show that the long-term stability of slopes in over-consolidated fissures clays is governed by residual strength through the mechanism of progressive failure. He also found that once the drained residual strength has been reached, additional shearing will not change its value. Bjerrum (1967) indicated that on over-consolidated clay need not contain fissures for its long-term stability to be governed by residual strength.

2.1.2 Relationship between residual strength with soil index properties

From the view point of geotechnical engineering it is important to decide the residual strength parameters as quick as possible in an acceptable precision. For that purpose, many investigators tried to correlate the residual shear strength parameters with soil index properties such as clay content and Atterberg limit (Lupini et al. 1981; Mesri and Diaz 1986; Stark and Eid 1994). The clay fraction is defined as percentage by weight of particles smaller than 0.002 mm and liquid limit provides an adequate indication of clay mineralogy. Skempton (1985) and Lupini et al. (1981) concluded that particle reorientation will be significant only in clays containing platy clay minerals and having a clay fraction exceeding about 20-25%. If the clay fraction (CF) is less than about 25%, the clay behaves much like a sand or silt with angles of residual shearing resistance typically greater than 20° .

Many correlation between the residual shear strength and clay fraction or plasticity have been proposed by different authors. Fig. 2.2 shows the correlation postulated by Skempton including correlations reported by other authors Lupini (1981). Some authors also have suggested that there is a better correlation between the residual friction angle and the plasticity index than any other parameter. Fig. 2.3 and 2.4 summarize the correlations of this type reported by different authors (Seycek, 1978; Hatipoglu et al., 2013). Although the good correlation between the residual strength and some soil properties was found, Lupini et al (1982) pointed out that these correlations cannot be generalized. He stated that other properties, such as the particle shape, grading,

mineralogy, pore water chemistry, ect., affect remarkably on the residual strength of soils.

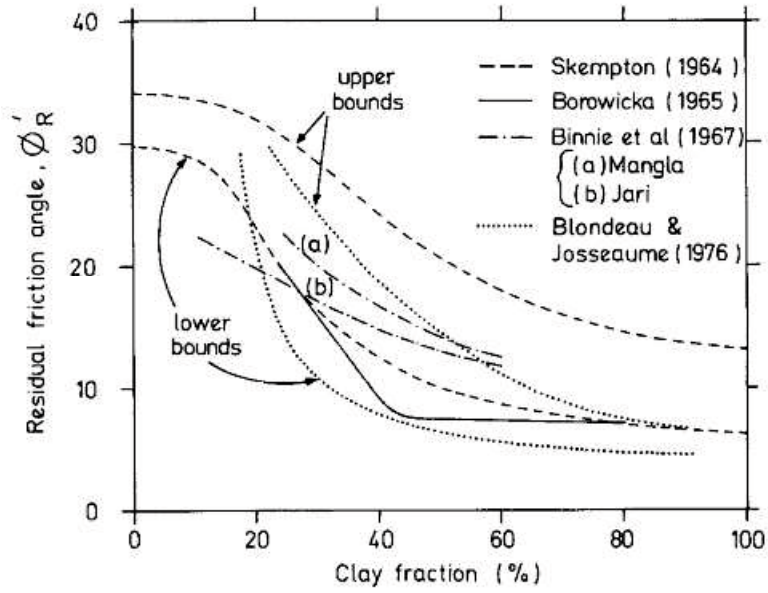


Figure 2.2 Relationship between the residual friction angle and the clay fraction (Lupini et al., 1981).

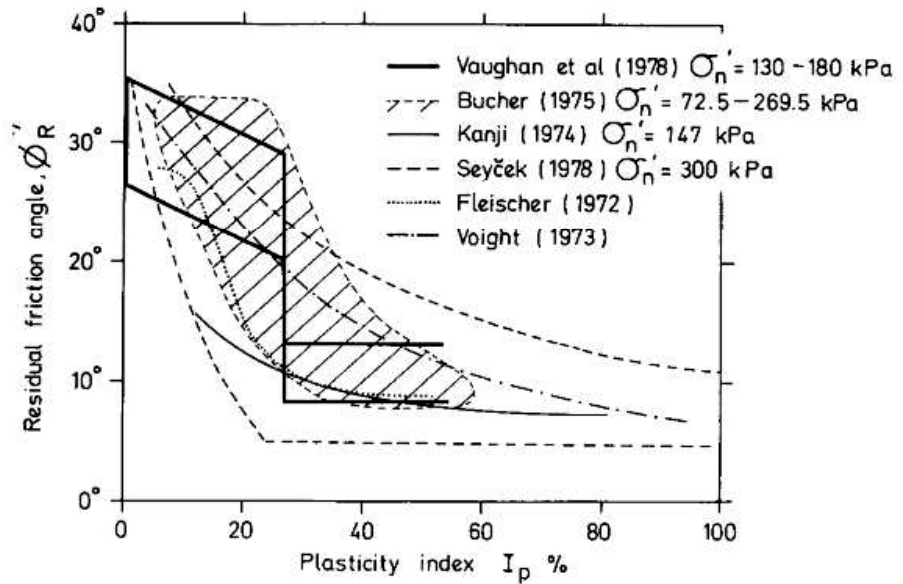


Figure 2.3 Relationship between the residual friction angle and plasticity index (Seycek, 1978).

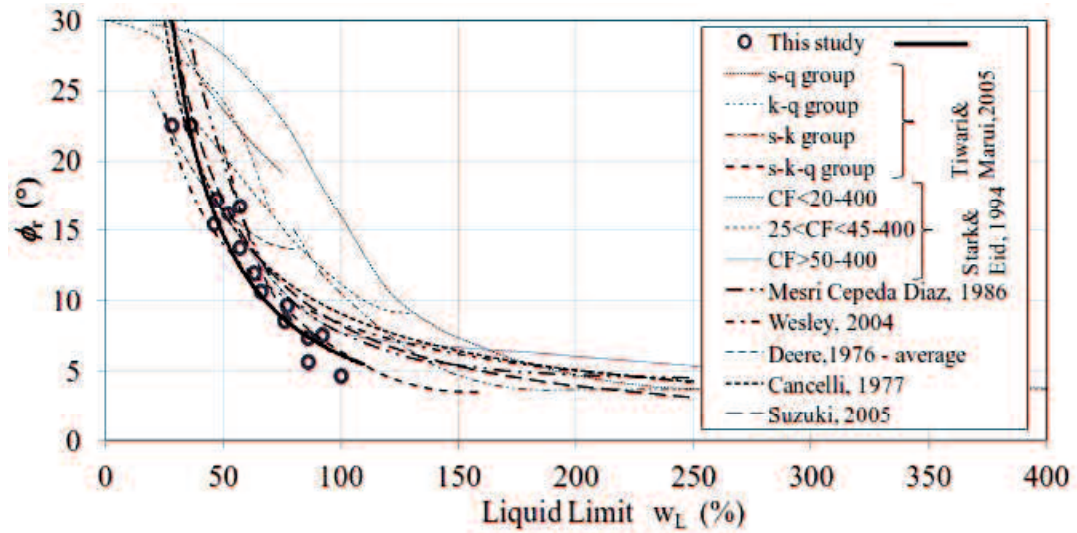


Figure 2. 4 The variation of residual shear strength angle with liquid limit (Hatipoglu et al., 2013).

More recently, Stark and Eid (1994) postulated that correlations based on only clay-size fraction or clay plasticity tend to overestimate the drained residual friction angle. In addition, the nonlinearity of the residual failure envelope was not estimated. This led to low estimation of the safety factor in soil stability analysis problems because small changes in the residual friction angle results in substantial changes in the calculated factor of safety. The authors also suggest that the residual failure envelope can be approximated by a straight line for cohesive soils that have a clay fraction less than 45%. For cohesive soils with clay fraction larger than 50% and a liquid limit between 60 and 220, they demonstrated that the nonlinearity of the drained residual failure envelope was significant. As a consequence, the authors proposed a new drained residual strength correlation which is a function of the liquid limit, clay fraction, and the effective normal stress (Fig. 2.5).

Recently, Stark et al. (2005) based on new experimental data revised the correlation in Fig. 2.5 and presented a new empirical correlation only for the relationship of an effective normal stress of 100 kPa (Fig. 2.6). The new relationship was shifted slightly upward (less than 1°), which increased the stress dependency of the secant residual friction angle for soils with a clay fraction less than or equal to 20%. The relationship for an effective normal stress of 400 and 700 kPa were not changed from Stark and Eid (1994).

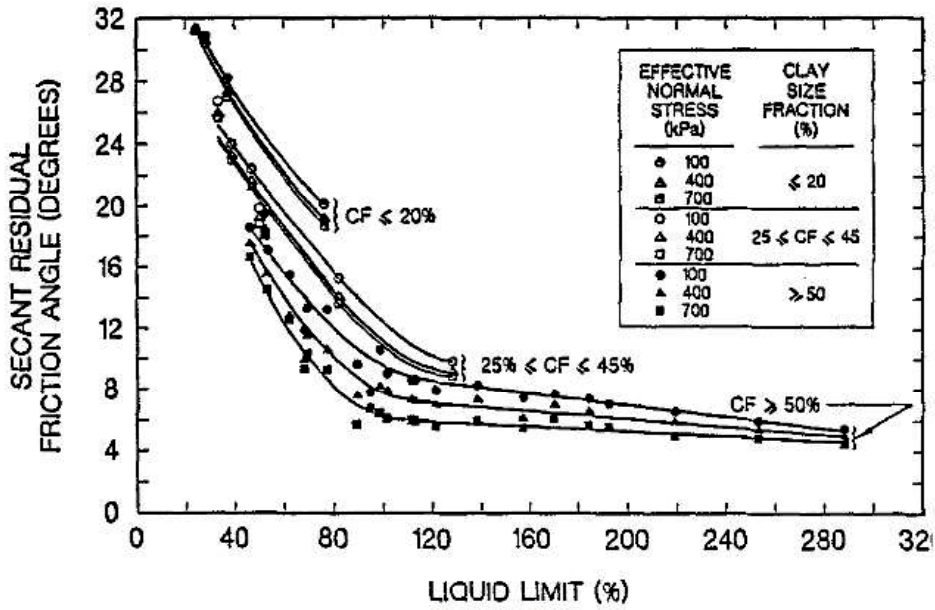


Figure 2. 5 Relationship between the secant residual friction angle and liquid limit, clay fraction, and the effective normal stress (Stark and Eid, 1994).

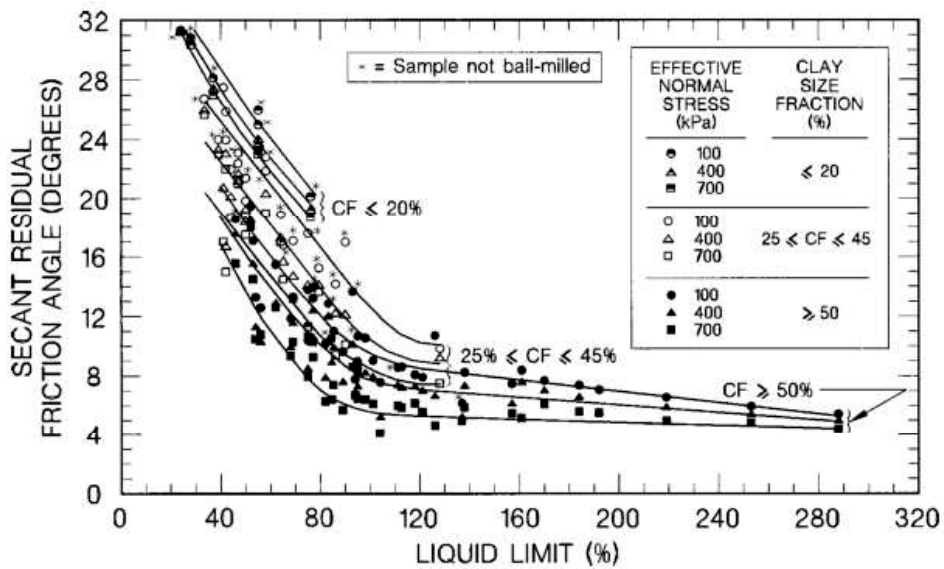


Figure 2. 6 Relationship between the secant residual friction angle and liquid limit, clay fraction, and the effective normal stress (Stark et al., 2005).

The residual strength is mostly dependent on the percentage of clay particles present and their type. Apart from the clay fraction, the mineralogy of the clay also has an effect on residual strength, especially when the clay fraction is large. The clay mineralogy that

are common in clay and shales are platy structures, and are therefore subject to alignment when sheared. This leads to high residual friction angles, commonly greater than 25° .

Lupini et al. (1981) also suggested again that all these correlations, which are characterized by a large amount of scatter in the data, cannot be general. This reasoning, on the one hand, is consistent with Mesri and Ceped-Diaz's (1986) statement that the correlation need not be general. However, it is valuable to be able to predict the residual strength from the clay fraction or plasticity index, for a particular site where relationship can be developed when variation of the other factors are negligible. Kalteziotis (1993) also stated that although correlations between residual strength and index properties of soils should not be generalized, it must be noted that for soils with a similar composition and geological history these correlations can be valid and of great importance in geotechnical engineering, and especially in the study of reactivated landslides.

Attempts to correlate ϕ_r with soil mineralogical composition were also made by Tiwari and Marui (2005). They proposed a reliable method for the estimation of ϕ_r with mineralogical composition, which not only brought about less deviation from the measured ϕ_r but also minimized the range of estimation error compared to that commonly used method. Their study based on the results of more than 35 mixtures of smectite, kaolinite, mica, feldspar, and quartz as major constituent minerals, thus the applicability of this method is wider than the other methods proposed so far (Figs. 2.7 and 2.8)

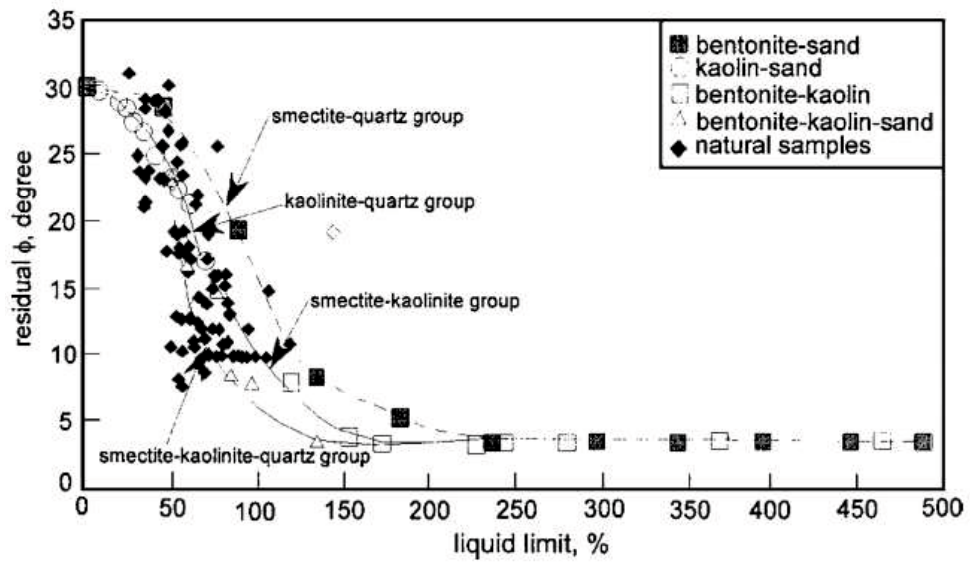
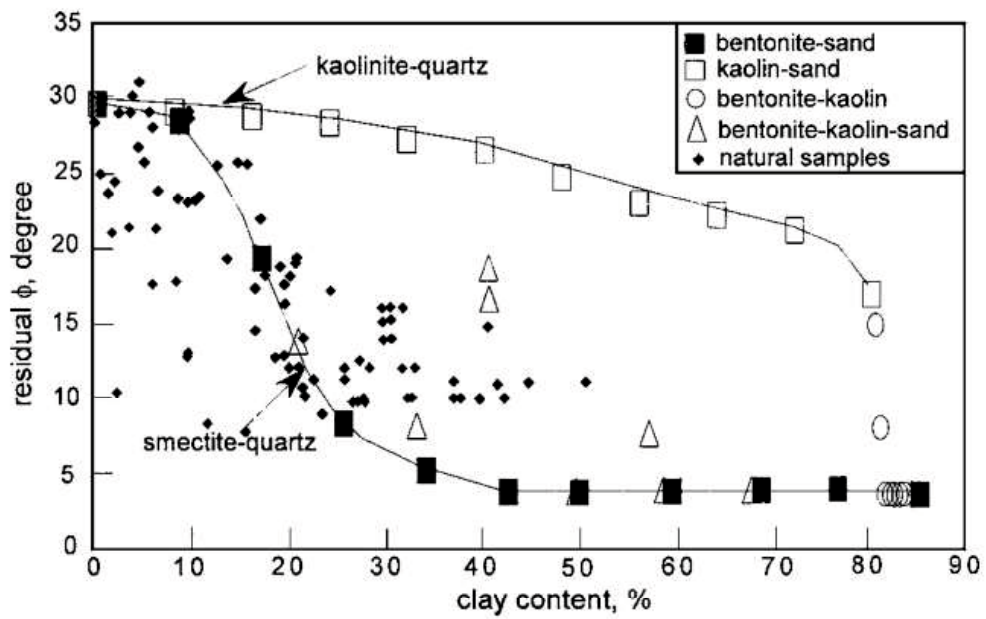


Figure 2. 7 Variation in ϕ_r with clay fraction and liquid limit (Tiwari and Marui, 2005).

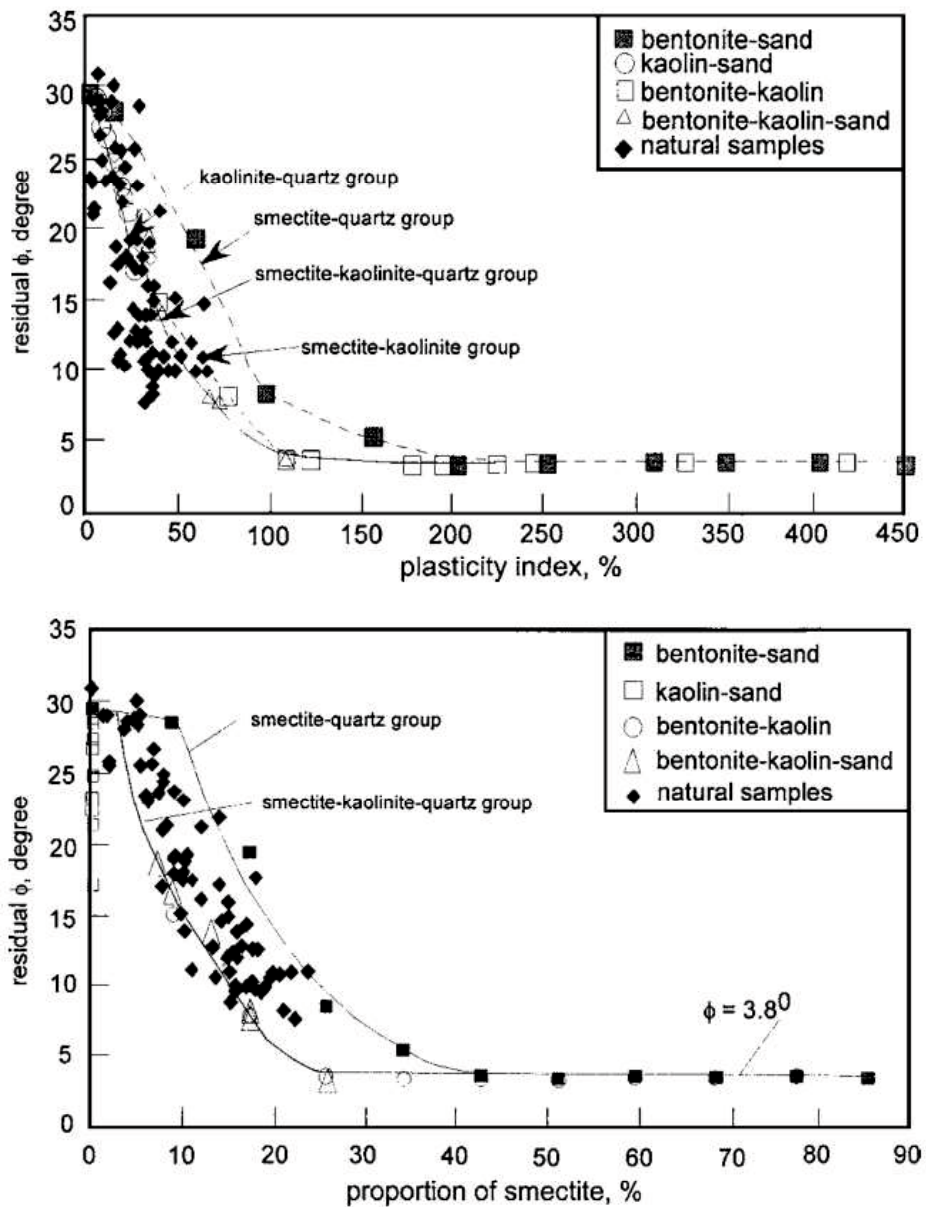


Figure 2. 8 Variation in ϕ_r with plasticity index and proportion of smectite (Tiwari and Marui, 2005).

The magnitude of the drained residual strength is controlled by the type of clay mineral and quantity of clay-size particles. The liquid limit provides an indicator by the type of clay mineral and the clay-size fraction indicates the quantity of particles smaller than 0.002 mm. Therefore, both the liquid limit and clay-size fraction should be used to estimate the drained residual friction angle. *In summary, it could be said a general statement that residual of friction angle decreases with increasing liquid limit, plasticity index, clay fraction and effective normal stress.*

2.1.3 Nonlinearity of residual failure envelope

Many investigators found that the drained residual strength failure envelope is nonlinear (Bishop et al., 1971; Lupini et al., 1981, Skempton, 1985; Stark et al., 1992; 1994) illustrated in Figs 2.9 and 2.10. Bishop et al. (1971) shown that the brown London clay to have a curved envelope but the blue London clay a straight envelope. The nonlinearity is significant for cohesive soils with a clay size fraction greater than 80% and a liquid limit between 60 and 220. Nevertheless, a straight line relationship was often used for fitting the result of tests on over-consolidated clays. Recent studies have established that, particularly at low stress level, there is a distinct curvature of the residual failure envelope, and the residual angle of shearing resistance ϕ_r is dependent on the stress level (Lupini et al., 1981; Stark et al., 2005). Stark and Eid (1994) conducted a series of drained ring-shear tests using thirty-two different clays and clay shales, and it was found that the drained residual envelope is nonlinear. They also stated that the difference in contact area results in a nonlinear residual failure envelope.

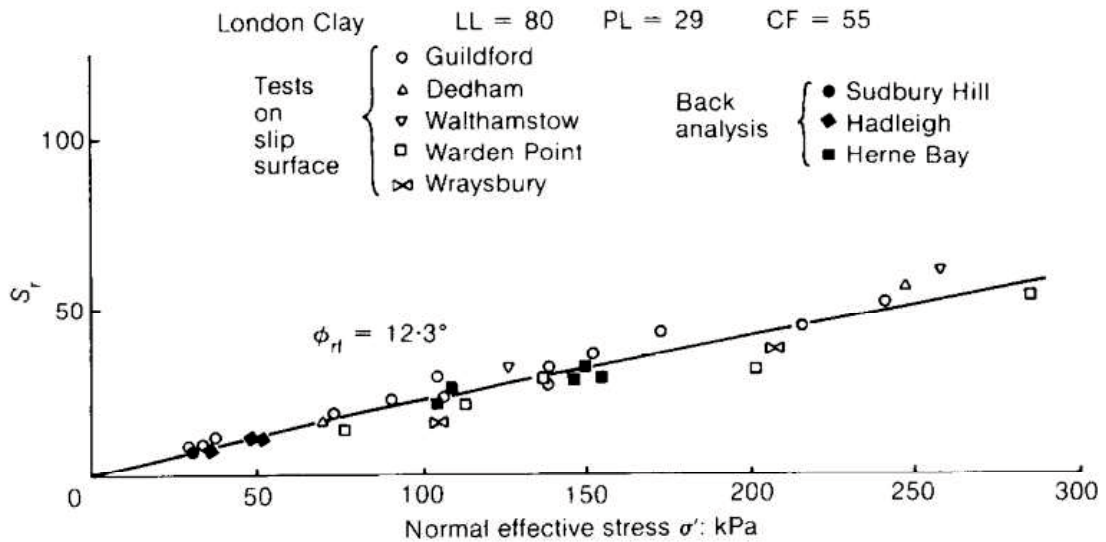


Figure 2. 9 Field residual strength for London clay (Skempton, 1985)

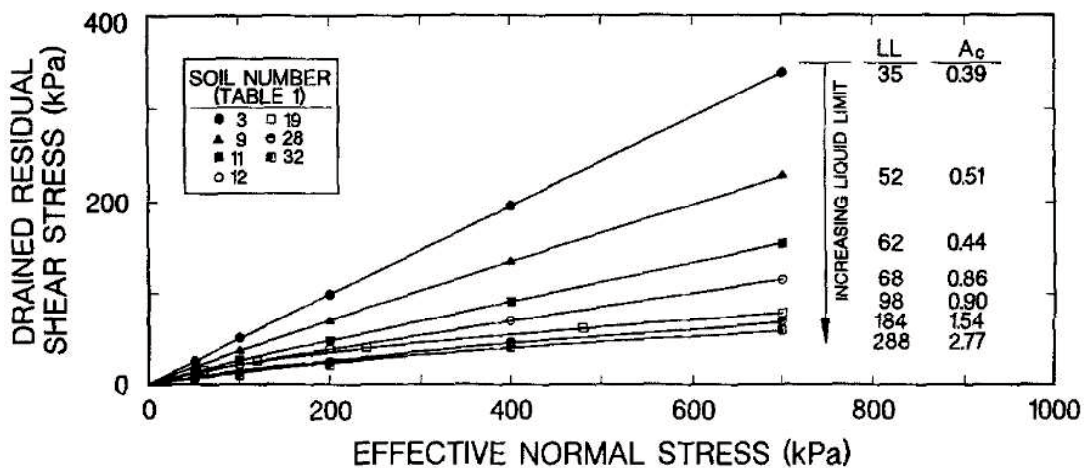


Figure 2. 10 Effect of clay mineralogy on drained residual failure envelopes (Stark and Eid, 1994)

On the other hand, some researchers stated that the residual shear strength envelope was linear. Townsend and Gilbert (1976) based on the tests conducting on various clay shales from Brazil and American stated that the residual strength envelope is accurately described by a straight line through the origin. Stark and Eid (1994) also suggested that the residual failure envelope can be approximated by a straight line for cohesive soils that have a clay fraction less than 45%. For cohesive soils with clay fraction larger than 50% and a liquid limit between 60 and 220, they demonstrated that the nonlinearity of the drained residual failure envelope was significant

Kalteziotis (1993) conducted a program of residual strength on a number of Hellenic soil types (Marls, Clays, and Flysch) using the Bromhead ring shear apparatus and found that ϕ_r was constant for normal stress between 50 and 400 kPa, it means the effective residual friction angle is independent of normal effective stress. At high clay content the residual friction angle was controlled by the properties of the predominant clay minerals whereas at low clay contents it was the mineralogical composition of the silt-sized grains that determined ϕ_r .

Hawkins and Privett (1985) highlight the curved nature of the residual failure envelope, particularly at effective normal stresses below 200kPa and in soil with high clay fraction. They also stated that ϕ_r should not be considered as constant for a particular material, but a parameter which changes with the effective normal stress. When the

effective normal stress increases, the failure envelope becomes straighter and the residual friction coefficient approaches to constant value. A new drained residual strength correlation is described that is a function of the liquid limit, clay-size fraction, and effective normal stress as mentioned in previous section (Stark and Eid, 1994). The correlation can be used to estimate the entire nonlinear residual failure envelope or a secant residual friction angle that corresponds to the average effective normal stress on the slip surface (Fig. 2.10).

On the other hand, Mesri and Abdel-Ghaffar (1993) indicated the significant influence of the cohesion intercept on the location of the slip surface and the factor of safety. It is still common practice to assume a best fitted straight line would give a small c_r . This residual cohesion is often ignored in design. This assumption is consistent in the case of low effective normal stress, and may result in erroneous calculated results in the stability analysis of existing slopes.

2.1.4 Residual shearing mechanism

Lupini et al. (1981) defined three possible modes of residual shear behavior (Fig. 2.11), depending on the proportion of platy particles presents in the soil and the coefficient of inter-particle friction of the platy particles. The three possible modes of residual shear are as follows:

Turbulent mode: This mode occurs when behavior is dominated by rotund particles or in soils dominated by platy particles when the coefficient of interparticle friction between these particles is high. Residual strength is high, no preferred particle orientation occurs and brittleness is due to dilatant behavior only. The residual friction angle in this mode depends primarily on the shape and packing of the rotund particles and not on the interparticle friction. A shear zone, once formed, is a zone of different porosity only and it is considerably modified by subsequent stress history.

Sliding mode: This mode occurs when behavior is dominated by platy, low friction particles. A low strength shear surface of strongly oriented platy particles then develops. The residual friction angle depends primarily on mineralogy, pore water chemistry and on the coefficient of interparticle friction. A shear surface, once formed, is not

significantly affected by subsequent stress history. Brittleness during first shearing is due primarily to preferred particle orientation.

Transitional mode: This mode occurs when there is no dominant particle shape, and involves turbulent and sliding behavior in different parts of a shear zone. The properties of the soil in residual shear change progressively across the transitional range from those of turbulent shear to those typical of sliding shear. In this mode the residual friction angle is sensitive to small changes in grading of the soil, and the changes in grading is required to cross this range entirely are typically small. Finally, the authors state that the residual friction angle depends on the normal effective stress and this dependence is typically greatest for the sliding mode of behavior.

According to Skempton (1985), the residual shear strength of soils with clay fractions exceeding 50% is almost entirely controlled by the sliding friction of the clay minerals, and further increase in clay fraction has little effect. Of the clay less than about 25%, “turbulent” or “rolling” shear occurs without the influence of clay particle alignment. For value of clay fraction between 25% and 50%, there is a “transitional” type of behavior, and the residual strength depends on the percentage of clay particles as well as on their nature.

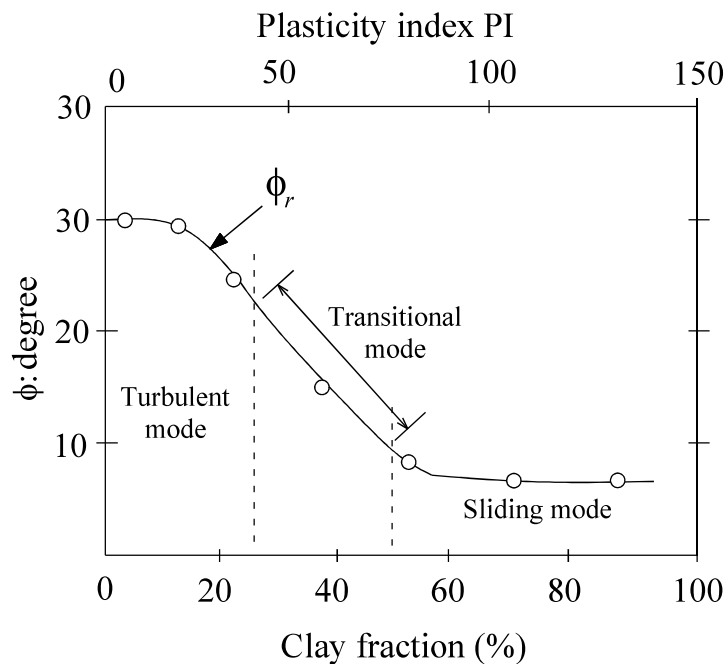


Figure 2. 11 Ring shear tests on sand-bentonite mixtures (after Lupini, Skinner and Vaughan, 1981)

2.1.5 Effect of shear displacement rate on residual strength

With some soils, the residual strength can be sensitive to the rate at which the soil is sheared. This influence of shear rate on residual strength of clay was presented by [La Gatta \(1970\)](#), [Skempton \(1985\)](#), [Tika et al. \(1996, 1999\)](#), [Suzuki et al. \(2000\)](#), [Lemos et al. \(1986, 2003\)](#), [Carrubba et al. \(2006\)](#), [Meehan et al. \(2006, 2007\)](#), [Mohammad et al. \(2013\)](#), [Deepak R. B. \(2013\)](#). The influence of different rates of shear must be taken into account for evaluation of residual strength on natural pre-existing shear surfaces. Rates of shear on such surfaces can vary considerably from very slow movements in some reactivated landslides to very fast displacement caused by earthquakes ([Kalteziotis, 1993](#)).

[La Gatta \(1970\)](#) found that increasing the shear displacement rate from 0.006 mm/min increased the residual strength of Cucuracha Shale (LL = 65%; PI = 20%; CF = 48%) by 35%. [Skempton \(1985\)](#) has mentioned that the residual strength is little affected by variation in the slow rates of displacement in the usual laboratory tests, but at rates faster than about 100mm/min all samples showed a rise in strength to a maximum, followed by a decrease to an approximately steady minimum value. [Tika et al. \(1996\)](#), [Lemos et al. \(2003\)](#) described that, if a shear surface formed at residual strength by slow shear rate under drained condition, then subjected to a fast shear rate, the following features are typically observed ([Fig. 2.12](#)):

- (a) There is an initial threshold strength on the shear surface, mobilized at a negligibly small displacement. The threshold strength is a function of the displacement rate and is considerably in excess of the slow drained residual strength.
- (b) There is often a further increase in strength on the shear surface with fast displacement up to a maximum value, the fast peak strength, which is again a function of the displacement rate.
- (c) The strength is then likely to drop with further fast displacement to a minimum value, the fast residual strength. The fast residual strength usually remains higher than the slow drained residual strength, but it may drop to a lower value.

- (d) If, after fast shearing of a soil that shows transitional and sliding shear mode, the shear surface is tested slowly, an initial slow peak strength greater than the slow drained residual strength is measured, indicating that fast shearing causes disordering of the shear surface.

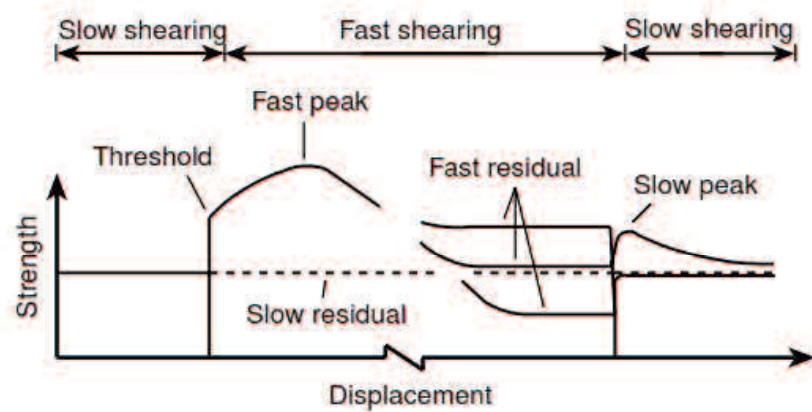


Figure 2. 12 Summary of the observed rate-dependent phenomena for residual strength
(Tika et al., 1996)

Three types of variation of the fast residual strength with an increasing displacement rate were observed: *a positive rate effect*, *a neutral rate effect* and *a negative effect*. Soils with turbulent shear exhibit a neutral or negative rate effect. Soils with transitional shear mode exhibit a negative rate effect. Soils with a sliding shear mode show a positive or a negative rate effect. Suzuki et al. (2000) has also reported the rate of displacement from 0.02 to 2.0 mm/ min significantly influenced the residual strength of kaolin clay and mudstone (Fig. 2.12). Another research from Carrubba et al. (2006) also agreed to above contents. In addition, they suggested that viscous effects and fabric modification may explain part of the gain in strength observed at peak strength in neutral or negative rate effect. A further problem was mentioned involved a cyclic contraction and dilation of the specimen caused an increase a pore pressure build-up, that was a main reason of loss of strength and thus the negative rate effect. Parathiras (1995) proposed an alternative hypothesis, based on the observation that, in presence of water, the negative rate effect only occurred when the sample developed a non-planar shear surface. Petley et al. (1999) have introduced a numerical model to describe the interplay between the pore water

pressure generation and negative rate effect. Their findings agree with those of [Parathiras \(1995\)](#).

Otherwise, based on a series of “fast” ring shear tests were performed in the Bromhead ring shear device to examine the effect of shear rate on the strength measured along existing slickensided discontinuities in Rancho Solano Fat Clay, [Meehan et al. \(2006, 2007\)](#) supposed that the fast ring shear test results could not be used to accurately quantify the effect of loading rate on the shear strength measured along slickenside surfaces. Similarly to previous researches, [Deepak \(2013\)](#) concluded that the residual strength of kaolin clay is negligible with the shearing rate 0.037 mm/min to 0.162 mm/min and hardly increase in residual strength occurred with the shearing rate varying from 0.233 mm/min to 0.586 mm/min. [Mohammad et al. \(2013\)](#) also done a series of slow and fast ring shear tests in kaolinite and deduced that the rate dependency of the residual shear strength might be influenced by changes in the test procedure that is applied. This effect appears to be more noticeable at low effective normal stresses where more scatter in the slow measured residual strength in observed.

From these studies, although the rate effect mechanism on the residual strength has not sufficiently clarified yet, but their significance in earthquake engineering design is obviously considerable and some following hypotheses have been suggested:

- Changes in shear strength at increasing rates of shear displacement can be attributed to the changes in effective normal stress that are caused by shear-induced pore water pressure along the shear plane ([Skempton 1985](#))

- The negative rate effect only occurred when the sample developed a non-planar shear surface which bring about great opportunity for generating the pore water pressure within the shear surface ([Parathiras, 1995; Petley et al., 1999](#)).

- Changes in shear strength at increasing rates of shear displacement can be attributed to structural changes in the shear zone ([Tika et al. 1996](#)), and

- Changes in shear strength at increasing rates of shear displacement can be attributed an influence by changes in the test procedure ([Mohammad et al. 2013](#)).

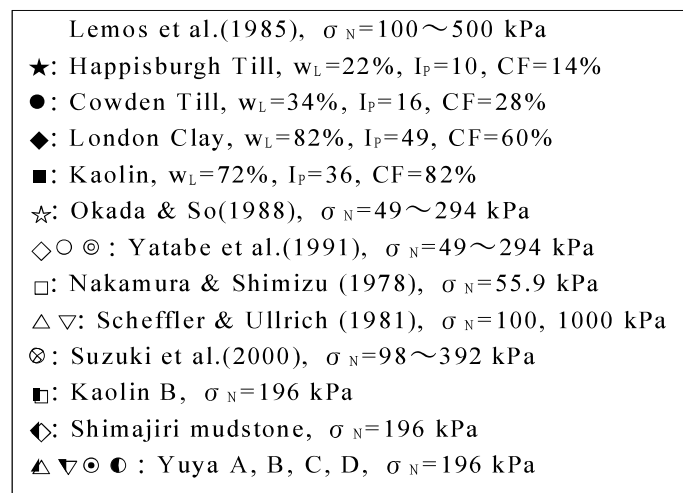
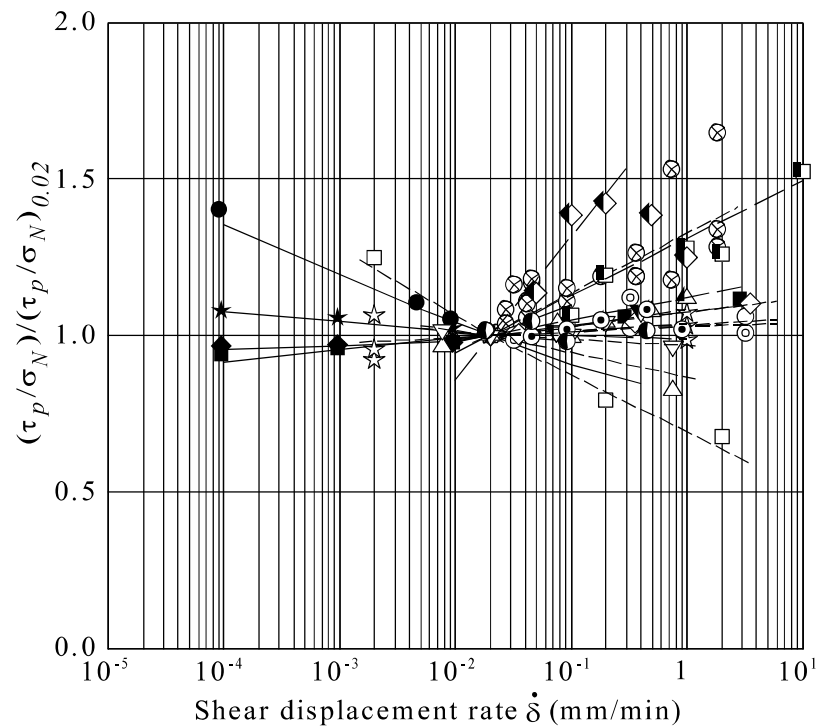


Figure 2. 13 Rate effect of residual strength observed in various soils (after Nakamura and Shimizu, 1978; Scheffler and Ullrich, 1981; Lemos et al., 1985; Okada and So, 1988; Yatabe et al. 1991; Suzuki et al., 2000; made by Prof. Suzuki)

2.1.6 Residual shear strengths of clays and its application to the evaluation of landslides stability

Based on the interpretation of torsional ring shear tests on clays, mudstones, shales, and claystones and the results of slope stability analyses, Stark et al. (2005) stated that

in stability analyses, an effective stress cohesion equal to zero should be used in residual shear strength conditions (pre-existing shear surfaces, e.g., old landslides, shear zones, slickensided surfaces, or fault gouges) because the particle bonds, structure, and stress history have been reduced or removed and the clay particles are oriented parallel to the direction of shear. Therefore, the residual shear strength is controlled by the frictional resistance of the face-to-face contacts of the oriented particles and should be represented by only a residual friction angle or a stress dependent failure envelope that passes through the origin. In first-time slide situations it is recommended that the effective stress cohesion be assigned a zero. The authors also recommended that the stress dependent failure envelope or a secant friction angle corresponding to the average effective normal stress on the slip surface be used in a stability analysis to model the effective stress dependent behavior of the residual and fully softened shear strengths.

Some recent researches shown that “healing” or “strength gain” is realized in time on preexisting slip surfaces at residual state. And shear stress required to reactivate a landslide is suggested to be larger than the drained residual shear strength determined using laboratory tests. [Bishop et al. \(1971\)](#) tested an undisturbed blue London clay specimen. After the test was ceased for two days to consider the capacity of “healing”, no gain strength was observed when shearing was restarted.

[Gibo et al. \(2002\)](#) investigated strength recovery in two specimens obtained from slip surfaces. Tests were performed on remolded normally consolidated specimen at effective normal stress ranging from 30 to 300 kPa using rest period of two days. They concluded that it is reasonable to consider the recovered strength in a stability analysis of a reactivated landslide dominated by silt and sand particles and at low effective normal stress less than 100 kPa.

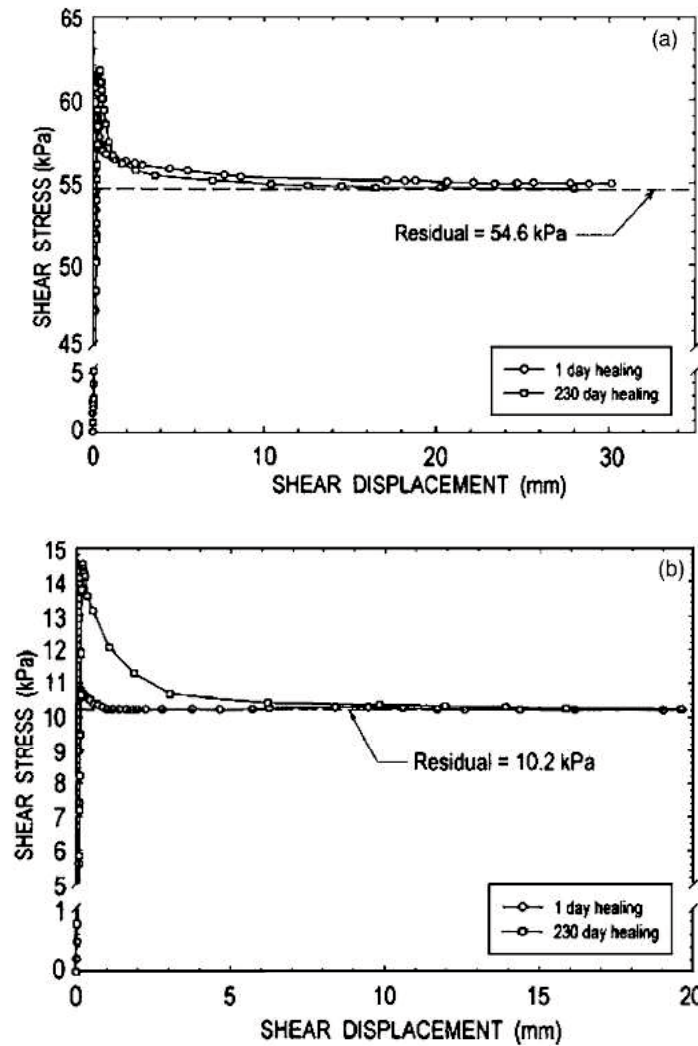


Figure 2.14 Reactivated shear strength versus displacement for different times of aging: (a) Duck Creek shale; (b) Otay bentonitic shale (Stark et al., 2005)

Stark et al. (2005) based on preliminary results of healing ring-shear tests indicate that preexisting shear surfaces may undergo healing or strength gain. After a 230-day aging, strength gain of 13% and 43% on soil samples of low plasticity ($PI = 12$, $AI = 0.63$) and high plasticity ($PI = 59$, $AI = 0.81$), respectively (Fig. 2.14). The magnitude of healing appears to increase with increasing soil plasticity, and this increase could have important implications for the size, timing, and cost of landslide remediation. The strength gain with time may be more important in high plasticity soil because of the large difference in the fully softened and residual shear strength of these materials and thus the large potential for strength gain. However, the strength gain due to healing appears to be lost after small shear displacement.

Carrubba and Del Fabbro (2008) conducted similar torsional ring shear tests as Stark et al. (2005) on Rosazzo (LL = 45%) and Montona (LL = 51%) flyschs from northern Italy, aging time of up to 30 days, and at normal stress of 25, 50, and 100 kPa. The results shown that the strength gains are about 20% for the Rosazzo and about 30% for the Montona. The strength gain at reactivation is greater for the Montona, which contains more silty-sandy particles. They also indicated that the strength gains in samples with remarkable percentage of fine fraction are lower than those recorded in samples with the same mineralogy but greater grain-size distribution.

Stark and Hussain (2010) also investigated the gain in strength along a preexisting shear surface with time. Tests were carried out on four natural clay soils with a range of plasticity (LL = 37%-112%), arrange of effective normal stress from 100 to 600 kPa, and rest periods of up to 90 days for all effective normal stresses and 300 days for an effective normal stress of 100 kPa. The researchers suggested that the mobilized shear strength is greater than the drained residual strength of the slip surface material. However, it is possible in shallow landslides or at shallower depths of a deep-seated landslide (depth of 5 m or less) and is negligible in deep-seated landslides with depths greater than 5 m. The observed recovered strength in ring and direct shear tests even at an effective normal stress of 100 kPa is lost with a small shear displacement and the benefit of this strength for the repair of shallow landslides or the shallower portion of a deep-seated landslide may not be economically significant. This leads to the conclusion that the observed strength gain has limited practical significance in the analysis and repair of landslides. However, the strength gain may be useful in explaining the behavior of shallow landslides, such as amount and rate of slope creep and stability prior to reactivation. This findings also are consistent with that of Hussain and Stark (2011) and Bhat et al. (2013).

Fig. 2.15 summarizes the test results presented by previous studies using the ratio between the drained recovered shear strength (τ_{rec}) and drained residual strength (τ_r) as a function of rest time. All soils exhibit a strength gain above the residual strength at effective normal stress of 100 kPa or less irrespective of different devices and test procedures.

In certain special field conditions, changes in a number of external factors may contribute to an increase in shearing resistance on a preexisting shear surface. The shear strength may increase as a result of penetration and reinforcing action of tree roots, especially in the case of shallow slip surfaces (e.g., thin colluviums). The shear strength of the shear zone may also increase as a result of chemical changes, including accumulation of salt especially in coastal areas, precipitation of carbonates and iron compounds, and exchange of lower valence to higher valence cations. For shallow landslides, suction resulting from drop of groundwater level below the slip surface is expected to temporarily increase shear strength. Ignoring suction in stability analyses is expected to lead to an underestimation of actual factor of safety. Severe desiccation and non-uniform swelling may also disrupt the slip surface and lead to a temporary increase in shear strength on preexisting shear surfaces (Mesri and Sarihan, 2012).

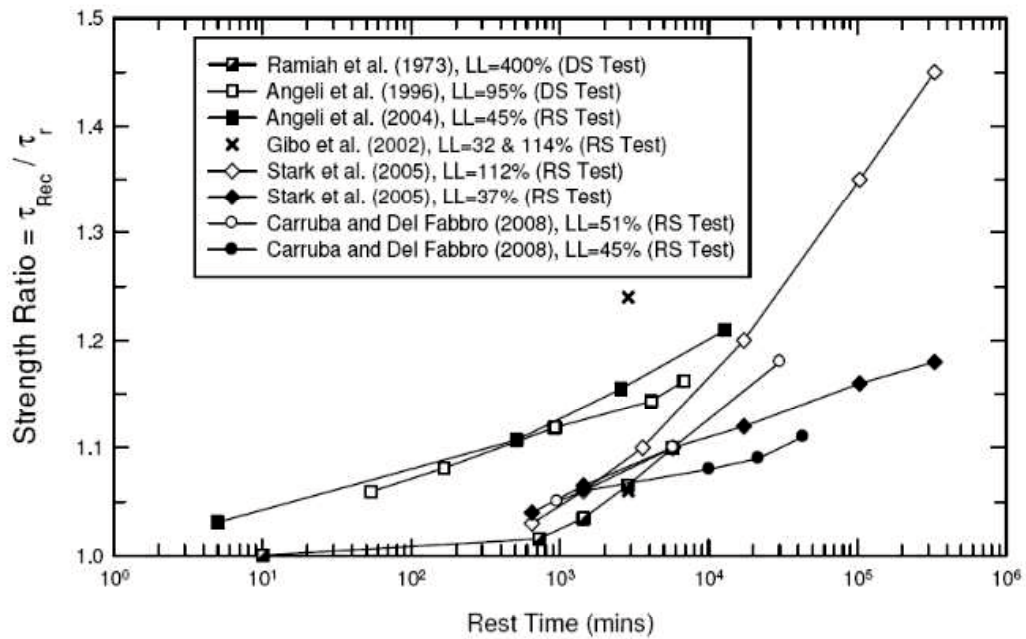


Figure 2. 15 Summary of published strength recovery test results for effective normal stress of 100 kPa or less (Stark, 2010)

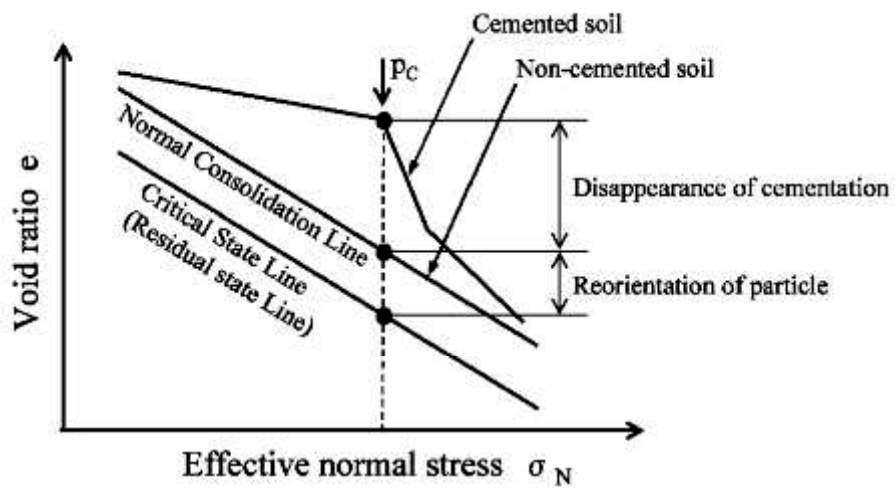
2.2 Characteristics of naturally cemented clay

An important feature of all naturally cemented clays is the bonding that takes place between particles as a result of diagenesis. This occurs because of carbonate

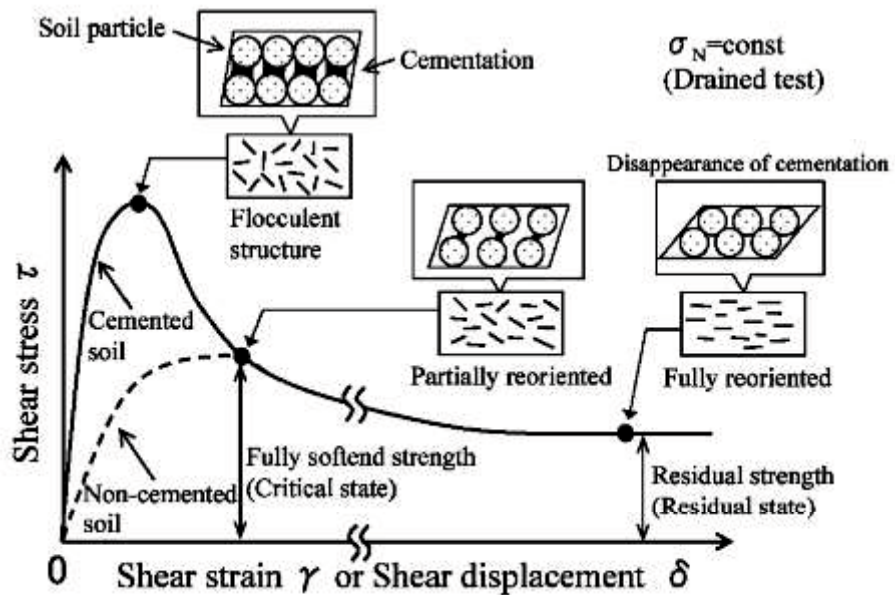
precipitation and the growth of carbonate crystals on the soil grains. Natural cementation increases the resistance of soil to deformation. Therefore, when the cementation is broken, failure will occur, accompanied by a significant magnitude and rate of subsequent deformation. There are many common mechanical characteristics amongst different types of cemented soils, such as yield stress, initial stiffness, peak strength, residual strength, and dilatancy. The “metastable” structure which is broken down with straining is usually attributed to relative weak cementation and bonding between the particles.

[Abramson et al. \(1996\)](#) stated that soils exhibiting progressive failure are clay and shale possessing chemical bonds that have gradually disintegrated by weathering. [Leroueil and Vaughan \(1990\)](#) revealed that the mechanical behaviours of naturally cemented soils such as claystone, sandstone, and weak rocks are similar, even when the cementation results from different causes. This finding also consistent with [Sangrey \(1972\)](#). Consequently, the artificially cemented clay samples are expected to simulate many of the characteristics of naturally cemented clays. The effects of bonding in artificial clays are only significant for stresses below an apparent pre-consolidation stress value. They are considered to be sensitive to stress changes and the duration of loading during testing.

According to the literature, the concept of aging often refers to the cementation of clays forming over many years. The mechanical behaviour of aged clay is characterized by three main factors: delayed compression and cementation over a long period of geological time, a consolidation yield stress higher than the effective overburden pressure, and “stress overshooting” in an e -log p relation ([Bjerrum, 1967](#)). According to [Suzuki et al. \(2007\)](#), the concept of residual strength for a cemented clay can be extended in terms of the disappearance of cementation, in addition to the reorientation of platy clay particles parallel to the direction of shearing. The drained shear and dilatancy behaviors of soils with and without the cementation that pass through the critical state and reach the residual state are schematically illustrated in [Fig. 2.16](#). It should be noted that slope failure and landslides involving such aged clays occurs frequently in many parts of the world. Thus, when considering the stability of a landslide slope consisting of naturally cemented clay such as mudstone, it is important to understand the residual strength characteristics of undisturbed soil samples having natural cementation.



(a) Relation between e and σ_N



(b) Relation between τ and γ (or δ)

Figure 2. 16 Schematic diagram showing one-dimensionally consolidation and drained shear behaviors in (a) void ratio and effective normal stress relation and (b) shear stress and shear strain relation for cemented and non-cemented soils, respectively

(Suzuki et al, 2007)

2.3 Residual strength characteristics of cemented clay soils

Mitchell (1993) stated that the engineering behaviour of the clay is governed by the inter-particle force fabric. When soft clay admixed with cementing agents, it would have a specific micro-fabric formed because the cement agents tend to cover the spacing between clusters and weld the fabric (Miura et al., 2001). Considering the undrained shear response, the resistance mobilized due to the cementation and fabric can take place simultaneously (Fig. 2.17).

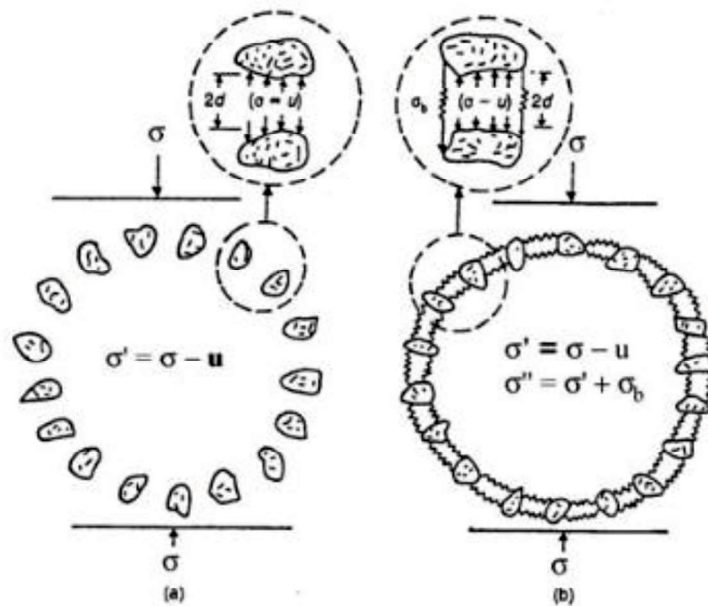


Figure 2. 17 (a) Microfabric of uncemented clay and (b) Structure of the induced cemented clay (Horpibulsuk et al., 2003)

Wissa et al. (1965) reported that the residual strength shows no effect from cementation and can be described by a single strength envelope that is independent of the amount of cementation. Fischer et al. (1978) stated that cemented Drammen clay behaves as a non-cemented clay with an OCR of about 1.7. Clough et al. (1981) concluded that the failure envelopes of both cemented and un-cemented sands are essentially straight lines with nearly the same slope. The cohesion intercept increases with increasing amount of cement and the friction angle is not affected by cementation.

Kasama et al. (2000) indicated that the failure envelope of cemented clay is parallel to that of non-cemented clay based on the results of a consolidated undrained triaxial compression test conducted on cemented Ariake clay. They also suggested a possible reason for different effects on the frictional strength is that cement mixing not only generates cementation between soil particles, but also supplies fine grains to the untreated soil through very fine particles in the cement agent. They also implied that the contribution from the cementation bond to the shear resistance is still available, even when the cementation bond was broken down during shear.

Recent results by Horpibulsuk et al. (2004, 2005) on two kinds of clay (Bangkok and Ariake clay) revealed that the failure envelope of the induced cemented clay is a single straight line for both pre- and post-yield states, which is different from that of uncemented clay. Furthermore, the role of the cement is mainly to increase the cohesion intercept with insignificant change in internal friction angle (Fig. 2.18). Sasanian and Newson (2014) also pointed out that the residual shear strength of cemented soil increases at a slower rate than peak strength increases, as a function of increasing curing time or cement content. It could be realized that a little literature have referred to the residual shear strength characteristics of cemented clay soils. Thus, a sufficiently explained mechanism at residual state of such kind of soils has not been elucidated up to present.

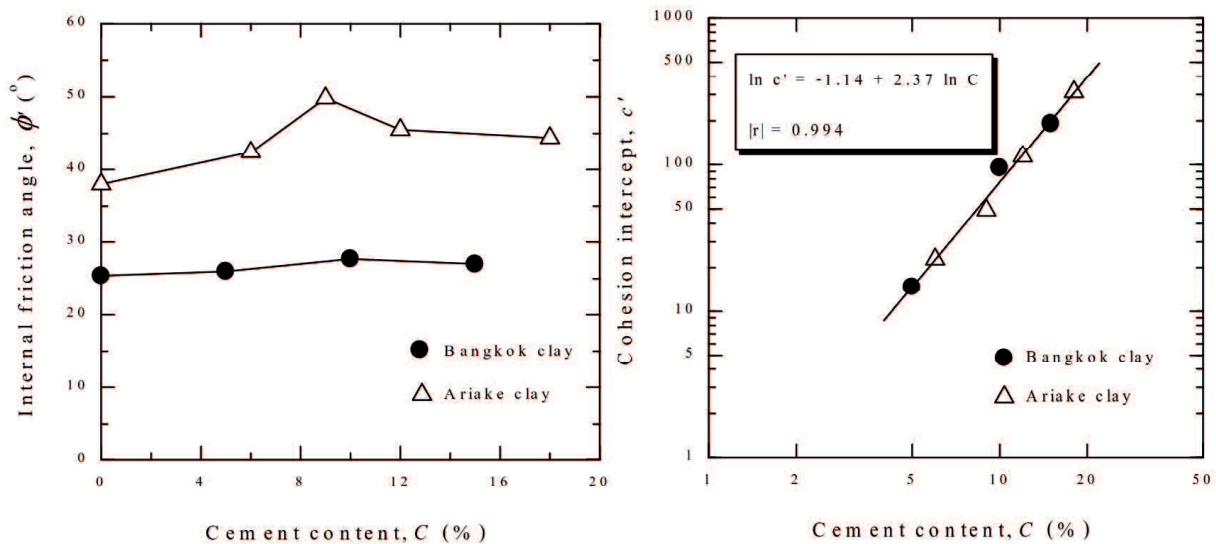


Figure 2. 18 Relationship between friction angle and cohesion intercept versus cement content of induced cemented Bangkok and Ariake clays (Horpibulsuk et al., 2005)

2.4 Multistage ring-shear test technique

Multistage test procedure can be performed on the ring-shear apparatus. Using this method, a single specimen is sheared to its residual state, changing the normal stress, and then shearing the same specimen to its residual state again. The acceptability of the multistage technique has been mainly based on test results for over-consolidated clays, which suggested that stress history has no effect on the measured residual strength.

For some very soft soils, continuously increasing normal stress in multistage test may result in the loss of soil through the gap between upper and lower confining ring during long shear displacement, that further contributing to the drawback of multistage ring-shear technique. Bromhead (1979) stated that it is quite important to allow time enough to a very soft sample, which being consolidated under an consecutively increasing level of loading, to avoid the excessive loss of soil through the gap between two halves. Thus, the multistage ring-shear test should only be carried out with a limit number of stages, corresponding to a number of normal stresses, to obtain the more effective results.

The multistage ring-shear testing (MRST) technique has been used by many researchers in the past for determining shear strength parameters of various types of soils, for instances, Lupini et al. (1981), Anderson and Hammoud (1988), Tika et al. (1996), Harris and Watson (1997). Bishop et al. (1971) show that residual strength is independent of stress history, i.e. loading sequence in multistage tests, because a unique curve exists for τ/σ_N values dependent only on the magnitude of normal stress.

Anderson and Hammoud (1988) stated that this technique is satisfactory for clays exhibiting turbulent or transitional shearing mode, that is, soils with a percentage of clay particles less than 50%. If soils contain more than 50% clay particles, they will exhibit a sliding mode of shearing and different results are likely to be obtained from multiage and single-stage tests. This conclusion not only because of the inaccurate values of residual strength obtained from multistage test, but also because the brittleness of the clay, which may be an important parameter in evaluating the engineering behavior.

Tiwari and Marui (2004) used the MRST technique on five variation kinds of natural soils, which all showed similar effective residual internal friction angle

irrespective of testing method. They also concluded that multistage technique provides objective oriented quick shear testing as the shear strength for various displacement ranges can be measured. [Harris and Watson \(1997\)](#) recommended the use of a multistage test as an optimal procedure for ring-shear test, particularly for those using the Bromhead ring-shear apparatus, by which resulted in a value for the drained residual shear strength within three working days. They also obtained the residual shear strength values to be considered close to those derived from back analyses of slope failures.

2.5 Cyclic degradation in clay in dynamic ring-shear test device

According to the literature, many researches have been conducted to investigate the cyclic behavior of soils based on cyclic triaxial and cyclic simple shear tests. Another group of studies have been performed on dynamic ring-shear apparatus. As a result, the available results have provided a great deal of dynamic response of clayey soils. For instances, [Osipov et al. \(1984\)](#) investigated the microfabric of clayey soil by means of a scanning electron microscope (SEM) before, during, and after cyclic loading. They concluded that soil microstructure was not ruptured by vibration during the shear process; rather, disruption of some structural bonds was followed by their rapid restoration, and overall microstructure remained intact. [Mortezaie et al \(2013\)](#), [Soralump et al. \(2016\)](#) stated that clay soil with higher over-consolidation ratio and plasticity index exhibit a small degradation in cyclic strength ([Fig. 2.19](#)). In addition, they also suggested that the cyclic pore water pressure build up may not be a dominant contributor to the cyclic degradation of normally consolidated clays ([Matasovic and Vucetic, 1995](#)). [Proctor and Khaffaf \(1985\)](#) observed that no significant variation in the effect of frequency with respect to the number of cycles. As stated by [Yasuhara et al. \(1982\)](#), in repeated or dynamic shear test in laboratory, frequency should be identified as an additional factor influencing the mechanical property of clay. Furthermore, it is evident that the strength and deformation properties of contact surface between different soil layers during static and dynamic loading remains to be clarified ([Sassa et al., 1995](#); [Onoue et al., 2006](#); [Wakai et al., 2010](#)).

Cemented clays generally have the low permeability by which an excess positive pore pressure is likely to be generated under cyclic loading and consequently the shear resistance gets reduced. Further, the presence of cementing agents can cause the

complication of the material behavior. The structure of clays is characterized as a combination of fabric and bonding. Naturally cemented clays were formed over long periods of time because of diagenesis as a result of precipitation of cementing agents in marine and arid environments, weathering, or by long-term crystal growth between grains (Sangrey, 1972). The presence of the discontinuity bedding planes on slopes consisting of naturally cemented clay soils is found in many areas due to previous movement caused by landslides or tectonic forces. Nevertheless, to date, relatively little literature has been published on the effect of dynamic loading on pre-existing shear surface of soil, especially cemented clayey soil. Additionally, the cyclic degradation of cemented clayey soil carried out by a dynamic ring-shear test has never been published. Consequently, the primary objective of this research is to evaluate the change degree of the cyclic degradation of lightly cemented kaolin clay that model actual behaviors of new or pre-existing slip surfaces of soil, as well as contribute the more deeply understanding to a largely unexplored area.

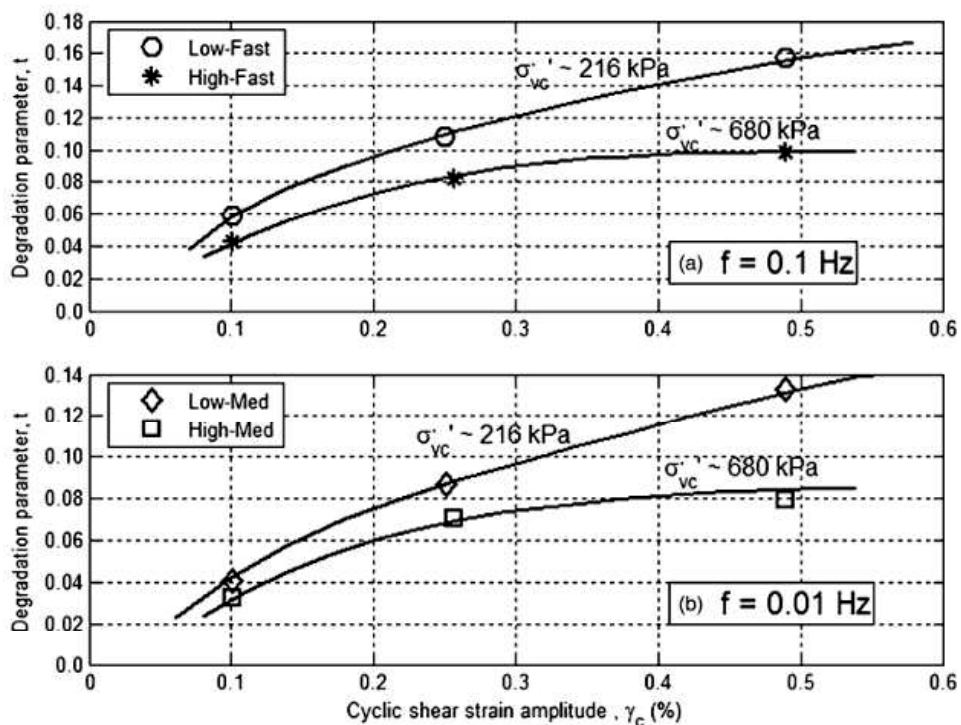


Figure 2. 19 The effect of vertical consolidation on cyclic degradation for two samples of kaolin (Mortezaie et al 2013)

2.6 Review of typical earthquake-induced landslides occurring along the bedding plane in Japan

Earthquake-induced landslides, which are usually found along the bedding plane of alternating beds of different kinds of deposit, are common phenomena in Japan. The 2004 Mid-Niigata Prefecture earthquake (M6.8) triggered 362 landslides more than 50 m wide, and 12 large-scale landslides of more than one million cubic meters, and the total volume of all landslides was about one hundred million cubic meters ([Ministry of Land, Infrastructure and Transport 2004](#)). The landslides was found to be occurred on the boundary between weathered mudstone and un-weathered mudstone. The characteristics of weathering of mudstone in mountainous areas in central Japan described and discuss by [Chigira \(1990\)](#), who also stated that the weathering of mudstone is affected by the presence of the other rock, such as sandstone, conglomerate, and coal, when it intercalates in these rocks. [Figs. 2.20, 2.21, and 2.22](#) show some earthquake-induced landslides occurring along the bedding plane of alternating beds of different kinds of deposit in Japan.



Figure 2. 20 Landslide dam in the 2004 Niigata Prefecture Chuetsu Earthquake (taken by Prof. [Suzuki](#))



Figure 2. 21 Bedrock Sliding Tuffaceous sandstone on slip surface at Yokowatashi in Nagaoka city (taken by Prof. [Suzuki](#))



Figure 2. 22 Large-scale landslide in the 2004 Niigata Prefecture Chuetsu Earthquake (taken by Prof. [Suzuki](#))

It is revealed that planar sliding surfaces seem to be essentially for the generation of landslides triggered by this earthquake. Planar bedding-parallel sliding surfaces were formed at the boundary between the overlying permeable sandstone and underlying siltstone or along the bedding planes of alternating beds of sandstone and siltstone, and they typically resulted in from the reactivation of parts of previous landslides (Chigara and Yagi, 2006; Wang et al., 2007).

Beside, reactivation of weathered mudstone slides was investigated which included the Aburao, Tanesuhara, and Mitsumine landslides. The surface morphology of these landslides showed ductile deformation with fewer large open cracks, occasionally between mudstone and weathered mudstone.

An investigation conducted by Sassa et al. (2005) at two large-scale rapid landslides (Higashi Takezawa and Terano) after the 2004 Mid-Niigata prefecture earthquake revealed that previous landslides in both areas probably occurred at the sliding surface in the weathered part of silt just below the sand layer; however the rapid landslides triggered by the mid-Niigata earthquake formed their sliding surface within the sand layer.

In the case of the 2007 Mid-Niigata offshore earthquake, Has and Nozaki (2014) referred the significance of bedding plane as a sliding surface. Slopes consisted of alternating beds of sandstone and siltstone are easily sheared along bedding plane because of weak surface strength. This also support important role of bedding plane in controlling both the landslide mechanism and activity.

A case study of reactivated landslides which occurred in Hyogo Prefecture (“Kuchi-Otani landslide) was investigated by Grachev et al. (2005). The landslide was reactivated in 2003 with approximate 1.5 million m³ of landmass at an estimated rate of about 1 mm per month. According to the data obtained by borehole’s inclinometers, the sliding surface is located near the boundary of stiff black mudstone and soft silty clay (Fig. 23).

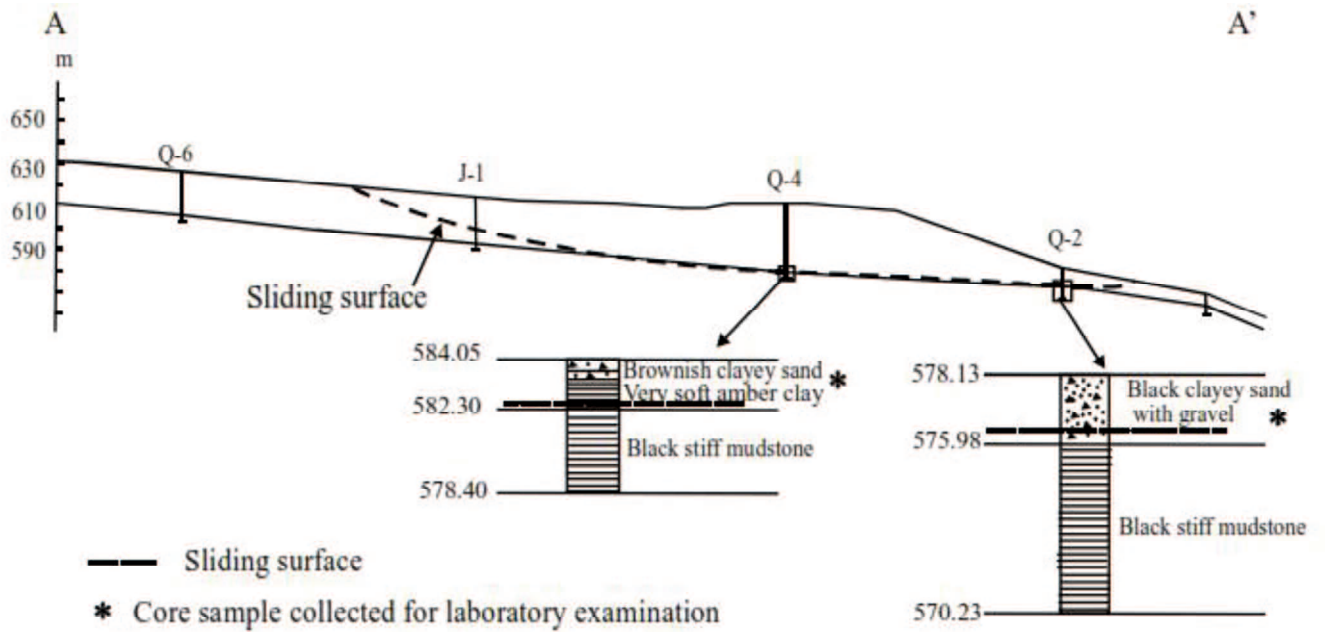


Figure 2. 23 A cross section of “Kuchi-Otani” landslide (Grachev et al. (2005))

Tiwari et al. (2005) conducted a study focusing on the residual strength of weathered mudstone for six landslides in the Niigata Prefecture of Japan. All landslides are located within a radius of about 6 km, and have similar geologic, geohydrology, and climatic conditions. A representative geologic profile of the Iwagami landslide area is shown in Fig. 2.24 indicates that the sliding surfaces of all the landslides are located at the contact between highly weathered and less weathered tertiary black mudstone layers. The shear zones are composed of 0.2-0.45 m thick clayey soil, formed due to crushing and weathering of mudstone during the shearing process.

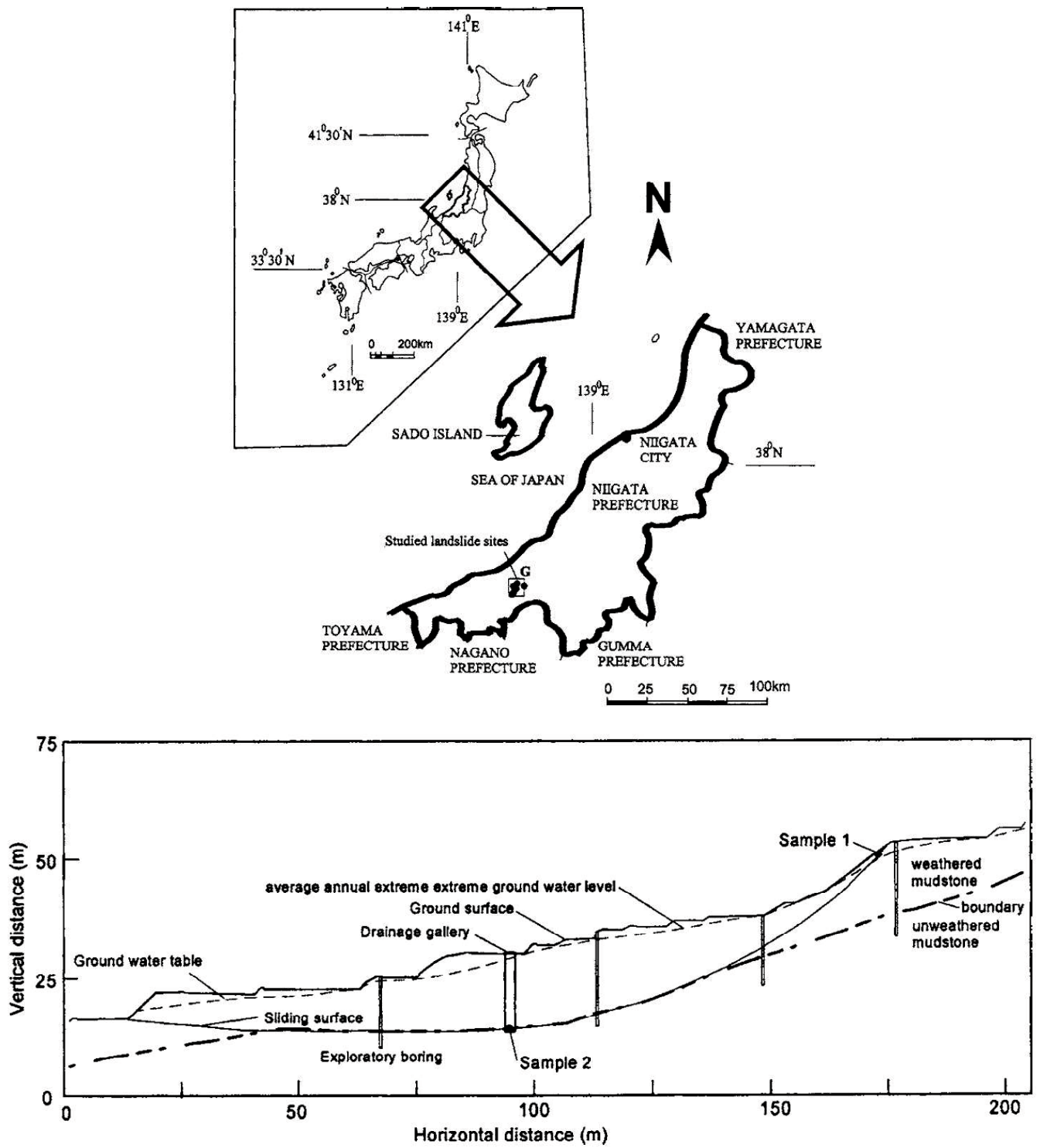


Figure 2. 24 Geographic location and cross section of Iwagami landslide (Tiwari et al., 2005)

Chapter 3 EXPERIMENTAL TESTING PROGRAMME

3.1 Introduction

Residual strength parameters are usually determined using a ring-shear apparatus. Based on previous researches, approximately comparable values of residual strength were found using various types of laboratory shear device and testing procedure (La Gatta, 1970; Bishop et al., 1971; Townsend and Gilbert, 1973; 1976; Sassa et al., 2003, 2004). The simplicity, convenience, less cost, and requirement of less sample volume are the main characteristics of the Bromhead ring shear apparatus, developed by Bromhead (1979), which that has brought about it being popularly used for commercial testing. The results obtained from this device on both remolded and undisturbed samples are consistent with those from much more sophisticated equipment. Conversely, the main factor affecting the measured residual strength is the magnitude of the wall friction that is developed along the inner and outer circumferences of the confined specimen (Bromhead, 1986; Stark and Vettel, 1992; Meehan et al., 2007).

At present, the reversal direct shear test is widely used to measure the drained residual strength of clays and clay shales even though it has several limitations. The primary limitation is that the soil is sheared forward and then backward until a minimum shear resistance is measured. Each reversal of the shear box results in a displacement that is usually less than 0.5 cm. As a result, the specimen is not subjected to continuous shear deformation in one direction, and thus a full orientation of the clay particles parallel to the direction of shear may not be obtained (Stark and Eid, 1994). In addition, the cross sectional area of the specimen is changing during shear, arising high local concentrations of strain, and a substantial amount of soil is usually extruded out of the exposed shear plane during the test. These limitations result in residual strength that is higher than the residual values obtained from ring-shear devices (Bromhead, 1979; Stark and Eid, 1994). The main advantages of the this device would appear to be the ready availability of suitable equipment, the simple method of operation, and the short drainage path which results in short time tests. Stark et al. (1992) stated that a ring shear apparatus and remolded specimens be used to estimate the field residual strength. In

contrast, a reversal direct shear was not recommended to measure the field residual strength on remolded, not precut specimens.

The ring-shear apparatus was developed specifically for the purpose of determining residual strength. The advantages and disadvantages of most ring-shear devices constructed prior to 1971 are reviewed by [Bishop et al. \(1971\)](#). The major advantages of the ring shear test are followed:

- The sample is sheared continuously in one direction for any magnitude of displacement without uninterrupted shear process. This allows clay particles of an intact, remoulded specimens to be oriented parallel to the direction of the shear and the development of a residual strength condition.
- The cross sectional area of the shear plane is constant during shear. Uniform stress and strain conditions along the shear plane are desirable for reliable interpretation of results.
- Because of thinner sample, process of shearing could be conducted at faster shear rate.
- Less laboratory supervision is required.

However, like any other testing device, the ring shear apparatus has some issues and limitations accompanying with it. That includes non-uniform stress and strain distributions, soil extrusion, difficult undrained testing procedure, wall friction, and the effect of varying stress around the edges of the sample during shearing are difficult to access.

3.2 Monotonic ring-shear apparatus

[Figs. 3.1, 3.2 and 3.3](#) show the test apparatus, which has basically the same principle as the Bishop-type apparatus ([Bishop et al., 1971](#)). The ring-shaped specimen has an inner diameter of 6 cm, an outer diameter of 10 cm, and a wall thickness of 2 cm ([Fig. 3.4](#)). The dimensions of the ring-shear device result in a ratio of outer to inner ring diameters of 1.7. [Table 3.1](#) provides the features of ring-shear apparatus from Universities and Institutes, compared with the device used in this study. The specimen was subjected to shear forces at a height of 1 cm above the base plate. During testing,

the shear stress, normal stress, frictional force, and vertical displacement were all measured and automatically recorded. The frictional force along the perimeter of the rings, which was generated by vertical displacement of the specimen, was measured with a load cell attached to the loading frame via a linking yoke connected to the upper ring (Suzuki et al., 1997). This feature is very essential for the ring-shear apparatus because it ensure to measure the total normal stress acting on the soil specimen with high accuracy. In this apparatus, the load-receiving plate did not rotate, but was instead supported using a ball bearing to prevent deviation from the normal force. In this test, the net normal stress acting on the shear surface was calculated based on the measured frictional force.

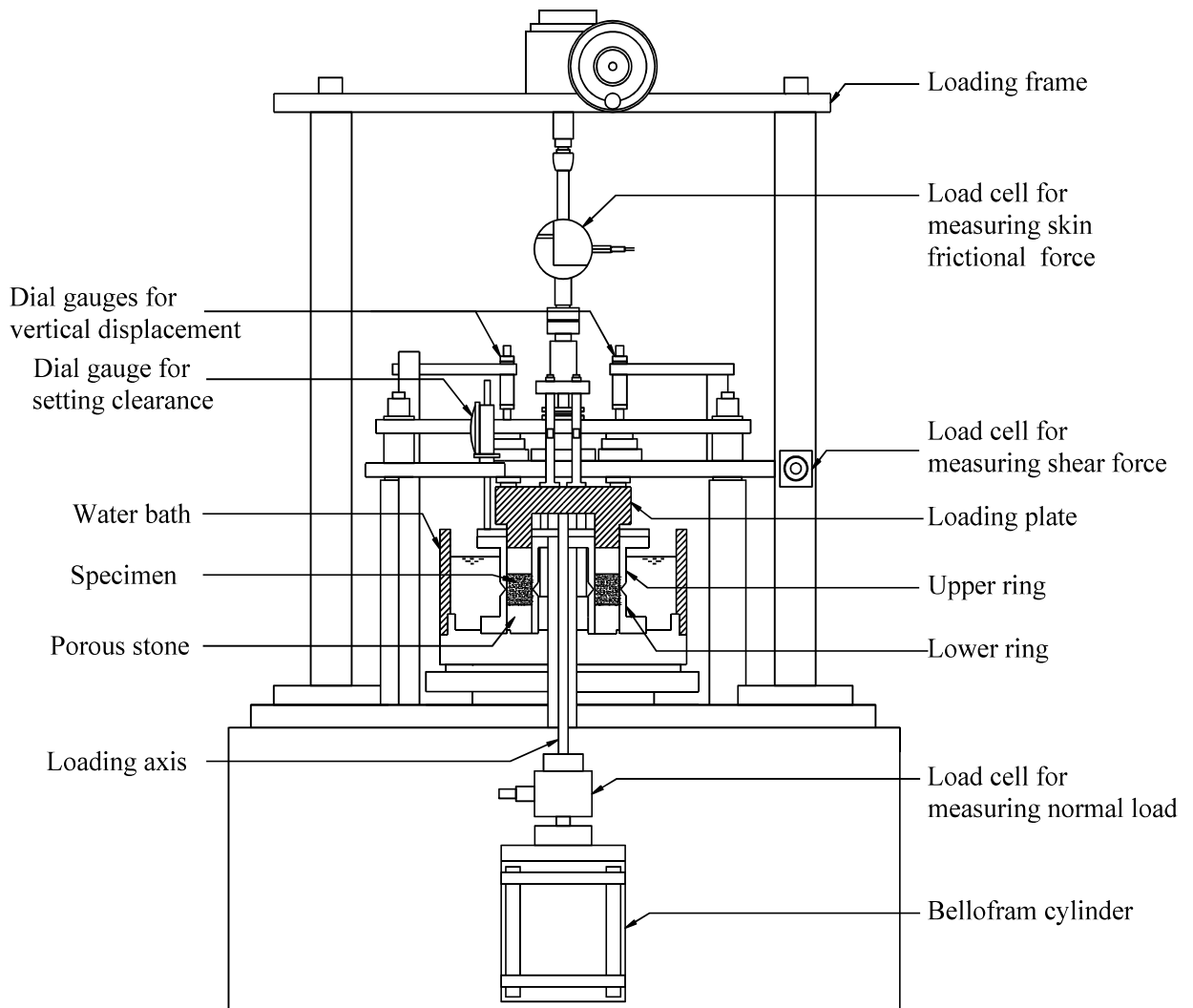


Figure 3.1 Essential features of ring-shear test apparatus.



Figure 3.2 Front view of ring shear-test apparatus

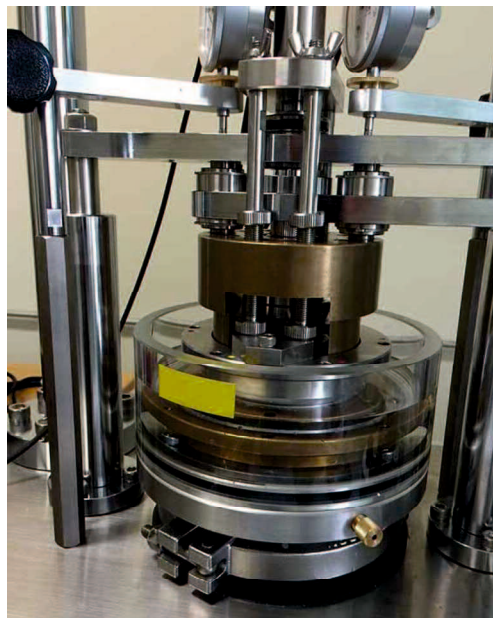


Figure 3.3 Shear box containing test sample

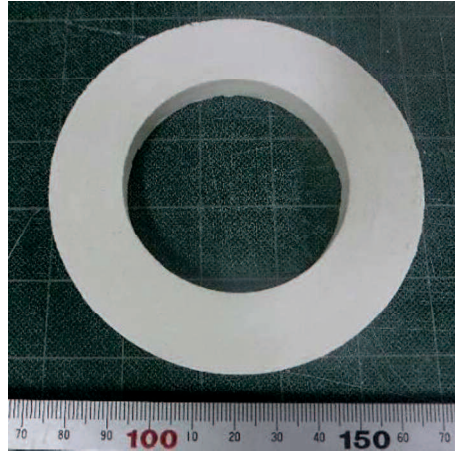


Figure 3. 4 A typical testing specimen for monotonic ring-shear test

Table 3. 1 Features of ring-shear apparatus from Universities and Institutes, compared with the device used in this study (summarized by Prof. Suzuki)

Researcher	Research organization	Outer diameter r_o (cm)	Inner diameter r_i (cm)	r_i/r_o	Annulus thickness h (cm)	h/r_o	Height (cm)
Suzuki et al.	Shinshu Univ.	10	6	0.6	2	0.2	2
Umezaki et al.	Shinshu Univ.	7	4.2	0.6	1.4	0.2	2
Ogawa et al.	Nagaoka Univ.	15	10	0.67	2.5	0.17	2
Yatabe et al.	Ehime Univ. of Technology	16	10	0.67	3	0.19	2
		10	8	0.8	1	0.1	1
Nakamura et al.	Tokyo Univ. of Agriculture and Technology	12	6	0.5	3	0.25	3
Kamai et al.	Nihon Univ.	12	8	0.67	2	0.17	2
Sassa et al.	Kyoto Univ.	35	25	0.71	5	0.14	-
Yamashita et al.	Aratani Civil Engineering Consultants	21.5	10	0.47	5.75	0.27	2
Gibo et al.	Ryukyu Univ.	10	6	0.6	2	0.2	3
Yoshimi et al.	Tokyo Institute of Technology	26.6	21.4	0.8	2.6	0.1	2.7
Yasuda et al.	Tokyo Denki Univ.	15	10	0.67	2.5	0.17	2.5
Nakamura	Public Works Research Institute	25	17	0.68	4	0.16	0.9-1.9
		22	15	0.68	4	0.16	0.9-1.9
		15	10	0.67	4	0.16	0.9-1.9
Bishop et al	London Univ.	15.24	10.16	0.67	2.54	0.17	1.91
La Gatta	Harvard Univ.	7.12	5.08	0.71	1.02	0.14	0.2-0.25
Scheffler et al.	Leipzig Institute of Technology	9.4	4.96	0.53	2.22	0.24	1.6
Bucher	Swiss Federal Institute of Technology	24	16	0.67	4	0.17	1.6
Bromhead	Kingston Univ.	10	7	0.7	1.5	0.15	0.5
Stark et al.	Illinois Univ.	10	7	0.7	1.5	0.15	1
Suzuki et al.	Yamaguchi Univ.	10	6	2	2	0.2	2

3.3 Dynamic ring shear apparatus

A consolidation-constant volume cyclic loading ring-shear test apparatus was used to obtain the purpose of the study. For common undrained cyclic loading ring-shear tests, shear-torque-controlled (STC) and shear-displacement-controlled (SDC) methods are often used to apply the cyclic loading. The testing device used in this investigation is a kind of shear-torque-controlled method. Figs 3.5, 3.6, and 3.7 show the test apparatus. This cyclic shear machine consists of a cyclic ring-shear test apparatus and pneumatic servo controller, two bellofram cylinders, constant volume-control device, dynamic strain data logger, and personal computer for data recording. The ring-shaped specimens had an inner diameter of 4.2 cm, an outer diameter of 7 cm, and a wall thickness of 2 cm (Fig. 3.8). The area of shear surface is approximately 24.63 cm². The maximum shear speed in the center of sample is 10 cm/s, maximum frequency of cyclic loading is 5 Hz, and the maximum rate of data recording is 200 readings/s. Table 3.2 provides the features of some previous dynamic ring-shear apparatus in comparison to the device used in this study.

The specimen is sheared by rotating the lower haft of the shear box in both direction, while the upper haft of the shear box is restrained by two resistance transducers, from which shear resistance is measured. During testing, the cyclic shear resistance, τ_{cN} , vertical consolidation stress, σ_N , frictional force, horizontal displacement, δ , and vertical displacement, v , were all measured and automatically recorded. It is noted that the pore water pressure was not measured in this device. The normal load on the failure plane is calculated by subtracting the side friction on the upper confining rings from the total applied normal stress. Shear forces developed across the failure plane during testing are transferred through the upper confining rings and loading platen to the moment-transfer arms. A pair of force transducers measure the moment carried by the moment transfer arms.

The most essential limitation of this device is that it is impossible for the pore water pressure to be measured. This leads to the lack in the evaluation of cyclic strength characteristics of cemented clay soil. In addition, dimension of specimen is smaller than that in the monotonic ring-shear test, which bring out an insufficient comparison between monotonic and dynamic ring-shear strength. This comparison is very necessary

in this study. Furthermore, it is difficult to measure the peak cyclic strength in early few cycles of shear stage due to bellowram cylinder and pneumatic servo controller. Consequently, only main cyclic degradation parameter is evaluated in relevant subsequent chapter.

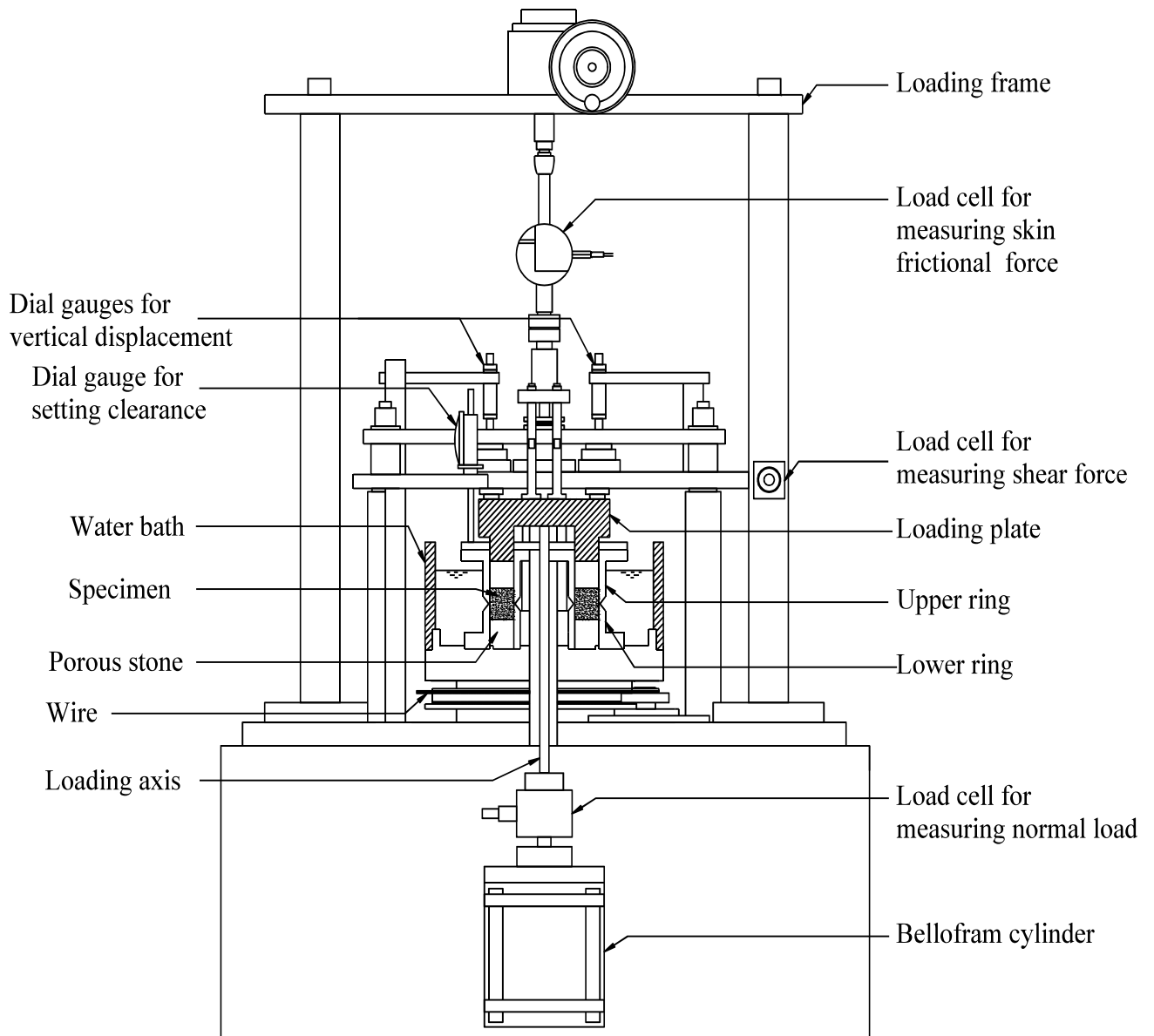


Figure 3. 5 Essential features of consolidation-constant volume cyclic loading ring-shear apparatus.

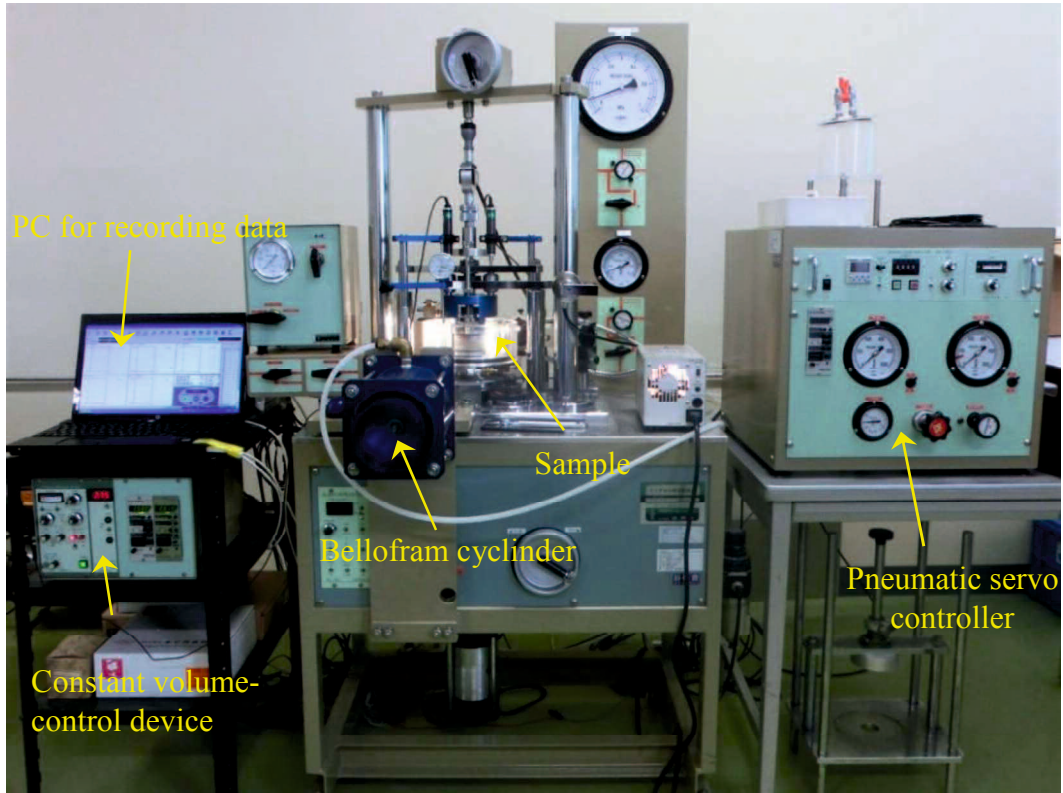


Figure 3. 6 Front view of consolidation-constant volume cyclic loading ring-shear apparatus.



Figure 3. 7 Shear box containing test sample

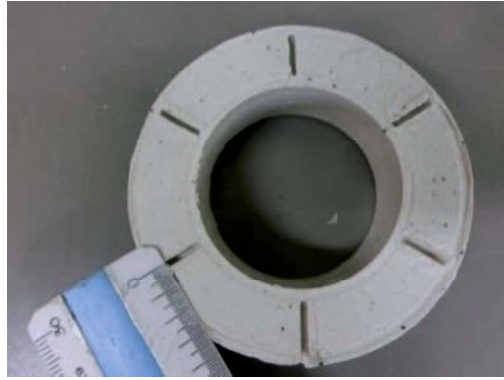


Figure 3. 8 A typical testing specimen for dynamic ring-shear test

Table 3. 2 Features of previous dynamic ring-shear apparatus, compared with the device used in this study

Authors	Bishop et al. (1971)	Hungr and Morgenstern (1984)	Tika (1989)	Garga and Sendano (2002)	Sassa (1992) DPRI-3	Sassa (1996) DPRI-4	Sassa (1997) DPRI-5	Sassa (1997) DPRI-6	Sassa (2004) DPRI-7	This study
Shear box										
Inner diameter (cm)	10.16	22	10.16	9.2	21	21	12	25	27	4.2
Outer diameter (cm)	15.24	30	15.24	13.3	31	29	18	35	35	7
Max. height of sample	1.9	2	1.9	2	9	9.5	11.5	15	11.5	2
Ratio of max. height/width	0.75	0.5	0.75	0.98	1.8	2.38	3.83	3	2.88	
Shear area (cm ²)	101.34	326.73	101.34	72.45	408.41	314.16	141.37	471.24	389.56	24.63
Max. normal stress	980	200	980	660	500	3000	2000	3000	500	980
Max. shear speed (cm/s)	-	100	9.33	-	30	18	10	224	300	10
Cyclic torque control testing (max)	No	No	No	No	0.5 Hz	5 Hz	5 Hz	5 Hz	5 Hz	5 Hz
Undrained testing and pore pressure monitoring	No	No	No	No	Yes	Yes	Yes	Yes	Yes	No
Max. data acquisition rate (reading/sec)	-	-	10	-	12	200	200	200	1000	200

3.4 Material and Specimen

Soil samples used in this study were a common type of commercially available kaolin from Japan. They were obtained in powdered form to ensure purity and uniformity. In addition, ordinary Portland cement (OPC) was used as the cementation agent for preparing artificially cemented samples. As described below, the amount of cement was defined as the percentage of the dry weight of the OPC to clay sample. Nine sample types were used for monotonic ring-shear tests, namely: kaolin only (0% cemented kaolin), 2% cemented kaolin, 4% cemented kaolin (as a normal specimen), and combinations of 0% and 0% cemented kaolin, 0% and 2% cemented kaolin, 0% and 4% cemented kaolin, 2% and 2% cemented kaolin, 2% and 4% cemented kaolin and 4% and 4% cemented kaolin as combined specimens. For convenience, these nine sample types were referred to as “0% cement”, “2% cement”, “4% cement”, “0% + 0% cement”, “0% + 2% cement”, “0% + 4% cement”, “2% + 2% cement”, “2% + 4% cement” and “4% + 4% cement”, respectively.

Table 3. 3 Physical properties of kaolin and cemented kaolin clay

Properties	Sample	Characteristic values
Liquid limit (%)	Kaolin	62
Plasticity index		21.8
Clay fraction (%)		35.3
Soil particle density (g/cm ³)	Kaolin	2.618
	Kaolin + 2% cement	2.620
	Kaolin + 4% cement	2.621

Four sample types: 0%, 4%, 4%+2%, and 4%+0% were chosen for multistage ring-shear tests; and four sample types: 0%, 2%, 2%+2%, and 0%+2% for dynamic ring-shear tests, respectively. Their physical properties are given in [Table 3.3](#). These combinations of cement kaolin samples are given in [Table 3.4](#) and simultaneously exhibited in [Fig. 3.9](#). In this study, the cement content added to kaolin was mainly determined on the basis of the value of the hardness of the soil measured at a landslide slope site in the Mid Niigata Prefecture earthquake. The strength of the cemented soil itself is similar to that of the in-situ soil to some extent. As mentioned above, earthquake-induced landslides occurred along the bedding plane as a slip surface. When the strength

of the soil has a discontinuity such as that of the bedding plane, the influence of the discontinuity on the stability of the landslide slope can be assessed quantitatively.

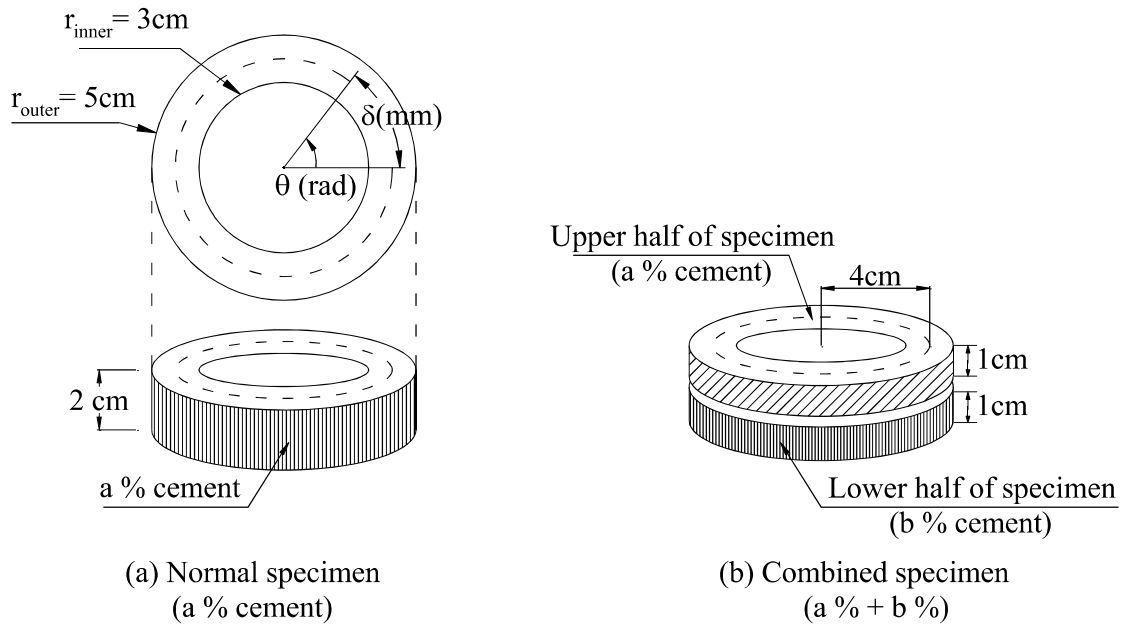


Figure 3. 9 Basic features of normal and combined specimens.

Table 3. 4 Types of combination for combined-cement kaolin samples.

Sample	Sample types	Types of combination	
		Upper half	Lower half
Combined specimen	0% + 0% cement	0% cement	0% cement
	0% + 2% cement	0% cement	2% cement
	0% + 4% cement	0% cement	4% cement
	2% + 2% cement	2% cement	2% cement
	2% + 4% cement	2% cement	4% cement
	4% + 4% cement	4% cement	4% cement

3.5 Preparation of normal and combined specimens

For any laboratory test conducted with artificially cemented samples, the reproducibility of the procedure is essential to the measured test results. Flow chart showing the test procedure is exhibited in Fig. 3.10. In this study, kaolin clay was first mixed with distilled water at approximately twice the liquid limit of kaolin, which is the optimum water content required to produce lightweight cemented clay commonly used in the laboratory, in order to produce a workable homogeneous state. Mixing was

accomplished using an electric mixer fitted with a paddle-type mixing blade for approximately 5 min until a homogeneous mixture was achieved. After that, OPC was added, in amounts of 2% or 4% of the dry mass of the clay, and the resulting slurry was mixed again to ensure homogenization of the sample. The uniform paste, which had suitable workability, was transferred using a spoon into a double-draining consolidation tank of 150 mm in diameter and 300 mm in height. The inside of the consolidation tank was highly polished and coated with a thin layer of vacuum grease to minimize friction between the tank and clay. Soaked circular filter papers were placed on the top and bottom of the consolidated sample. Prior to consolidation, a vacuum of about 98 kPa was applied to the tank, purging air bubbles trapped inside the slurry to prevent air entrapment (Fig. 3.11).

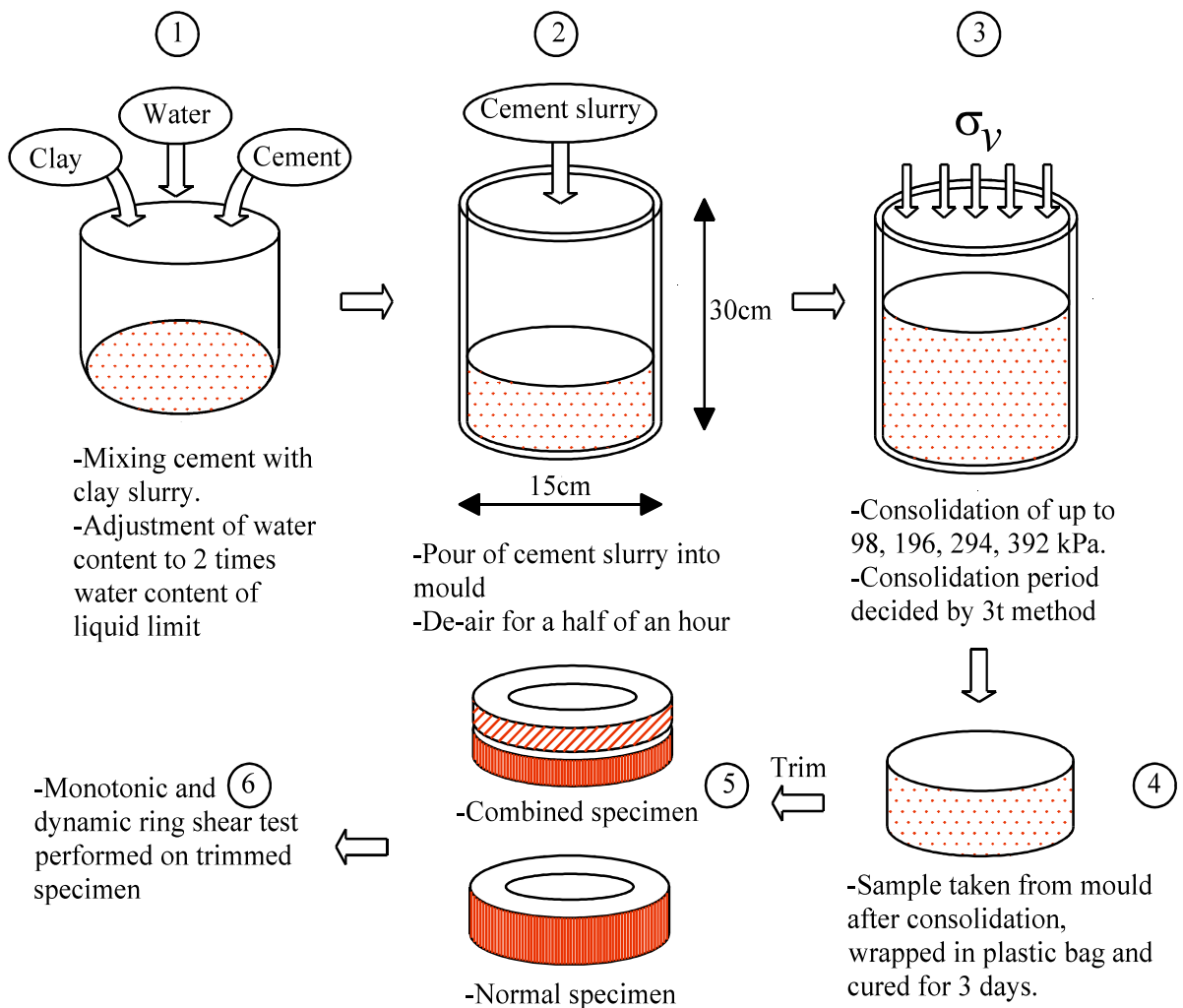


Figure 3. 10 Flow chart shows test procedure

Each sample was normally consolidated under a constant consolidation pressure until the end of primary consolidation was confirmed using a check based on the $3t$ method. The cylindrical samples were unloaded, wrapped in plastic bags to avoid significant variation of moisture content, and stored in a humidity chamber of constant temperature (20 ± 2 °C). To simulate cementation in natural cemented clay soils as best as possible, all samples were left to cure for 3 days. In addition, to investigate the effects of curing time on mechanical characteristics, the 2% and 4% cemented kaolin samples were cured for an additional 7, 14, and 28 days.



Figure 3. 11 Soil specimen in process of pre-consolidation



Figure 3. 12 A soil specimen in process of trimming



Figure 3. 13 Removing the inside soil core to make an annular specimen



Figure 3. 14 Completing specimen before transferring to the shear box



Figure 3. 15 Transferring a soil specimen to the shear box



Figure 3. 16 Final setting before ring shear test

Two types of specimens, normal and combined specimens, were tested in this study. A ring-shaped specimen was produced from the pre-consolidated and cured samples using a cutting tool. Two types of cutter rings with different heights of 1 cm and 2 cm were used for producing the combined and normal specimens, respectively. The sides of the cutting tool were coated with silicon grease to minimize side friction while sectioning. Considerable care was taken while setting up specimens because of the fragility of the cemented samples. Finally, the specimens were transferred to the ring shear apparatus (Fig. 3.12 to 3.16). Two stages were required to produce the combined specimens. First, one cutting tool with height of 1 cm was used to procure ring-shaped specimens having a 10 cm outer diameter, 6 cm inner diameter, and 1 cm height. Second, these specimens were transferred to a lower part of the ring shear box where they were

bonded to a second specimen having the same dimensions and composition to create a complete combined specimen. These procedure also are similar to that adopting for combined sample in dynamic ring-shear test. The only difference was the dimension of the sample.

3.6 Preparation of over-consolidation samples

In this study, the over-consolidated non-cemented and cemented kaolin samples were carried out in dynamic ring-shear tests. In order to create consolidation conditions, the sample was first reconsolidated at a given re-consolidation pressure until there was no change in the sample volume for approximately more than 1 hour. Afterward, the vertical load was decreased to a lower normal stress to achieve the expected over-consolidation state. The dynamic ring-shear test only was carried out when the vertical settlement of the soil sample became stable again under the new vertical load pressure.

Considering that the cemented clay soil could have suffered different stresses histories, here two series of tests were performed on 0% and 2% cemented kaolin samples under different over-consolidation ratios to examine the possible effects of stress history. Three values of pre-consolidation pressure were set in advance, namely 196kPa, 294 kPa, which were all effective normal stresses. Subsequently, corresponding to each level of pre-consolidation, the stress was decreased to around 98 kPa to obtain the OCRs of 2, 3, and 4. The initial effective normal stress was kept at approximately 98 kPa during this testing series.

3.7 Test procedure for monotonic ring shear test

Each specimen was normally reconsolidated under a constant consolidation stress, σ_c , for around 1 hour. The value of the consolidation stress applied in the ring shear test apparatus was greater than that of the preliminary consolidation pressure during the curing process. The additional consolidation stress may damage the cementation of the specimen. According to [Suzuki et al. \(2005\)](#), when the elapsed curing time reaches a certain value, the unconfined compressive strength of the cemented specimen cured under a higher overburden pressure was not lower than that cured under a preceding

overburden pressure. In other words, the additional overburden pressure did not influence the unconfined compressive strength of the cemented soil cured with an applied stress. Therefore, any damage to the cemented matrix induced by the application of the additional consolidation pressure can be neglected when evaluating the shear behaviour. To avoid swelling of the specimen due to submergence, pure water was poured into a water bath immediately after applying the consolidation stress. Subsequently, the specimen was sheared under a constant total normal stress, until the shear displacement, δ , became sufficiently large to reach the residual state. Here, δ is defined as an intermediate circular arc between the inner and outer rings. To minimize the friction between the upper and lower rings and the outflow of the sample from the shear surface, the gap between the rings was fixed at 0.10 mm. The frictional force along the perimeter of the specimen acted upward in the case of negative dilatancy and downward in the case of positive dilatancy. In this test, the net normal stress acting on the shear surface was calculated based on the frictional force measured by the load cell. When determining the gap between the upper and lower rings before the start of the shear test, changes in frictional force along the rings were measured and used to modify the normal stress accordingly.

3.8 Test procedure for dynamic ring-shear test

Test procedure for dynamic ring-shear test has distinct features differing from monotonic ring-shear test. After the specimen was adapted completely into the shear box. Subsequently, the specimen was sheared under a reversal shear stress with a given constant amplitude. During dynamic ring-shear tests, normal stress was kept constant, shear stress with the wave form of sine curve at 0.5 Hz frequency was applied. This frequency is chosen uniquely because the common frequencies of an earthquake is well known in ranges of 0.5 Hz to 15 Hz. Thus, the frequency of 0.5 Hz applied in this investigation can be applied to a range of soil dynamic behaviors. To minimize the friction between the upper and lower rings and the outflow of the sample from the shear surface, the gap between the rings was fixed at 0.10 mm.

The testing program consisted of three test series, each designed to investigate a particular effect of the cyclic behavior of cemented kaolin clay. Series 1 included the

cyclic tests conducted under three altered defined normal stress, the seconds for varying three cyclic shear stress amplitudes, and the thirds for different over-consolidation ratios, respectively. During each test, a normalized cyclic stress ratio, τ_{cN}/σ_{N0} , defined as the ratio of the maximum cyclic shear resistance to the initial normal stress, was measured in order to compare the obtained results for different types of sample. Here τ_{cN} is the average cyclic shear resistance in the N th cycle and to distinguish with τ_c defined as cyclic shear in previous section. During the cyclic shearing, the magnitude of vertical displacement was controlled constant as much as possible by volume-controlled device, by which hold the volume of specimen constant.

3.9 Determination of residual strength

The test results revealed that residual strength is an important parameter that must be calculated precisely without error. In this study, a hyperbolic approximation method was used to objectively determine the residual strength regardless of shear displacement, as suggested by [Suzuki et al. \(1997\)](#). The hyperbolic approximation was applied to the measured relationship between the stress ratio τ/σ_N and the shear rotation angle θ , which is defined as the angle of rotation about the vertical axis. The asymptotic value of the stress ratio at the residual state was designated as $(\tau/\sigma_N)_r$. The hyperbolic approximation parameters, a and b , are given by the offset and slope of a linear fit to the relationship between $\theta/(\tau/\sigma_N)$ and θ by the least squares method. If the approximated hyperbola is in good agreement with the measurement, then $(\tau/\sigma_N)_r$ is given as the inverse of b . The validity of the fit can be assessed using the correlation coefficient, r ([Fig. 3.17](#)). The applicability of the method was demonstrated based on the test results of kaolin and natural clays under various test conditions ([Suzuki et al., 1997](#)). Therefore, the residual strength of a soil sample can be determined by this method.

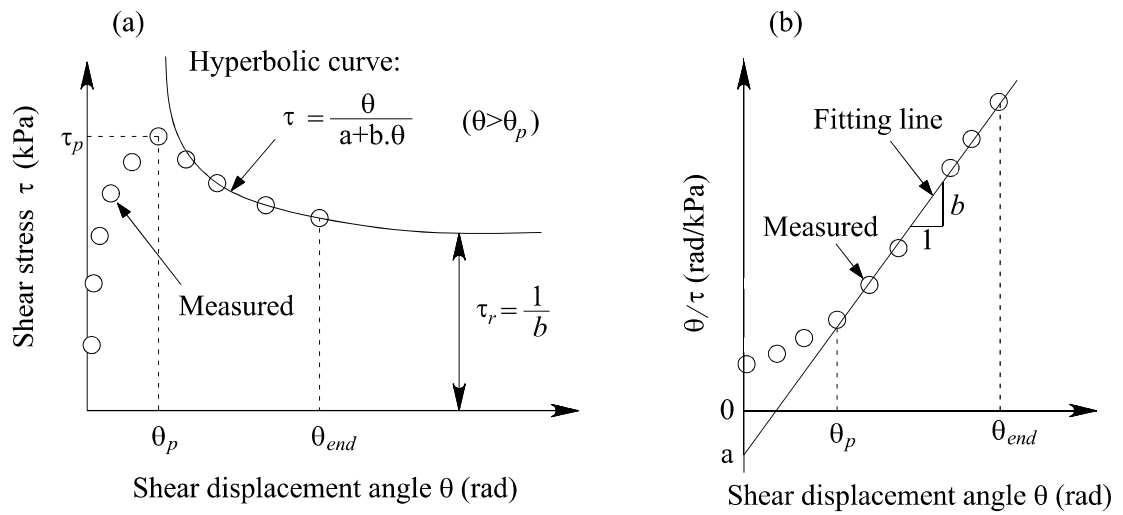


Figure 3. 17 Schematic diagram for determining the residual strength by a hyperbolic curve approximation (Suzuki et al., 1997)

Chapter 4 SHEAR BEHAVIOR OF DISCONTINUOUS PLANE MATERIALS IN MONOTONIC RING-SHEAR TEST

4.1 Shear behaviour and strength properties of normal and combined specimens

Test cases and test results of cemented and non-cemented kaolin samples are summarized in [Table 4.1](#). The test results were obtained under the curing conditions of a constant temperature and humidity, as mentioned before. Residual and peak shear strength values were calculated for target normal stresses of 98, 196, and 392 kPa. The shear displacement rate was set to 0.2 mm/min.

[Figs. 4.1 \(a\)-\(k\)](#) and [Figs. 4.2 \(a\)-\(k\)](#) contain a number of shear stress and shear displacement curves and the residual and peak failure envelopes for the samples tested. Here, the peak shear strength is defined as the maximum shear stress that a specimen exhibits under drained condition in the constant pressure ring shear test. In the case of the normal specimen, the shear stress initially rapidly increased and subsequently gradually decreased, accompanying the progress of shearing. Finally, it reached its residual state during which the shear stress became almost constant. As the added cement content increased, the peak and residual values of shear stress remarkably increased for each level of normal stress.

When the cementation around a shear surface in a specimen fully disappeared in the residual state stage, the residual shear strength was considered to be independent of the cement content. It can be seen from these results that the internal friction angle and apparent cohesion in the residual state are affected by the cement content. This is because the physical composition of the sample was primarily changed by adding fine cement particles. Further, the degree of reorientation of the particles along the shearing direction for cemented kaolin was much lower than that for pure kaolin. The aggregates of clay particles generated by chemical bonding did not decompose as shearing proceeded; hence, the sectional shape of the shear surface undulated.

In the case of combined specimen having an artificial bedding plane, the shear stress after the peak value rapidly decreased and then became almost constant. The behaviour observed in this combined specimen is very unique in that the sharp decrease in the

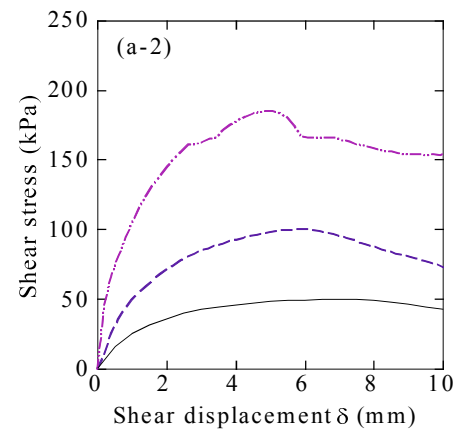
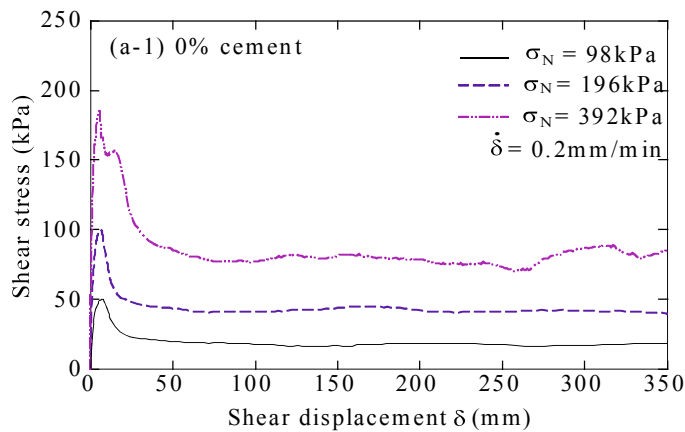
strength is characterized by a discontinuous plane. For this reason, the contact surface between two layers of different soils in the specimen is thought to act as a discontinuous plane. The specimen having this pre-existing surface is likely to reach residual state in earlier stages of shearing. Such a sudden reduction of shear strength on a bedding plane could cause large deformations resulting in catastrophic endings of earthquake-induced landslides.

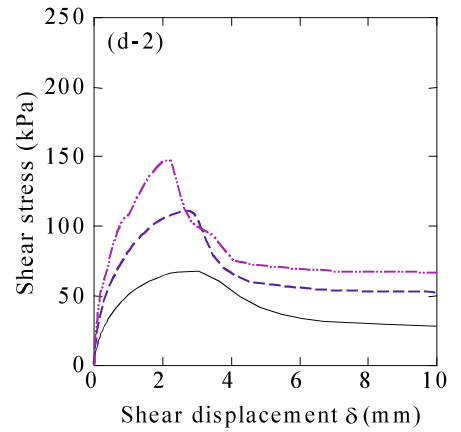
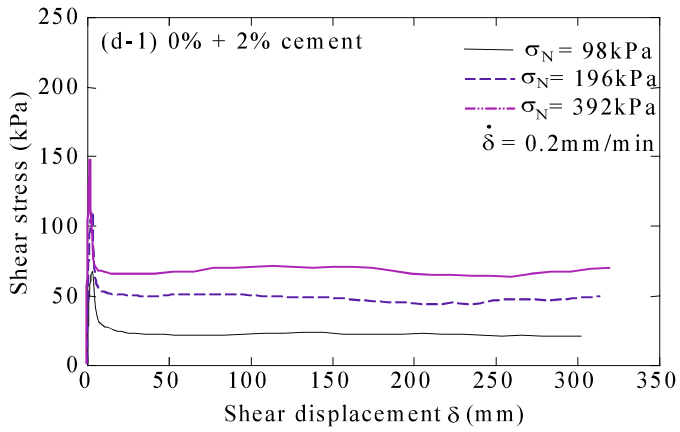
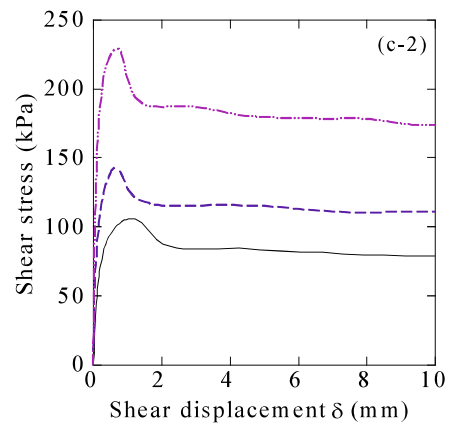
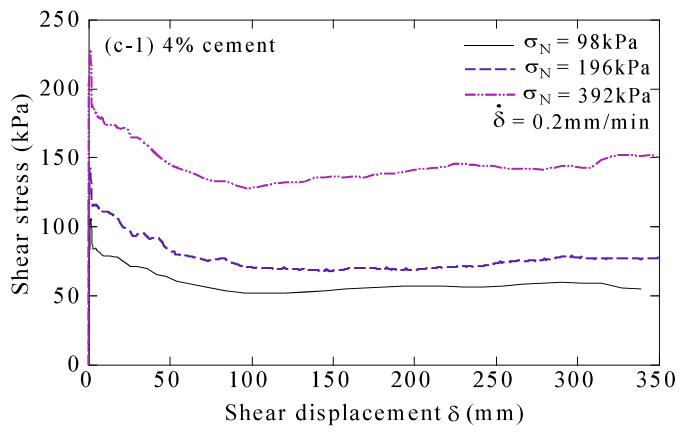
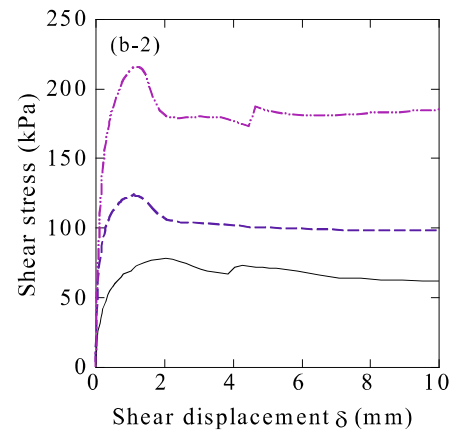
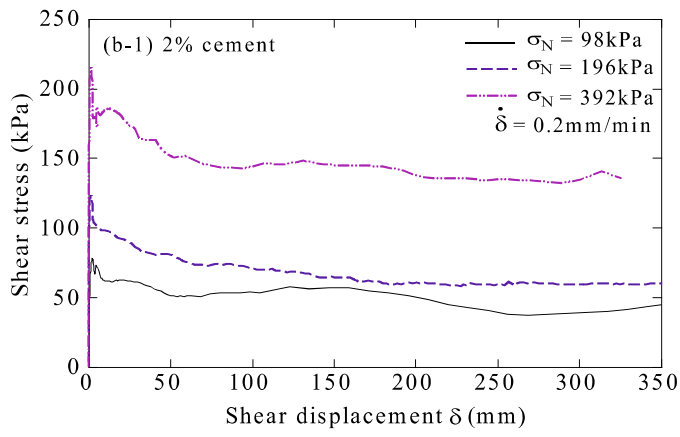
Figs. 4.2 (a)-(f) show that all envelopes demonstrated the apparent peak and residual cohesions except for the kaolin sample. In most cases, the residual failure envelopes are somewhat curved because of the progressive de-bonding with the increasing total stress (Lupini, 1981; Skempton, 1985; Stark and Eid, 1994). The data were fitted linearly to approximate the peak and residual failure envelopes obtained from the ring shear tests conducted on cemented and non-cemented kaolin, ranging at normal stresses from 98 kPa to 392 kPa. This modification is considered to be consistent with the preliminary purpose of study and other researchers (Stark and Eid, 1994). A high coefficient of determination R^2 (R is the coefficient of correlation) was obtained for all samples. The values of the strength parameters obtained in this investigation are summarized in Table 4.2.

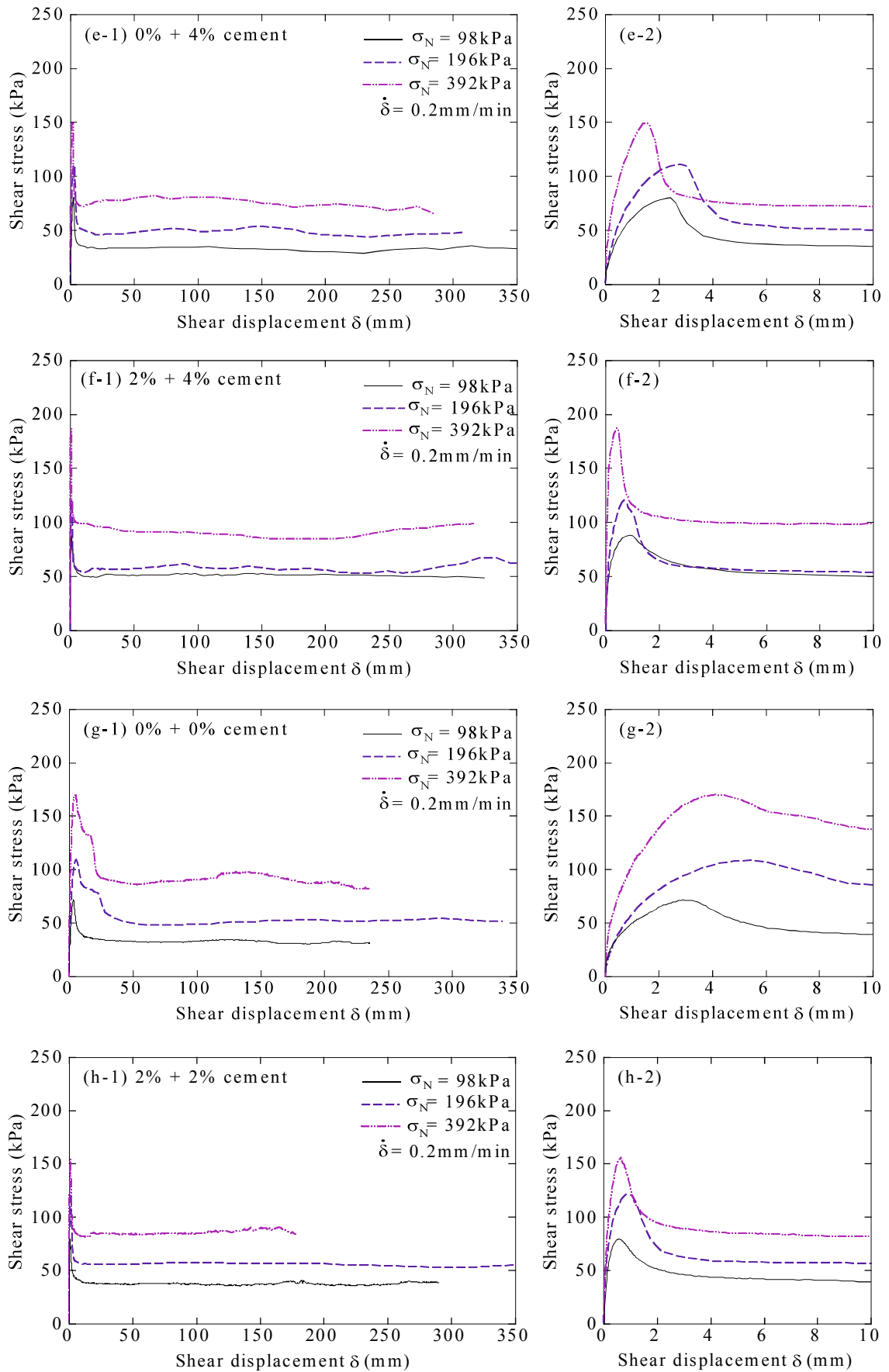
The value of the internal friction angle for kaolin, ϕ' , is 28.8° , and the value of the apparent cohesion, c' , is zero on the basis of a triaxial compression test. In general, the residual friction angle of kaolin seems to be about 70–80% of its peak value. In the present study, the residual friction angle of kaolin was almost half of the peak value. Suzuki et al. (2007) conducted a reversal box shear test to determine the residual shear strength of kaolin and found that the internal friction angles in the peak and residual states were 25.5° and 13.6° , respectively. The ratio of the residual value to the peak value was about 53%. It is considered that the results obtained from the present study are appropriate.

Table 4. 1 Test cases and test results of cemented and non-cemented kaolin samples

Soil sample	Test No.	Shear rate		Normal stress σ_N (at peak) (kPa)	Normal stress σ_N (at residual) (kPa)	Peak strength τ_p (kPa)	Residual strength τ_r (kPa)	Stress ratio at peak τ_p / σ_N	Stress ratio at residual τ_r / σ_N
		(mm/min)	(deg/min)						
0% cement	1-1	0.2	0.29	97	97	53.1	18.1	0.547	0.187
	1-2	0.2	0.29	202	202	102.5	42.4	0.507	0.210
	1-3	0.2	0.29	400	402	184.6	82.6	0.462	0.206
2% cement	2-1	0.2	0.29	96	97	78.1	42.0	0.813	0.433
	2-2	0.2	0.29	198	199	123.9	63.7	0.626	0.320
	2-3	0.2	0.29	393	393	215.2	135.1	0.547	0.344
4% cement	3-1	0.2	0.29	100	102	106.1	56.8	1.061	0.557
	3-2	0.2	0.29	198	197	145.6	78.1	0.735	0.396
	3-3	0.2	0.29	388	388	228.8	144.9	0.590	0.374
2% + 0% cement	4-1	0.2	0.29	91	101	67.9	21.6	0.746	0.214
	4-2	0.2	0.29	198	199	92.7	46.7	0.468	0.235
	4-3	0.2	0.29	412	412	147.0	66.2	0.357	0.161
2% + 4% cement	5-1	0.2	0.29	101	101	88.1	50.8	0.873	0.503
	5-2	0.2	0.29	197	206	119.6	59.5	0.607	0.289
	5-3	0.2	0.29	390	390	187.3	91.7	0.480	0.235
0% + 4% cement	6-1	0.2	0.29	100	101	80.2	32.8	0.802	0.325
	6-2	0.2	0.29	196	197	111.0	46.5	0.567	0.236
	6-3	0.2	0.29	381	389	149.0	71.9	0.391	0.185
0% + 0% cement	7-1	0.2	0.29	93	94	71.6	31.3	0.77	0.333
	7-2	0.2	0.29	191	191	108.9	51.8	0.570	0.271
	7-3	0.2	0.29	390	387	169.9	84.5	0.436	0.218
2% + 2% cement	8-1	0.2	0.29	76	76	79.8	37.9	1.051	0.498
	8-2	0.2	0.29	191	191	121.7	54.3	0.637	0.285
	8-3	0.2	0.29	411	412	179.6	86.9	0.376	0.211
4% + 4% cement	9-1	0.2	0.29	98	100	91.2	49.0	0.931	0.490
	9-2	0.2	0.29	216	216	129.5	61.7	0.560	0.285
	9-3	0.2	0.29	393	393	184.6	90.1	0.470	0.229







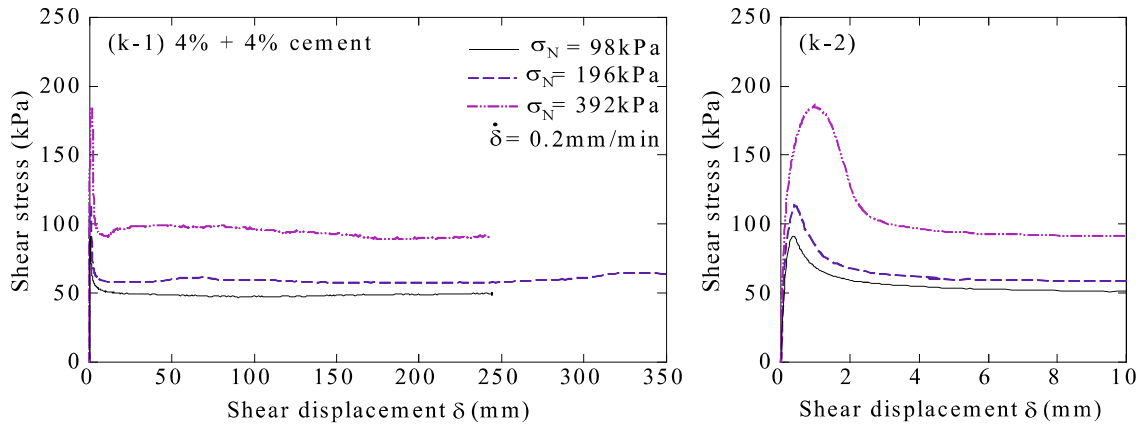
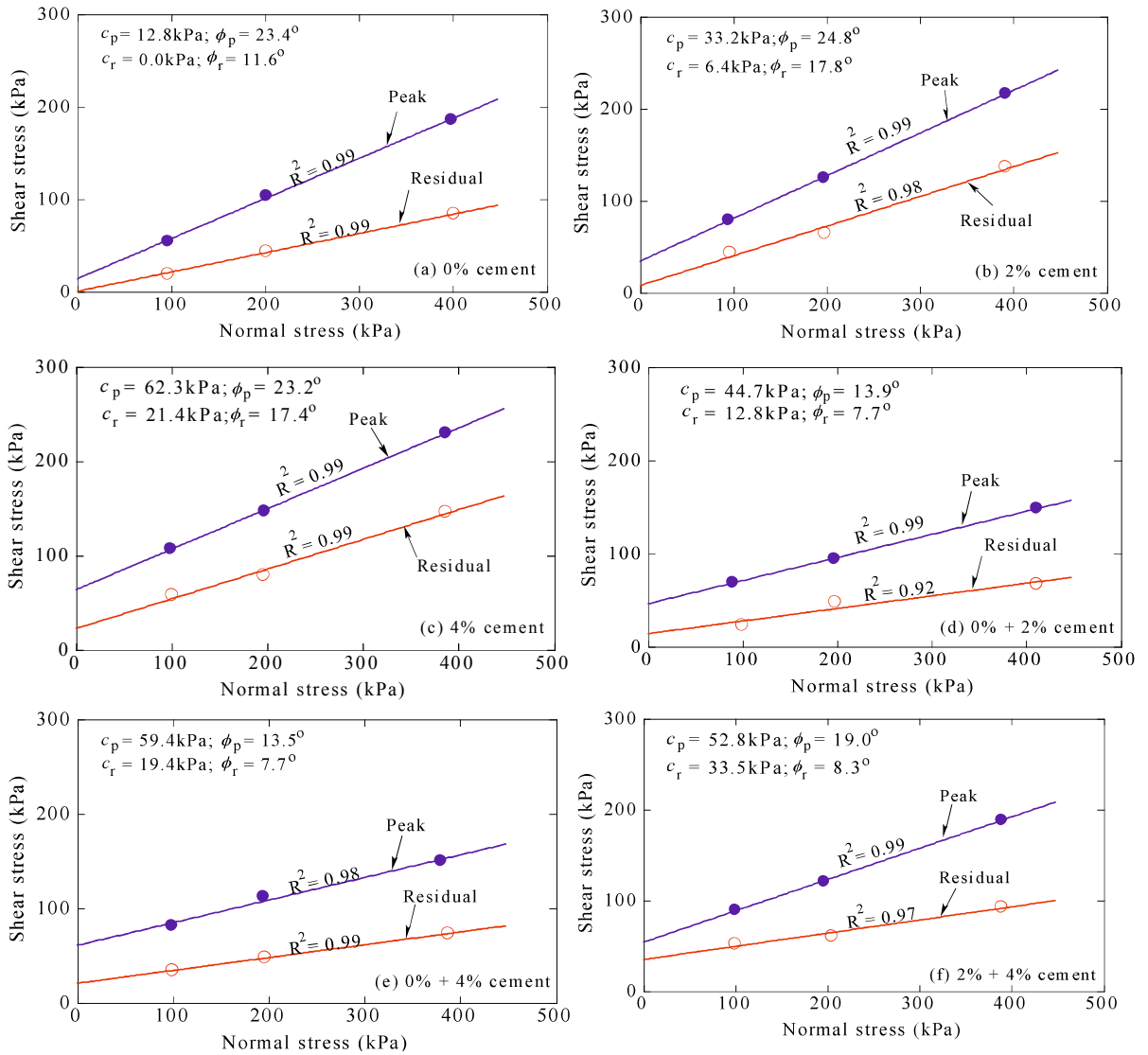


Figure 4. 1 Shear stress and shear displacement curves for (a)-(c) normal and (d)-(f) combined specimens.



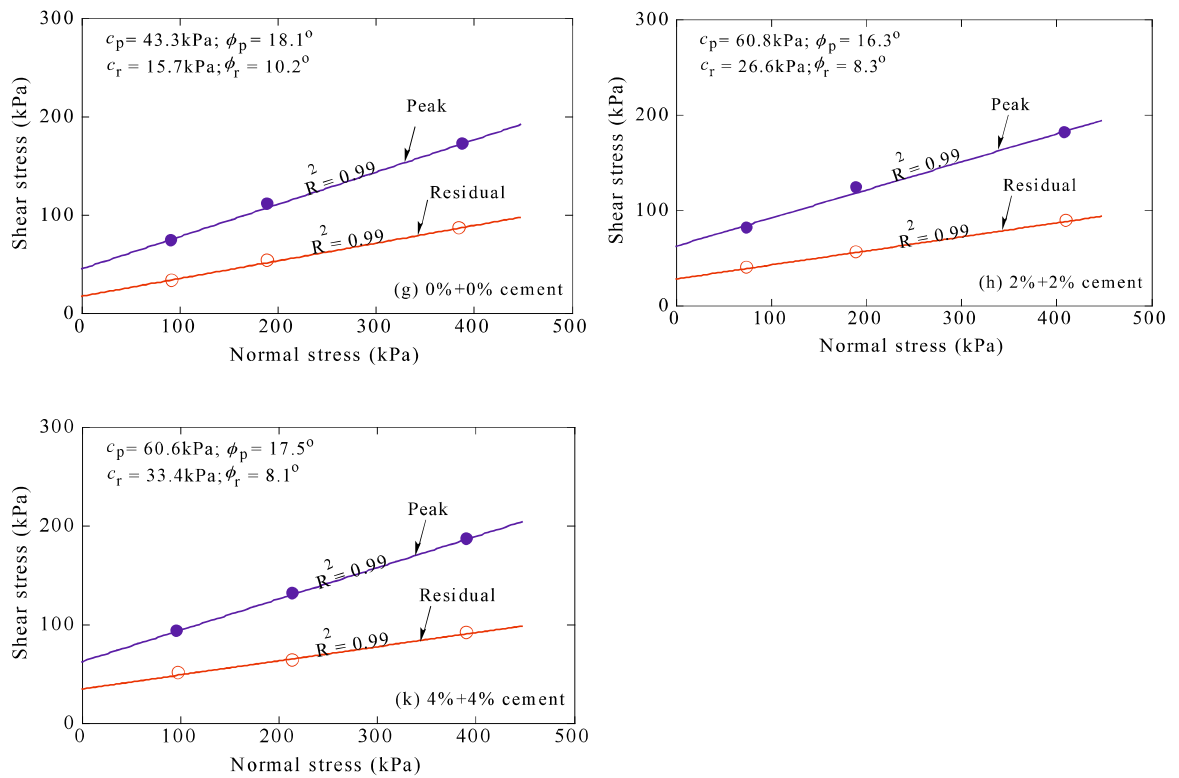


Figure 4. 2 Peak and residual drained failure envelopes for (a)-(c) normal and (d)-(f) combined specimens.

Table 4. 2 Summary of shear strength parameters of cemented and non-cemented kaolin specimens under a normal stress of 196 kPa

Type of specimen	Test ID	Peak friction angle (deg.)	Peak cohesion (kPa)	Residual friction angle (deg.)	Residual cohesion (kPa)
Normal	0% cement	23.4	12.8	11.6	0.0
	2% cement	24.8	33.2	17.8	6.4
	4% cement	23.2	62.3	17.4	21.4
Combined	0%+0% cement	18.1	43.3	10.1	15.7
	0%+2% cement	13.9	44.7	7.7	12.8
	0%+4% cement	13.5	59.4	7.7	19.4
	2%+2% cement	16.3	60.8	8.3	26.6
	2%+4% cement	19.0	52.8	8.3	33.5
	4%+4% cement	17.5	60.6	8.1	33.4

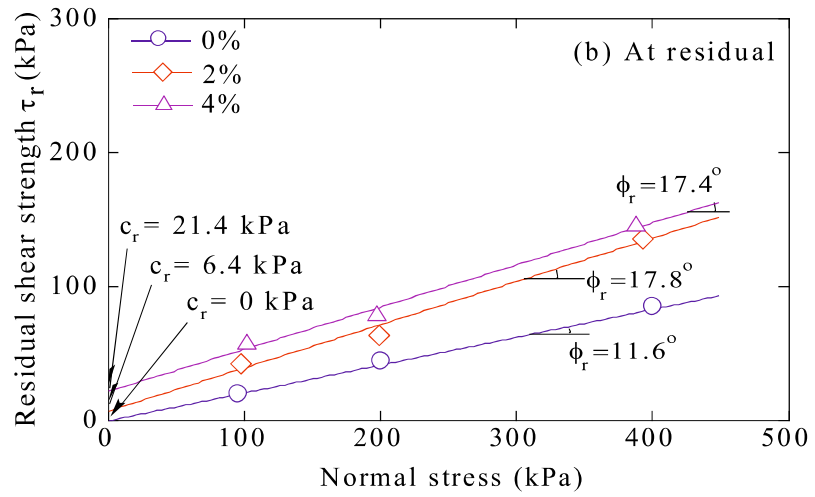
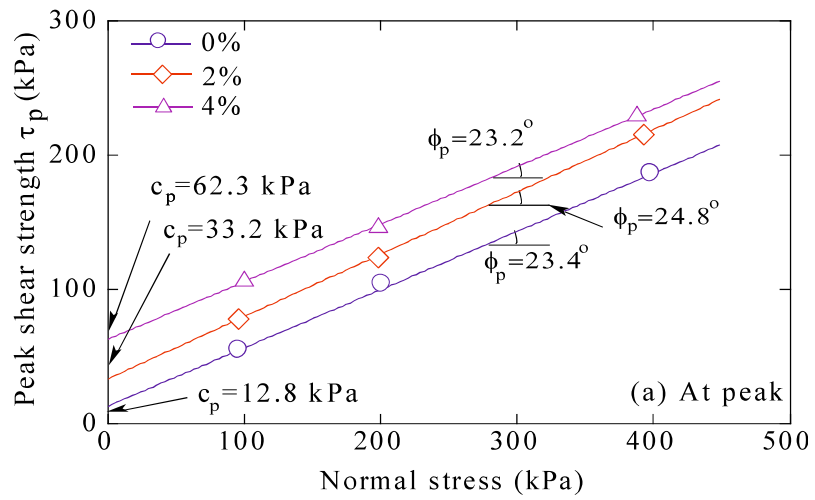
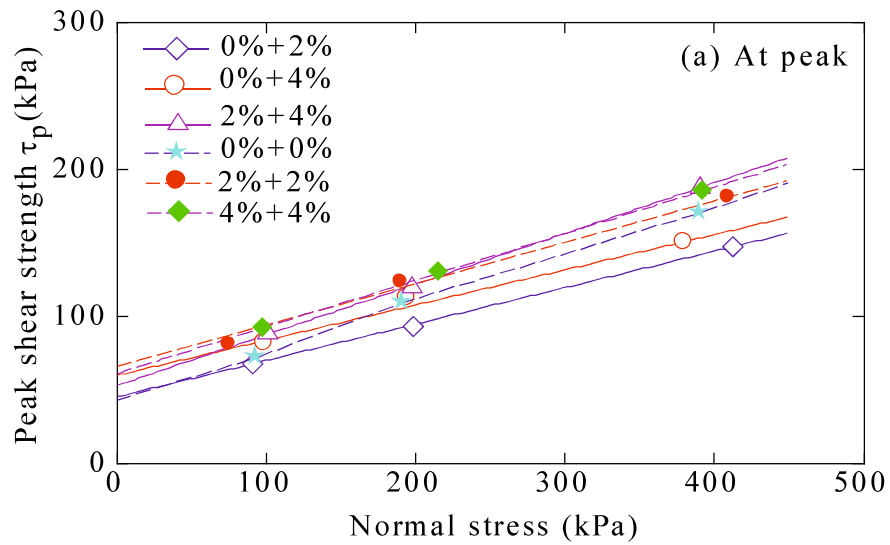


Figure 4. 3 Comparison of (a) peak and (b) residual drained failure envelopes for normal specimen with different cement contents.



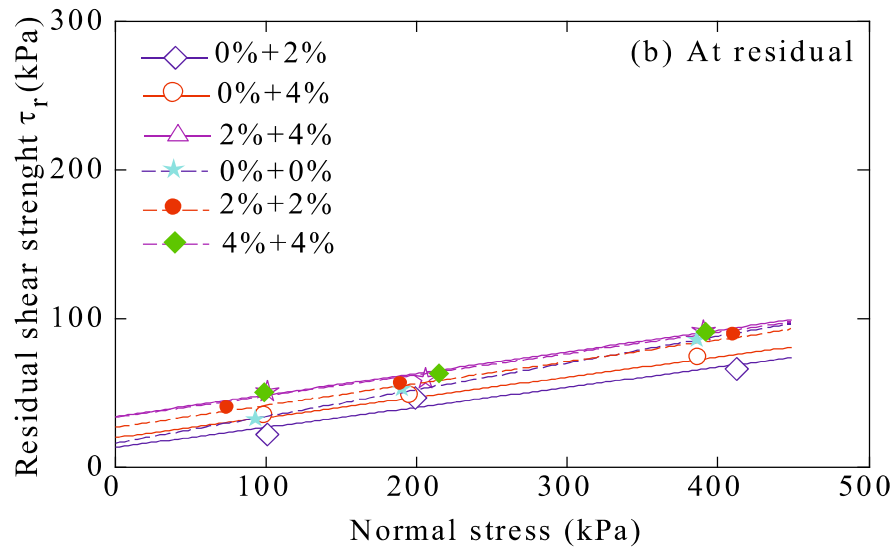


Figure 4. 4 Comparison of (a) peak and (b) residual drained failure envelopes for combined specimens with different cement contents.

Figs. 4.3 (a) and (b), and Figs. 4.4 (a) and (b) show the drained residual and peak failure envelopes to allow comparison of strength characteristics of the tested samples. These failure envelopes were the same as those in Figs. 4.2. All values of R^2 in Fig. 4.2 were greater than 0.92. Therefore, these values show that the compatibility of the fitting line with the measured values is high without any problems. It can be seen in Fig. 4.3 (a) that the failure envelopes at the peak state of each cemented kaolin specimen rise upwards in accordance with the cement content, and they seem to parallel the trend of pure kaolin (0% cemented kaolin). In addition, the failure envelope at the residual state of the 2% cemented kaolin is almost parallel to that of the 4% cemented kaolin. Furthermore, both straight lines appear to be steeper than the failure envelope of pure kaolin for a confined stress up to approximately 400 kPa, as shown in Fig. 4.3 (b). These findings are consistent with previous research (Clough et al., 1981; Kasama et al., 2000) and are thought to result from the cementation effect. Interestingly, this is also observed in the combined specimens, which demonstrated a similar trend. Because of higher cement content, the incline of the 2% + 4% cemented kaolin failure envelope at the peak state was steeper and greater in value than that of the 0% + 2% and 0% + 4% cemented kaolin specimens. The incline of the failure envelope at the residual state was almost the

same for all specimens irrespective of composition. The value of apparent cohesion was not always zero in the case of the 0% + 2% cemented specimen. This is thought to be attributed to the development of cementation in one half of the specimens.

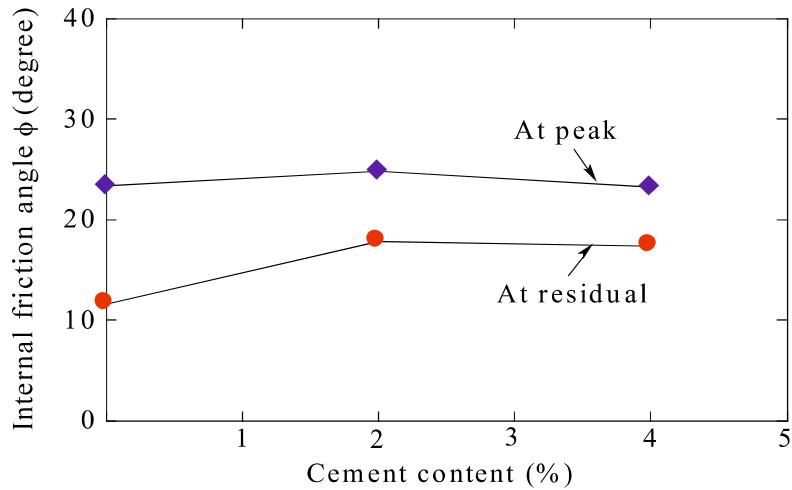


Figure 4. 5 Internal friction angle versus cement content for normal specimen.

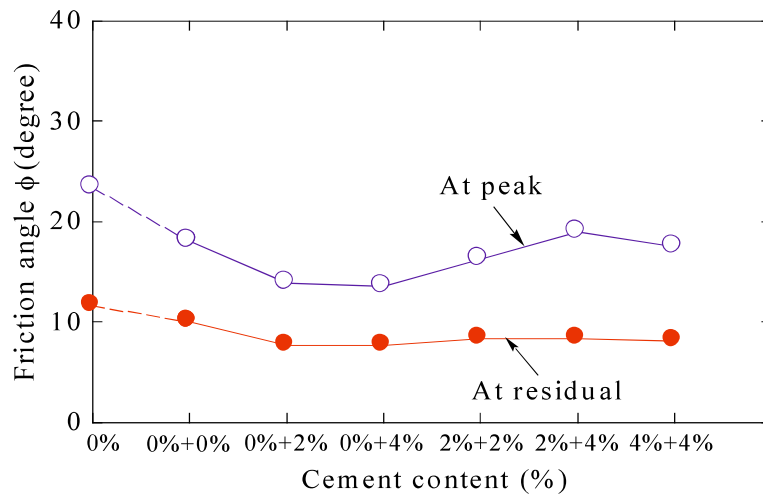


Figure 4. 6 Friction angle versus cement content for normal and combined specimens.

Figs. 4.5 and 4.6 show the values of the peak and residual friction angles as a function of cement content. In Fig. 4.5, the value of the peak friction angle hardly varied with cement content; thus, it was considered to be independent of the amount of cement. This characteristic is in agreement with the results of other research (Wissa et al., 1965;

Kasama et al., 2000; 2006). In contrast, the residual friction angle increased by 6.2° as the cement content increased from 0% to 2%, and after that decreased by only 0.4° , which was essentially insignificant. The residual friction angle is essentially independent of the cement content added to the soil. This change was possibly attributable to the changes in the physical properties of the soil mixed with the cement and to the changes in the shape and conditions of the shear surface formed by the development of cementation. There does not seem to be sufficient information in the literature related to significantly increasing residual friction angle for 2% cemented kaolin because in previous studies, residual strength is considered as to be independent of stress history, original structure, initial moisture content, cementation and others factors.

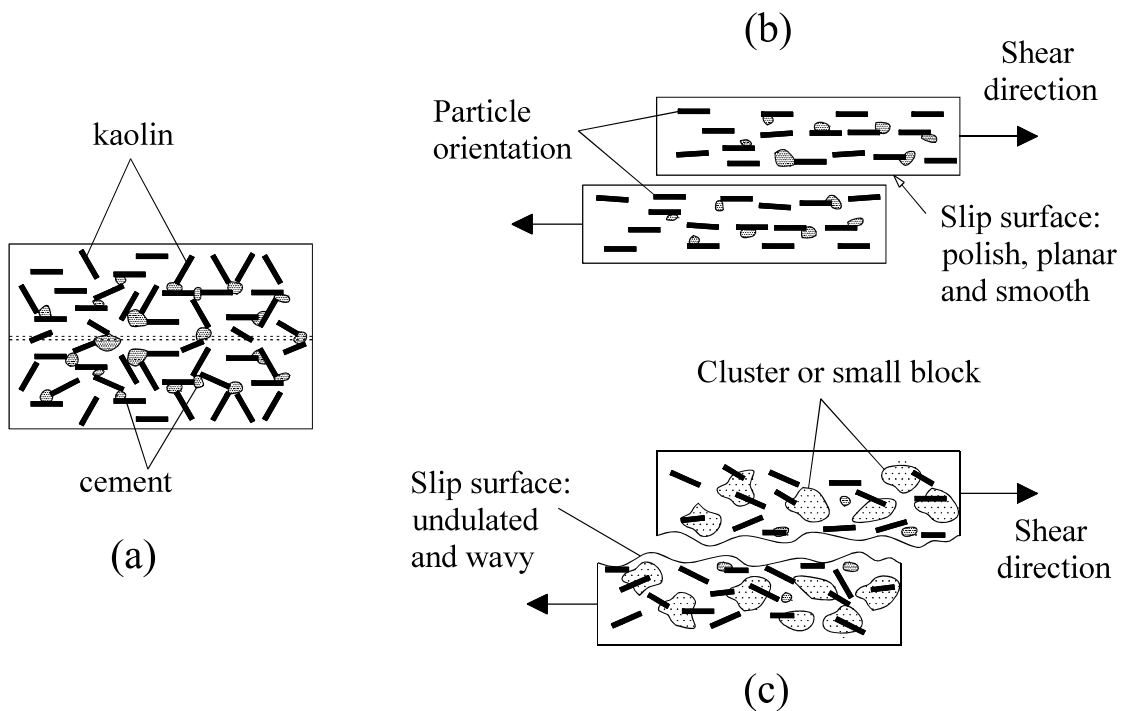


Figure 4. 7 Sketch pictures exhibit the theories using to explain the significantly increasing residual friction angle: (a) a cemented clay specimen before shearing, (b) development of slip surface based on previous researches, and (c) slip surface was undulated and wavy observing in this study.

Based on the observation of the slickensides of cemented samples after shearing, we realized that the slip surfaces were not smooth, planar, and polish in comparison with pure kaolin. Its slickensides were undulating, slightly wavy and occasionally two simultaneous slickensides developed at the gap between the upper and lower shear boxes and between the tip of a radial fin and sample. The addition of cement into kaolin result in soil aggregations (clusters), which act almost as single particles and interact to produce the strength and stiffness. Thus, the residual strength increases with the increase in the degree of cementation may be attributed an undulating and slightly wavy slickenside at the residual state under any normal stress, by which soil aggregations acting almost as single particles or small blocks cause an increasing friction angle. This theory is illustrated in [Fig. 4.7](#).

This theory is considered to be consistent with that of [Sorensen et al. \(2007\)](#). They stated that the behaviour of the cemented kaolin when sheared to high strains result in breaking the cementing, forming aggregates of cement-mixed kaolin, and that these kaolin aggregates contribute to changing the soil behaviour from that of a continuum to that of a granular (particulate) material. These clusters cannot be destroyed by large shear displacement at residual state.

As seen in [Fig. 4.6](#), the friction angles at the peak states of all combined specimens were smaller than that of the normal specimen with 0% cement. The residual friction angle for 0%+0% was 1.5° lower than that for 0%. The residual friction angle for 2%+2% and 4%+4% were 9.5° and 9.3° lower than those for 2% and 4%, respectively. The difference in the residual friction angle between the normal and combined specimens was increased in the cemented sample. This difference in the friction angle may result from a pre-existing shear surface inside the combined specimen. According to the literature, the process of producing the combined cement kaolin specimens as mentioned above is similar to a pre-shearing test procedure carried out by [Stark et al. \(1992\)](#), which resulted in residual strengths consistent with in situ conditions. The residual friction angle of combined specimens decreased significantly by 3.9° as the cement content changed from 0% to 0% + 2%. With further increases in cement content, the residual friction angles were almost constant. The variation of residual friction angle increased by 0.6° in the range from 0% + 2% to 2% + 4%. This tendency was similar to that of cemented kaolin, which was found to be independent of cement content. It is

believed that this was caused by the cementation effect, resulting in two halves of specimens with different degrees of hardening. The residual friction angle for the 2%+4% combined sample was significantly lower than that for the 2% normal sample. This may be due to the differences in the conditions of the slip surfaces between the normal and combined cemented specimens. The shear surface in the normal cemented specimen did not show a flat shape but complicated shapes because the aggregates have inter-particle bonding strength. On the other hand, the shear surface in the combined specimen developed along the discontinuous plane; thus, the reorientation of clay particles in the shearing direction was well developed compared with the normal cemented specimen. Therefore, the friction angle in the residual state for the combined specimen was lower than that for the normal cemented specimen.

Figs. 4.8 and 4.9 show the relationship between the cohesion intercept and cement content. It can be observed that the cohesion intercept at the peak and residual states increased remarkably with only small amounts of cement. Here, c_p and c_r should be considered as the parameters representing cementation property. This tendency is consistent with the findings of [Kasama et al. \(2000; 2006\)](#) and [Raftari et al. \(2014\)](#). It can be stated that cohesion is a basic parameter characterizing the effect of cementation on the residual strength of cemented soil, which also is especially important in bedding planes with low confining pressures where the effective cohesion plays an important role in stability and the prevention of landslides. In **Fig. 4.9**, the value of cohesions at peak and residual states for combined specimens were higher than those of the normal specimen with 0% cement. It was recognized that the value of cohesion was recovered to a certain degree, even in discontinuous planes.

Fig. 4.10 shows drained stress paths of cemented and non-cemented kaolin on the basis of shear stress measurements and total normal stresses on the shear surface. The stress paths of normal specimens with 2% and 4% cement exceeded the peak failure envelopes of normal specimens with 0% cement, and reached their respective peak failure envelopes. As previously mentioned, this behavior was caused by the effect of the cement content, resulting in increased shear strengths. **Fig. 4.11** shows a comparison of drained stress paths between combined and normal specimens. This result shows that the drained stress paths of combined specimens with 0% + 2% and 0% + 4% cement did not reach the peak failure envelope of pure kaolin having a normal stress value of around

400 kPa, but their peak values exceeded that of pure kaolin in the range below $\sigma_N = 200$ kPa. In contrast, the stress path of the combined specimen with 2% + 4% cement exceeded that of the 0% cement specimen over the entire range of normal stresses because of the higher cement content, even though it was a combined specimen. The peak strengths for the other cases were also equal to or higher than the peak failure envelope of non-cemented kaolin. It can be seen from this figure that the net normal stress acting on the shear surface fluctuated owing to the change in the skin friction generated between the upper rings and the specimen.

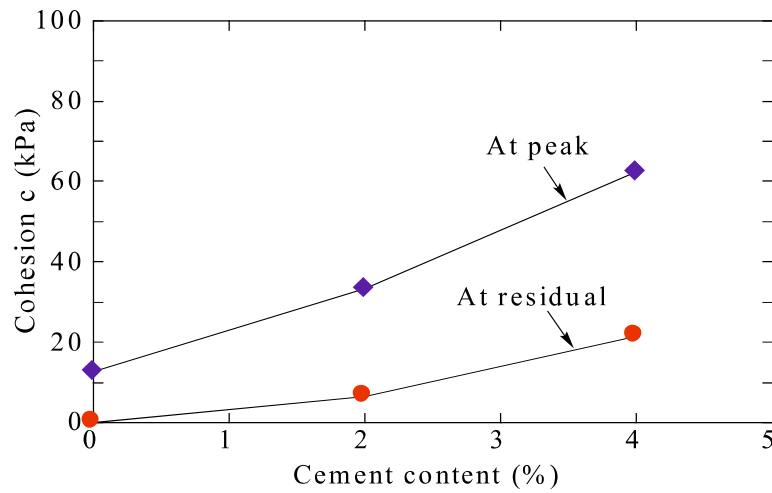


Figure 4. 8 Cohesion versus cement content for normal specimen.

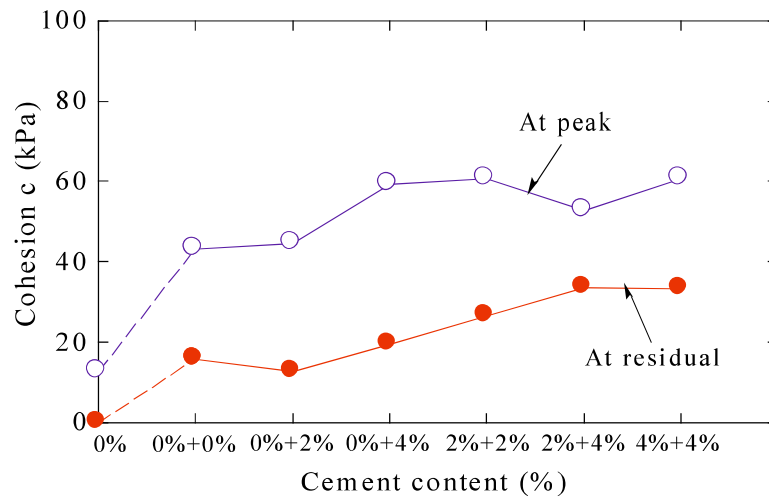


Figure 4. 9 Cohesion versus cement content for normal and combined specimens.

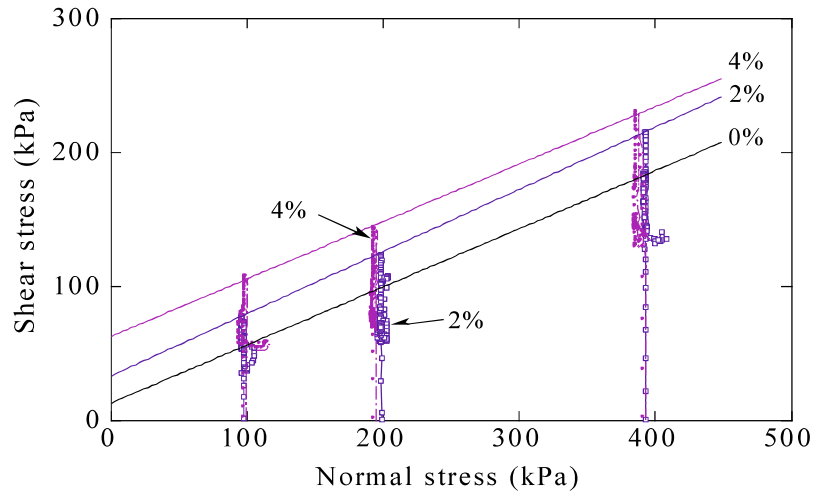
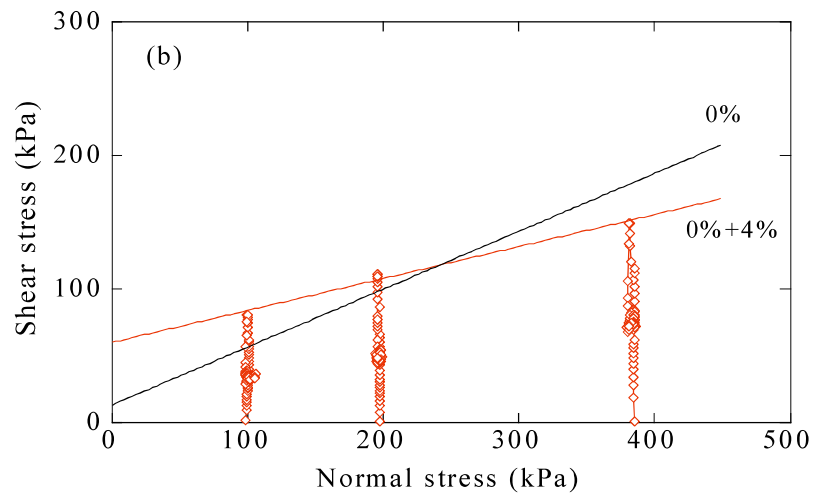
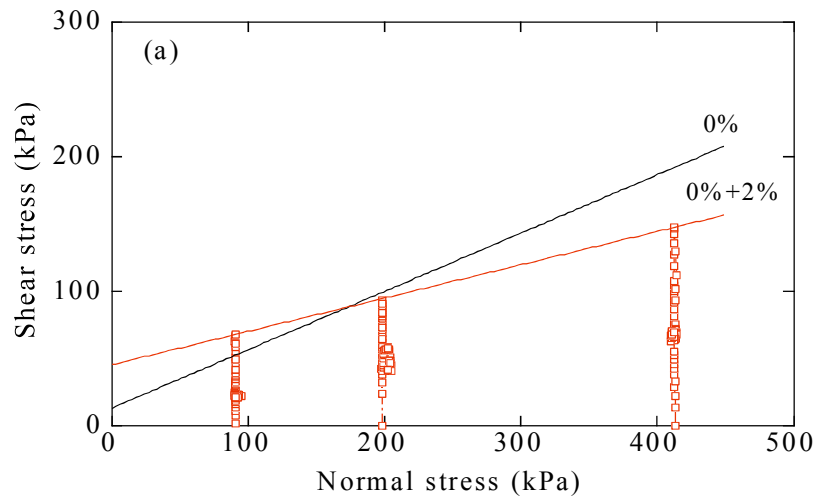


Figure 4. 10 Stress paths of normal specimen with different cement contents.



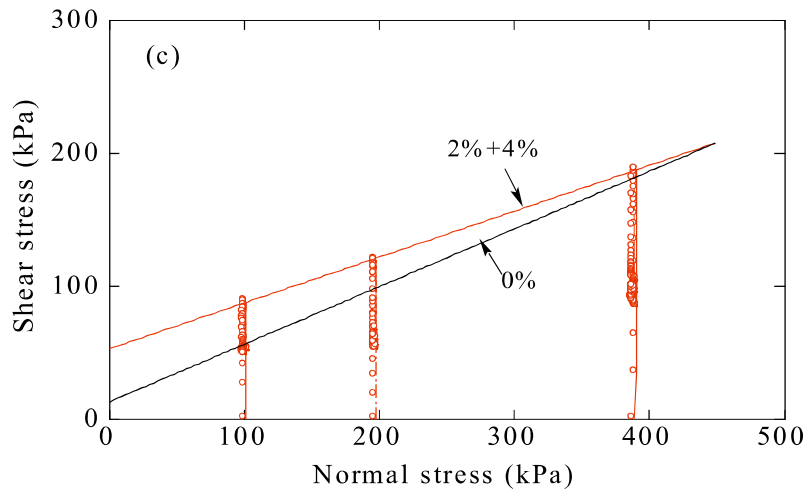
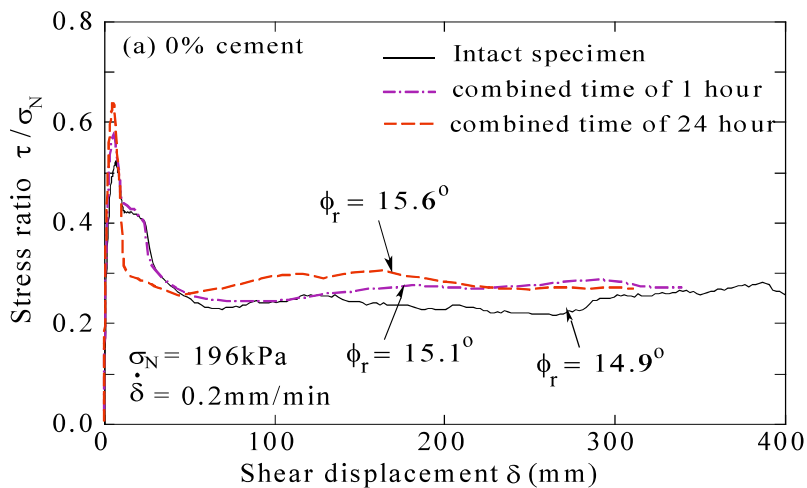


Figure 4. 11 Stress paths of combined specimen with different cement contents.

4.2 Effects of combination conditions on shear behaviour for combined specimens

For combined specimens, it was necessary to investigate the effect of combined time as well as the pre-shearing process on shear behaviour. The 0%, 2%, and 4% cemented kaolin samples were selected for these tests. The shear displacement rate was set to 0.2 mm/min. The normal stress was fixed at 196 kPa. All specimens used in this study were normally consolidated under a constant consolidation stress, σ_c , for 1 hour prior to shearing. Two halves of an intact specimen were cut, and then combined with each other according to the procedure used for combined specimens described in previous sections. The combined time was set to 1 hour and 24 hours. The results obtained from the combined samples were also compared to intact samples.



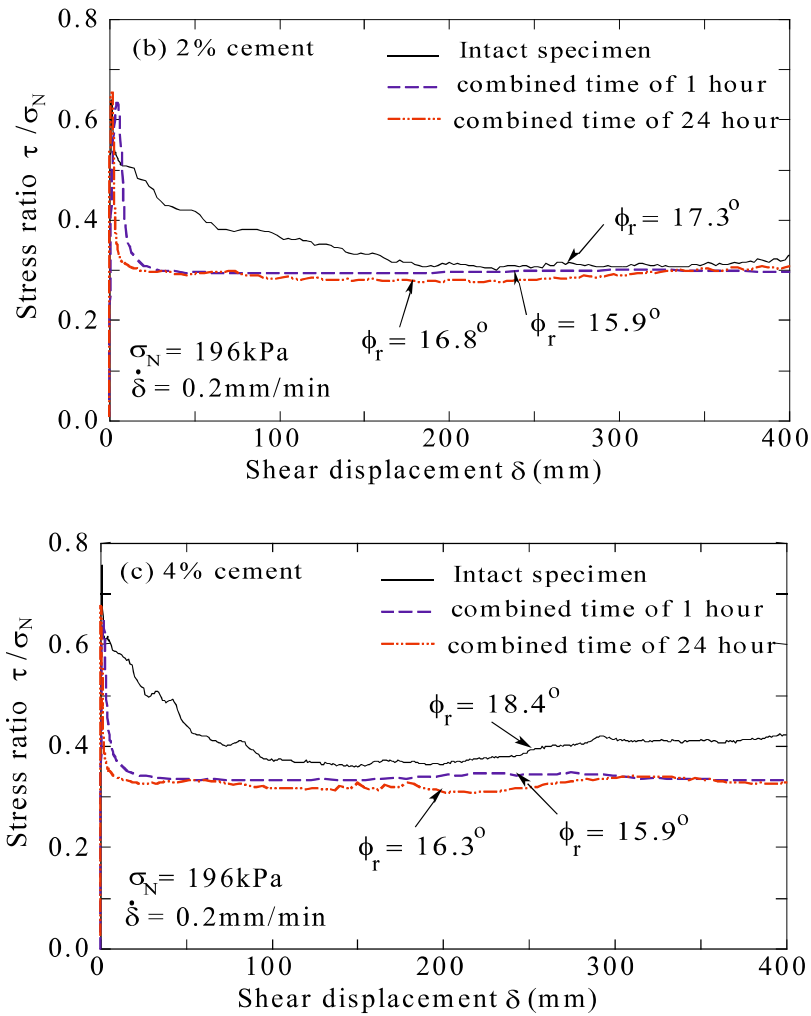


Figure 4. 12 Influence of combined time on shear behavior for normal specimens with different cement content.

Figs. 4.12 (a)-(c) show the effect of combined time on the stress ratio and shear displacement curves for test samples. It can be seen from these figures that the curves were differed insignificantly for combined times between 1 hour and 24 hours. The residual stress ratios of 0% and 2% cemented kaolin, compared between normal and combined specimens, were not observed to be noticeably different. In contrast, 4% cemented kaolin showed a considerably higher stress ratio for normal specimens at the residual and peak states than those of combined specimens. As the combined time became longer, the stress ratio reduced more rapidly. Details of the calculated results are presented in Table 4.3. The 0% cemented kaolin samples for a combined time of 24 hours showed a 3.3% higher value than equivalent samples with a combined time of 1

hour. The increase in strength from 1 hour to 24 hours of combined time was approximately 5.6% and 2.5% for 2% and 4% cemented kaolin samples, respectively. This could be attributed to further development of cementation on the shear surface with the passage of time after combining. Furthermore, these values are relatively small and can be considered to be constant irrespective of combined time.

Table 4. 3 Summary of stress ratio at residual state under various combined time and type of specimen for cemented and non-cemented kaolin specimens.

Sample	Type of specimen	Combined time (hour)	Stress ratio at residual state τ_r/σ_N	% increase or decrease compared intact specimen
Kaolin (0% cemented kaolin)	Intact	1 hour	0.267	0.0
	Combined	1 hour	0.271	+1.5
	Combined	24 hour	0.280	+4.9
2% cemented kaolin	Intact	1 hour	0.312	0.0
	Combined	1 hour	0.285	-8.6
	Combined	24 hour	0.301	-3.5
4% cemented kaolin	Intact	1 hour	0.332	0.0
	Combined	1 hour	0.285	-14.1
	Combined	24 hour	0.292	-12.0

4.3 Stress ratio versus normal stress

In order to evaluate how normal stresses affected the stress ratios on the shear surfaces, the relationships between stress ratios at peak and residual states (τ_p/σ_N), (τ_r/σ_N) and the normal stress σ_N are shown in Fig. 4.13 for normal specimens, respectively. Additionally, the relationships between (τ_p/σ_N), (τ_r/σ_N) and σ_N are shown in Fig. 4.14 for combined specimens, respectively. The stress ratio at a certain normal stress is defined as the inclination of a secant line at the normal stress on the failure line. Therefore, for the failure line with cohesion, when the normal stress is lowered, the stress ratio becomes higher. For all cases, the stress ratio at peak state considerably decreased with increased normal stress. For values of σ_N greater than 200 kPa, the stress ratio at the residual state was essentially constant and showed similar values for all compositions. For values of σ_N less than or equal to 100 kPa, there was a significant difference in the stress ratio. Such an increase in the stress ratio can be attributed to the existence of

apparent cohesion. Also, the values of the stress ratios at peak and residual states increased as the cement content increased. Under higher confined stresses, the bonding could be gradually broken, eventually leading to complete disappearance of cementation. Kaolin clay without cementation exhibits constant stress ratios, that are relatively unaffected by normal stress values exceeding 100 kPa. Based on the analysis above, it can be concluded that for a given value of confining stress, the influence of cementation is greater at low confining stresses and becomes smaller as the confining stress increases. According to our finding (Suzuki et al., 2007), this is a result of cementation-originated bonds being partially damaged by continuous large shear displacements.

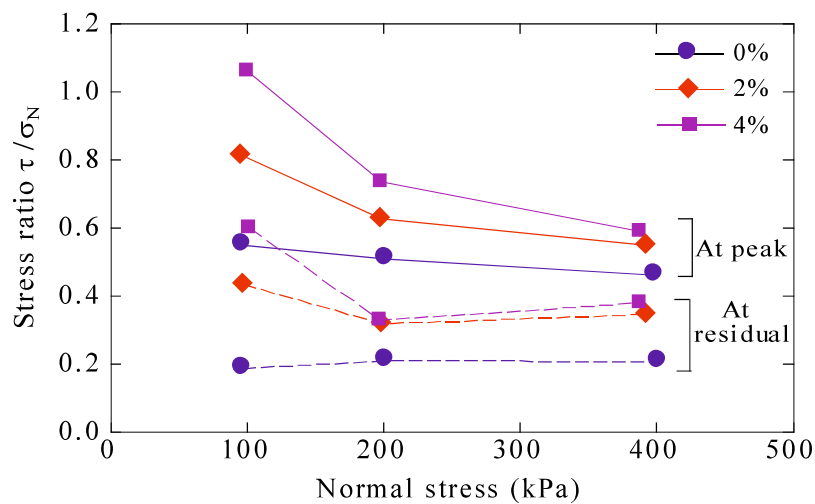


Figure 4. 13 Relationship between mobilized stress ratio (τ/σ_N) at peak and residual states and normal stress for normal specimens with different cement contents.

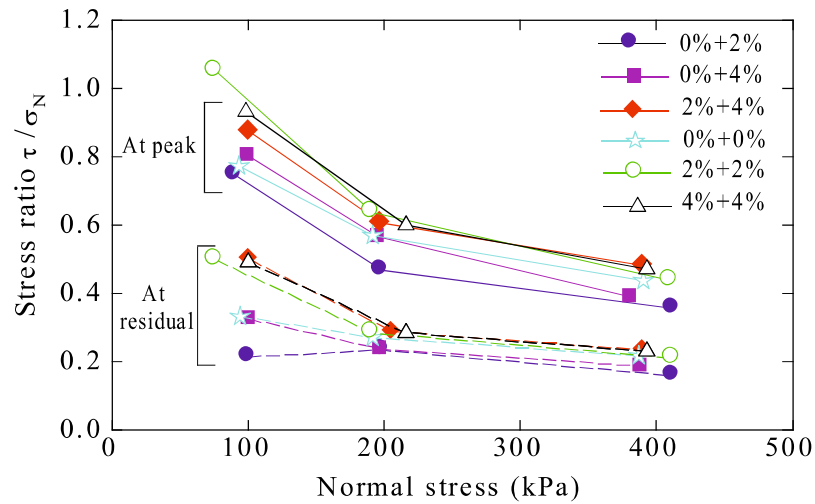


Figure 4. 14 Relationship between mobilized stress ratio (τ/σ_N) at peak and residual states and normal stress for combined specimens with different cement contents.

4.4 Effects of cement content in normal and combined specimens

Kaolin generally contains clay particles in which edge-to-face and edge-to-edge interlocking dominates the micro-structure. At most 2% and 4% cement content, the cementing material could not be identified in scanning electron microscope images (Lee, K.H. and Lee, S., 2002). From 5% to 10% cement content, the cementing structure could be seen, but not clearly. Only for cement contents greater than 10% did the available cementing structure become clearly apparent in SEM images. This means that the mechanical characteristics of kaolin with low cement content should change insignificantly as a function of cement content as well as curing time. However, as mentioned above, it is necessary to clarify the residual strength property of lightly-cemented clay related to earthquake-induced landslides occurring in areas containing natural cemented soil.

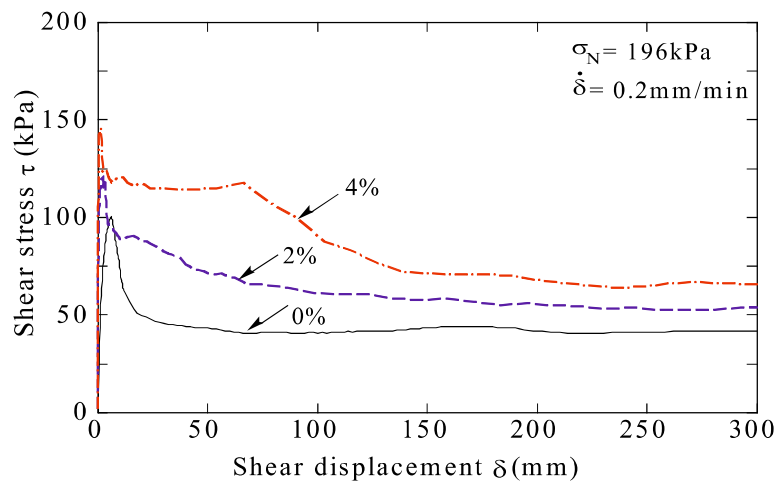


Figure 4. 15 Shear stress and shear displacement curves for cemented kaolin clay with various cement contents.

Fig. 4.15 shows the shear stress and shear displacement curves for cemented kaolin with various cement contents. The test results were obtained from 0%, 2% and 4% cemented normal specimens with an initial confining stress of 196 kPa and a curing time of 3 days. It can be seen from this figure that cement content highly influenced peak strengths, with cemented kaolin having significantly higher values than non-cemented kaolin for a given normal stress. Also, the shear stress at residual state appeared to increase with increased cement content. The specimens with higher cement content appeared to reach peak strength after only a small displacement. This indicates that increased cement content resulted in increased stiffness, thereby reducing the specific shear displacement at which peak strength is attained. This observation is consistent with results from the findings of [Horpibulsuk et al. \(2004, 2005\)](#), which conclude that the peak strength of cemented clay is a function of cementation, not interlocking. The interlocking is thought to affect only the residual strength. Furthermore, it can be recognized that shear stress and shear displacement relationships show an apparent trend from strain hardening to post-peak strain-softening behaviour, corresponding to an increase in the cement content.

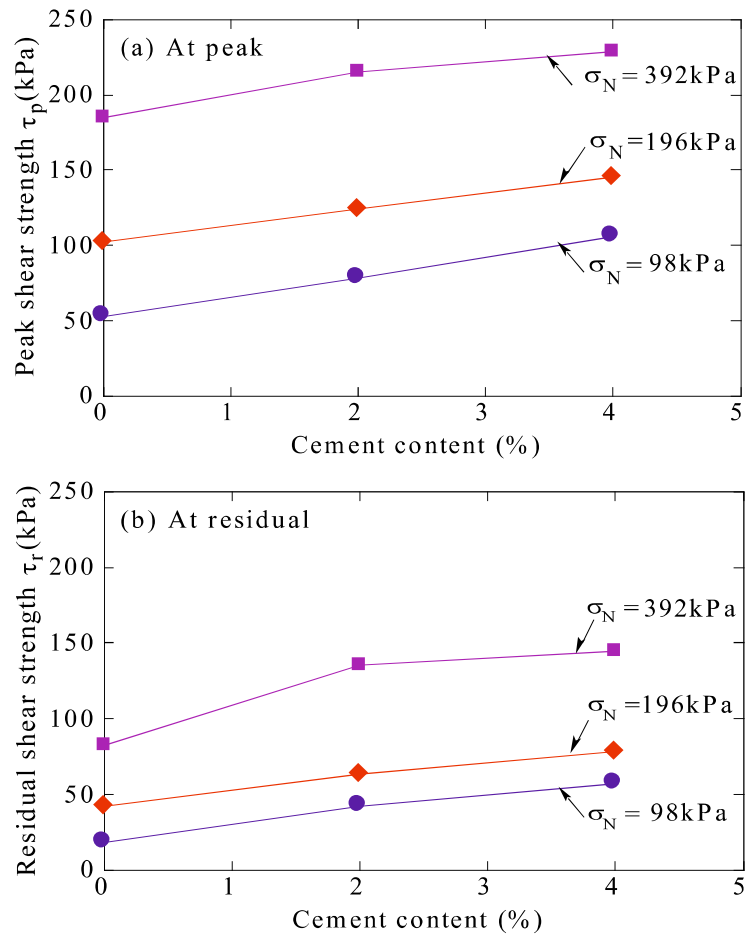
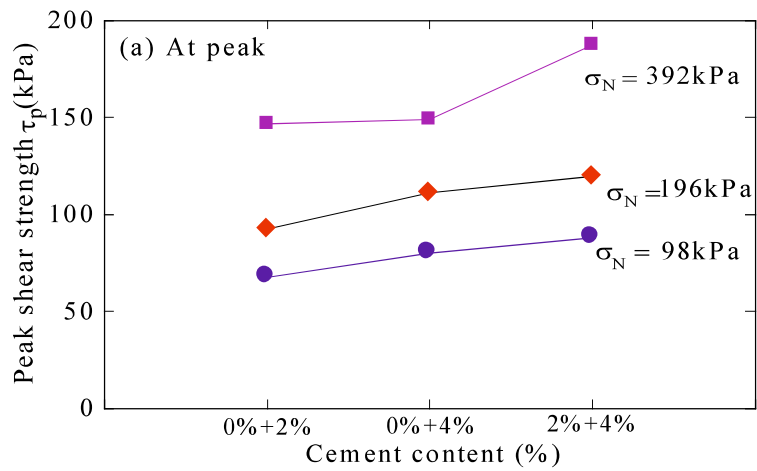


Figure 4. 16 Relationship between (a) peak and (b) residual drained shear strength and cement content for normal specimen.



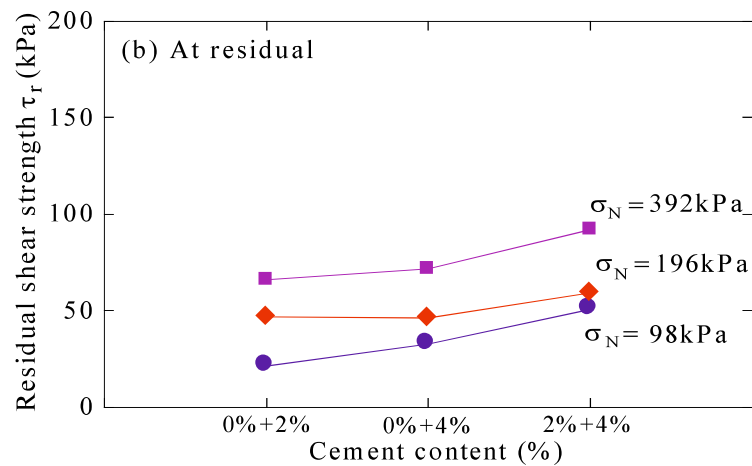


Figure 4. 17 Relationship between (a) peak and (b) residual drained shear strength and cement content for combined specimen.

Figs. 4.16 (a) and (b), and Figs. 4.17 (a) and (b) show the relationships between peak and residual drained shear strengths and the cement content for normal and combined specimens, respectively. For normal specimens, the peak and residual drained shear strengths increased slightly as cement content increased, and seemed to become insignificant at a normal stress of 392 kPa. The combined specimens demonstrated a similar trend of residual strength to that of the normal specimens. As mentioned in Fig. 4.6 and 4.9, the residual friction angle is independent of the average cement content for combined specimen, and the residual cohesion gradually increases with increasing the average cement content. This finding implies that the shear strength at the binding interface of combined specimens improved. Thus, the increase in both shear strengths is thought to result from adhesions on the pre-existing surfaces caused by continued cement hydration.

4.5 Effects of curing time on the residual strength of normal specimens

The effect of curing time on the residual strength of cemented kaolin was investigated by performing ring shear tests on cemented kaolin cured at various time intervals. According to Lee, K.H. and Lee, S. (2002), the strength of the cement-kaolin mixture does not improve over time after 28 to 56 days. Therefore, cemented kaolin samples referenced in this section were cured for the maximum period of 28 days. Figs.

4.18 (a) and (b) show the results of the ring shear test on 2% and 4% cemented kaolin samples with curing times of 3, 14, and 28 days. The shear displacement rate was fixed at 0.2 mm/min under a normal stress of 196 kPa. The calculated results showed the 2% cemented sample with 28 days of curing to have a residual strength approximately 25.3% higher than samples cured for 3 days. The corresponding strength increase was approximately 12.2% for the 4% cemented sample.

Fig. 4.19 presents the results for peak and residual strengths versus curing time. The residual strengths of 4% cemented kaolin slightly increased for curing time up to 28 days, whereas the residual strength of 2% cemented kaolin increased for curing time up to 14 days, after which they were nearly constant with curing time. The peak strength of 2% cemented kaolin also increased with curing time. In contrast, the measured peak strength of 4% cemented kaolin was nearly constant, thereby indicating that it was independent of curing time. A high peak strength developed rapidly even when the specimen was cured for only 3 days. This is because kaolin having higher cement content behaves in a more brittle manner, causing the cement bonds to fail upon small displacements. Cemented kaolin with lower cement content of 2% resulted in softening behaviour, depicted by the slight linear increase similar to that of the residual state. For only these test results, the influence of the curing time within 28 days did not significantly influence the peak and residual shear strengths. However, there may be an effect on both strengths for a curing time exceeding 28 days.

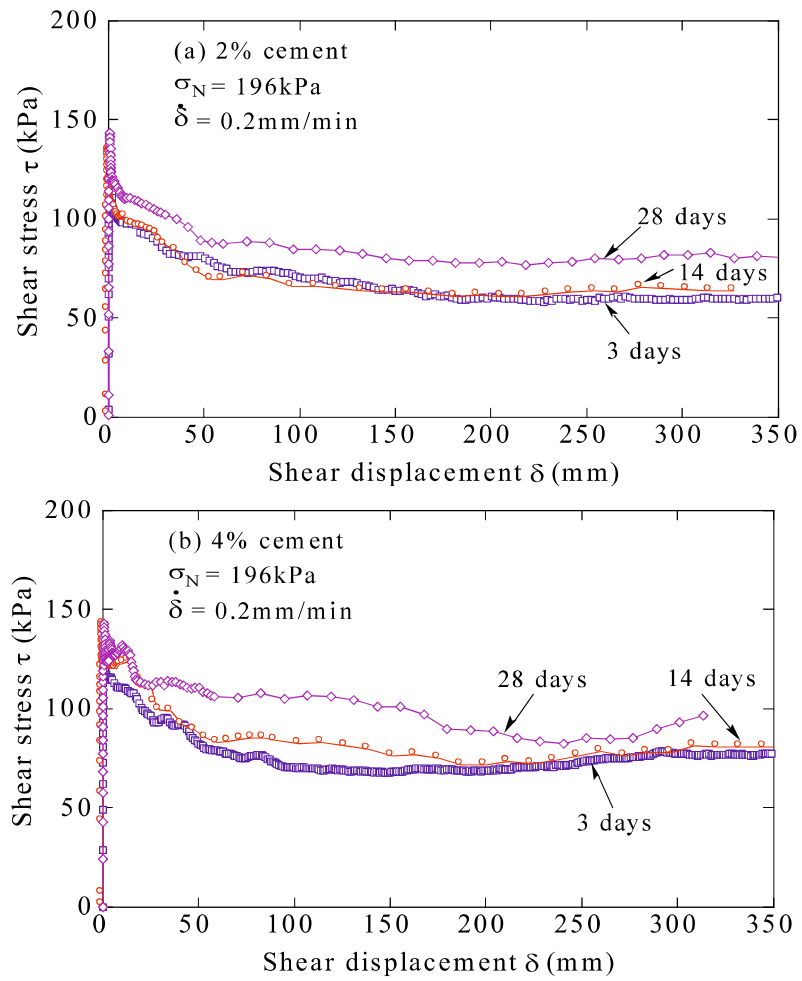


Figure 4. 18 Shear stress and shear displacement curves under different curing time for cemented kaolin specimen.

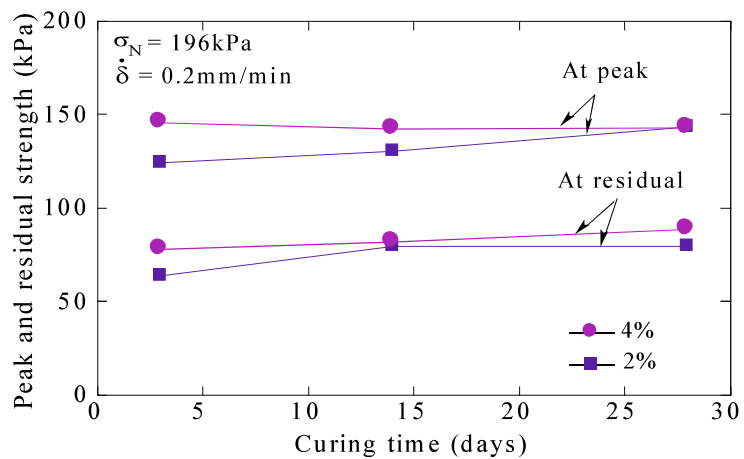


Figure 4. 19 Relationship between peak and residual strength, and curing time for 2% and 4% cement kaolin specimens.

4.6 Residual state characteristics of multistage ring-shear tests

An extensive investigation of the multistage ring-shear test was carried out on non-cemented and cemented kaolin samples, as well as two-part combinations of non-cemented and cemented kaolin samples, with target normal stress values of 98, 196, 294, and 392 kPa. The following four sample types were chosen in this additional study: 0%, 4%, 4% + 0%, and 4% + 2% cemented kaolin. On the other hand, the results of the single-stage tests of these samples are also used in this section for a comparative analysis. As mentioned in the previous section, the multistage technique should only be applied to a limited number of stages owing to soil loss throughout the gap between the two halves of the shear box. Thus, these confined normal stress levels are considered to be suitable for the multistage ring-shear test. In the present investigation, the single-stage test is defined as a single sample testing method for each normal stress (Method 1), and the multistage test consists of two methods, namely the increasing load multistage (Method 2) test and the reducing load multistage (Method 3) test. Here, the term ‘load’ is defined as the normal stress that a sample is subjected to in the process of increasing and decreasing the load during the multistage test. In this test, after the residual strength is obtained under the first normal stress, shearing is stopped, allowing the consolidation of the sample to occur for a short time period of 1 h. Thereafter, shearing is increased or decreased according to the subsequent stress levels. This procedure is repeated for a number of stress levels.

The shear stress–displacement curves obtained using the multistage ring-shear test for various types of specimens are shown in **Figs. 4.20 (a) and (b)**. For each test, the shear stress–shear displacement relationship at the residual state corresponding to four normal stress levels are plotted. These curves illustrate a clear variation in the residual strength as the normal stress is altered. The shear stress of the 4% cemented kaolin shows the highest value among all the tested specimens. It can also be observed from these figures that the peak strength can only be obtained during the first stage of the multistage test. Furthermore, after reaching the residual state during the first stage of the test, an additional displacement is necessary to obtain the different residual states for all the specimens.

Figs. 4.21 (a) and (b) show the relationship between normal stress and settlement obtained by conducting the multistage test on all the specimens. In method 2, the settlement increased with an increase in the normal stress, and the different stress values depended on the sample type. The settlement values of specimens obtained by method 3 increased rapidly in the first stage, and then decreased slightly thereafter as the normal stress increased. This reduction in settlement can be readily attributed to the dilatant behaviour of the soils. It can be apparently observed that the normal stress–settlement curve of the 4% + 2% combined-cement kaolin sample was similar to that of the 4% + 0% combined-cement kaolin sample, a characteristic that was different from the normal cemented samples.

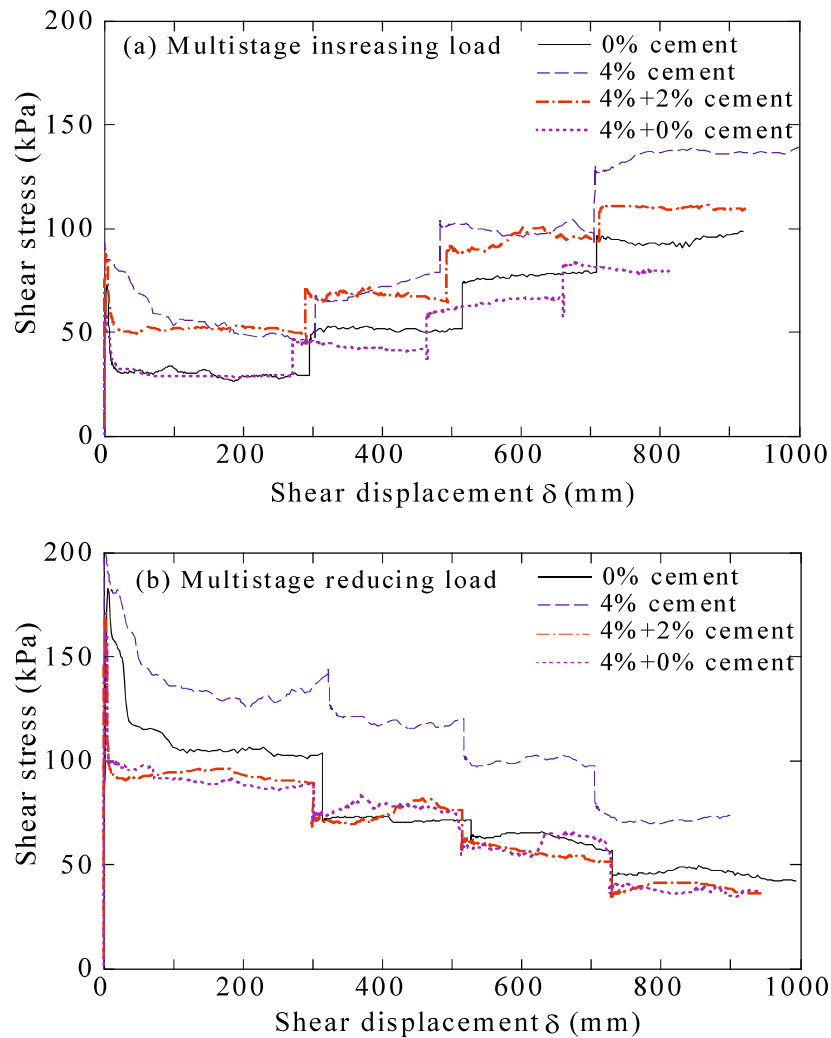


Figure 4. 20 Shear stress-displacement curves for four kinds of specimens by increasing (a) and reducing (b) load MRST.

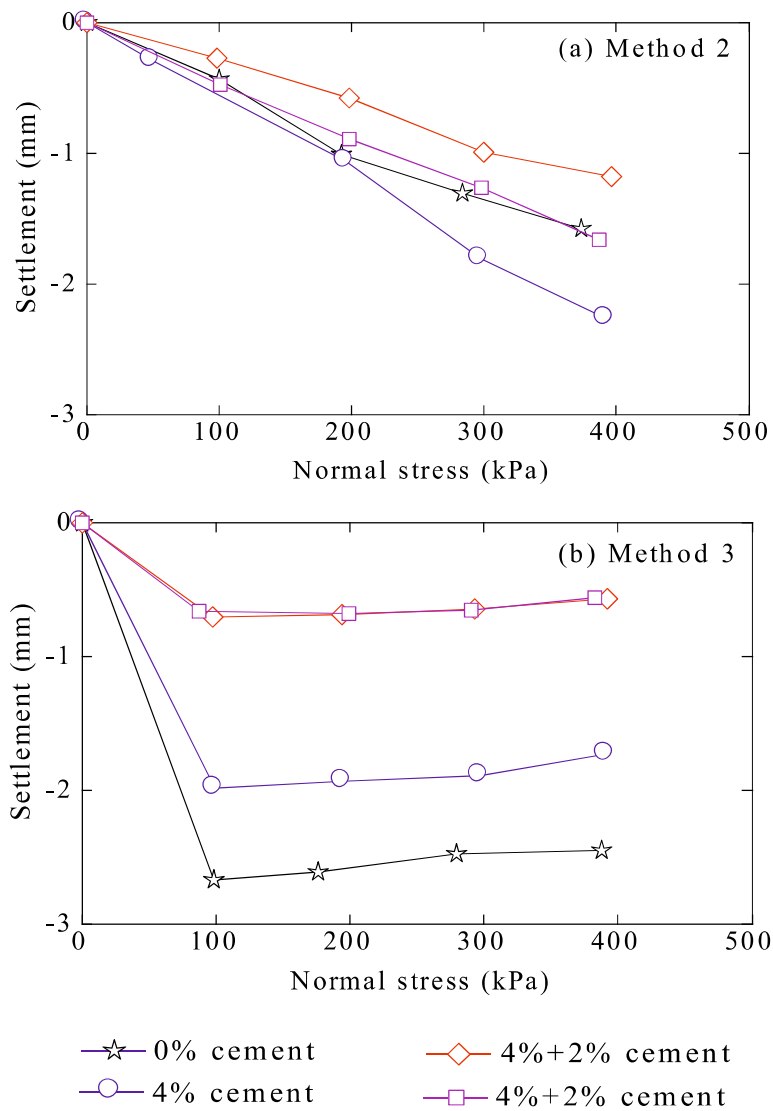
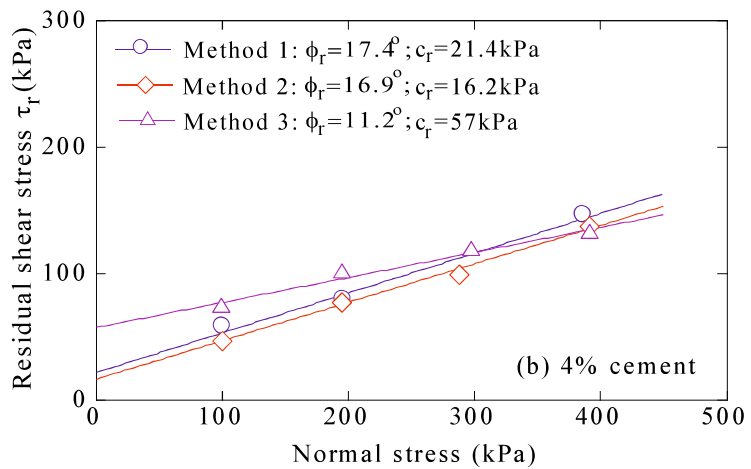
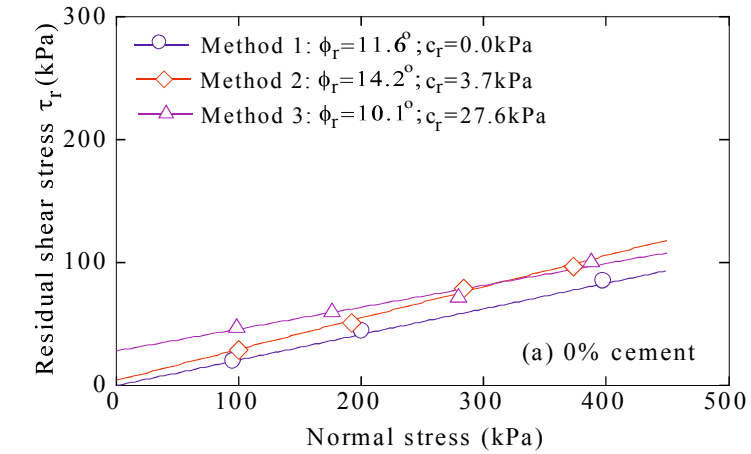


Figure 4. 21 Normal stress-settlement relationship for all specimens conducted by (a) method 2 and (b) method 3.

Figs. 4.22 (a)-(d) illustrate the residual shear strength envelope obtained by various testing methods for all the samples, from which the value of c_r and ϕ_r are seen to be well-defined. These figures show that all envelopes exhibit the apparent residual cohesions, irrespective of the sample type or the type of method used. In previous studies, the residual failure envelope had either been considered as a curve because of the progressive de-bonding with the increasing total stress (Lupini, 1981; Skempton, 1985; Stark and Eid, 1994), or as a linearly approximate straight line, depending on the purpose of the geotechnical designation, as well as soil materials. This problem was mentioned

in the chapter ‘literature review’ and has not been discussed further in this section. In this comparative evaluation, these envelopes are conveniently described as a straight line through the origin. It can be seen that the residual envelopes obtained by methods 1 and 2 in the 4% cemented kaolin sample and those obtained by methods 2 and 3 in the 4% + 2% cemented kaolin sample appear to be parallel to each other, suggesting that the value of ϕ_r is the same.



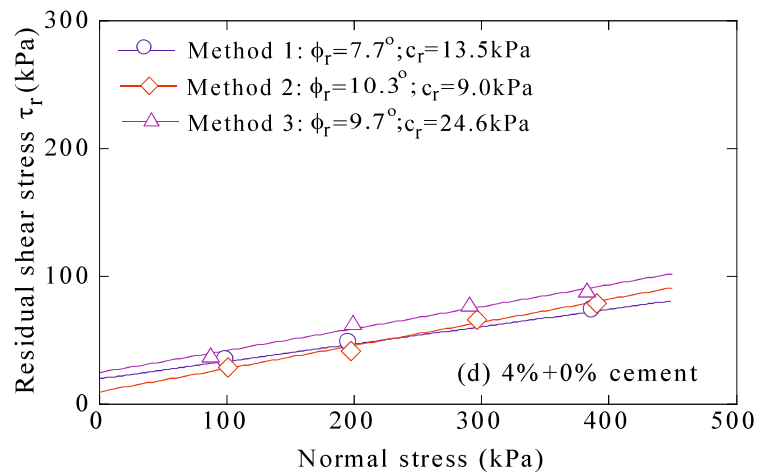
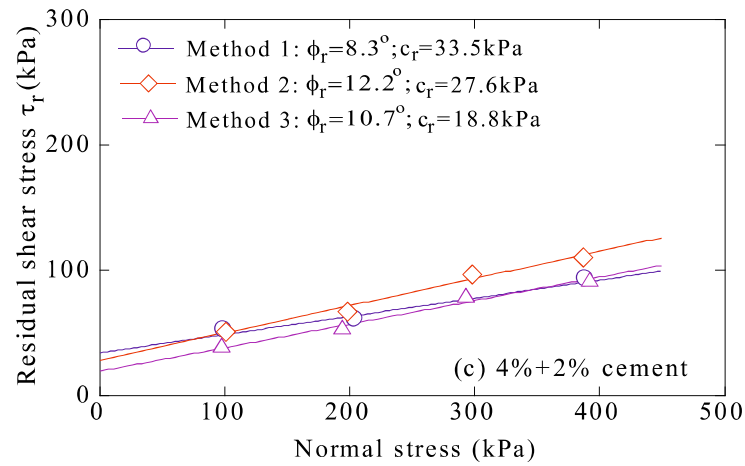


Figure 4. 22 Residual shear strength envelopes of all samples obtained by various testing methods.

Fig. 4.23 shows the residual friction angles obtained by all methods for all the tested samples. The residual friction angle obtained by method 2 was always higher than that obtained by method 1 for all samples, except for the 4% cement specimen. However, the residual friction angle obtained by method 3 was found to be lower for the normal samples, and higher for the combined samples, when compared with the friction angle obtained by method 1. This result indicated a different tendency between the two types of specimens. While comparing methods 2 and 3, it was found that the residual friction angle obtained by method 3 was always lower than that obtained by method 2 for all specimens. Additionally, although all the sample types showed a high difference in residual friction angles in the single-stage test, for instance, an absolute value of 9.7° was observed based on a comparison between the 4% and the 4% + 0% cemented kaolin

samples, in the multistage test, this difference was insignificant, with an absolute value of 1.5° being obtained by method 3 for all samples. The reason for this behaviour is not clear and needs further research. This behaviour partly contributes to the disadvantages of the multistage reducing load ring-shear test.

For the 0% cemented kaolin sample, ϕ_r increased from 11.6° , obtained using method 1, to 14.2° , obtained using method 2, while the difference between the values obtained by methods 1 and 3 is only 1.5° . For the 4% cemented kaolin sample, the values of ϕ_r obtained by methods 1 and 2 are similar, whereas the value of ϕ_r obtained by method 3 is significantly lower than that obtained by method 1 with a difference of 6.2° . It is not certain why the 4% cemented kaolin sample shows such a high difference between the ϕ_r values when the multistage reducing load test is conducted. This difference is attributed probably to the cementation bonds due to a series of consecutively reducing load during the multistage test. Furthermore, it can be assumed that cementation not only increases the cohesion intercept, with a value that is approximately three times higher than that for the single-stage test, but it also reduces the angle of internal friction. The measured friction angle was lower than that in single-stage of about 6.2° , a highest value of all tested specimens. For the combined samples, the residual friction angle of the 4% + 2% cement sample obtained by method 2 was 3.9° higher than that obtained by method 1. This difference was 2.6° for the 4% + 0% cement sample.

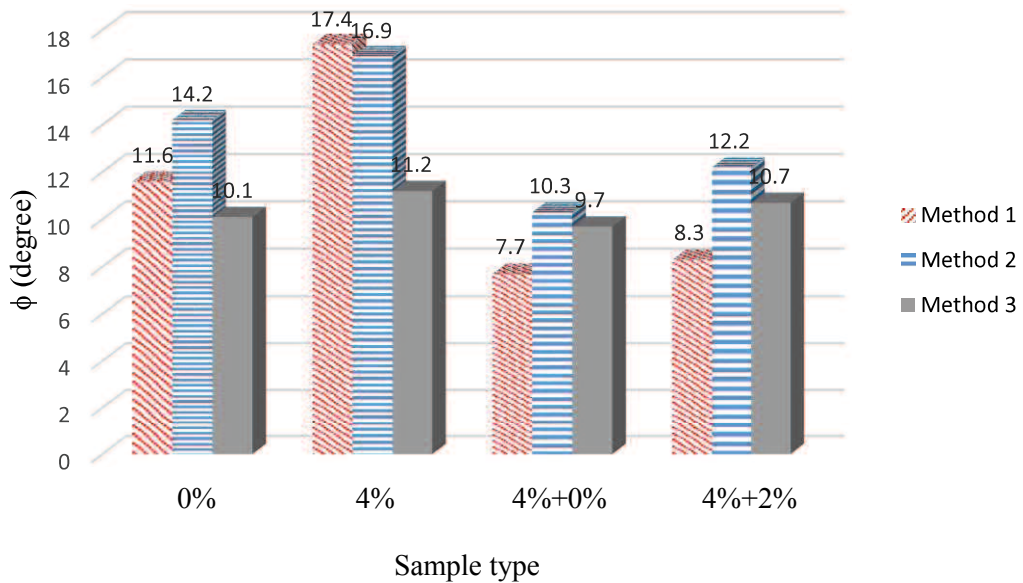


Figure 4. 23 Residual friction angle obtained by all methods.

Fig. 4.24 shows the residual cohesion intercept obtained by all the methods for all the tested samples. The residual cohesion intercept c_r obtained by method 2 was lower than that obtained by method 1 for all specimens, except for the 0% sample. This is due to a consecutive increment in the normal stress owing to the reduction of bonding between the clay particles. Meanwhile, the residual cohesion intercept obtained by method 3 was higher than those obtained by the other methods, except for the 4% + 0% cemented kaolin specimen, which may be due to an erroneous test. It can be clearly observed that the 4% cement sample exhibited the highest value of residual cohesion in the multistage reducing load test, with a measured value of 57 kPa, which is approximately three times compared to that obtained during the single-stage test. This observation probably has a relation with the dilatancy behaviour of the cementation material, which brings back a rebound of the bonds at the inter-particle surface in the process of reducing the normal stress. Another theory that may also be responsible for this observation is the development of slickensides for different sample types.

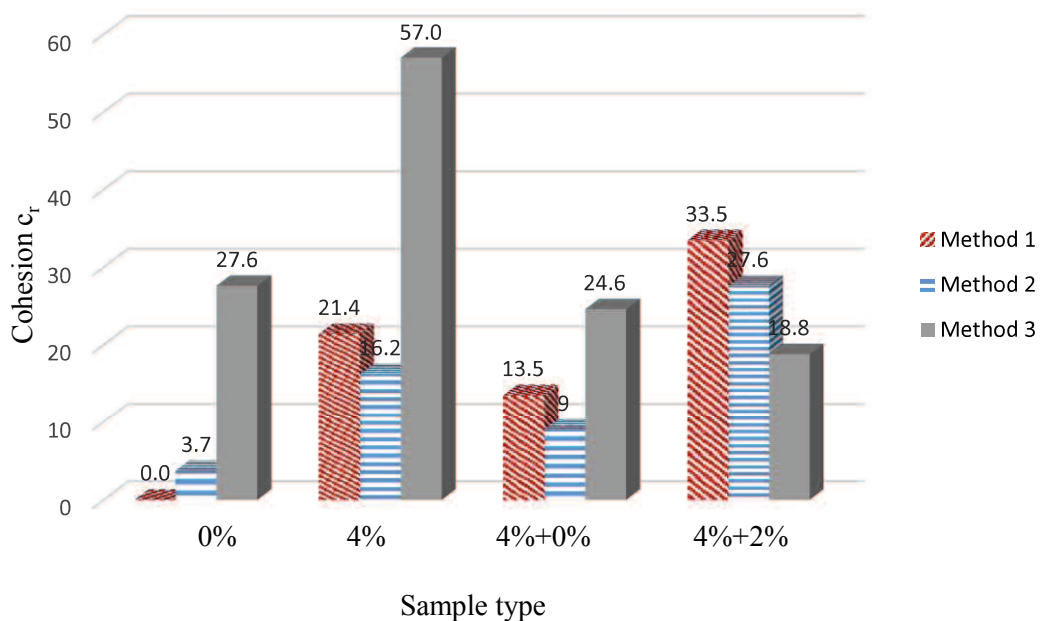


Figure 4. 24 Residual cohesion intercept obtained by all methods.

Based on the above mentioned results, between the two methods for the multistage ring-shear test, the multistage reducing load ring-shear test is the more -suitable method for the 0%, 4% + 0%, and 4% + 2% cemented kaolin samples, from a practical point of

view; it resulted in a wide range of residual friction angles, varying from 1.5° to 2.4°. A small variation is acceptable for stability analysis purposes. In contrast, the multistage increasing load ring-shear test is the more suitable method for the 4% cemented kaolin sample; the residual friction angle was only 0.5° in this case.

Figs 4.25 (a)-(d) illustrate the residual stress ratio (also defined as the residual friction coefficient τ_r/σ_N) plotted against the normal stress. For all specimens, it is apparent that there is a reduction in the residual stress ratio corresponding to the increased normal stress, and the ratio approaches a constant value in the end. This decrease is probably attributed to the increasing orientation of the clay particles under a higher normal stress. For kaolin, the residual stress ratio is nearly constant with an increase in the normal stress in method 2. It indicates that the residual friction angle is independent of the normal stress. In the 4% cemented kaolin sample, the τ_r/σ_N values at normal stress ranged from 98 kPa to 392 kPa, which is the widest range among all specimens. The percentage decrease in the residual stress ratio values is approximately 54.3%.

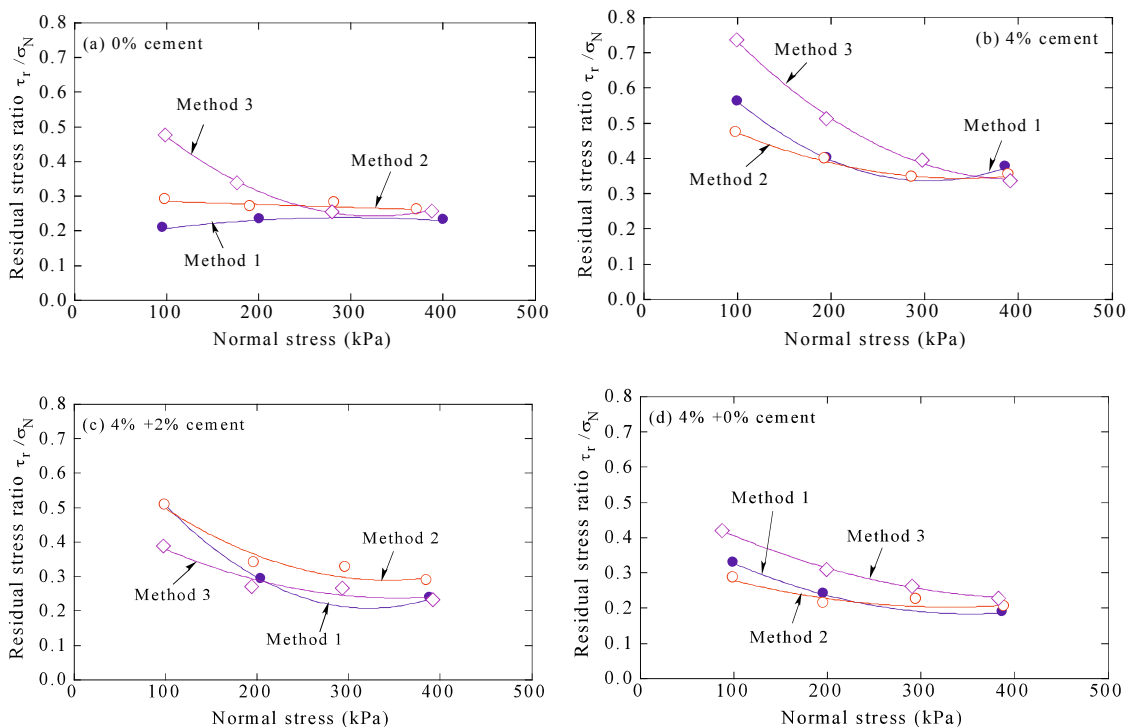


Figure 4. 25 Variation in residual strength for four kinds of specimen by all methods.

4.7 Observation the slickensides after test

Figs. 4.26 (a)-(d) show a visual inspection on the slickensides of the shearing zone in ring-shear tests for the 0%, 4%+0%, 2%, and 4% cemented kaolin specimens. As revealed by these photo, the slip surface of 4% cemented kaolin seemed to be undulating and non-planar, contrary to 0 % cemented kaolin which demonstrated a planar and polished slickenside. This occurred because the addition of 4% cement to kaolin clay results in a sample that becomes harder than normal. Hence, under a normal stress of 196 kPa, the slip surface did not develop completely. This implies that the degree of reorientation in the shearing direction became lower on an undeveloped rough shear surface so that the residual shear strength became higher. Thus, the residual strength of cemented kaolin for cement content higher than 4% is independent of the shearing rate for both normal and combined specimens. In addition, the process of multistage inducing load conducted on such slickensides may result in a turbulent zone, contributed to yield higher cohesion.

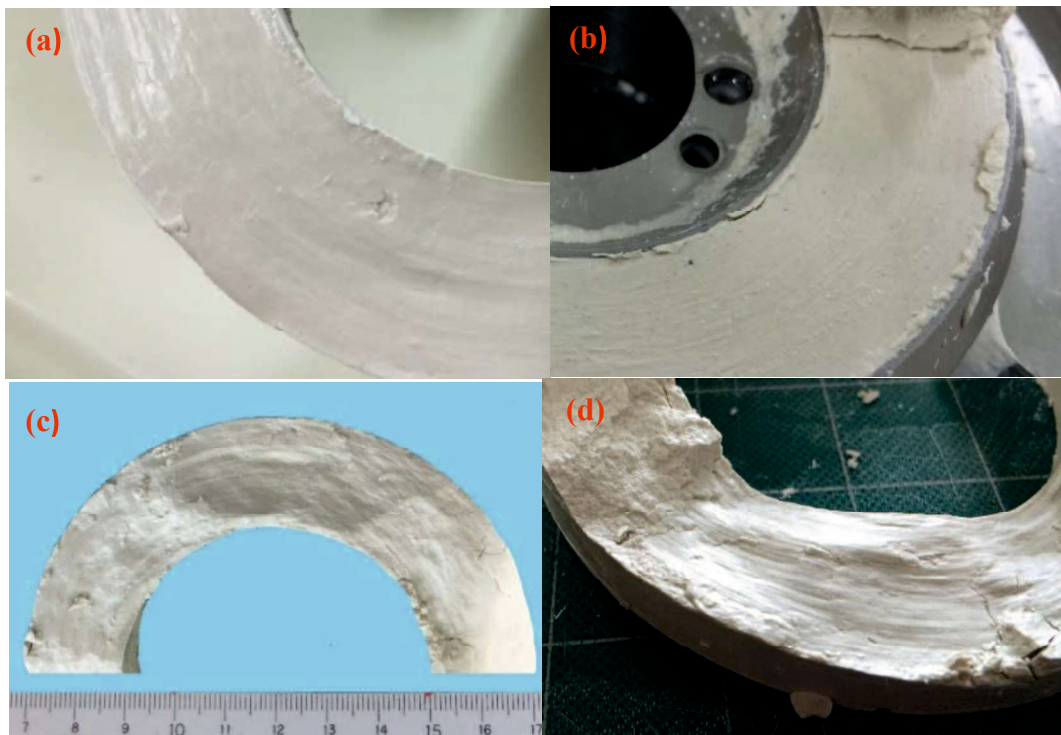


Figure 4. 26 Slickensides observed after ring-shear tests for (a) 0% cement, (b) 4%+0%, (c) 2%, and (d) 4% cemented kaolin specimens.

4.8 Summary

This Chapter 4 presents the results of monotonic ring-shear tests on cemented and non-cemented kaolin samples to investigate the strength characteristics of discontinuous plane materials. The presented results are discussed and compared to available data from the literature. This chapter also presents an experimental investigation into the multistage ring-shear test. The main conclusions can be summarized as follows.

1. The residual friction angle of cemented kaolin considerably increased by 6.2° with an increase in the cement content from 0% to 2%. This increase was not significant in cases where the cement content was increased beyond 2%.
2. The results of this study also show that the values of residual friction angle calculated on the contact surface between cemented and non-cemented kaolin specimens may be as much as 33.6% lower than those of pure kaolin. In addition, the intercept cohesion at the residual state, which can be fitted as a straight line passing through the origin, increased linearly according to cement content. The calculated average value of cohesion for combined cement kaolin samples was higher than that for cemented kaolin samples. These findings are quite meaningful in assessing the stability of earthquake-induced landslides that occur in areas with cemented soil. Especially, the residual cohesion on this discontinuous plane may control the instability of an earthquake-induced landslide rather than the residual friction angle.
3. For 0% and 2% cemented kaolin samples, the residual strength of combined samples was in good agreement with that of intact samples. In contrast, the residual strength of the 4% combined samples decreased by approximately 12.0–14.1% from that of intact samples.
4. The residual strength of cemented kaolin showed an insignificant increase with curing time up to 14 days, and then slightly increased with curing time. At a curing time of 28 days, the residual strengths of 2% and 4% cement-content samples were approximately 25.3% and 12.2% higher than those with 3 days curing, respectively. In contrast, the curing time showed a minimal effect on the strength at peak state.

5. The difference in residual friction angles measured by the increasing load multistage and the reducing load multistage ring-shear tests and those measured by single-stage ring-shear tests varied from a minimum of 0.5° to a maximum of 6.2° for all the tested samples. Between the two multistage methods, the multistage reducing load ring-shear test was recognized as the more -suitable method, which resulted in a wide range of residual friction angles, varying from 1.5° to 2.4° . In contrast, the multistage increasing load ring-shear test was the more -suitable method for the 4% cemented kaolin samples, which resulted in a residual friction angle of only 0.5° .
6. The effect of cementation on the residual cohesion intercept was identified for the 4% cemented specimen in the multistage reducing load test with a value that was approximately three times higher than that obtained in the single-stage test.

Chapter 5 RATE EFFECT ON RESIDUAL STRENGTH OF DISCONTINUOUS PLANE MATERIALS

5.1 Rate effects on residual strength at the contact surface between non-cemented and cemented clays

The effect of the shear displacement rate on residual strength is very important for evaluating residual strength of natural pre-existing shear surfaces, even though many researchers have found this effect to be small. Reactivated landslides could result from very slow movements to very rapid movements, such as those caused by earthquakes. In order to clarify the residual strength characteristics of cemented and non-cemented clays subjected to such fast shearing, a series of ring shear tests was carried with varying shear displacement rates across multiple specimens. The shear displacement rate was varied within a range of 0.04 to 20 mm/min. The normal stress, σ_N , was fixed at 196 kPa.

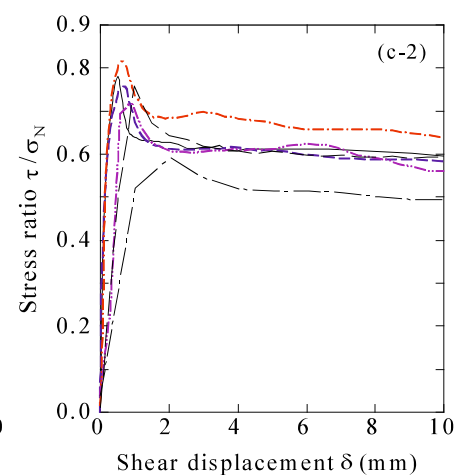
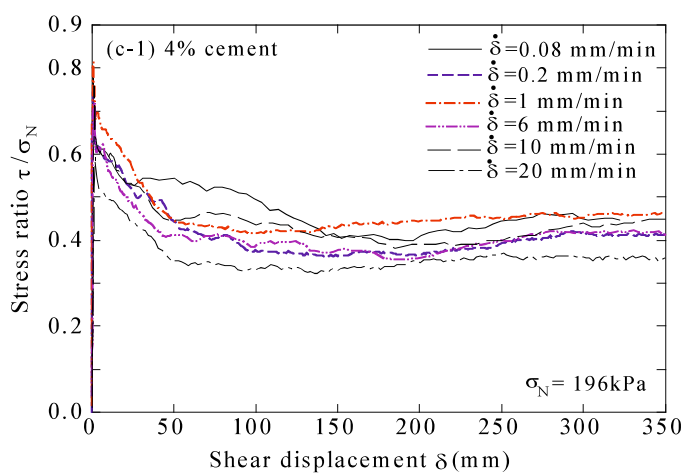
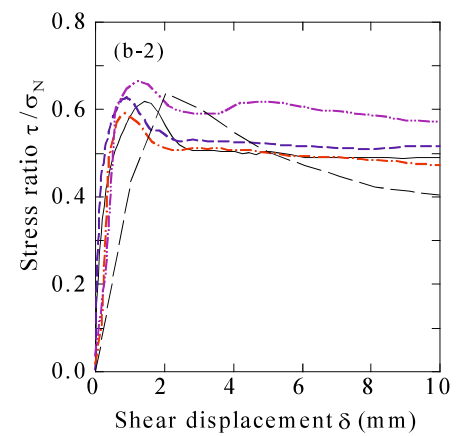
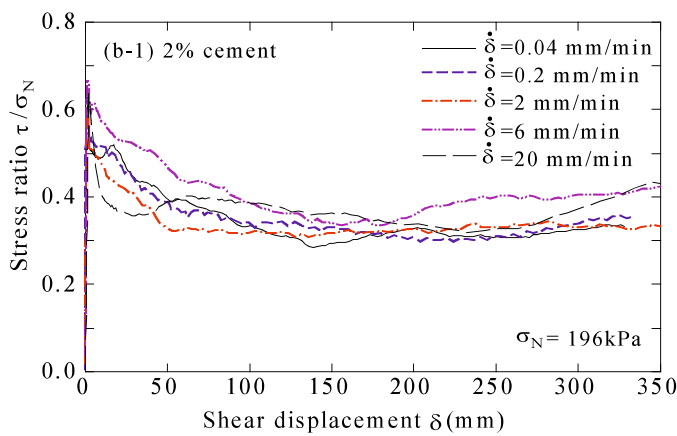
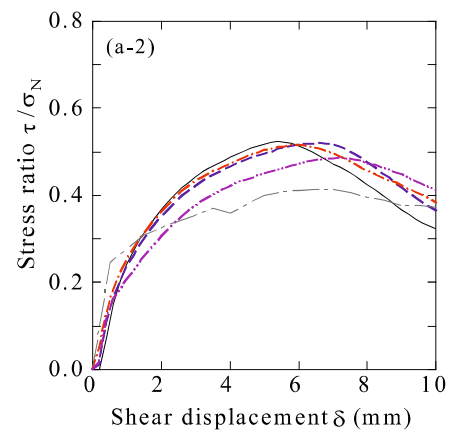
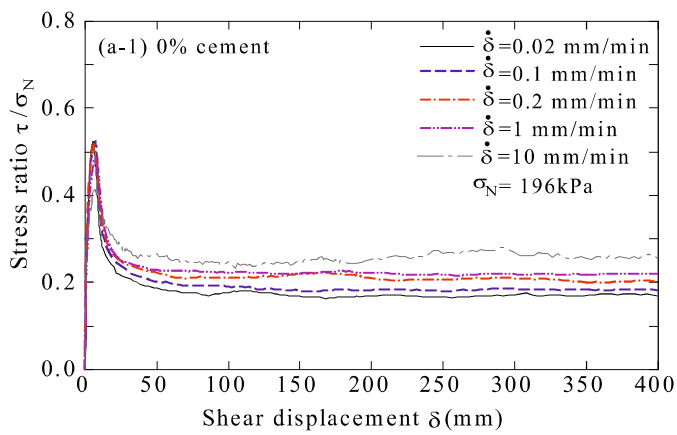
According to the literature, the magnitude of the residual strength can be affected less or more as the shear speed varies, because of differences in the types of clay soil. Investigations supporting this were conducted by various researchers; [Skempton \(1985\)](#), [Lemos et al. \(1985\)](#), [Tika et al. \(1996\)](#), [Suzuki et al. \(2000, 2001, 2007\)](#), [Bhat et al. \(2013\)](#), [Kimura et al. \(2013\)](#), [Khosravi et al. \(2013\)](#) and [Gratchev and Sassa \(2015\)](#). Amongst them, [Skempton \(1985\)](#) emphasized that the change in residual strength can be neglected when the shear displacement rate is changed within a range of 0.002 to 0.01 mm/min, a range generally adopted for laboratory tests. [Bhat et al. \(2013\)](#) investigated the effects of shearing rate on the residual strength of kaolin clay and concluded that the residual strength of kaolin clay was almost identical for shearing speeds of 0.073 mm/min and 0.162 mm/min but increased slightly as the shearing rate increased from 0.233 mm/min to 0.586 mm/min.

On the other hand, [Lemos et al. \(1985\)](#) pointed out that the residual strength either increased (positive rate effect), decreased (negative rate effect), or remained constant (neutral rate effect) depending on various factors such as clay fraction and dominant clay mineral type. [Tika et al. \(1996\)](#) showed that residual strength dependency on rate was significantly related to the change in the void ratio of the shear zone. In addition to the

positive and negative changes in the shear strength during fast shearing, a small increase in residual strength was found as the shear rate decreased (Gratchev and Sassa, 2015). Many factors such as pore water pressure, shear mode, and void ratio of shear zone were proposed to explain the dependence of residual strength on shearing speed. Thus, a mechanism controlling residual strength that explains general rate effects for all types of clays with varying amounts of cementation is still unknown. Furthermore, the rate dependence of residual strength for specimens having bedding planes has not yet been elucidated. The rate effect on residual strength at contact surfaces between non-cemented and cemented clays is discussed in this section. However it should be noted that test results used to evaluate the rate effect were analysed from a viewpoint of total stress, since pore water pressure inside the specimens was not measured by the ring shear device used in this study. Test cases and test results of cemented and non-cemented kaolin samples at various different shear speed are summarized in [Table 5.1](#)

Table 5. 1 Test cases and test results of cemented and non-cemented kaolin samples under different shear rates

Soil sample	Test No.	Shear rate		Normal stress σ_N (at peak) (kPa)	Normal stress σ_N (at residual) (kPa)	Peak strength τ_p (kPa)	Residual strength τ_r (kPa)	Stress ratio at peak τ_p / σ_N	Stress ratio at residual τ_r / σ_N
		(mm/min)	(deg/min)						
% cement	1-4	0.02	0.03	188	184	98.5	31.8	0.524	0.173
	1-5	0.1	0.14	189	181	97.8	33.1	0.519	0.183
	1-2	0.2	0.29	202	202	102.5	42.4	0.507	0.210
	1-6	1	1.43	204	203	99.0	44.1	0.485	0.217
	1-7	10	2.87	194	196	80.4	51.8	0.414	0.264
2% cement	2-4	0.04	0.06	196	199	121.3	61.4	0.619	0.308
	2-2	0.2	0.29	198	199	123.9	63.7	0.626	0.320
	2-5	2	2.9	197	197	116.5	64.5	0.591	0.327
	2.6	6	8.6	197	198	130.5	79.4	0.663	0.401
	2-7	20	29	195	214	124.1	83.3	0.636	0.389
4% cement	3-4	0.04	0.12	199	197	149.9	82.0	0.753	0.416
	3-2	0.1	0.29	195	194	145.6	78.1	0.747	0.403
	3-5	1	1.43	192	192	156.1	87.0	0.813	0.453
	3.6	6	8.6	200	200	138.9	77.5	0.695	0.388
	3-7	10	14.32	197	198	144.4	80.6	0.733	0.407
	3-8	20	29	202	202	148.5	84.7	0.735	0.420
2% + 0% cement	4-4	0.04	0.058	196	198	95.7	28.8	0.488	0.146
	4-2	0.2	0.29	198	199	92.7	46.7	0.468	0.235
	4-5	10	14.32	195	196	85.2	51.3	0.437	0.262
	4-6	20	29	201	202	82.1	55.6	0.408	0.275
2% + 4% cement	5-4	0.08	0.12	201	202	122.0	53.8	0.607	0.266
	5-2	0.2	0.29	197	206	119.6	59.5	0.607	0.289
	5-5	2	2.9	196	198	123.4	62.9	0.630	0.318
	5-6	10	14.32	191	192	112.9	71.9	0.591	0.375



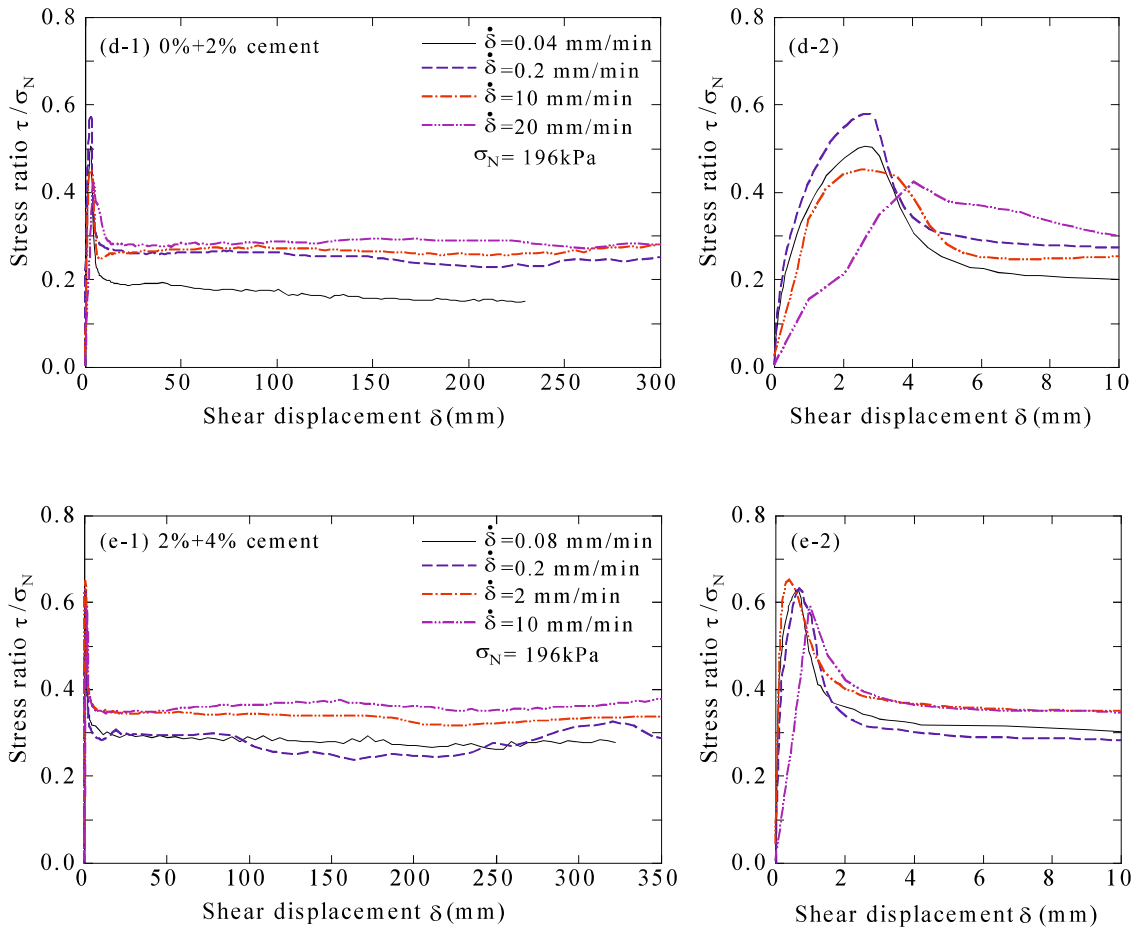


Figure 5.1 Shear behaviors of normal and combined specimens tested under various shear displacement rate.

Figs. 5.1 (a)-(e) show the relationships between the stress ratio and the shear displacement for the various samples under different shear displacement rates. Here, the stress ratio is defined as the value of shear stress divided by total normal stress. It can be seen that the stress ratio and shear displacement curves were dependent on the shear displacement rate. For the case of normal specimens, the stress ratio for each cemented sample gradually decreased with increased shear displacement, whereas the stress ratio for non-cemented clay rapidly decreased. The difference in shear behaviour may be caused by a disappearance of cementation. On the other hand, for combined specimens, the stress ratio rapidly decreased and nearly reached a constant value as shearing progressed. As the shear displacement rate increased exponentially, the stress ratio rose rapidly, and then dropped accompanied by a fluctuation of the stress ratio. These figures show that almost all samples are affected by changes in the shear displacement rate.

Figs. 5.2 (a) and (b), and Figs. 5.3 (a) and (b) demonstrate the effect of shearing rate on stress ratio based on a detailed comparison for different cases. In the case of normal specimens, both the peak and residual stress ratios were primarily affected by changes in the shear displacement rates for a range of 0.02 mm/min to 20 mm/min. The measured stress ratio at peak state for 0% cement decreased above 0.2 mm/min. This phenomenon may be induced by generation of unknown excess pore water pressure near the shear surface resulting in a reduction of the effective normal stress. These findings are in good agreement with previous results (Suzuki et al., 2000; 2001). In contrast, the measured stress ratios at peak state for 2% and 4% cement tended to remain almost constant over the whole range of shear displacement rates. This implies that the pore water inside the specimen did not migrate as a result of cementation.

On the other hand, the residual stress ratio of 2% cemented kaolin was almost constant at shear rates below 2 mm/min, and slightly increased as the shear rate increased. The stress ratio at the residual state for 0% cemented kaolin slightly increased when the shear rate was larger than 0.1 mm/min. This trend is similar to previous results of pure kaolin (Suzuki et al., 2000, 2001), which suggests that only 2% cement kaolin shows an insignificant effect of fast shearing on the residual strength. Suzuki et al. (2001, 2007) also reported that the rate of displacement affects the residual strength of clays in a range of 0.02 to 2.0 mm/min, and suggested that the rate effect of residual strength depends on the physical properties of the soil such as plasticity index, clay fraction and activity. This is thought to be a result of any physicochemical change of material in slip, specifically, an increase in viscosity of the sheared soil or an increase in real contact area of the shear surface. For 4% cemented kaolin, the residual stress ratio exhibited an unclear trend that may be considered approximately constant (neutral rate effect) as the shearing displacement rate increased. This neutral rate effect could be attributed to undulating shear behaviour resulting from poor or discontinuous slickenside development, which appears to exhibit a correlation to turbulent shear mode.

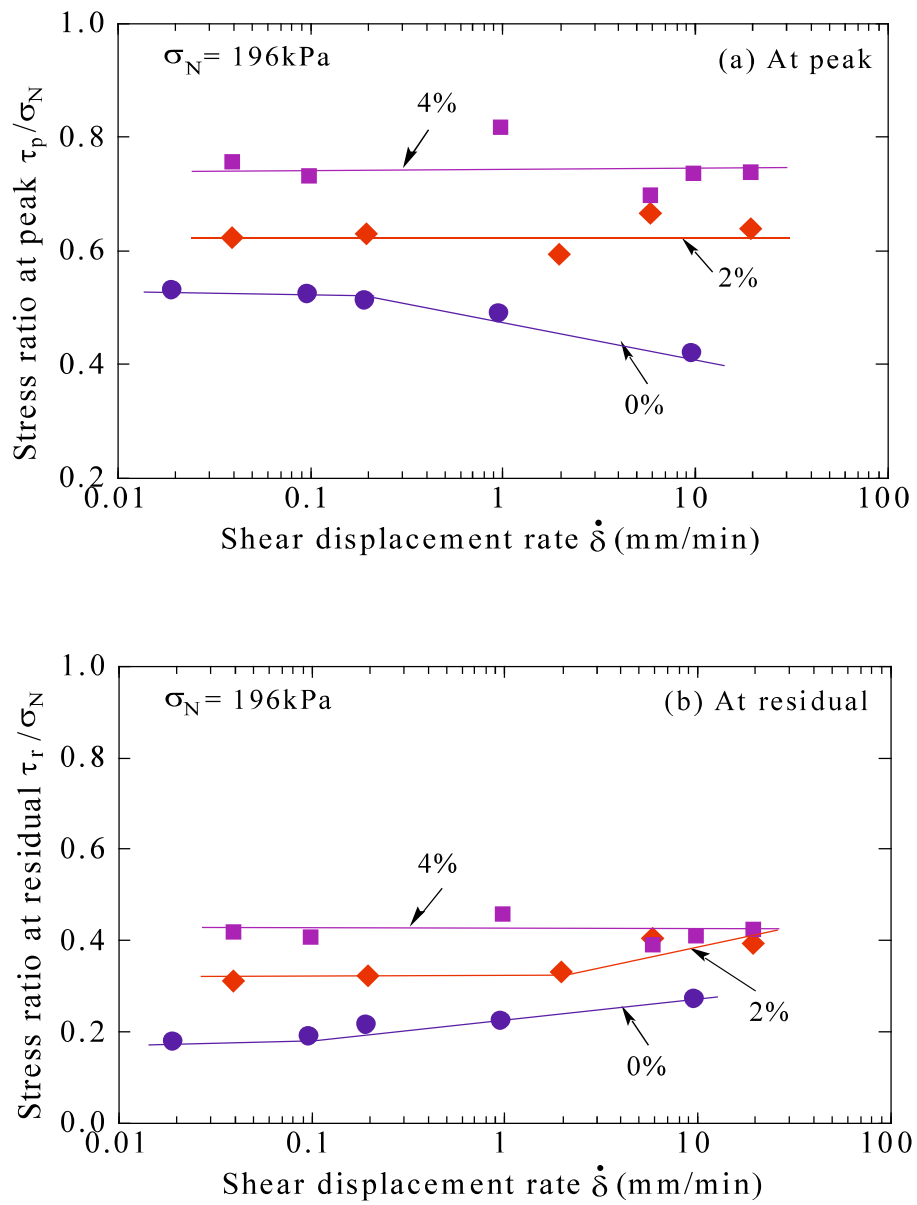


Figure 5. 2 Variation of stress ratio at (a) peak and (b) residual states with shear displacement rate for normal specimen with various cement contents.

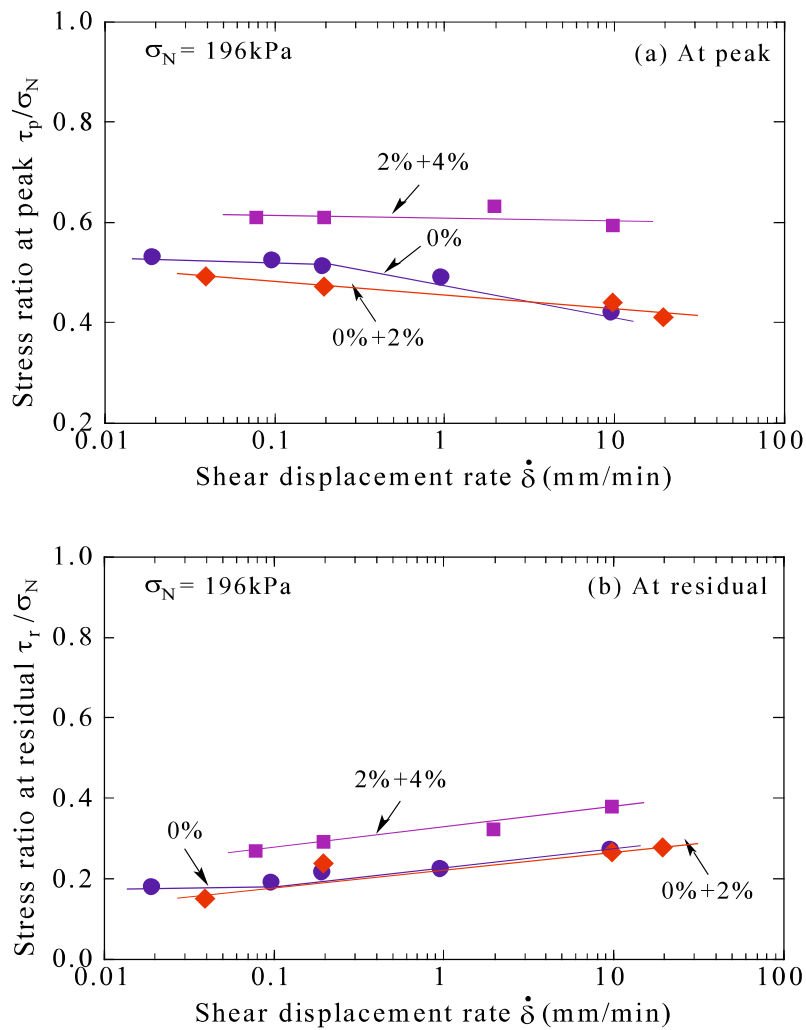


Figure 5. 3 Variation of stress ratio at (a) peak and (b) residual states with shear displacement rate for normal and combined specimens.

Next, in the case of combined specimens, the stress ratio at peak state for 0% + 2% cement decreased with increased shear displacement rate, similar to the trend found in the case of pure kaolin (0% cement). This decrease may result from the generation of pore water pressure in upper half of specimen during fast shearing which results in a reduction of the effective normal stress on the contact surface. For 2% + 4% cement, the stress ratio at peak state did not change due to the entrapment of pore water in each half of specimen. The stress ratio at the residual state of combined specimens, as well as normal specimens, increased linearly according to increasing shear displacement rate. As mentioned above, the slip failure occurred on the contact surface between two material layers having different hardness values resulting from the cementation process.

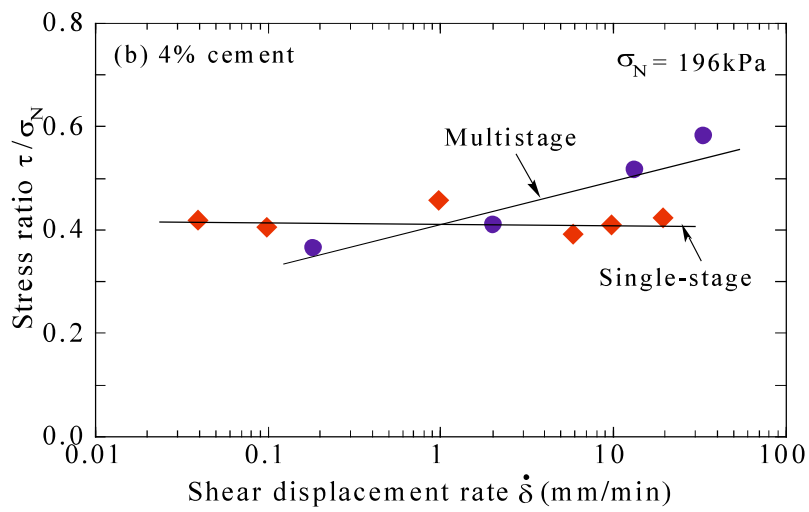
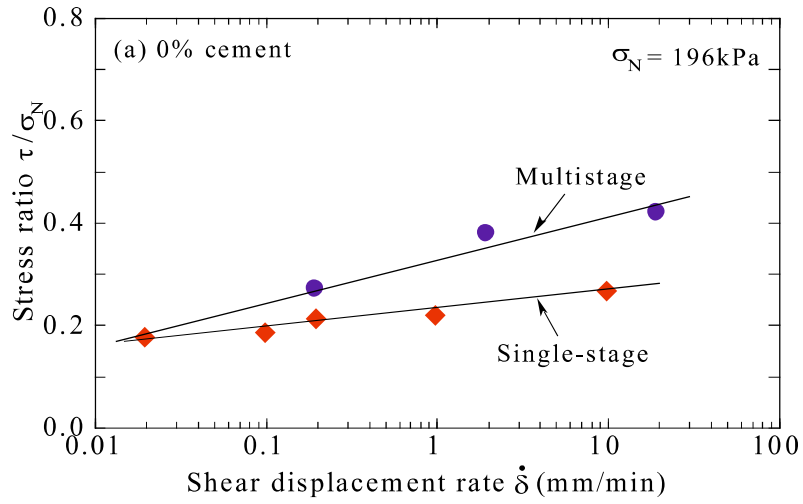
This possibly reorients the particles in the shearing direction inside the shear zone during fast shearing, which increases the residual strength. Hence, the damaging degree of cementation may be considered to be responsible for the rate effect on the residual shear strength of combined specimens. In addition, an increase in real contact area of the shear surface, a change in viscosity, or a decrease in the void ratio inside the shear zone as the shear speed increases, could additionally contribute to the positive rate effect.

5.2 Effect of increasing shear-rate multistage ring-shear test on the residual strength of cemented and non-cemented kaolin samples

Figs. 5.4 (a)-(d) show shear rate versus stress ratio for all specimens by increasing shear-rate in single- and multi-stage tests. All specimens in multistage test show an increase in stress ratio when shear speed consecutively increased with a different tendency corresponding to each specimen. The tendency for an increase in multistage fast residual strength may be due to the viscous effect and to structural changes in the shear zone. It should be noted that high rates of shear may result in disturbance of the residual soil fabric (aligned clay particles) with consequent increase in inferred strength. On the semi-log plot, the stress ratio of kaolin rapidly rise up with a tendency that far above from the single-stage test. Kaolin generally contains clay particles in which edge-to-face and edge-to-edge interlocking dominates the micro-structure. Once sheared to residual state in a ring-shear apparatus, they demonstrate a thin polished continuous shear surface.

In contrast, for 4% cemented kaolin, the stress ratio is almost constant in single-stage, whereas that in multistage increase with a same tendency as 0% cemented kaolin. The residual strength of the 4% cemented kaolin samples that was constant irrespective of shearing speed, could be attributed the undulating or incompletely developed shear surface caused by stiffness resulting from cementation. Hence, under a normal stress of 196 kPa, the slip surface did not develop completely. On the other hand, under a series of increasing load in multistage test, a well-defined shear surface was created with characteristics nearly similar to 0% cemented kaolin, which resulted in an increase in the residual stress ratio. For combined-cement kaolin specimens with a pre-existing shear surface showed a similarly increases tend in stress ratio by both methods. This is due to the well orientation of clay particles and platy clay minerals parallel to the

direction of shearing on a well-defined pre-cut shear surface. Hence, for these application of results is quite meaningful in quickly assessing the stability of reactivated landslides that occur in areas with cemented soil.



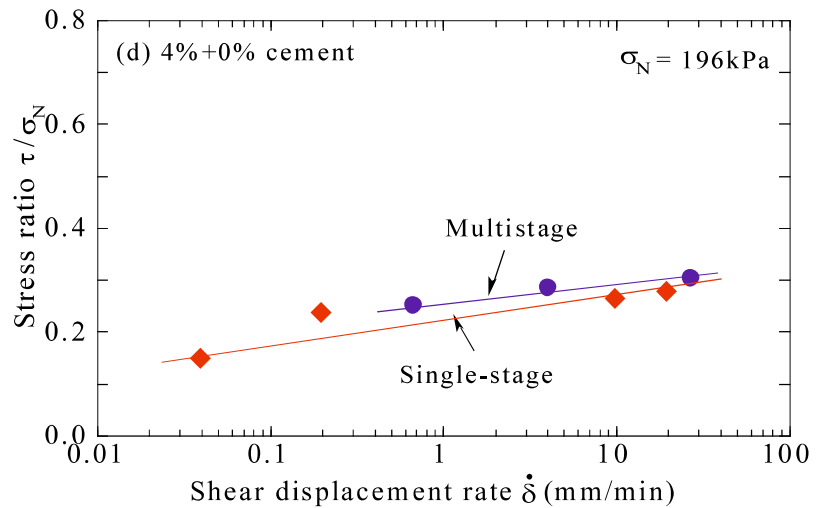
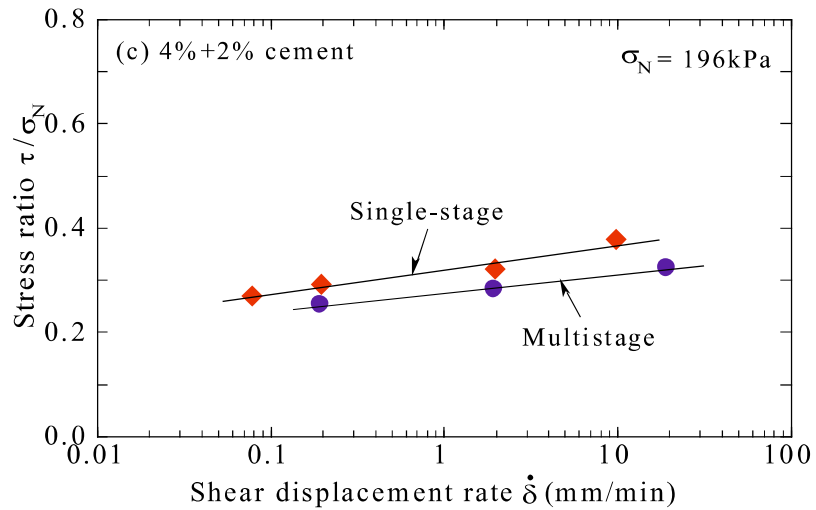


Figure 5. 4 Shear displacement rate versus stress ratio for all specimens by increasing shear-rate in single- and multi-stage tests.

5.3 Summary

The main conclusions of Chapter 5 are summarized as follows:

1. The effect of cement content on rate dependency of residual strength was identified for cemented specimen. The results show that 2% cemented kaolin samples exhibited an increase in residual strength corresponding to increases in shear rate. In contrast, the residual strength of the 4% cemented kaolin samples was constant irrespective of shearing speed.

2. The residual strength was found to increase slightly with increasing shear displacement rate for each combined cemented specimen. This positive rate effect was similar to that of pure kaolin. Therefore, the rate dependency of residual strength exhibited in sample having a bedding plane.
3. The residual stress ratio of 4% cemented kaolin samples in shear rate single-stage and multistage ring-shear tests could not be completely evaluated because their slip surface seemed to be undulating and non-planar in single-stage test.
4. The stress ratio of combined samples in single-stage and multistage ring-shear tests increased with a practically similar tendency as the shear displacement rate increased. This increase is different for 0% and 4% cemented kaolin, thus, it is suggested that the multistage technique may give erroneous results for these clayey soils. It is recommended that it is possible and convenient to perform multistage fast shear-rate ring-shear tests on cemented pre-existing landslides soils to quickly evaluate the effect of shear velocity on the residual strength characteristics.

Chapter 6 CYCLIC DEGRADATION OF DISCONTINUOUS PLANE MATERIALS IN DYNAMIC RING-SHEAR TEST

6.1 Introduction of cyclic degradation

One of the most essential parameters evaluated in this study is the degradation parameter, t , which measures the degree of cyclic degradation during the process of the continuously increasing number of cycles of N . When soil is subjected to cyclic loading in undrained condition, its stiffness and strength decreases, and is accompanied by changes in pore water pressure as the number of cycles increases. This phenomenon is defined as cyclic degradation and is illustrated in Fig. 6.1. Index ζ and parameter t were originally introduced by Idriss et al. (1978) in a research on the cyclic degradation of marine clay deposits. In the process of dynamic shear, the secant shear modulus, G_{sN} , is defined as follows:

$$G_{sN} = \frac{\tau_{cN}}{\gamma_c} \quad (6.1)$$

where

γ_c : the cyclic shear strain amplitude

τ_{cN} : the average of the cyclic shear resistance in the N th cycle.

In the cyclic strain-controlled mode, the degradation index can be expressed as in the following:

$$\zeta = \frac{G_{sN}}{G_{s1}} = \frac{\tau_{cN}/\gamma_c}{\tau_{c1}/\gamma_c} = \frac{\tau_{cN}}{\tau_{c1}} \quad (6.2)$$

In the cyclic stress-controlled mode, the cyclic degradation with N can be defined with the degradation index, ζ^* , which is the same as ζ (Mortezaie et al, 2013).

$$\zeta^* = \frac{G_{sN}}{G_{s1}} = \frac{\tau_c/\gamma_{cN}}{\tau_c/\gamma_{c1}} = \frac{\gamma_{c1}}{\gamma_{cN}} = \frac{\delta_{c1}}{\delta_{cN}} \quad (6.3)$$

Here,

δ : the shear displacement defined as an intermediate circular arc between the inner and outer rings.

δ_{c1} , δ_{cN} : the ring shear displacement for cycles 1 and N , respectively.

$\delta_{c1} = \delta_{cN}$ in the first cycle of the shearing process.

The degradation parameter, t , can be expressed as in the following:

$$t = -\frac{\log \zeta^*}{\log N} \quad (6.4)$$

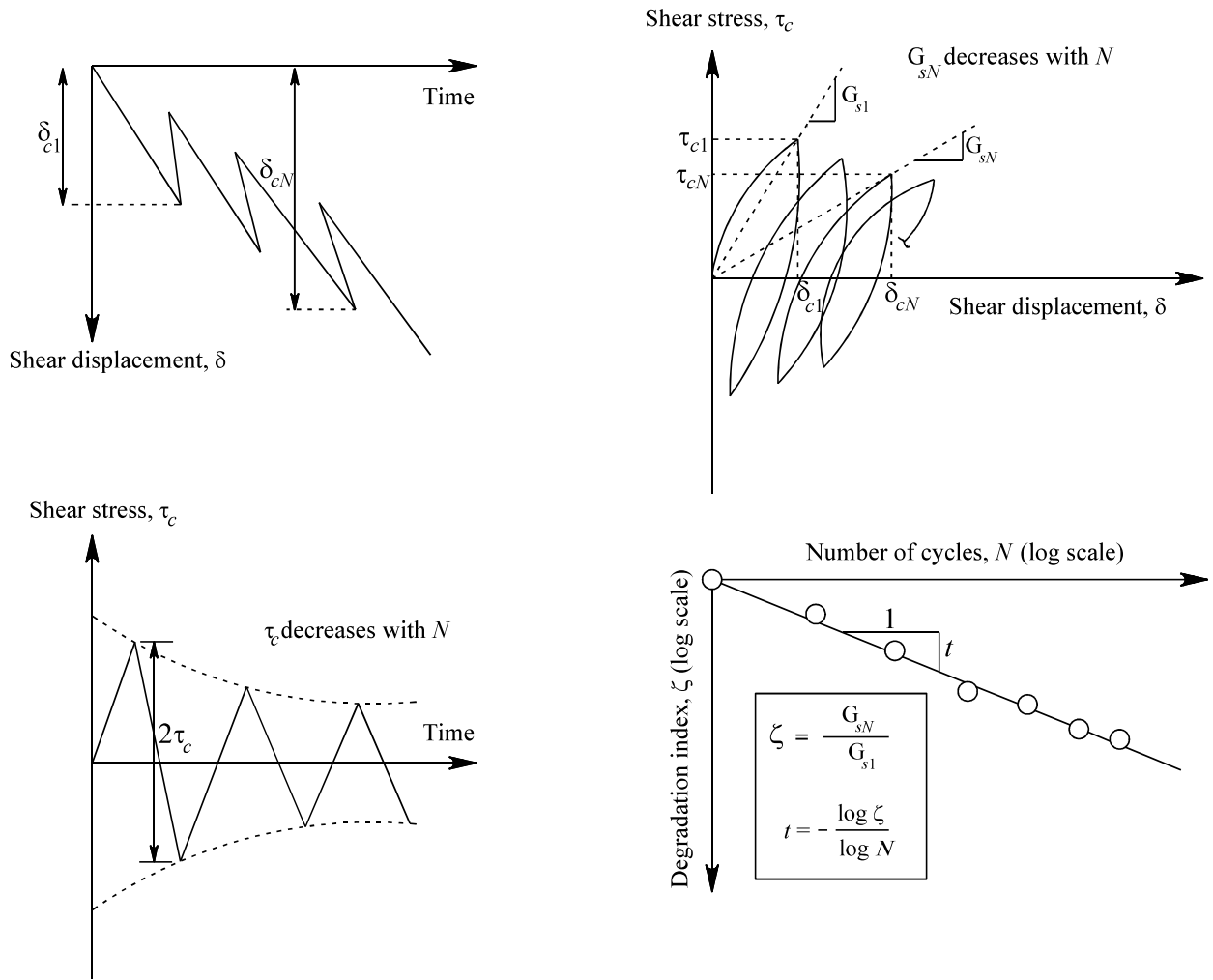


Figure 6. 1 Schematic illustrating the phenomenon of cyclic degradation and the definition of parameters

For many clays, the relationship between ζ and N in a log–log scale is represented as an approximately straight line. The slope of this line is the degradation parameter, t , as a result of the applied constant shear-torque τ_c . Parameter t has been extensively used in past research for the evaluation of the cyclic degradation in several types of clay (Matasovic, N. and Vucetic, M., 1995; Mortezaie et al, 2013; Soralump et al., 2016).

These studies were mainly conducted using test devices such as those used in the cyclic direct simple shear test and the cyclic triaxial compression test. Consequently, the evaluation of the cyclic degradation using a consolidation-constant volume cyclic-loading ring-shear test apparatus would contribute to the body of knowledge on the complex cyclic behaviour of clays, particularly that of cemented clay soil.

6.2 Effect of confining pressure on cyclic degradation of discontinuous plane materials

In this study, a total of 26 cyclic shearing tests were conducted. The test results are summarized in [Table 6.1](#). The value of the degradation parameter t was calculated and plotted for the first 20 cycles of shear displacement. All tests were carried out at vertical consolidation stress loads of 98, 196, and 294 kPa. The applied shear-torque amplitudes were approximately 30, 60, and 90 kPa, and the loading frequency was selected to be constant at a value of 0.5 Hz for all specimens. In the analysis of the dynamic ring shear test, it was assumed that failure of a sample would occur when the shear displacement, δ , would be approximately 2 mm.

6.2.1 Evaluation of the change of in the degradation parameter t under different confining pressure

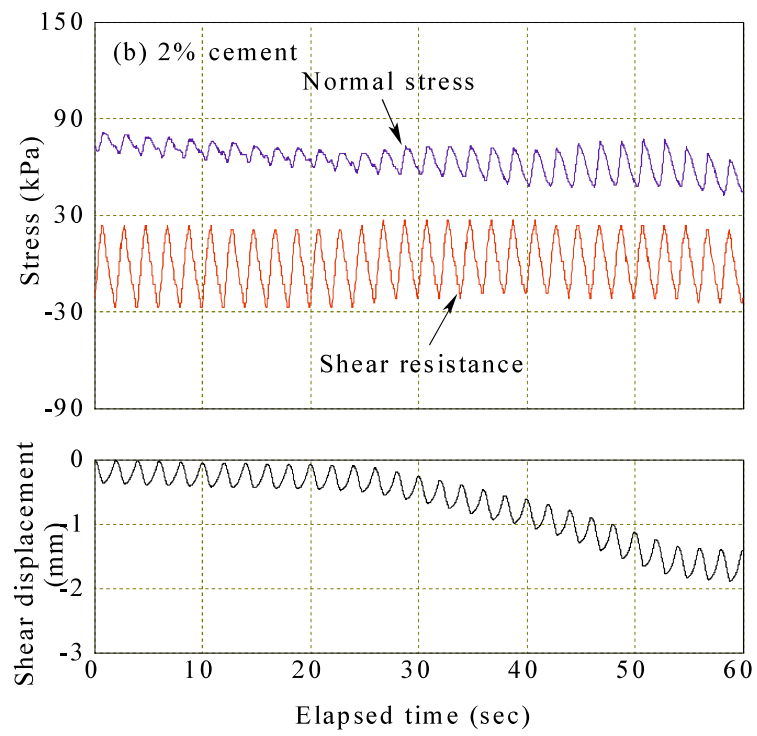
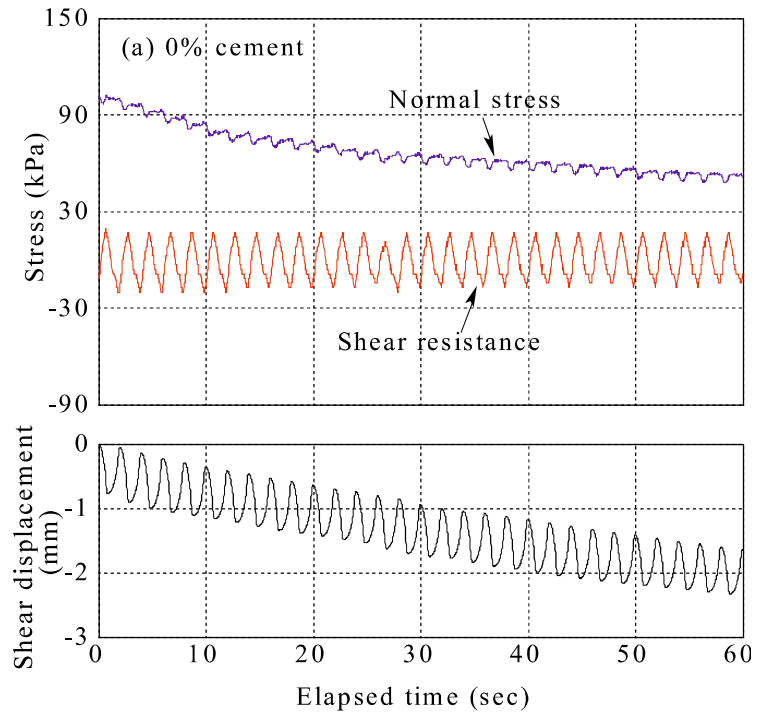
[Figs. 6.2 \(a–d\)](#) present typical results of cyclic loading behaviour, depicting time series data of normal stress, shear stress, and shear displacement. During the process of shearing, σ_N was reduced to maintain a constant volume condition. As pore water pressure was not measured in this study, the variation in the vertical stress required to maintain constant volume may be considered equivalent to the increase in pore water pressure that would have developed inside the specimen during cyclic loading. These figures indicate that the specimens experienced significant deformation according to the type of specimen caused by the shear load on the sliding surface. The displacement and the displacement rate increased with the difference between the shear load and the shear resistance and the loading time. It should be noted that when clay soil is subjected to cyclic loading, its strength and stiffness decreases with the number of cycles. This degradation is considered to be one of the most important phenomena in the analysis of

soil dynamics. As can also be seen in Figs. 6.2 (a–d), the shear displacement and the displacement rate increase with the difference depending on types of specimens. During the first few cycles, the mobilized cyclic shear resistance at peak state cannot be easily identified. This behaviour is thought to be different from that of other types of soil, such as sand, silt, or sandy clay.

Table 6. 1 Test cases and test results of cemented and non-cemented kaolin samples in dynamic ring-shear test

Test	Test	w _o (%)	ρ _{to} (g/cm ³)	S _{ro} (%)	e _o	σ _c (kPa)	σ _N (kPa)	OCR	Shear torque (kPa)	τ _f (at δ=2mm)(kPa)	(τ _{cN} /σ _{N0})	t(at N=20)
0% cement	K1	68.7	1.542	96.4	1.864	98	98	1.0	30	17.0	0.174	0.522
	K2	67.8	1.574	99.1	1.790	98	98	1.0	60	11.4	0.116	0.441
	K3	66.3	1.579	98.5	1.762	98	98	1.0	90	14.2	0.145	0.462
	K4	61.4	1.650	98.8	1.611	196	196	1.0	60	22.7	0.116	0.376
	K5	57.4	1.641	99.6	1.503	294	294	1.0	60	28.4	0.097	0.304
	K6	61.8	1.607	98.9	1.635	196	98	2.0	90	12.8	0.130	0.427
	K7	56.5	1.639	99.3	1.489	294	98	3.0	90	15.6	0.159	0.414
	K8	55.2	1.635	97.3	1.485	392	98	4.0	90	19.9	0.203	0.343
2% cement	C1	71.3	1.547	98.3	1.900	98	98	1.0	30	17.0	0.174	0.815
	C2	70.7	1.555	98.3	1.901	98	98	1.0	60	17.0	0.174	0.440
	C3	71.0	1.551	98.5	1.886	98	98	1.0	90	14.2	0.145	0.456
	C4	63.9	1.584	96.4	1.701	196	196	1.0	60	21.3	0.109	0.351
	C5	61.4	1.611	98.8	1.623	294	294	1.0	60	31.2	0.106	0.180
	C6	65.3	1.582	98.4	1.736	196	98	2.0	90	21.3	0.217	0.417
	C7	59.4	1.621	98.7	1.576	294	98	3.0	90	24.1	0.246	0.401
	C8	61.2	1.624	99.8	1.606	392	98	4.0	90	31.2	0.319	0.189
2%+2% cement	CC1	69.8	1.554	98.4	1.858	98	98	1.0	30	18.5	0.188	0.617
	CC2	71.0	1.559	99.5	1.870	98	98	1.0	60	21.3	0.217	0.504
	CC3	71.7	1.545	98.5	1.907	98	98	1.0	90	21.3	0.217	0.427
	CC4	64.7	1.593	99.5	1.704	196	196	1.0	60	27.0	0.138	0.388
	CC5	59.2	1.630	99.4	1.560	294	294	1.0	60	29.8	0.101	0.324
2%+0% cement	CK1	64.8	1.546	94.7	1.791	98	98	1.0	30	12.8	0.130	0.506
		72.9	1.620	100	1.790							
	CK2	64.8	1.546	94.8	1.787	98	98	1.0	60	15.6	0.159	0.454
		72.9	1.620	99.5	1.782							
	CK3	67.9	1.603	99.8	1.736	98	98	1.0	90	17.0	0.174	0.381
		69.4	1.551	97.9	1.856							
	CK4	61.4	1.650	99.8	1.562	196	196	1.0	60	15.6	0.080	0.429
		62.8	1.570	95.9	1.716							
	CK5	61.4	1.652	99.6	1.566	294	294	1.0	60	21.3	0.072	0.400
		62.8	1.574	96.4	1.708							

Note: curing time of 3 days for all samples; $f=0.5$ Hz for all tests; for 2%+0% cement: $\frac{A}{B}$, A: upper part of 0% cement and B: lower part of 2% cement; w_o: initial water content; ρ_{to}: initial wet density; S_{ro}: initial degree of saturation; e_o: initial void ratio; t: degradation parameter.



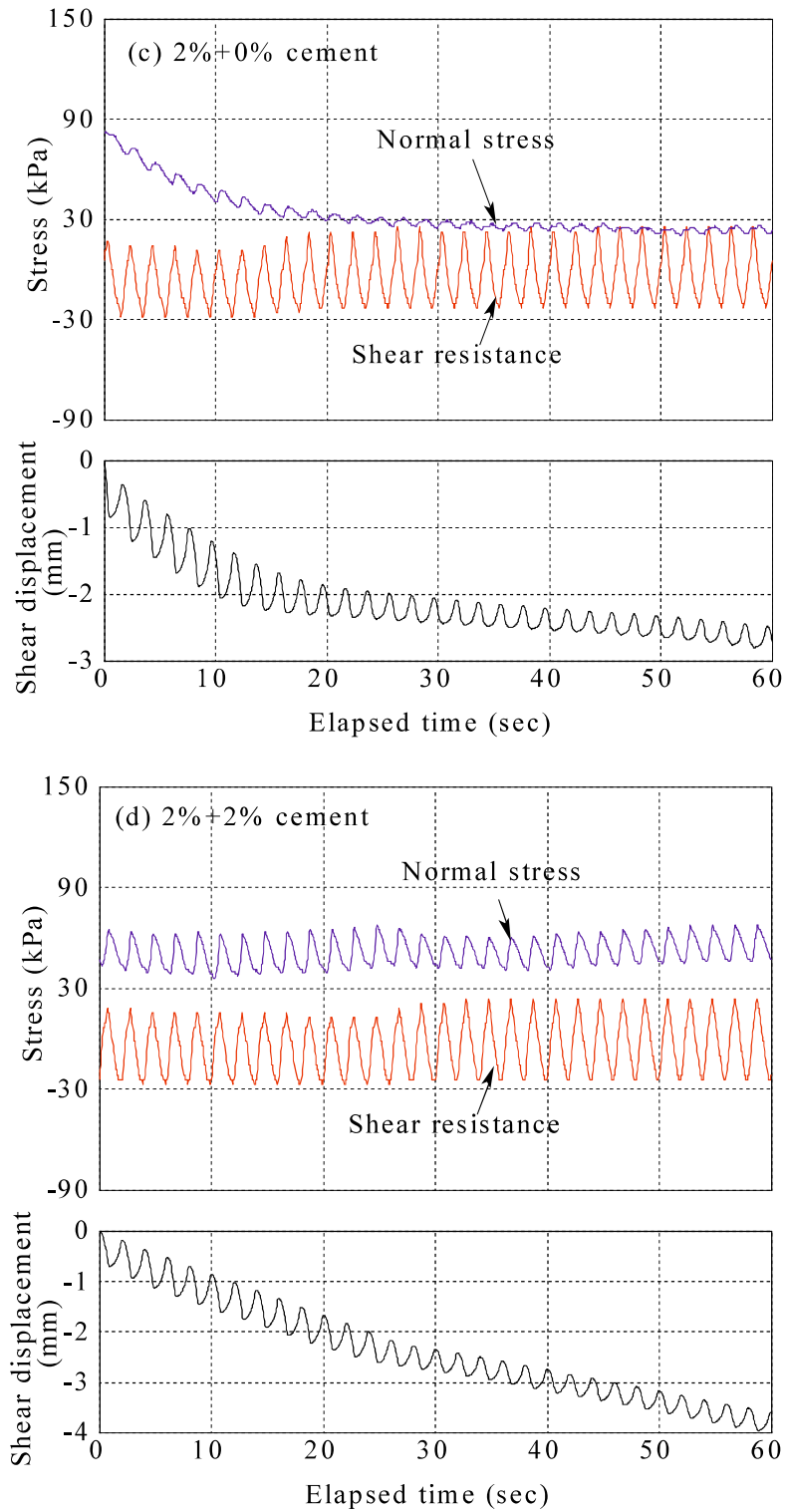
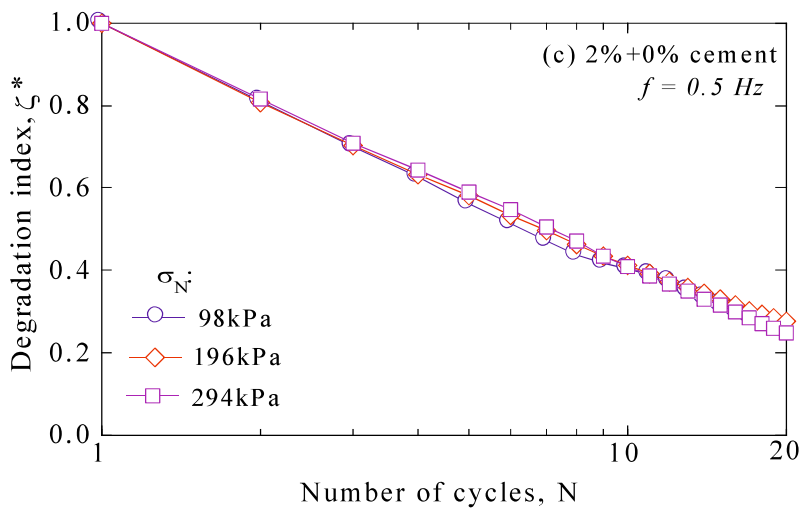
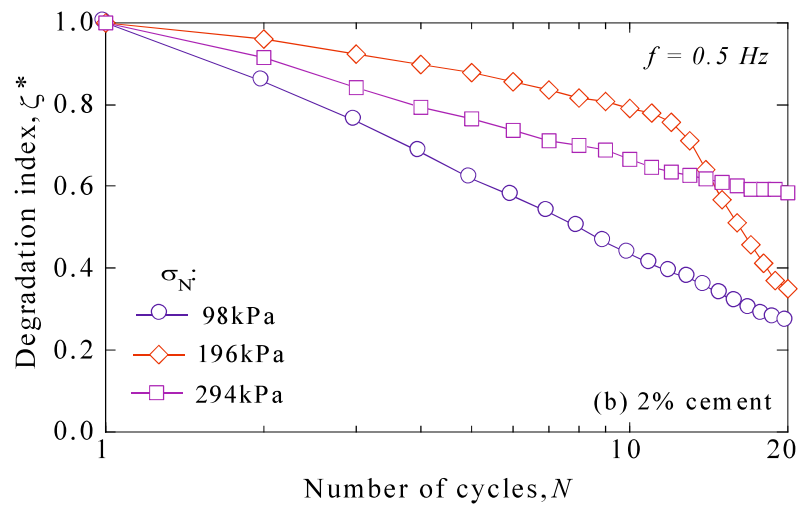
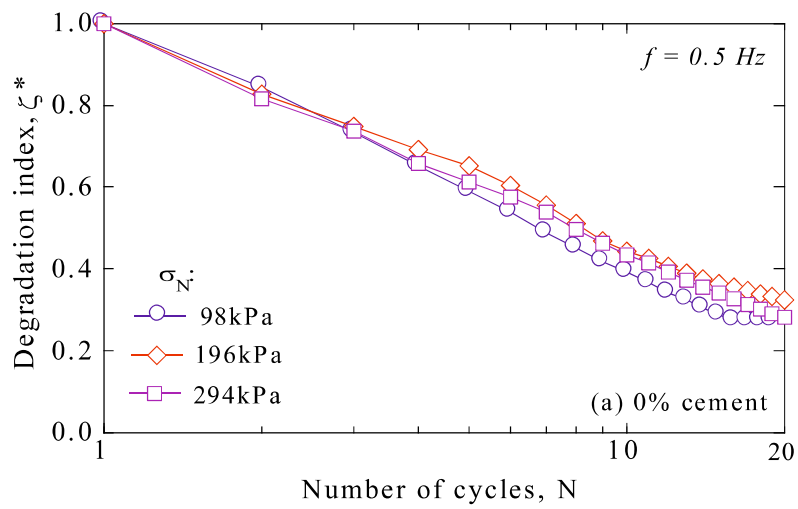


Figure 6. 2 Typical time series data for CRSTs on 0%, 2%, 0%+2%, and 2%+2% cemented kaolin specimens: $f = 0.5$ Hz; shear-torque = 60 kPa; normal stress = 196 kPa.

The influence of σ_N on the cyclic degradation is illustrated in Figs. 6.3 (a–d), 6.4, 6.5, and 6.6 (a–d) for all specimens under different normal stresses. Logarithmic scales are used to clearly demonstrate the differences in the response for a small number of cycles. During the testing, the shear-torque amplitude was set to 60 kPa, while the frequency of the shear loadings was 0.5 Hz. During the cyclic stages of loading, different distinct types of cyclically induced responses and deformations were identified. When the initial shear stress was applied, a large deformation took place owing to mobilized cyclic shear resistance degradation. With the increase in confining pressure, the number of cycles required to reach failure obviously increased for all cases. Cementation resists the dynamic loading; however, after the specimens lost the cementation formed between clay particles owing to the continuous cyclic loading, shear displacement occurred rapidly and failure may occur. At a lower normal stress of 98 kPa, the influence of the number of cycles on the degradation index was observed to not be significant, which indicates the effect of condition of specimen is approximately the same. This trend becomes to be more clearly at a higher normal stress of 198 kPa (Figs. 6.4 and 6.5).

For the 2% cemented kaolin, tests conducted at a higher level of the initial normal stress, particularly at a normal stress of 294 kPa, indicate that specimens suffer from slight deformation. This tendency is thought to be owing to the addition of 2% cement, which enhanced the stiffness and strength of the specimen. Thus, it is assumed that this shear-torque amplitude of 60 kPa was not high enough to cause the failure of the specimens; the shear displacement was limited, and the sample presented a relatively small shear deformation. On the other hand, for the 2% + 0% cemented kaolin, shown in Fig. 6.3 (c), the curves of the degradation index as a function of the number of cycles are almost similar among the different normal stress levels. This means that σ_N has a relatively small effect on t for this type of specimen. The reason for this behaviour is due to pre-existing surface that made of 0% and 2% cement content two half of specimen which results in relatively very weak bond. This tendency is different from the 2% + 2% cement specimen which shows the clearly diverse trend of cyclic degradation with the increase in normal stress in spite of a combined specimen. It is suggested that the cohesion remains mostly on the bedding plane. Both trends observed for the 2% and the 2% + 2% cemented kaolin indicate that cementation has a significant influence on the cyclic degradation.



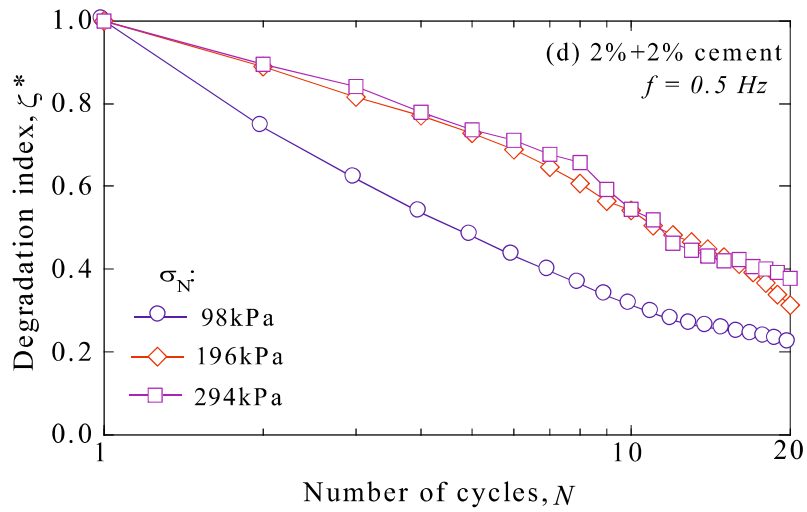


Figure 6. 3 Relationship between the cyclic degradation index, δ^* , and the number of cycles, N , for all types of specimen under different normal stresses.

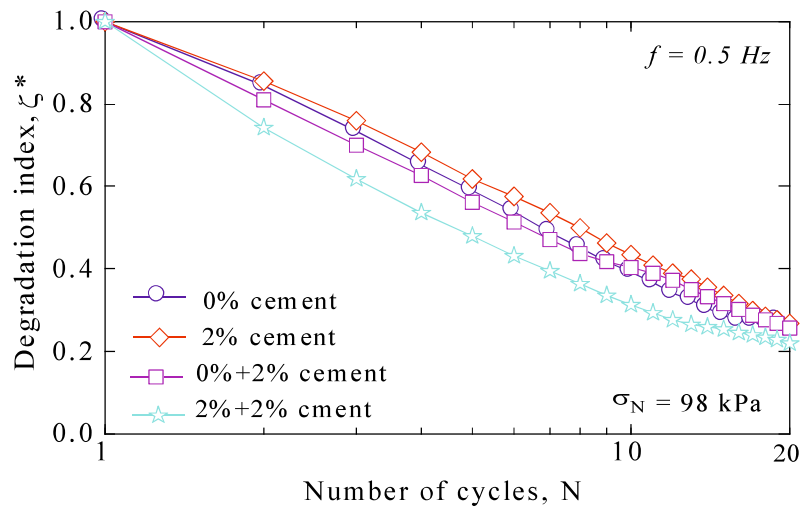


Figure 6. 4 Comparison of the degradation index with the number of cycles, N , for all types of specimens under constant normal stress, $\sigma_N = 98 \text{ kPa}$

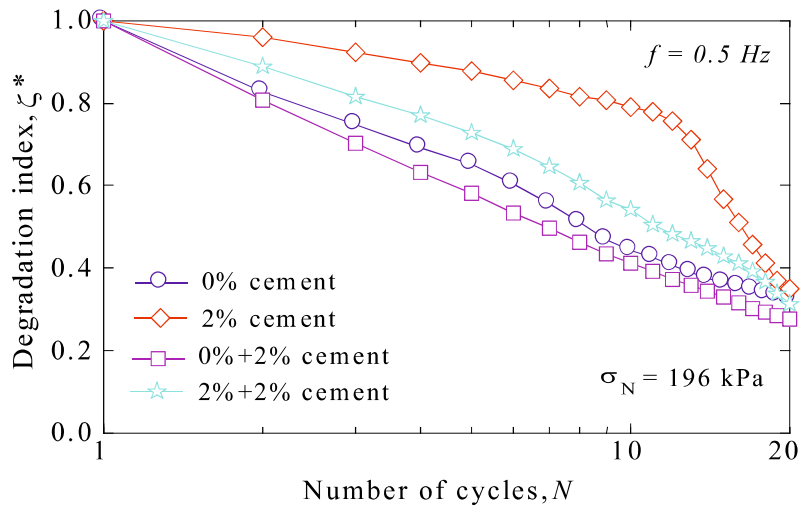
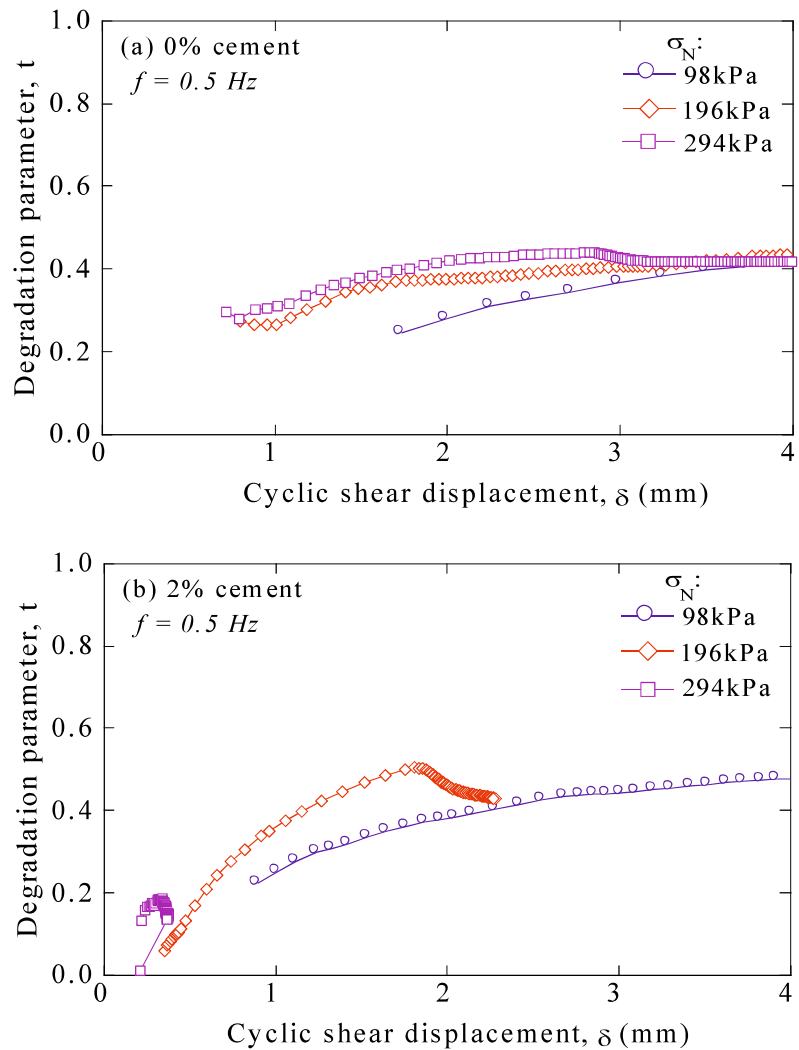


Figure 6. 5 Comparison of the degradation index with the number of cycles, N , for all types of specimens under constant normal stress, $\sigma_N = 196$ kPa



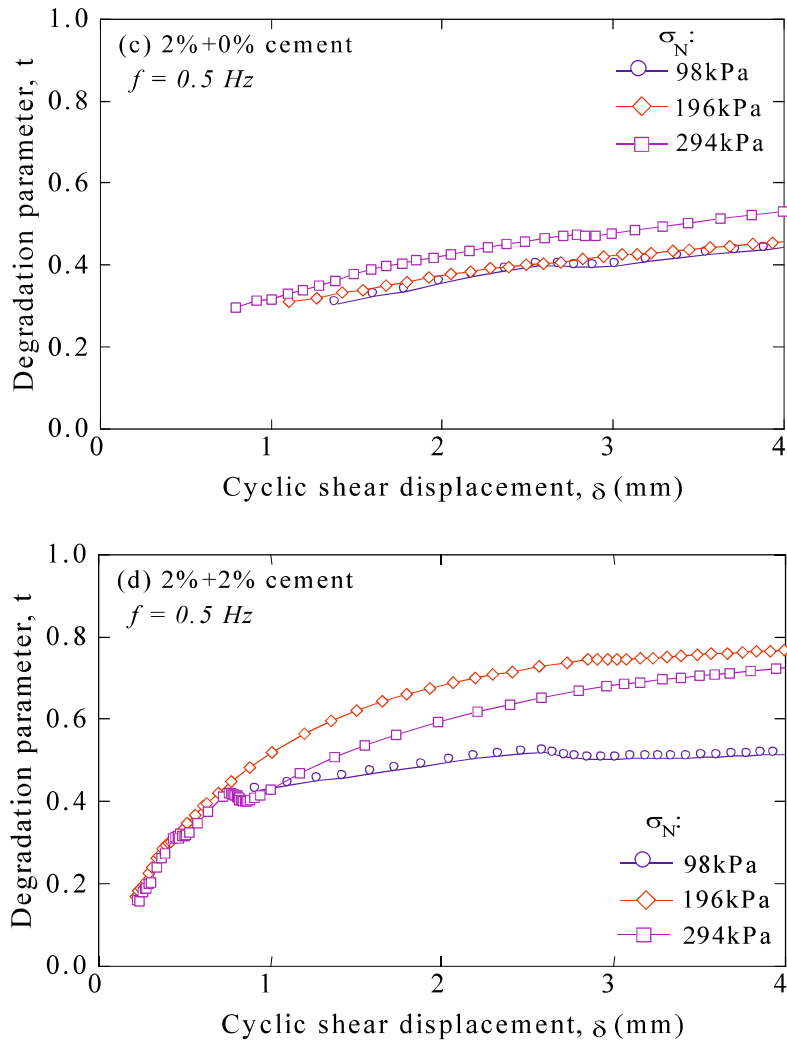


Figure 6. 6 Effect of normal stress, σ_N , on the degradation parameter, t , for all types of specimens.

A comparison of the effect of σ_N on the degradation parameter, t , for all types of specimens is presented in Fig. 6.7. The results clearly indicate that t reliably decreases with the increase in normal stress at different levels. This tendency is consistent with previous research (Mortezaie et al., 2013; Soralump et al., 2015). The calculated results, listed in Table. 6.1, show that if σ_N increases from 98 kPa to 294 kPa (increases three times), t decreases by 31.1%, 59.1%, 11.9%, and 35.7% for the 0%, 2%, 2% + 0%, and 2% + 2% cemented kaolin, respectively. The results also show that the value of t for the 2% cement specimen is approximately two times higher than that of the 0% cement specimen, owing to the cementation. The effect of the increase in the vertical compression on parameter t is observed not to be significant for the 2% + 0% specimen.

This relatively small reduction in the degradation may result from a pre-existing shear surface inside the combined specimen. The 2% + 0% cement combined specimen consists of two halves with different degrees of hardening, and the bond between the 0% half and the 2% half is not particularly strong. Furthermore, the re-orientation of clay particles in the shearing direction was well developed, compared to that in the normal cemented specimen. Therefore, the degradation of the 2% + 0% combined specimen was lower than that of the other specimens. Although the 2% + 2% cement also has a pre-existing surface, the value of t decreases nearly to the same as that of the 0% cement specimen because the bond available on two halves of cementation specimens. The reason behind this tendency should be further studied in future research.

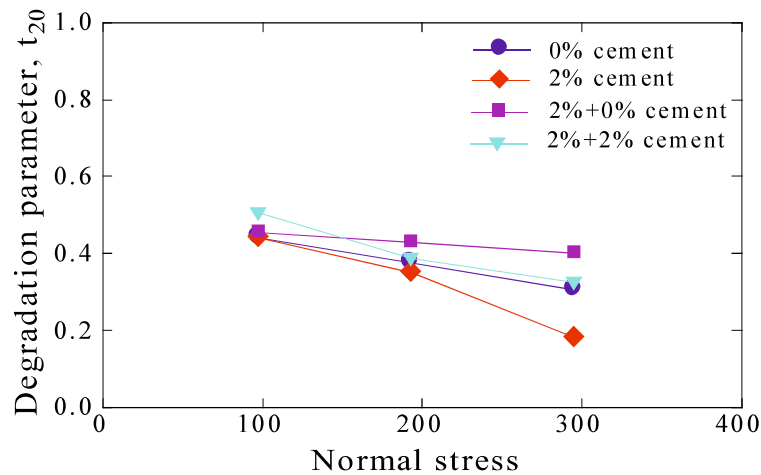


Figure 6. 7 Comparison of the effect of σ_N on the degradation parameter, t_{20} , for all types of specimen.

At $\sigma_N = 98$ kPa, the largest difference in the magnitude of t is only found to be 0.064 between the 2% and the 2% + 2% cemented kaolin. Conversely, this difference is 0.285 at $\sigma_N = 294$ kPa, which is significantly higher than 0.064. This means that the effect of the consolidation stress on t becomes higher as the consolidation stress becomes higher. This may be explained in terms of different void ratios, which will be described in more detail in the next section, under incremental normal stress, shown in Table 6.1. At lower σ_N , the void ratio is higher; this creates a great opportunity for the build-up of pore water pressure, which would reduce the effective stresses, and would thus induce a higher rate

of softening. This physical evidence only reveals a limited aspect of factors affecting the degradation parameter. There may be certain other factors that need to be studied further; for instance, the changes in clay microstructure may be responsible for the cyclic degradation.

6.2.2 Evaluation of the normalized cyclic stress ratio under different confining stress levels

Fig. 6.8 shows the normalized cyclic stress ratio (NCSR) versus the number of cycles under different normal stress levels. In this study, the NCSR is defined as the ratio of maximum shear resistance in an instant cycle to the initial effective normal stress, τ_{cN}/σ_{N0} . From Fig. 6.8, it can be seen that τ_{cN}/σ_{N0} increases with the decrease in the number of cycles (N_f) at a constant vertical consolidation value, under a pre-defined failure state of shear displacement, $\delta = 2$ mm. Conversely, the NCSR of pure kaolin does not seem to be influenced by the increase in normal stress, and is presented as an approximately straight line as the number of cycles increases. The $(\tau_{cN}/\sigma_{N0})-N_f$ curves of the 2% and 2% + 2% cemented specimens were almost the same, and they were higher than those of other specimens. The effect of cementation on the cyclic stress ratio was identified, and it remained to a certain degree, even in discontinuous planes. It can be stated that the increasing cyclic stress ratio is due to the addition of cement into the kaolin clay, thus increasing the hardness and the bonding inside the specimen, which influence the cyclic behaviour of cemented kaolin.

From the results listed in Table. 6.1, the increase in the confining normal stress from 98 to 294 kPa causes decrease in the normalized cyclic stress ratios by approximately 16.4%, 39.1%, 54.7%, and 53.4% for the 0%, 2%, 2% + 0%, and 2% + 2% cemented kaolin, respectively. The reduced NCSR values for the two cement-combined specimens were 53.4% and 54.7%, which indicate a small difference between them. In contrast, owing to the effect of cementation, the NCSR of the 2% cemented kaolin specimen decreases over two times compared to pure kaolin. As the number of cycles increases to approximately 100, the respective τ_{cN}/σ_{N0} ratios of the 0%, 2%, and 2% + 2% specimens seem to be identical among them. This trend may be due to the complete damage of

cementation by the high number of cycles, after which the behaviour of the cemented specimens is similar to that of the non-cemented specimens.

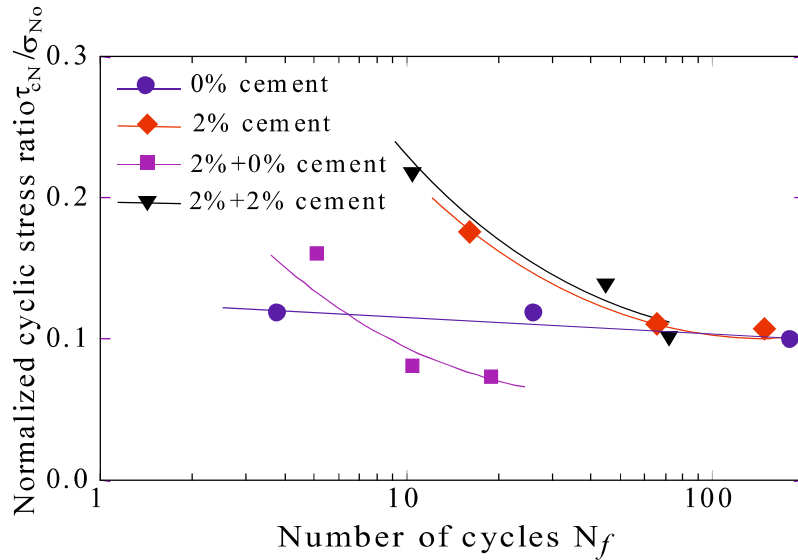
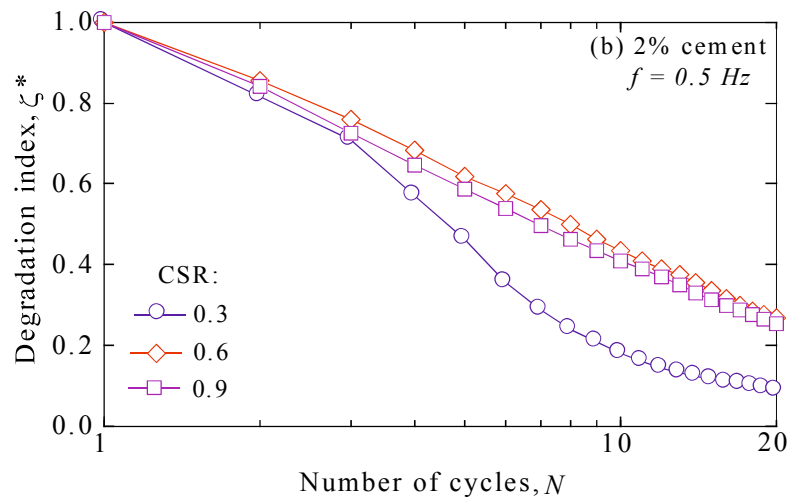
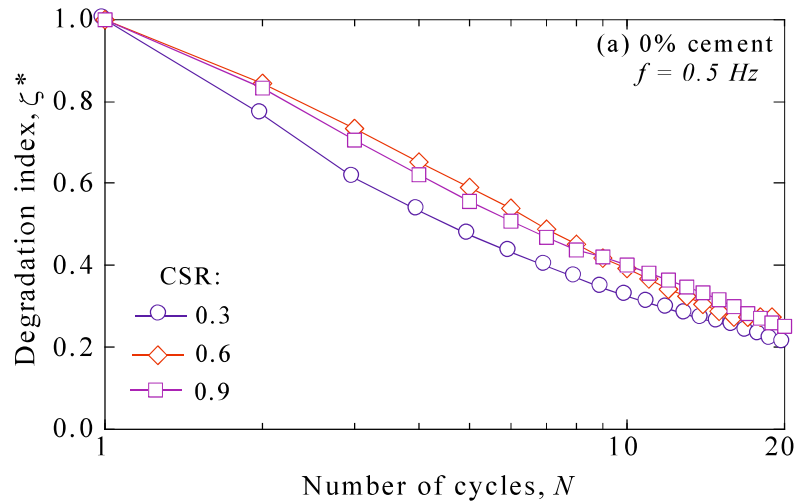


Figure 6. 8 Normalized cyclic stress ratio versus the number of cycles under the different normal stress at shear displacement, $\delta = 2\text{mm}$.

6.3 Effects of the shear-torque amplitude on cyclic degradation of discontinuous plane materials

In the second part of this investigation, the cyclic shear responses of cemented and non-cemented kaolin samples are studied with respect to different shear-torque amplitudes at the same cyclic loading frequency of 0.5 Hz. The process of evaluation was carried out with procedures similar to those previously mentioned. The constant normal stress amplitude of 98 kPa was adopted through this test series. To clearly analyse the results of the effect of different shear-torque amplitudes on the cyclic degradation, the ratio of the applied shear-torque to the initial normal stress, $\text{CSR} = \tau_c/\sigma_{N0}$, was used in this section. The influence of CSR on the cyclic degradation is presented in Figs. 6.9 and 6.10 for all specimens. It can be observed that the degradation parameter t decreases with the increase in CSR. A detailed comparison of the effect of σ_N on the degradation parameter, t , for all types of specimens is presented in Fig. 6.11. The degradation parameter of the 2% cemented kaolin is clearly observed to decrease

the most compared to the other specimens. On the other hand, the decreasing trend of the two cement-combined specimens appears to be the same. Furthermore, the data listed in Table 6.1 also reveal that at the same lower CSR, the tendency of t for the four sample types is significantly different with a value of approximately 0.309, and this gradually decreases to reach the value of merely 0.035 for a CSR of 0.9. As the CSR increases from approximately 0.3 to 0.9, parameter t decreases by 11.5%, 44.0%, 30.8%, and 24.7% for the 0%, 2%, 2% + 2%, and 2% +0% cemented kaolin, respectively. The addition of 2% cement content to kaolin is thought to be the main reason for the significant decrease in t for the 2% cement sample.



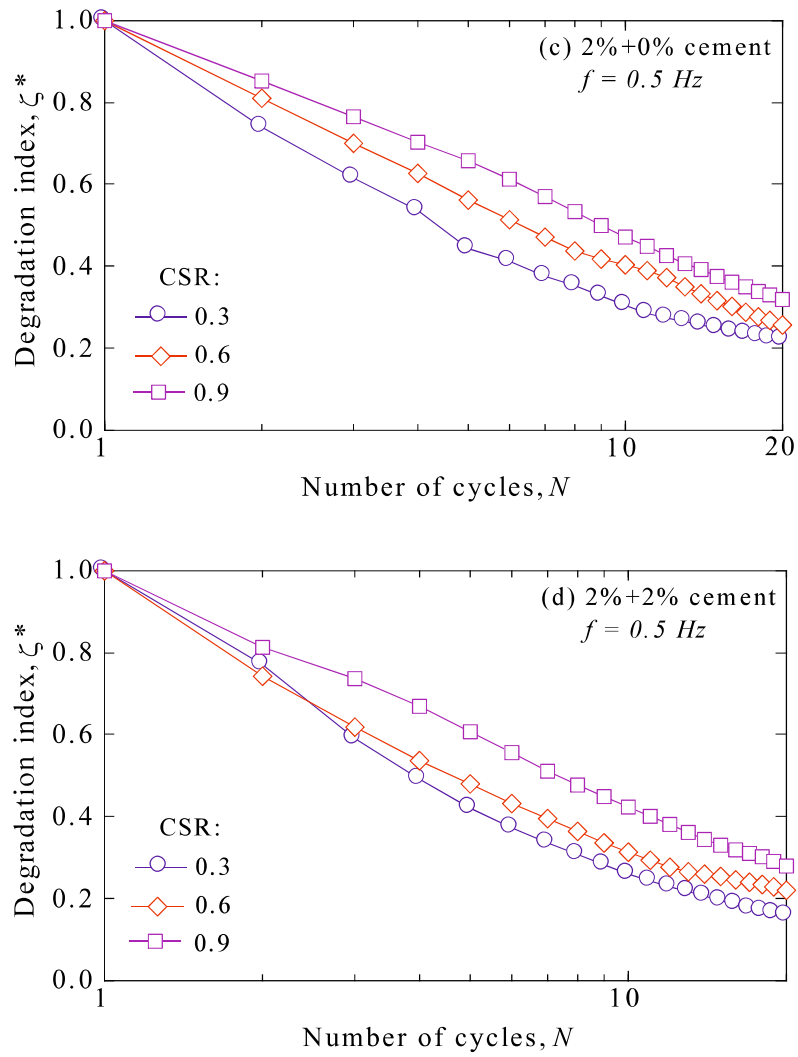
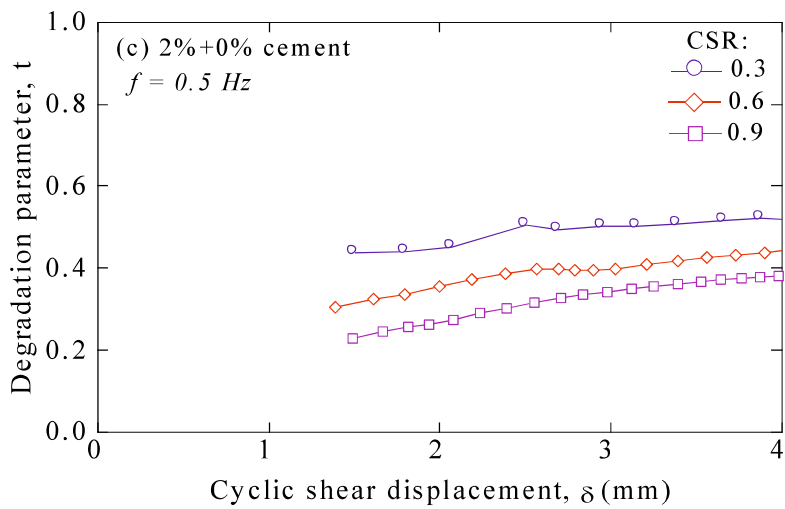
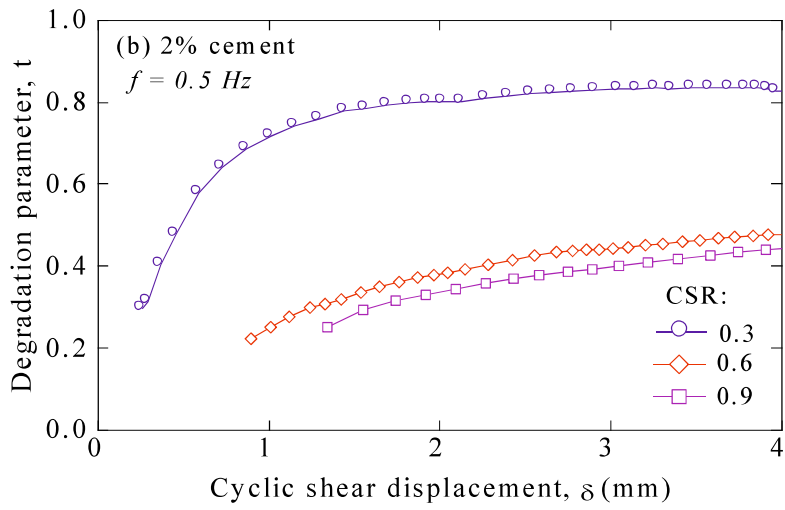
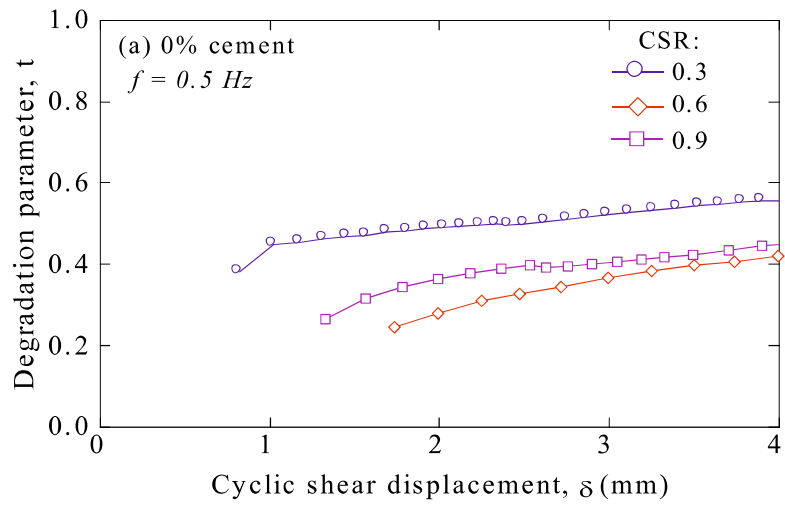


Figure 6. 9 Relationship between the cyclic degradation index, δ^* , and the number of cycles, N , for all types of specimen under different cyclic stress ratios.



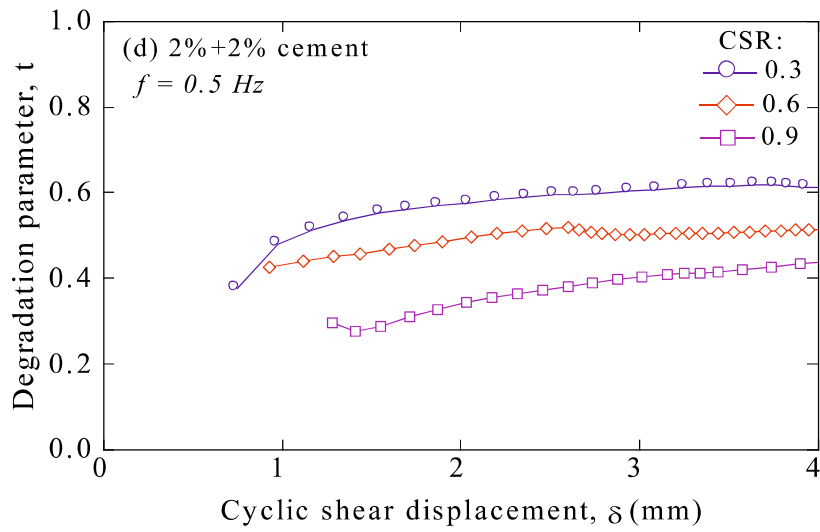


Figure 6. 10 The effect of the cyclic stress ratio, CSR, on degradation parameter, t , for all types of specimen

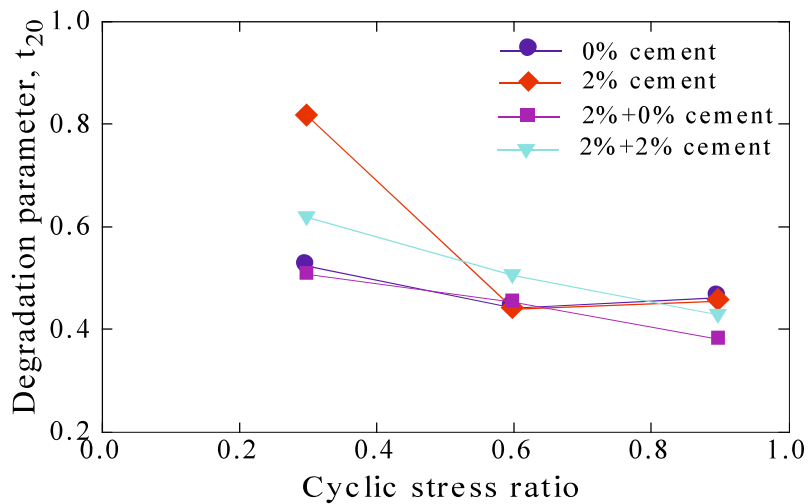


Figure 6. 11 Comparison of the effect of the cyclic stress ratio, CSR, on the degradation parameter, t_{20} , for all types of specimens.

6.4 Effect of the over-consolidation ratio on the cyclic degradation of discontinuous plane materials

Considering that the cemented soil could have suffered different stress history, in the present study, two series of tests were performed on the 0% and 2% cemented kaolin

samples under different over-consolidation ratios (OCRs) to examine the possible effects of stress history. After the specimens were consolidated at normal stresses of 196 kPa, 294 kPa, and 392 kPa, the stress decreased to 98 kPa to obtain the OCRs of 2, 3, and 4. The initial effective normal stress was maintained at approximately 98 kPa during this testing series.

6.4.1 Change in the degradation parameter t under different over-consolidation ratios

The results of the evaluation of the degradation parameter t for two types of specimens with OCRs from 1 to 4 are illustrated in Fig. 6.12 and 6.13. It is well-known that over-consolidated samples are stronger, and fail at larger N_f values than the normally consolidated ones when subjected to the same value of τ_c/σ_{N0} . Furthermore, the sample with the highest OCR exhibited less degradation and pore water pressure build-up. At OCR = 4, the relationship between the number of cycles and the degradation index of the 2% cemented kaolin specimen seems to be an apparent curve. The decreasing degree of parameter t under different OCRs for the 0% and 2% cement specimens is compared in Fig. 6.14. It can be seen that as OCR increases from 1 to 3, the change in the cyclic degradation is small. Lower OCR values can result in a great opportunity for generating the pore water pressure, through which the pore water pressure can be reduced, resulting in a higher rate of softening. This tendency becomes clear as OCRs increase beyond 4. The data presented in Table. 6.1 show that when OCRs increase from 1 to 4, the degradation parameter t decreases by 25.7% and 58.5% for the 0% and 2% cemented kaolin. The decrease in parameter t of the 2% cement is two times higher than that of pure kaolin, at the same OCR value. This value most likely occurs because the addition of 2% cement content into kaolin clay further enhances its OCR and its stiffness, which may cause a substantial decrease in cyclic degradation. On the other hand, the result regarding pure kaolin is consistent with previous studies. For instance, [Vucetic and Dobry \(1988\)](#) found that when the OCR increased from 1 to 4 for clay with a PI between 25 and 55, the degradation parameter t may decrease by 35–40%.

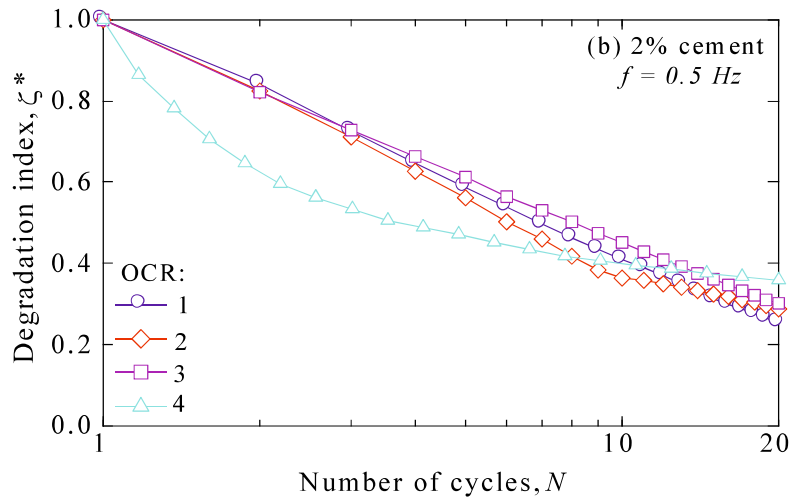
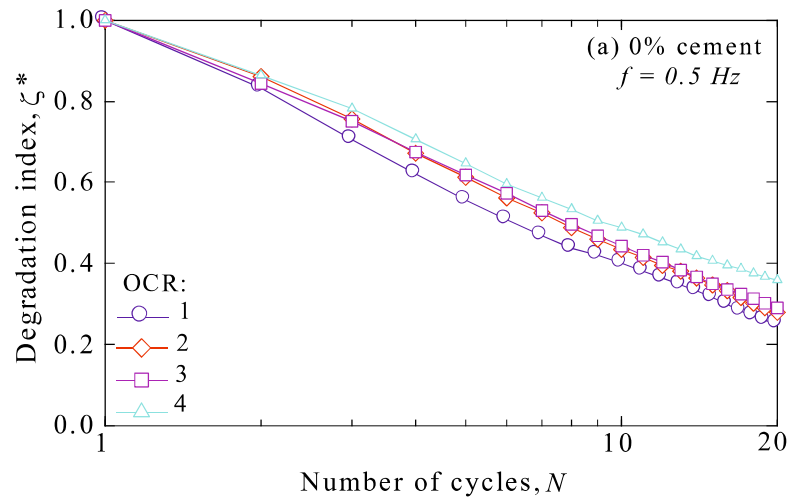


Figure 6. 12 Relationship between the cyclic degradation index, δ^* , the and number of cycles, N , for the 0% and 2% cemented kaolin specimens.

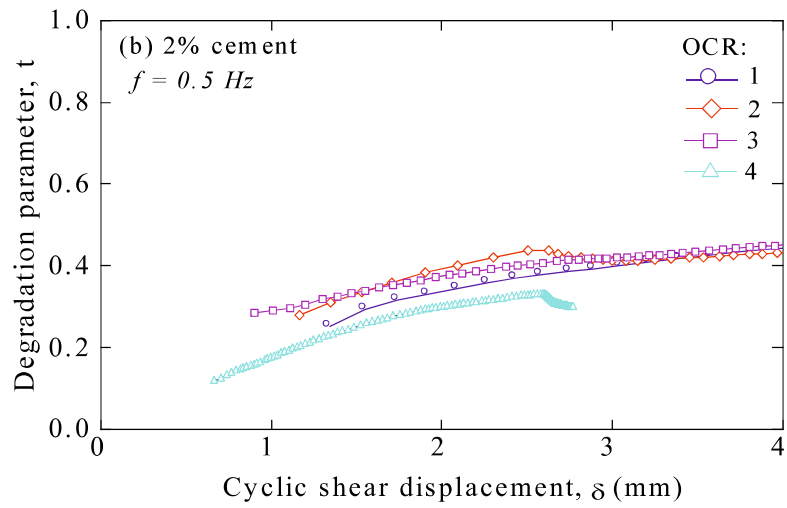
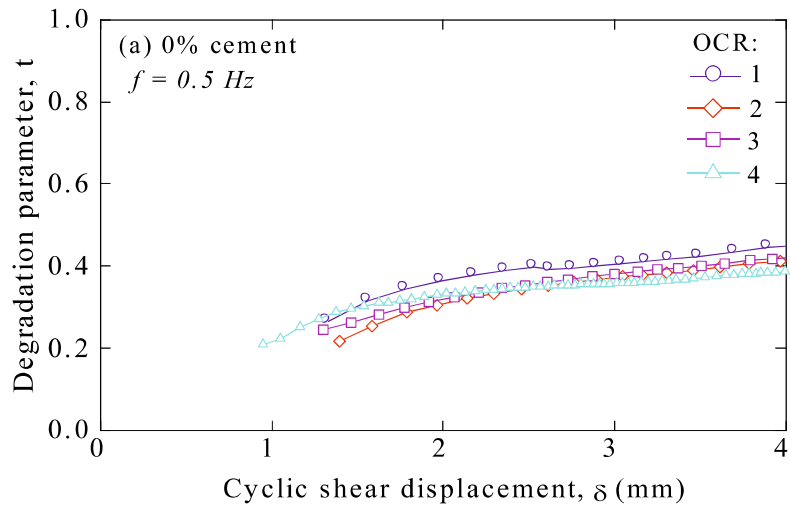


Figure 6. 13 Effect of OCR on the degradation parameter, t , for the 0% and 2% cemented kaolin specimens.

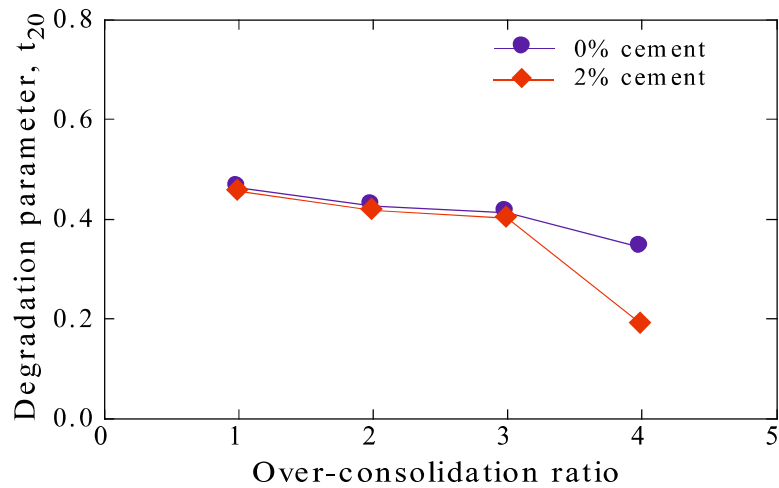


Figure 6. 14 Comparison of the effect of OCR on the degradation parameter, t_{20} , for the 0% and 2% cemented kaolin specimens.

Another possible explanation is that over-consolidation produces an increase in the amount of contacts between soil particles, and thus improves its stability against dynamic loading. Cemented clays typically have low permeability and a lower void ratio owing to over-consolidation. Excess positive pore pressure is not likely to be generated under cyclic loading because specimens have been consolidated at a high normal stress to obtain the defined OCR. The initial void ratio, e_0 , of the 2% and 0% cemented kaolin specimens was found to be 1.762 and 1.886 at $\sigma_c = 98$ kPa, and 1.485 and 1.606 at $\sigma_c = 392$ kPa, respectively. The difference in the above-mentioned values of the initial void ratios expressed in percentages is 15.7% and 14.8% for the two specimens, respectively. Considering based on experimental meaning, two values almost were equivalent, which would result in the same degradation parameter. Nevertheless, the degradation of the 2% cemented kaolin specimen decreases by substantially more than two times compared to that of the 0% cemented kaolin specimen. This indicates that the effect of cementation on parameter t was substantially identified.

6.4.2 Partial evaluation of pore water pressure based on normal stress change during cyclic loading for over-consolidated cemented and non-cemented specimens

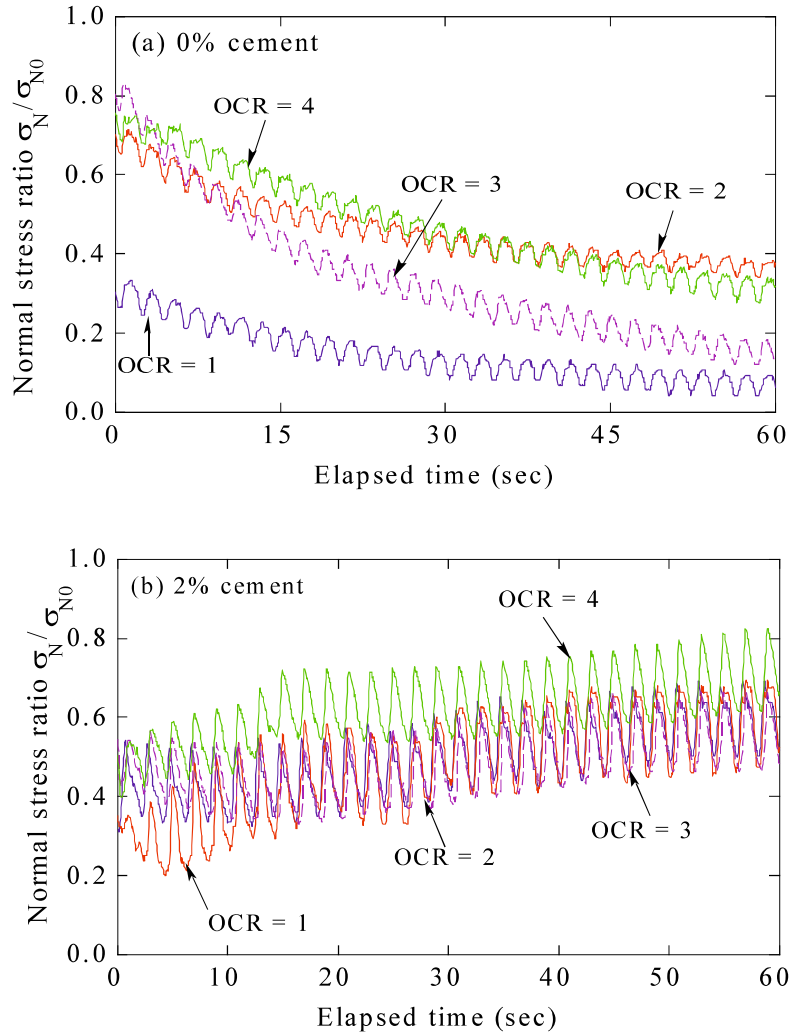


Figure 6. 15 Comparison of the vertical normal stress change during cyclic loading for the (a) 0% and (b) 2% cemented kaolin specimen with the different OCRs

The diagrams in Fig. 6.15 were additionally plotted to allow for a preliminary evaluation of the pore water pressure change, for various OCRs of the 0% and 2% cemented kaolin specimens versus the elapsed time. As mentioned previously, the change in the vertical stress required to maintain constant volume is equivalent to the pore water pressure change. In this manner, the cyclic pore water pressure of the 0%

cemented kaolin specimen, presented in Fig. 6.15, can be considered to develop as a positive value. Conversely, an unclear increasing and decreasing trend was observed for the 2% cemented kaolin specimen, which suggests that negative cyclic pore water pressure was generated inside the cemented specimen. This tendency strongly supports the above statement related to the physical evident of void ratio due to the soil to be compacted by over-consolidation process. This trend also suggests that the cyclic pore water pressure build-up may not be a dominant factor contributing to the cyclic degradation of cemented clay. Moreover, this result is in good agreement with that obtained by Matasovic, N. and Vucetic, M. (1995).

6.4.3 Mobilized cyclic stress ratio versus the number of cycles under different over-consolidation ratios

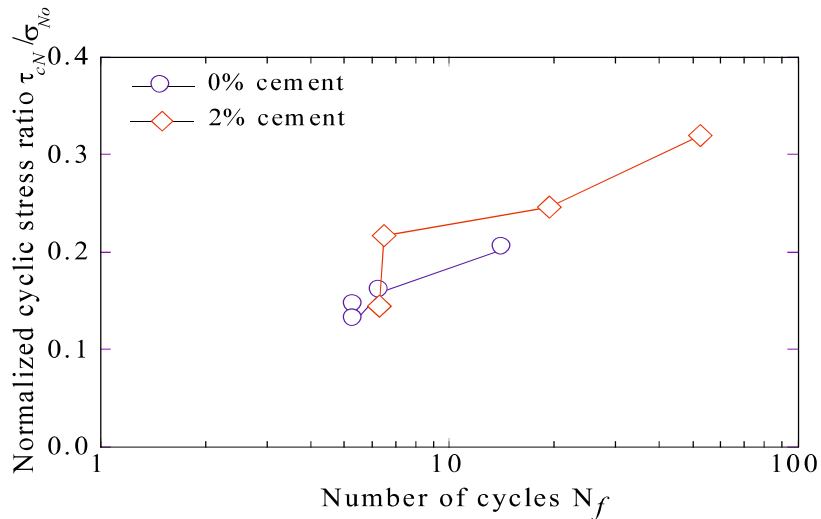


Figure 6. 16 Mobilized cyclic stress ratio versus the number of cycles under the different over-consolidation ratio for the 0% and 2% cemented kaolin specimens.

Fig. 6.16 shows the mobilized cyclic stress ratio versus the number of cycles for the shear displacement of 2 mm under different over-consolidation ratios for the 0% and 2% cemented kaolin specimens. As previously mentioned, OCRs of below 3 do not seem to affect the cyclic response of pure kaolin. Consequently, the scatter is found to be minimal, as shown in the figure. On the other hand, the cyclic ratio of the 2% cement specimen significantly increased with an increase in the over-consolidation ratio from 1

to 4. In addition, the required number of cycles to reach the failure state was considerably higher than the normal. Meanwhile, as expected, a sample with a higher OCR could exhibit greater shear resistance.

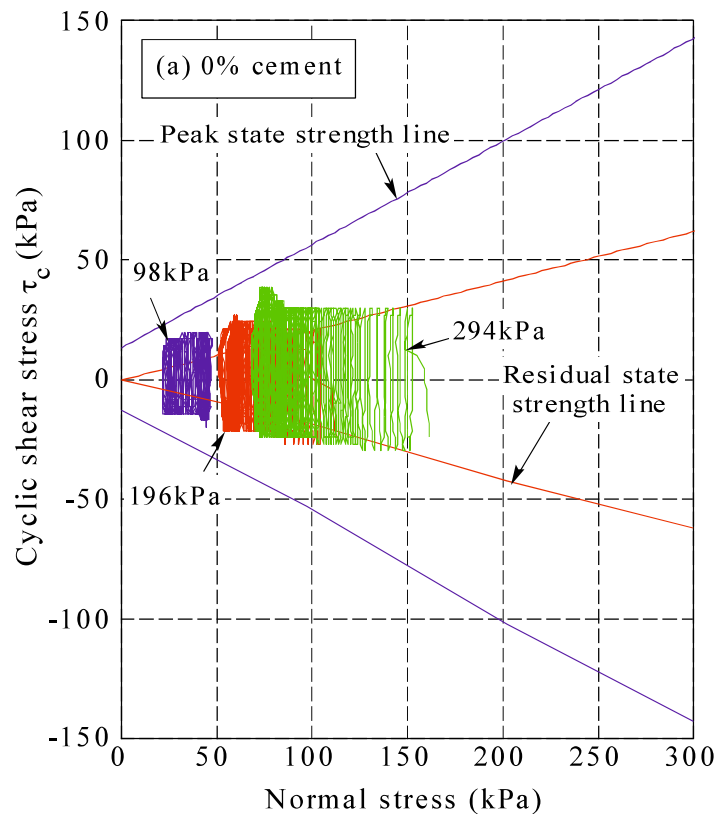
6.5 The stress paths based on a comparison between the shear strength of dynamic and monotonic ring-shear test

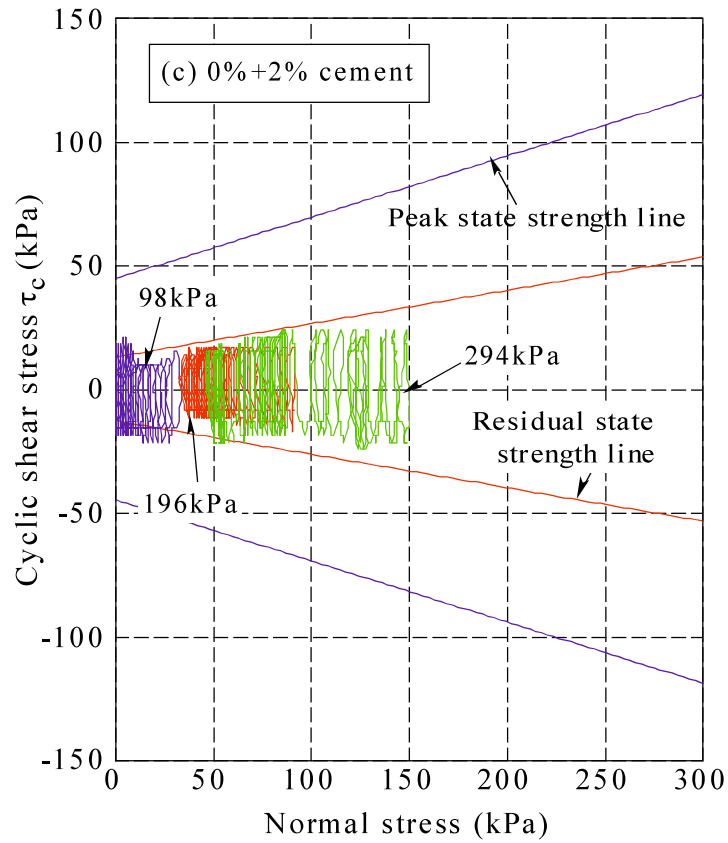
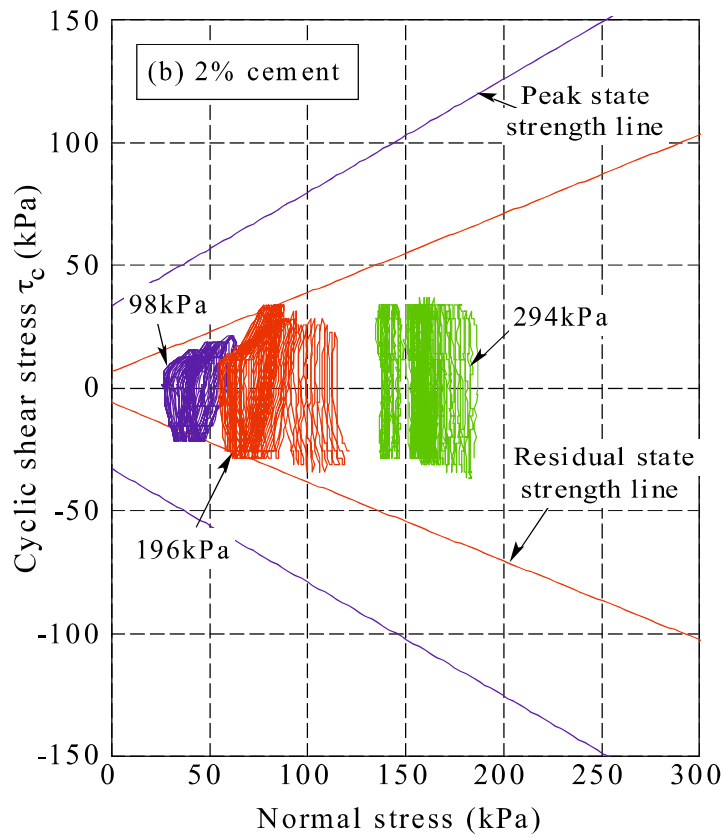
Fig. 6.17 shows the relationship between σ_N and τ_c , plotted in terms of stress paths and failure envelopes for the dynamic and the monotonic ring-shear test, respectively. The peak and the residual state failure envelopes obtained from the study in Chapter 4 are employed for purposes of comparison. For the 0% cement specimen, the stress paths surpassed its residual state strength line; however, they did not reach its peak state strength line for all three levels of normal stress. The cyclic shear strength may be considered to be an approximately average value between the peak and the residual strength. For the 2% cement specimen, the stress paths reach its residual strength line only at normal stress levels lower than 198 kPa. At a higher normal stress, 294 kPa, the stress paths did not coincide with its residual strength line. This behaviour, paired with Fig. 6.3 (c), indicates once more that the 2% cement specimen only slightly suffers from cyclic loading within a shear-torque amplitude of 60 kPa, and there was no sign of failure regarding these results. The cementation may not have been significantly influenced by cyclic loading.

For combined specimens with a bedding plane, the stress paths barely reached their residual strength line. For the 0% + 2% combined specimen, the stress paths barely surpassed its residual straight line (RSL) for a normal stress below 98 kPa. More specifically, all stress paths of the 2% + 2% cement specimen during cyclic shearing did not distinctly reach its residual strength line. This observation suggests that the cyclic strength of the 2% + 2% cement specimen is, essentially, lower than its residual static strength obtained from the monotonic ring-shear test. As mentioned in the previous section, the residual friction angle of the 2% + 2% cement specimen decreased by approximately 9.5° compared to that of the 2% cement specimen. In this case, it seems that the cyclic shear resistance of cement-combined specimens with a pre-existing slip surface decreased significantly compared to the static residual strength. The behaviour

observed in this cement-combined specimen is extremely unique, in that the decrease in the cyclic shear resistance is characterized by a discontinuous plane. Furthermore, in the dynamic ring-shear test, the total normal stress always changes to maintain constant volume; this leads to the decrease in effective normal stress, and causes decrease in the cyclic strength. Such a reduction of cyclic shear resistance on a bedding plane could cause substantial deformations, resulting in catastrophic endings of earthquake-induced landslides.

The results presented here are merely preliminary evaluations based on a comparison between the static and the dynamic strength obtained from the monotonic and the dynamic ring shear test. There are still many factors that influence the compared results, such as the differences in sample dimension, the constraint of applied loading conditions, and the shear speed, which are required to be further studied in future research. Nevertheless, these findings may meaningfully contribute to the body of knowledge regarding the cyclic behaviour of discontinuous plane materials, particularly that of cemented clay soils.





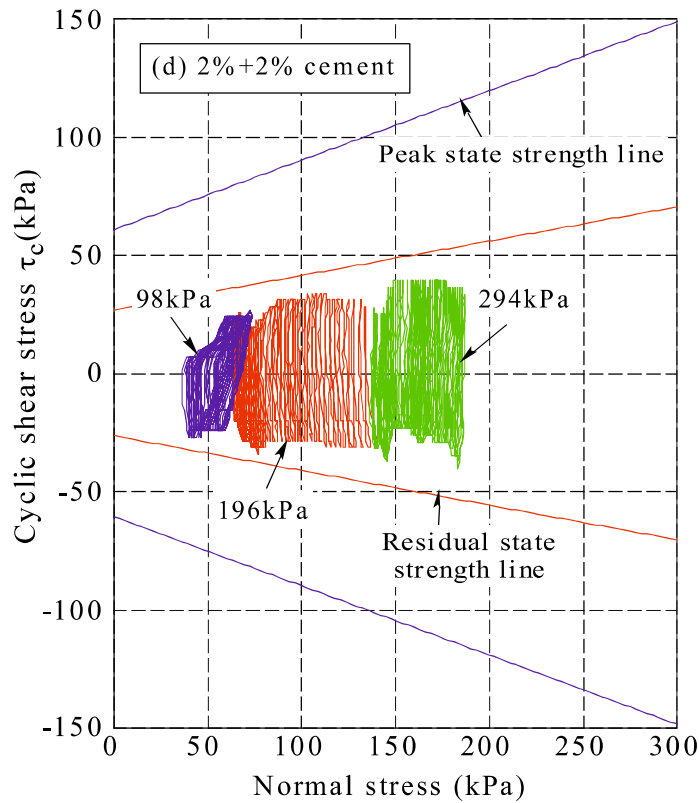


Figure 6. 17 Stress paths and peak and residual strength line of the (a) 0% cement, (b) 2% cement, (c) 0%+2% cement and (d) 2%+2% cement specimen during cyclic shearing, respectively; $f = 0.5$ Hz, shear torque = 60 kPa.

6.6 Summary

The results of the dynamic ring-shear test were analysed with respect to the effect of the confining pressure, the shear-torque amplitude, and over-consolidation on the cyclic degradation. The following conclusions can be drawn from the analysis of the test results in Chapter 6:

1. The experimental results clearly demonstrated that the degradation parameter t consistently decreased with the increase in vertical normal stress, shear-torque amplitude, and OCR for all samples.
2. The effect of vertical consolidation stress on parameter t for the 2% + 0% cemented kaolin sample appeared to be insignificant. On the other hand, when σ_N increased from 98 kPa to 294 kPa (approximately three times), t decreased by 31.1%, 59.1%, and 23.0% for the 0%, 2%, and 2% + 2% cemented kaolin,

respectively. This result means that the t of the 2% cemented kaolin is highly sensitive to variations in normal stress.

3. As the applied CSR approximately increased from 0.3 to 0.9, parameter t decreased by 11.5%, 44.0%, 30.8%, and 24.7% for the 0%, 2%, 2% + 2%, and 2% + 0% cemented kaolin, respectively. The addition of 2% cement content to kaolin confirmed again that the t of the 2% cemented kaolin is highly sensitive to variations in the shear-torque amplitude.
4. As OCR increased from 1 to 4, the value of t decreased by approximately 25.7% and 58.6% for the 0% and 2% cemented kaolin samples, respectively. This decrease is equivalently equal to that of the non-cemented and the cemented kaolin samples as σ_N increased from 98 kPa to 294 kPa.
5. The normalized cyclic stress ratio (τ_{cN}/σ_{N0}) increased with the decrease in the number of cycles (N_f) at a constant vertical consolidation value, under a pre-defined failure state for all samples except for the pure kaolin sample. The effect of cementation on τ_{cN}/σ_{N0} can be observed in the (τ_{cN}/σ_{N0})– N_f curve for the 2% and 2% + 2% cemented specimens, which was higher than that of other samples. On the other hand, the τ_c/σ_{N0} of pure kaolin did not seem to be influenced by the increase in normal stress. The reason behind such a tendency is not apparent in the present study.
6. Limited data suggest that the 2% cemented kaolin sample under a normal stress of 294 kPa and a shear-torque amplitude of 60 kPa did not present a failure state defined as cyclic shear displacement had reached a magnitude of 2 mm. This may be a subject of future investigation in relation to threshold shear strain in cemented clay soils..

Chapter 7 CONCLUSIONS AND RECOMMENDATIONS FOR FUTURE RESEARCH

7.1 Conclusions

This research represents a laboratory-based experimental study into the monotonic and dynamic strength characteristics of discontinuous plane in ring shearing. The occurrence of earthquake-induced landslides has increased in Japan, as well as in many areas of the world. As a consequence, it is realized that the strength and deformation properties of the contact surface between different soil layers during static and dynamic loading remains to be clarified and improved further.

Lightly cemented kaolin was used as discontinuous plane material in order to simulate realistic mechanical behaviour of slip surfaces occurring between two layers having different degrees of cementation. Both two series of monotonic and dynamic ring-shear tests was performed under various conditions on non-cemented and cemented kaolin, as well as two-layered specimen combined by attaching cemented kaolin to non-cemented kaolin.

Through the investigation, the current findings add substantially to our understanding of a typical case of of land sliding due to development of slip surface in cemented clayey material, also contribute to the body of knowledge on the complex behavior of clays, as well as cemented clay soils. Note that the results of the study are based on the slightly limited test results conducted on specified material and it is possible for this study to apply to cases of earthquake-induced landslides or failure slopes that occur in cemented clay soils having similar properties to artificially cemented kaolin. The following conclusions from analysis of the test results are presented below:

1. It has been found that the addition of 2% and 4% cement content affected scarcely on the peak friction angle of cemented kaolin. It means that failure envelopes at the peak state of cemented kaolin parallel with that of pure kaolin, and whose the internal friction angle are approximately in the same ranges.

2. For all tested samples, the residual failure envelopes produced in this study did not show pronounced curvature. Consequently, they can be considered linear for a range of 98 kPa to 392 kPa, regardless of cement content. Moreover, for the purpose of the stability analysis of landslide and failure slopes, it is commonly suggest that it is necessary to linear approximately of a segment of nonlinear drained residual failure envelopes of cemented kaolin samples, by which result in the residual cohesion. A high coefficient of determination R^2 (R is the coefficient of correlation) was obtained for all samples.
3. The residual friction angle of cemented kaolin considerably increased by 6.2° with an increase in the cement content from 0% to 2%. This increase then was not significant in cases where the cement content was increased beyond 2%. It is unclearly that the residual friction angle increases with the increase in the degree of cementation, which is scarcely referred in the literature. Based on the observation of the slickensides of cemented samples after shearing, we realized that the slip surfaces were not smooth, planar, and polish in comparison with pure kaolin. Its slickensides were undulating, slightly wavy and occasionally two simultaneous slickensides developed at the gap between the upper and lower shear boxes and between the tip of a radial fin and sample. The addition of cement into kaolin result in soil aggregations (clusters), which act almost as single particles and interact to produce the strength and stiffness. Thus, the residual strength increases with the increase in the degree of cementation may be attributed an undulating and slightly wavy slickenside at the residual state under any normal stress, by which soil aggregations acting almost as single particles or small blocks cause an increasing friction angle.
4. The values of residual friction angle for combined specimens may be as much as approximately 33.6% and 56.7% lower than those of pure and cemented kaolin, respectively. The addition of cement into kaolin not only increases the bond strength between soil particles, but also results in the presence of finer particles. Accompanied by hardening, these finer particles contributed to the development of a planar and polish pre-existing slip surface. This interface appears to increase a slip frictional coefficient, as well as reduce gradually the soil frictional coefficient, by which lead to a reduction of the residual friction.

5. For a comparison between intact and combined samples, 0% cemented kaolin was shown a good agreement in the residual friction angle between two sample types with a different value of 1.5° . In contrast, the residual friction angles of the 2% and 4% cement-combined samples decreased by approximately 9.5° and 9.3° from that of intact samples.
6. The cohesion intercept at the residual state for combined samples, which can be fitted as a straight line passing through the origin, increased linearly according to cement content. The calculated average value of cohesion for combined cement kaolin samples was higher than that for normal cemented kaolin samples. Furthermore, the residual cohesion intercept of 2% and 4% cement increased with the degree of cementation. These findings are quite meaningful in assessing the stability of earthquake-induced landslides that occur in areas with cemented soil. Especially, the residual cohesion on this discontinuous plane may control the instability of an earthquake-induced landslide rather than the residual friction angle.
7. The residual strength of cemented kaolin showed an insignificant increase with curing time up to 14 days, and then slightly increased with curing time. At a curing time of 28 days, the residual strengths of 2% and 4% cement-content samples were approximately 25.3% and 12.2% higher than those with 3 days curing, respectively. In contrast, the curing time showed a minimal effect on the strength at peak state.
8. The effect of cement content on rate dependency of residual strength was identified for cemented specimen. The results show that 2% cemented kaolin samples exhibited an increase in residual strength corresponding to increases in shear rate. In contrast, the residual strength of the 4% cemented kaolin samples was constant irrespective of shearing speed. The constant shearing rate effect observed with 4% cemented kaolin could be attributed the undulating or incompletely developed shear surface caused by stiffness resulting from cementation. Hence, the residual strength of cemented kaolin for cement content greater than 2% is independent of the shearing rate.

9. The residual strength was found to increase slightly with increasing shear displacement rate for each combined cemented specimen. This positive rate effect was similar to that of pure kaolin. Therefore, the rate dependency of residual strength exhibited in sample having a bedding plane.
10. The difference in residual friction angle, measured by the increasing load multistage and the reducing load multistage ring-shear tests and those measured by single-stage ring-shear tests varied from a minimum of 0.5° to a maximum of 6.2° for all tested samples. Between multistage two methods, the multistage reducing load ring-shear test was recognized as the more suitable method, which resulted in a wide range of residual friction angles, varying from 1.5° to 2.4° . In particular, 4% cemented kaolin sample exhibited a converse tendency, which shown that the multistage increasing load is more reasonable. This finding leads to the recommendation of inapplicability of the multistage technique for cemented clay soil, which may bring about erroneous results.
11. The effect of cementation on the residual cohesion intercept was identified for the 4% cemented specimen in the multistage reducing load test with a value that was approximately three times higher than that obtained in the single-stage test.
12. The residual stress ratio of 4% cemented kaolin samples in shear rate single-stage and multistage ring-shear tests could not be completely evaluated because their slip surface seemed to be undulating and non-planar in single-stage test. This evaluation may be obtained if single-stage ring-shear test is conducted at much greater shear displacement at which residual condition of cemented specimen would be achieved completely.
13. The stress ratio of combined samples in single-stage and multistage ring-shear tests increased with a practically similar tendency as the shear displacement rate increased. This increase is different for 0% and 4% cemented kaolin, thus, it is suggested that the multistage technique may give erroneous results for these clayey soils. It is recommended that it is possible and convenient to perform multistage fast shear-rate ring-shear tests on cemented pre-existing landslides soils to quickly evaluate the effect of shear velocity on the residual strength characteristics.

14. The experimental results clearly showed that degradation parameter t consistently decreased with increasing vertical normal stress, shear-torque amplitude, and OCR for all tested samples.
15. The effect of vertical consolidation stress on the parameter t for 2%+0% cemented kaolin sample appeared to be insignificant. On the other hand, if σ_N increases from 98 kPa to 294 kPa (approximately 3 times), t decreases by 31.1%, 59.1%, and 35.7% for 0%, 2%, and 2%+2% cemented kaolin, respectively. The decrease degree of 2% cemented kaolin is found to be over 2 times compared to pure kaolin. This result means that the t of 2% cemented kaolin is highly sensitive to the variation in normal stress.
16. As the applied cyclic stress ratio (CSR) approximately increased from 0.3 to 0.9, parameter t decreased by 11.5%, 44.0%, 30.8%, and 24.7% for 0%, 2%, 2%+2%, and 2%+0% cemented kaolin, respectively. The 2% cemented kaolin decreases over 4 times compared to pure kaolin. The addition of 2% cement content to kaolin confirms again that the t of 2% cemented kaolin is highly sensitive to the variation in shear-torque amplitude.
17. As OCR increased from 1 to 4, the value of t reduced approximately 25.7% and 58.6% for 0% and 2% cemented kaolin samples, respectively. This decrease is equivalently equal to that of non-cemented and cemented kaolin samples as σ_N was increased from 98 kPa to 294 kPa.
18. The normalized cyclic stress ratio (τ_{cN}/σ_{N0}) increased with the decrease in the number of cycles (N_f) at a constant vertical consolidation value under a pre-defined failure state for all sample exception to pure kaolin sample. The effect of cementation on τ_{cN}/σ_{N0} is identified as the τ_{cN}/σ_{N0} and N_f curve for 2% and 2%+2% cemented specimens was higher than that in other samples. On the other hand, the τ_c/σ_{N0} of pure kaolin seems not to be influenced by increasing normal stress. This reason for such a tendency is not apparent in the case of this study. As the number of cycles increases approximately beyond 100, τ_{cN}/σ_{N0} of 0%, 2%, and 2%+2% seem to be identical.

19. Limited data suggest that the 2% cemented kaolin sample conducted under a normal stress of 294 kPa and a shear-torque amplitude of 60 kPa did not show a failure state defined as cyclic shear displacement had reached a magnitude of 2 mm. This may lead to a subject of future investigation in relation to threshold shear strain in cemented clayey soils.
20. When clay soil of un-drained condition is cyclically loaded, pore water pressure develops and is always positive; however, it may be negative in over-consolidated clays. In the case of pure kaolin with OCRs up to 4, the pore water pressure was always positive. Conversely, for over-consolidated 2% cemented specimen, a high OCR caused a negative, high pore water pressure, which then seemed to reach a low, positive value. This type of response is considered as a result of the increase in stiffness and strength owing to the cementation. Further research is needed to quantify the generation of pore-water pressure in cemented clay soils.
21. The stress paths of the cement-combined specimen did not even reach its residual strength line. The cyclic shear resistance of the discontinuous plane materials decreased significantly compared to the static residual strength. These results are only preliminary evaluations based on a comparison between the static and the dynamic strength obtained from the monotonic and the dynamic ring shear test. There are still many factors that influence the compared results, such as the difference in sample dimension, the constraint of applied loading conditions, and the shear speed. Nevertheless, these findings may meaningfully contribute to the body of knowledge regarding the cyclic behaviour of discontinuous plane materials, particularly that of cemented clay soils.
22. Finally, the practical applicability of discontinuous plane material were confirmed by experimental work, as well as in-situ investigation. The reproducibility of artificially cemented kaolin in this study was mainly determined on the basis of the value of the hardness of the soil measured at a landslide slope site in the Mid Niigata Prefecture earthquake. The strength of the cemented soil itself is similar to that of the in-situ soil to some extent. As mentioned above, earthquake-induced landslides occurred along the bedding plane as a slip surface. When the strength of the soil has a discontinuity such as

that of the bedding plane, the influence of the discontinuity on the stability of the landslide slope can be assessed quantitatively.

7.2 Recommendations for future research

The experimental work in this study has contributed significant data into monotonic and dynamic shear strength characteristics of discontinuous planes consisting of soil layers with varying cementation. In the view of the findings and discussion, the following recommendations are made for future work:

1. Measuring the pore water pressure: To build a more general framework of strength characteristics of discontinuous planes, further tests should be carried out to examine in more detail the influence of the pore water pressure during the shearing process in both monotonic and dynamic ring-shear test.
2. In process of shearing a soil sample, the pore water may migrate from upper part to lower part. This tendency could influence on the residual shear strength. Thus, the investigation of water content at the slip surface is suggested to be necessary to clarify the mechanical behavior of soil material at slide surface.
3. Residual strength characteristic between different soil layers: Ring shear strength properties of discontinuous planes simulated by various cemented and non-cemented kaolin sample types has been investigated in this study. To extend these findings, it would be of interest to examine if similar sample types that could be performed on combined samples composing of different soil layers, such as clay and clayey sand soil or clay and sand as well, to ensure its applicability to many kinds of soils with different cases. This could be part of more detailed study of the simulation of the behavior of realistic slip surfaces.
4. Investigation of shear zone using scanning electron microscopy (SEM) technique: This is one of most common methods using to investigate shear surface microstructure in ring-shear test. Thus, future research considering the examination of SEM at shear surface is recommenced.
5. Long-term curing time effects in artificially cemented kaolin on residual shear strength: The performed tests on artificially cemented kaolin only investigated

the influence of curing times up to 30 days. The effects of curing time on residual strength were highlighted, so in order to clear this up, additional tests need be carried out to investigate the residual strength development to longer curing times.

6. Threshold shear strain in cemented clayey soil: The 2% cemented kaolin sample conducted under a normal stress of 294 kPa and a shear-torque amplitude of 60 kPa did not show a failure state defined as cyclic shear displacement had reached a magnitude of 2 mm. This may lead to a subject of future investigation in relation to threshold shear strain in cemented clayey soil using ring-shear apparatus, as well as triaxial compression apparatus.
7. It is recommended to perform more strain-controlled ring-shear tests in order to clarify the trends observed for cemented kaolin specimen in this study.
8. Regarding residual strength of cemented clay soils, the shear displacement conducted in this study may be not enough to complete the residual state. Thus, it is suggested that an efficient method to result in much deformation is necessary.

REFERENCES

1. Abramson, L.W., Lee, T.S., Sharma, S. and Boyce, G.M. (1996). Slope stability and stabilization methods, John Wiley & Sons, 2-3.
2. Anderson, W.F and Hammoud, F. (1988). Effect of testing procedure in ring shear tests. *Geotechnical Testing Journal*, GTJODJ, Vol. 11, No. 3, pp. 204-207.
3. Ansal, A.M., and Erken, A. (1989). Undrained behavior of clay under cyclic shear stress. *Journal of Geotechnical Engineering*, ASCE, Vol.115, No. 7, pp. 968-983.
4. Bishop, A.W., Green, G.E., Garga, V.K., Andresen, A, Brown, J.D. (1971). A new ring shear apparatus and its application to the measurement of residual strength. *Géotechnique*, Vol. 21, No. 4, pp. 273-328.
5. Bjerrum, L. (1967). Engineering geology of Norwegian normally consolidated marine clays as related to settlements of buildings. Seventh Rankin Lecture, *Géotechnique*, Vol.17, pp. 83–118.
6. Burland, J.B. (1990). On the compressibility and shear strength of natural clays. *Géotechnique*, Vol. 40, No. 3, pp. 329-378.
7. Bhat, D.R., Bhandary, N.P., Yatabe, R. (2013). Effect of shearing rate on residual strength of kaolin clay. *EJGE*, Vol. 18, Bund. G: pp. 1387-1396.
8. Bhat, D.R., Yatabe, R, and Bhandary, N.P. (2013). Study of pre-existing shear surface of reactivated landslides from a strength recovery perspective. *Journal of Asian Earth Science*, Vol. 77, pp. 243-253.
9. Bhat, D.R., Bhandary, N.P., Yatabe, R. (2013). Experimental study of strength recovery from residual strength on kaolin clay. *International Journal of Civil, Architectural, Urban Science and Engineering*, Vol. 7, No. 1, pp. 67-73.
10. Bromhead, E.N. (1979). A simple ring shear apparatus. *Ground Engineering*, Vol. 17, No. 2, pp. 40-44.
11. Carrubba, P. and Colonna, P. (2006). Monotonic fast residual strength of clay soils. *Rivista italiana di Geotecnica, Technical Notes*, pp. 32-51.

12. Carrubba, P., and Del Fabbro, M. (2008). Laboratory investigation on reactivated residual strength. *Journal of Geotechnical and Geoenvironmental Engineering* ASCE 134, No. 3, pp. 302-315.
13. Chigira, M. (1990). A mechanism of chemical weathering of mudstone in a mountainous area. *Engineering Geology*, Vol. 29, pp. 119-138.
14. Chigira, M. and Yagi, H. (2006). Geological and geomorphological characteristics of landslides triggered by the Mid Niigata prefecture earthquake in Japan. *Engineering Geology*, Vol. 82, pp. 202-221.
15. Clough, G. W., Sitar, N., Bachus, R.C., Rad, N. S. (1981). Cemented sands under static loading. *Journal Geotechnical Engineering ASCE*, Vol. 107, No. 6, pp. 799-817.
16. Cuccovillo, T. and Coop, M. R. (1999). On the mechanics of structured sands. *Géotechnique*, Vol. 49, No. 6, pp. 741–760.
17. Fisher, K.P., Andersen, K.H., Moum, J. (1978). Properties of an artificially cemented clay. *Canadian Geotechnical Journal*, Vol. 15, No. 3, pp. 322-331.
18. Garga, V.K, and Infante, J.A. (2002). Steady state of sands in a constant volume ring shear apparatus. *Geotechnical Testing Journal*, Vol. 25, No. 4, pp. 1-8.
19. Gibo, S., Egashira, K., Ohtsubo, M. (1987). Residual strength of smectite-dominated soils from the Kamenose landslide in Japan. *Canadian Geotechnical Journal*, Vol. 24, No. 3, pp. 456-462.
20. Gibo, S., Egashira, K., Ohtsubo, M., Nakamura, S. (2002). Strength recovery from residual state in reactivated landslides. *Géotechnique*, Vol. 52, No. 9, pp. 683–686.
21. Grachev, I., Sassa, K., and Fukuoka, H. (2005). The shear strength of clayey soils from reactivated landslides. *Annuals of Disas. Prev. Res. Inst., Kyoto Univ.*, No. 48B, 2005.
22. Gratchev, I.B., Sassa, K., Osipov, V.I., and Sokolov, V.N. (2006). The liquefaction of clayey soils under cyclic loading. *Engineering Geology*, Vol. 86, pp. 70-84.

23. Gratchev, I.B, Sassa, K. (2015). Shear strength of clay at different shear rates. *Journal of Geotechnical and Geoenvironmental Engineering ASCE*, Vol. 141, No. 5.
24. Harris, A.J and Watson, P.D.J. (1997). Optimal procedure for the ring shear test. *Ground Engineering*, Vol. 30, pp. 26-28.
25. Has, B., and Nozaki, T. (2014). Role of geological structure in the occurrence of earthquake-induced landslides, the case of the 2007 Mid-Niigata Offshore Earthquake, Japan. *Engineering Geology*, Vol. 182, Part A, 19 November 2014, pp. 25-36.
26. Hatipoglu, M., Cevikbilen, G., Bayin, A., and Iyisan, R. (2012). Residual shear strength of cohesive soils. *Journal of Faculty of Mining, Geology and Civil Engineering*, Vol. 2013/1, pp. 33-38.
27. Hawkins, A.B., and Privett, K.D. (1985). Measurement and use of residual strength of cohesive soils. *Ground Engineering*, Vol. 18, No. 8, pp. 22-29.
28. Horpibulsuk, S., Miura, N., and Nagaraj, T.S. (2003). Assessment of strength development in cement content clays with Abram's law as a basic". *Géotechnique*, Vol. 53, No. 4, pp. 439-444.
29. Horpibulsuk, S., Miura, N., Bergado, D.T. (2004). Undrained shear behavior of cemented admixed clay at high water content. *Journal of Geotechnical and Geoenvironmental Engineering ASCE*, Vol. 130, No. 10, pp. 1096-1105.
30. Horpibulsuk, S. (2005). Mechanism controlling undrained shear characteristics of induced cemented clays. *Lowland Technology International* Vol. 7, No. 2, pp. 9-18.
31. Horpibulsuk, S., Miura, N., and Nagaraj, T.S. (2005). Clay-water/cement ratio identity for cement admixed soft clays. *Journal of Geotechnical and Geoenvironmental Engineering*, ASCE, Vol. 131, No. 2, pp. 187-192.
32. Hussain, M., and Stark, T.D. (2011). Bach-analysis of pre-existing landslides. *Geo-Frontiers 2011*, pp. 3659-3668.

33. Idriss, I. M., Dobry, R., and Singh, R. D. (1978). Nonlinear behavior of soft clays during cyclic loading. *J. Geotech. Engrg. Div.*, Vol. 104(GT12), pp. 1427-1447.
34. Jurko, J., Sassa, K., and Fukuoka, H. (2008). Study on seismic behavior of nonplastic silt by means of ring-shear apparatus. *Landslides*, Vol. 5: pp. 189-201.
35. Kalteziotis, N. (1993). The residual shear strength of some Hellenic clayey soils. *Geotechnical and Geological Engineering*, Vol. 11, pp. 125-145.
36. Kasama, K., Ochiai, H., Yasufuku, N. (2000). On the stress-strain behaviour of lightly cemented clay based on an extended critical state concept. *Soil and Foundations*, Vol. 40, No. 5, pp. 37-47.
37. Kasama, K., Zen, K., Iwataki, K. (2006). Undrained shear strength of cement-treated soils. *Soil and Foundations*, Vol. 46, No. 2, pp. 221-232.
38. Khosravi, M., Meehan, C.L., Cacciola, D.V., Khosravi, A. (2013). Effect of fast shearing on the residual shear strengths measured along pre-existing shear surfaces in kaolinite. In: *Proceedings of Geo-Congress 2013*: pp. 245-254.
39. Kimura, S., Nakamura, S., Vithana, S.B., Sakai, K. (2013). Shearing rate effect on residual strength of landslide soils in the slow rate range. *Landslides*, Vol. 11, No. 6, pp. 969-979.
40. Kinoshita, A., Shibasaki, T., Hasegawa, Y., Yamaoka, T., Yamazaki, T. (2013). Mechanism of earthquake-induced rapid landslides occurring along the bedding plane of weathered soft rock. *Journal of the Japan Landslide Society*, Vol. 50, No. 3, pp. 103-112 (in Japanese).
41. La Gatta, D.P. (1970). Residual strength of clay and clay-shales by rotation shear tests, *Soil Mechanics Series No.86*, Harvard University, Cambridge, Massachusetts.
42. Lee, K.H., Lee, S. (2002). Mechanical properties of weakly bonded cement stabilized kaolin. *Journal of Civil Engineering, KSCE*, Vol. 6, No. 4, pp. 389-398.
43. Lemos, L.J.L., Skempton, A.W., Vaughan, P.R. (1985). Earthquake loading of shear surface in slopes. In *Proceedings of the 11th International Conference on Soil Mechanics and Foundation Engineering*, Vol.4, pp.1955-1958.

44. Lemos, L.J.L. (2003). Shear behaviour of pre-existing shear zones under fast loading – Insight on the landslide motion. *Proc., Int. Work: Occurrence and Mechanism of Flow-like landslides in Natural slopes and Earthfills*, Sorrento, Italy, pp. 229-236.
45. Leroueil, S., Vaughan, P.R. (1990). The general and congruent effects of structure in natural soils and weak rocks. *Géotechnique*, Vol. 40, No. 3, pp. 467-488.
46. Lupini, J.F., Skinner, A.E., Vaughan, P.R. (1981). The drained residual strength of cohesive soils. *Géotechnique*, Vol. 31, No. 2, pp. 181-213.
47. Matasovic, N. and Vucetic, M. (1995). Generalized cyclic-degradation pore pressure generation model for clay. *Journal of Geotechnical Engineering*, ASCE, Vol. 121, No. 1, pp. 33-42.
48. Meehan, C.L, Duncan, J.M, Brandon, T.L, and Boulanger, R.W. (2006). An experimental study of the dynamic behavior of slickensided surfaces. Report of a study performed by the Virginia Tech Center for Geotechnical Practice and Research, April, 2006.
49. Meehan, C.L, Brandon, T.L, and Duncan, J.M. (2007). Measuring drained residual strength in the Bromhead ring shear. *Geotechnical Testing Journal*, ASTM, Vol. 30, No. 6, pp. 466-473.
50. Mesri, G. and Cepeda-Diaz, A.F. (1986). Residual shear strength of clays and shales. *Géotechnique*, Vol. 36, No. 2, pp. 269-274
51. Mesri, G. and Abdel-Ghaffar, M.E.M. (1993). Cohesion intercept in effective stress-stability analysis. *Journal of Geotechnical Engineering*, ASCE, Vol. 119, No. 8, pp. 1229-1249.
52. Mesri, G. and Shahien, M. (2003). Residual shear strength mobilized in first-time slope failures. *Journal of Geotechnical and Geo-environmental Engineering*, ASCE, Vol. 129, No. 1, pp. 12-31.
53. Mesri, G and Sarihan, N.H. (2012). Residual shear strength measured by laboratory tests and mobilized in landslides. *Journal of Geotechnical and Geo-environmental Engineering*, ASCE, Vol. 138, No. 5, pp. 585-593.

54. Mitchell, J.K. (1993). *Fundamental of soil behavior*. John Willey and Sons, Inc., New York.
55. Miura, N., Horpibulsuk, S., and Nagaraj, T.S. (2001). Engineering behaviour of cement stabilized clay at high water content. *Soils and Foundations*, Vol. 41, No. 5, pp. 33-45.
56. Moore, R. (1991). The chemical and mineralogical controls upon the residual strength of pure and natural clays. *Géotechnique*, Vol. 41, No. 1, pp. 35-47.
57. Mortezaie, A. R., and Vucetic, M. (2013). Effect of frequency and vertical stress on cyclic degradation and pore water pressure in clay in the NGI simple shear device. *Journal of Geotechnical and Geo-environmental Engineering*, ASCE, Vol. 139, No. 10, pp. 1727-1737.
58. Mortezaie, A., and Vucetic, M. (2016). Threshold shear strains for cyclic degradation and cyclic pore water pressure generation in two clays. *Journal of Geotechnical and Geo-environmental Engineering*, ASCE, 04016007-1-13.
59. Ministry of Land, Infrastructure and Transport (2004). Quick report for Landslides triggered by 2004 Niigata Chuetsu earthquake. http://www.mlit.go.jp/kisha/kisha04/05/051101_2_.html.
60. Onoue, A., Wakai, A., Ugai, K., Higuchi, K., Fukutake, K., Hotta, H., Kuroda, S., Nagai, H. (2006). Slope failures at Yokowatashi and Nagaoka College of Technology due to the 2004 Niigata-ken Chuetsu Earthquake and their analytical considerations. *Soils and Foundations*, Vol. 46, No. 6, pp. 751-764.
61. Osipov, V., Nilolaeva, S., Sokolov, V. (1984). Microstructural changes associated with thixotropic phenomena in clay soils. *Geotechnique*, Vol. 34, No. 2, pp. 293-303.
62. Parathias, A.N. (1995). Displacement rate and shear direction effects on the residual strength of plastic soils. *Proc. 7th Int. Conf. Soil Dynamics and Earthquake Engineering*, pp. 67-72.
63. Petley, D.J, and Taylor, P. (1999). Modelling rapid shearing of cohesive soils along undulating shear surfaces. *Proc. 7th Int. Symp. Slope Stability Engineering*. Shikoku, Japan, Vol. I, pp. 745-750.

64. Proctor, D.C, and Khaffaf, J. (1984). Cyclic triaxial tests on remolded clays. *Journal of Geotechnical Engineering*, ASCE, Vol. 110, No. 10, pp. 1431-1445.
65. Public Works Research Institute, 2006, Snow Avalanche and Landslide Research Center News, No.39, <http://www.pwri.go.jp/jpn/about/pr/publication/nignews/nn39/news02.htm> (in Japanese).
66. Raftari, M., Rashid, A.S.A., Kassim, K.A., Moayedi, H. (2014). Evaluation of kaolin slurry properties treated with cement. *Measurement*, Vol. 50, pp. 222-228.
67. Ramiah, B.K., Dayalu, N.K., and Purushothamaraj, P. (1970). Influence of chemicals on residual strength of silty clay. *Soils and Foundations*, Vol. 10, pp. 25-36.
68. Sangrey, D.A. (1972). Naturally cemented sensitive soils. *Géotechnique*, Vol. 22, No. 1, pp. 139-152.
69. Sasanian, S., Newson, T.A. (2014). Basic parameters governing the behavior of cement-treated clays. *Soil and Foundations*, Vol. 54, No. 2, pp. 209-224.
70. Sassa, K., Fukuoka, H., Scarascia-Mugnozza, G., Evans, S. (1995). Earthquake-induced landslides: distribution, motion and mechanisms. *Soils and Foundations Special Issue on Geotechnical Aspects the January 17 1995 Hyogoken-Nanbu Earthquake*: pp. 53-64.
71. Sassa, K., Wang, W., and Fukuoka, H. (2003). Performing undrained shear tests on saturated sands in a new intelligent type of ring shear apparatus. *Geotechnical Testing Journal*, Vol. 26, No. 3, pp. 1-9.
72. Sassa, K., Fukuoka, H., Wang, W., and Ishikawa, N. (2004). Undrained dynamic-loading ring-shear apparatus and its application to landslide dynamics. *Landslides*, Vol. 1, pp. 7-19.
73. Sassa, K., Fukuoka, H., Wang, F., and Wang, G. (2005). Dynamic properties of earthquake-induced large-scale rapid landslides within past landslide masses. *Landslides*, Vol. 2, pp. 125-134.

74. Seycek, J. (1978). Residual shear strength of soils. *Bull. Int. Ass. Eng. Geol.* Vol. 17, pp. 73-75.
75. Skempton, A.W. (1964). Long-term stability of clay slopes. Fourth Rankine lecture. *Géotechnique*, Vol. 14, No. 2, pp. 77–102.
76. Skempton, A.W. (1985). Residual strength of clays in landslides, folded strata and the laboratory. *Géotechnique*, Vol. 35, No. 1, pp. 3-18.
77. Soralump, S., and Prasomsri, J. (2016). Cyclic pore water pressure generation and stiffness degradation in compacted clays. *Journal of Geotechnical and Geo-environmental Engineering*, ASCE, Vol. 142, No. 1: 04015060, pp. 1-13.
78. Sorensen, K.K, Baudet, B.A., and Simpson, B. (2007). Influence of structure on the time-dependent behavior of a stiff sedimentary clay. *Géotechnique*, Vol. 57, No. 1, pp. 113-124.
79. Stark, T.D., Vettel, J.J. (1992). Bromhead ring shear test procedure. *Geotechnical Testing Journal*, Vol. 15, No. 1, pp. 24-32.
80. Stark, T.D., and Eid, H.T. (1992). Comparison of field and laboratory residual shear strengths. Proc., Stability and Performance of Slopes and Embankments II, No. 31, Vol. 1, ASCE, New York, GSP 876-889.
81. Stark, T.D., and Eid, H.T. (1993). Modified Bromhead ring shear apparatus. *Geotechnical Testing Journal*, ASTM, Vol. 16, No. 1, pp. 100-107.
82. Stark, T.D., Eid, H.T. (1994). Drained residual strength of cohesive soils. *Journal of Geotechnical Engineering*, ASCE, Vol. 120, No. 5, pp. 856-871.
83. Stark, T.D., Choi, H. and McCone, S. (2005). Drained shear strength parameters for analysis of landslides, *Journal of Geotechnical and Geo-environmental Engineering*, ASCE, Vol 131, No. 5, pp. 575-588.
84. Stark, T. and Hussain, M. (2010). Drained residual strength for landslides. *Proceeding of GeoFlorida 2010: Advances in Analysis, Modeling and Design*, pp. 3217-3226.

85. Stark, T. and Hussain, M. (2010). Shear strength in pre-existing landslides. *Journal of Geotechnical and Geoenvironmental Engineering*, Vol. 136, No. 7, pp. 957-962.
86. Suzuki, M., Umezaki, T., Kawakami, H. (1997). Relation between residual strength and shear displacement of clay in ring shear test. *Journal of the Japan Society of Civil Engineers* 575 (III-40): pp. 141-158 (in Japanese).
87. Suzuki, M., Umezaki, T., Kawakami, H., Yamamoto, T. (2000). Residual strength of soil by direct shear test. *Journal of the Japan Society of Civil Engineers* 645 (III-50): pp. 37-50 (in Japanese).
88. Suzuki, M., Yamamoto, T., Tanikawa, K., Fukuda, J., Hisanaga, K. (2001). Variation in residual strength of clay with shearing speed. *Memoirs of the Faculty of Engineering Yamaguchi University*, Vol. 52, No. 1, pp. 45-49.
89. Suzuki, M., Taguchi, T., Fujimoto, T., Kawahara, Y., Yamamoto, T., Okabayashi, S., (2005). Effect of loading condition during curing period on unconfined compressive strength of cement stabilized soil, *Journal of Japan Society of Civil Engineers*, 792(III-71), pp. 211-216 (in Japanese).
90. Suzuki, M., Tsuzuki, S., Yamamoto, T. (2007). Residual strength characteristics of naturally and artificially cemented clays in reversal direct box shear test. *Soils and Foundations*, Vol. 47, No. 6, pp. 1029-1044.
91. Suzuki, M., Fujimoto, T., and Taguchi, T. (2014). Peak and residual strength characteristics of cement-treated soils cured under different consolidation conditions. *Soils and Foundations*, Vol. 54, No. 4, pp. 687-698.
92. Tabana, K. and Vucetic, M. (2010). Threshold shear strain for cyclic degradation of three clays. *Fifth International Conference on Recent Advances in Geotechnical Earthquake Engineering and Soil Dynamics*, May 24-29, 2010, San Diego, California. Paper 30.
93. Tika, T.E., Vaughan, P.R., Lemos, L.J.L. (1996). Fast shearing of pre-existing shear zones in soil. *Géotechnique*, Vol. 46, No. 2, pp. 197-233.
94. Tika, T.E., and Hutchinson, J.N. (1999). Ring shear tests on soil from the Vaiont landslide slip surface. *Géotechnique*, Vol. 49, No. 1, pp. 59-74.

95. Tiwari, B. and Marui, H. (2001). Concept of shear strength measurement and modification of stability analysis during countermeasure planning of landslides. *Journal of the Japan Landslide Society*, Vol. 38, No. 3, pp. 213-224.
96. Tiwari, B. and Marui, H. (2003). Estimation of residual shear strength for bentonite-kaolin-Toyoura sand mixture. *Journal of the Japan Landslide Society*, Vol. 40, No. 2, pp. 124-133.
97. Tiwari, B. and Marui, H. (2004). Objective oriented multistage ring shear test for shear strength of landslide soil. *Journal of Geotechnical Engineering*, ASCE, Vol. 130, No. 2, pp. 217-222.
98. Tiwari, B. and Marui, H. (2005). A new method for the correlation of residual shear strength of the soil with mineralogical composition. *Journal of Geotechnical and Geo-environmental Engineering*, ASCE, Vol 131, No. 9, pp. 1139-1150
99. Tiwari, B., Brandon, T.L., Mauri, H., and Tuladhar, G.R. (2005). Comparison of residual strengths from back analysis and ring shear tests on undisturbed and remoulded specimens. *Journal of Geotechnical and Geo-environmental Engineering*, ASCE, Vol 131, No. 9, pp. 1071-1079.
100. Toyota, H., Nakamura, K., Sugimoto, M., Sakai, N. (2009). Ring shear tests to evaluate strength parameters in various remoulded soils. *Géotechnique*, Vol. 59, No. 8, pp. 649-659.
101. Townsend, F.C and Gilbert, P.A. (1973). Tests to measure residual strengths of some clay shales. *Géotechnique*, Vol. 23, No. 2, pp. 267-271.
102. Townsend, F.C and Gilbert, P.A. (1976). Effects of specimen type on the residual strength of clays and clay shales. *Soil Specimen Preparation for Laboratory Testing*, ASTM STP 599, American Society for Testing and Materials, pp. 43-65.
103. Vithana S.B., Nakamura, S., Kimura, S., Gibo, S. (2012). Effects of overconsolidation ratios on the shear strength of remoulded slip surface soils in ring shear. *Engineering Geology*, Vol. 131–132, pp. 29–36.

104. Vucetic, M., and Dobry, R. (1988). Degradation of marine clays under cyclic loading. *Journal Geotechnical Engineering*, Vol. 114, No. 2, pp. 133-149.
105. Yasuhara, K., Yamanouchi, T., and Hirao, K. (1982). Cyclic strength and deformation of normally consolidated clay. *Soils and Foundations*, Vol. 22, No. 3, pp. 77-91.
106. Yatabe, R., Yagi, N., Enoki, M., 1991, Ring shear characteristics of clay in fractured-zone-landslide. *Journal of the Japan Society of Civil Engineers* 436 (III-16): pp. 93-101 (in Japanese).
107. Yatabe, R., Yagi, N., Mukaitani, M., Enoki, M., 1996, Influence of shear test method and restraint condition of residual strength of soil. *Journal of the Japan Society of Civil Engineers* 554 (III-37): pp. 139-146 (in Japanese).
108. Wakai, A., Ugai, K., Onoue, A., Kuroda, S., Higuchi, K. (2010). Numerical modelling of an earthquake-induced landslide considering the strain-softening characteristics at the bedding plane. *Soils and Foundations*, Vol. 50, No. 4, pp. 533-545.
109. Wissa, A.E.Z., Ladd, C.C., Lambe, T.W. (1965). Effective stress strength parameters of stabilized soils. In Proceedings of the 6th International Conference on Soil Mechanics and Foundation Engineering, pp.412-416.
110. Wang, H.B, Sassa, K., and Xu, W.Y. (2007). Analysis of a spatial distribution of landslides triggered by the 2004 Chuetsu earthquakes of Niigata prefecture, Japan. *Natural Hazards*, Vol. 41, pp. 43-60.

ACKNOWLEDGMENTS

I am sincerely and respectfully grateful to my supervisor Professor Motoyuki Suzuki for the support, help and valuable guidance he gave me throughout this work. His technical support was invaluable and thus having a research work with him has always been a great opportunity for me.

My sincere thanks also go to committee of my dissertation examination: Prof. Hiroshi Matsuda, Prof. Yukio Nakata, Prof. Yoshimoto Norimasa, and Dr. Tran Thanh Nhan for their valuable advice and comments during the examination of this dissertation.

I extended my thanks to all of my laboratory members who have contributed in various ways towards this study: Mr. Takuya Yamamoto, Mr. Naoki Otani, Mr. Yuho Inoue, Mr. Nguyen Thanh Duong. Particular thanks should be given to doctoral fellow, Mr. Atsusi Kouyama for his kindness and help. Many thanks are due to all my friends at Yamaguchi University and Ube city.

I also would like to express my grateful acknowledgement to Vietnam Ministry of Education and Training (MOET), and Vietnam International Education Development (VIED) for their financial support of my doctoral research in Yamaguchi University. I would like to express my grateful acknowledgement to Mien Trung University of Civil Engineering (MUCE), Phu Yen province, Vietnam, for their substantial support of my research.

Living and working in Japan has always been a great experience, and my thanks goes to the Library and International Student Office of Yamaguchi University, Ube International Student House Office, Saruta Apartment Office, Tokiwa Kogyo Society, and Yaochi company for their help and niceness during my stay in Yamaguchi University and Ube city. I shall always remember very kind Japanese people.

Finally, I would like to express special thanks to my wife, Hoang Hao and my beloved daughter, Bao Chau for their love, patience, encouragement and for being always by my side during stay in Japan. I could never thank them enough for all of the sacrifices they have made for me.